THE UNIVERSITY
of EDINBURGH

Investigations into Inflammation and Apoptosis in the 'Perimenstrual' Human Endometrium and a Mouse Model of Menstruation

Gregory Armstrong

Thesis for the degree of Doctor of Philosophy

The University of Edinburgh

2016

Declaration

In accordance with the requirements of the University of Edinburgh, I hereby declare that the studies undertaken in this thesis were the unaided work of the author, except where due acknowledgement is made.

I acknowledge that the whole genome array and subsequent bioinformatics analyses described in the introduction to Chapter 5 were performed by JA Maybin with the assistance of E Marshall, and supported by funding from an MRC grant awarded to HOD Critchley. This work has been published previously in JA Maybin's 2011 University of Edinburgh PhD thesis.

All other work described herein has not previously been submitted or accepted for another degree or professional qualification.

Gregory Armstrong

March 2016

Abstract

Menstruation is triggered by a fall in circulating progesterone (P_4), and to a lesser extent, oestradiol (E_2) concentrations, and characterised by classical inflammatory features in the endometrium: breakdown of the basal lamina, tissue oedema and an influx of migratory leucocytes. During and following menstruation, endometrial inflammation is resolved and the endometrium is repaired. The successful resolution of acute inflammation in other tissues involves apoptosis and the phagocytic clearance of apoptotic cells.

Human endometrial tissues were collected with informed patient consent and local research ethics committee approval. C57Bl/6 mice underwent an induced menstruation protocol (via sequential E_2 and P_4 exposure followed by P_4 withdrawal), both with and without experimental inhibition of apoptosis (using the pan-caspase inhibitor, Q-VD-OPh).

Coordinated apoptosis and neutrophil recruitment were *hypothesised* to be components of the menstrual event and to precede menstrual shedding in the human endometrium. Immunoreactivity histoscoring for cleaved caspase-3 (CC3) revealed extensive apoptosis in the normal human endometrium early in the 'perimenstrual' period, and careful stereological delineation of neutrophil ($elastase^+$) recruitment showed a significant influx coincident with menstrual tissue breakdown.

Apoptosis and neutrophil recruitment were *hypothesised* to follow similar courses in the endometria of mice undergoing an induced menstruation protocol, recapitulating human menstrual events. Immunoreactivity histoscoring for CC3 and stereological investigation into neutrophil ($Ly6G^+$) recruitment in mouse endometrial tissues revealed almost identical extents and timings of apoptosis and neutrophil recruitment in women.

Whole genome array evidence of differential apoptosis-related gene transcription in the endometria of women with heavy menstrual bleeding (HMB) compared to those of women with normal menstrual bleeding (NMB) led to the *hypothesis* that apoptosis may be dysregulated in women with HMB and that perhaps this may delay timely repair of the endometrium and lead to prolonged bleeding in consequence. Candidate differentially-regulated gene transcripts identified by the whole genome array were validated by means of RT-qPCR, although immunoreactivity histoscoring for CC3 did not reveal any differences in apoptosis or its localisation between women with NMB and HMB at the menstrual cycle time-points examined.

Building on evidence of apoptotic transcriptional dysregulation in the endometria of women with HMB, it was *hypothesised* that experimental inhibition of apoptosis (via Q-VD-OPh) in a mouse model of induced menstruation could delay endometrial repair and delay resolution of endometrial inflammation. Some evidence of delayed early repair was obtained, alongside the discoveries of delayed inflammatory gene transcription and increased decidual proliferation ($BrdU^+$) in apoptosis-inhibited mice.

Apoptosis precedes the classical inflammatory features of menstruation in the human and mouse endometrium, with inhibition of apoptosis in the latter altering repair and the inflammatory micro-environment. An apoptosis-inhibited mouse model of menstruation may therefore represent a viable model for the further study of heavy menstrual bleeding.

Lay Summary

Sex steroids prepare the endometrium (lining of the womb) to support the development of a foetus during pregnancy, but in the absence of a successful pregnancy, this womb lining is shed in a process called menstruation. Menstruation shares many of the features that are associated with acute injury and wound healing, including the attraction of certain kinds of immune cells from the blood. Resolving the injury and repairing the tissue in acute injury involves a form of programmed cell death called 'apoptosis'. The *hypothesis* of this work is that apoptosis is also important in resolving menstruation, and that problems coordinating this process may interfere with the successful completion of menstruation.

To examine whether this might be the case, patient womb samples were collected with written informed consent from participating women and with permission from local research ethics committees. Womb samples were also collected from mice, using an experimental model in which menstruation is simulated – this made it possible to experimentally manipulate how apoptosis took place in the womb and to examine its effects. A variety of techniques were used to accomplish this, all with an aim to determining how, when and where important events were taking place in the womb.

This work discovered that apoptosis is indeed important in menstruation and that its timing is very tightly controlled, both in women and in our mouse model. Certain immune cells were discovered to be attracted to the womb at precise times, which may play a role in how the womb is able to repair itself. Changes in how the womb controls apoptosis were discovered in women who suffer from heavy menstrual bleeding. When we experimentally prevented mouse wombs from undergoing apoptosis, many of the features that we see in the wombs of women with heavy menstrual bleeding were

seen – it is hoped that this animal model may represent a means to further studying (and treating) heavy menstrual bleeding.

Acknowledgements

I would like to thank my supervisors, Professors Hilary Critchley and Adriano Rossi for their support, encouragement and advice throughout my PhD. These three years have been a tremendously rewarding experience, and I'd like to offer my supervisors my gratitude for the opportunity to have learned so much from them. I feel I could not have asked for better supervisors, nor for more welcoming lab groups.

To Hilary, I am very grateful indeed: for her support in my studies; for thoughtful, considered guidance; and, when I broached my interest in pursuing a career in medicine, for consistent encouragement at every stage of the (somewhat stressful) process.

I would like to thank Adriano for helping me refine my ideas, writing and scientific arguments, and for never making me feel as though he didn't have time to answer my questions (no matter how silly they were).

I'd like to give a special thank you to "Frau Dr." Alison Murray for her seemingly limitless patience in teaching me to work with mice, for reassuring me when I was apprehensive or when things weren't going well, and for helping me appreciate that they really can be endearing, timorous wee beasties.

To Professor Philippa Saunders, I would like to express my thanks for her invaluable advice and support, without which these experiments could not have taken place.

A great big thank you to Dr. Moira Nicol and the many members of the HODC lab, for teaching me laboratory techniques, enduring my forgetfulness and for generally making me feel so at home in the lab – even (and especially!) when experiments were not going exactly to plan. I have enjoyed working with them immensely.

I would like to thank my officemates and lab friends for their support and friendship over the course of my PhD. I will miss celebrating successes with them (and will even miss commiserating over the occasional failure). I always looked forward to coming into work – though never more than on our end-of-the-month "CRH social" days!

To Catherine Murray and Sharon McPherson, our clinical research nurses, I am profoundly thankful for their help in sourcing patient samples and information, as well as for cheerfully letting me talk their ears off in the process.

Thank you to Abby Dobyns for writing a fantastic ImageJ macro for assisting cell nucleus counting, saving me hours of anguish (as well as likely sparing the stereology microscopes a few choice swearwords).

I would like to also thank my parents, family, friends and Lucy. My parents I'd like to thank for believing in me and supporting me unconditionally – I have always tried to be as funny and as generous with my time as they are. My brothers I'd like to thank for always joking with me (or at least putting up with my dumb jokes!) and helping me to always see the humour in things. Being able to share my holidays with you all was always the highlight of the year for me. And Lucy I'd like to thank for putting up with my slightly nocturnal work habits and for enduring an admittedly cavalier attitude to the occasional looming deadline.

Finally and most especially, I would like to thank the countless patients who so graciously volunteered and donated in support of medical research – this work would not have been possible without them.

List of Abbreviations

ACTB	Beta-actin
ATP5B	Adenosine triphosphate synthase subunit beta, mitochondrial
B2M	Beta-2 microglobulin
BCA	Bicinchoninic acid
BCG	Bacillus Calmette-Guérin
BLAST	Basic local alignment search tool
BrdU	5-bromo-2'-deoxyuridine
BSA	Bovine serum albumin
cAMP	Cyclic adenosine monophosphate
CC3	Cleaved caspase-3
CCL2	C-C motif chemokine ligand 2
CD	Cluster of differentiation
cDNA	Complementary 2'-deoxyribonucleic acid
COCP	Combined oral contraceptive pill
cRNA	Complementary ribonucleic acid
CS-FCS	Carbon-stripped foetal calf serum
CTGF	Connective tissue growth factor
CTTN	Cortactin
C_q	Quantification cycle
CXCL1	C-X-C motif chemokine ligand 1
CXCL8	C-X-C motif chemokine ligand 8
DAB	3,3'-diaminobenzidine
DAPI	4',6-diamidino-2-phenylindole
DIABLO (SMAC)	direct IAP-binding protein, low pI (Second mitochondria-derived activator of caspases)
DMSO	Dimethyl sulphoxide
DNA	2'-deoxyribonucleic acid
E_2	17β-oestradiol
EDTA	Ethylenediaminetetraacetic acid
EHD3	EH-domain containing 3
ER	Oestrogen receptor

ERRFI1	ERBB receptor feedback inhibitor 1
FACS	Fluorescence-activated cell sorting
FDMC	Finnish DNA Microarray Centre
FIGO	Fédération Internationale de Gynécologie et d'Obstétrique
FKBP5	FK506 binding protein 5
FRET	Fluorescence resonance energy transfer
GAMP	Goat anti-mouse (peroxidase) secondary antibody
GAPDH	Glyceraldehyde 3-phosphate dehydrogenase antibody
GARabP	Goat anti-rabbit (peroxidase) secondary antibody
GARP	Goat anti-rat (peroxidase) secondary antibody
GC	Glucocorticoid
GLUL	Glutamate-ammonia ligase
GO	Gene ontology
GR	Glucocorticoid receptor
GUSB	Beta-glucuronidase
H&E	Haematoxylin and eosin
HAMP	Horse anti-mouse (peroxidase) secondary antibody
HARabP	Horse anti-rabbit (peroxidase) secondary antibody
HIER	Heat-induced epitope retrieval
HMB	Heavy menstrual bleeding
HRP	Horseradish peroxidase
HSP90AB1	Heat shock protein HSP 90-beta
HSPA5 (GRP78)	Heat shock 70 kDa protein 5 (Glucose-regulated protein, 78 kDa)
Ig	Immunoglobulin
IGFBP1	Insulin-like growth factor-binding protein 1
LNG-IUS	Levonorgestrel-releasing intrauterine system
LOX	Lysyl oxidase
LPS	Lipopolysaccharide
mAb	Monoclonal antibody
MDM	Monocyte-derived macrophage
MIQE	Minimum Information for publication of quantitative real-time PCR experiments
MMP	Matrix metalloproteinase
MPO	Myeloperoxidase

mRNA	Messenger ribonucleic acid
MT1	Metallothionein 1
NBF	Neutral-buffered formalin
NF-κB	Nuclear factor of kappa light polypeptide gene enhancer in B-cells
NFKBIA (IκBα)	Nuclear factor of kappa light polypeptide gene enhancer in B-cells inhibitor alpha
NHS	National Health Service
NICE	National Institute for Health and Care Excellence
NOS3 (ENOS)	Nitric oxide synthase type 3 (Endothelial nitric oxide synthase)
NSAID	Non-steroidal anti-inflammatory drugs
NSET	Non-surgical embryo transfer device
P_4	Progesterone (pregn-4-ene-3,20-dione)
pAb	Polyclonal antibody
PBMC	Peripheral blood mononuclear cell
PBS	Phosphate-buffered saline
PMN	Polymorphonuclear leucocyte
PR	Progesterone receptor
Q-VD-OPh	Quinolyl-valyl-O-methylaspartyl-[2,6-difluorophenoxy]-methyl ketone
RabASP	Rabbit anti-sheep (peroxidase) secondary antibody
RGS2	Regulator of G-protein signalling 2
RIPA	Radioimmunoprecipitation assay
RNA	Ribonucleic acid
RPMI	Roswell Park Memorial Institute medium
RT-qPCR	Reverse transcription quantitative polymerase chain reaction
SEB	Staphylococcal enterotoxin B
SEM	Standard error of the mean
SGK1	Serum-/glucocorticoid-regulated kinase 1
TBS-T	Tris-buffered saline with Tween 20/polysorbate 20
TBX2	T-box transcription factor 2
THRA	Thyroid hormone receptor alpha
Tris	Tris(hydroxymethyl)aminomethane
TUNEL	Terminal deoxynucleotidyl transferase (TdT)-mediated dUTP-biotin nick end labelling

Table of Contents

List of Figures

List of Tables

1. Literature Review

1.1 Hormonal Regulation of the Human Endometrium & the Menstrual Cycle

The menstrual cycle sees the human uterus exposed to an environment of cyclically-expressed ovarian sex steroids crucial to the regulation of growth and differentiation of its outermost layer, and in the absence of an implanting conceptus, shedding and subsequent tissue restoration. Chief amongst these sex steroids are 17β-oestradiol (E_2) and pregn-4-ene-3,20-dione (progesterone; P_4), whose concentrations fluctuate in a well-characterised manner through the menstrual cycle (**Figure 1**).

The endometrium is the outermost layer of the uterus, consisting of a multicellular stroma overlain by a simple columnar epithelium. In comparison to other mucous membranes, the thickness and cellular constituents of the endometrium vary considerably in response to the sex steroid environment. The endometrial stroma, largely connective tissue composed of fibroblast-like endometrial stromal cells, contains a number of tubular glands contiguous with the luminal surface, spiral arteries, and is host to various fluctuating populations of recruited leucocytes.

The principal function of the non-pregnant endometrium is to maintain uterine patency, whereas that of the pregnant endometrium is to become the decidua, contributing to the formation of the placenta and support of the developing foetus.

1.1.1 Proliferative Phase

The endometrial endocrine environment is first dominated by oestradiol in the early, 'proliferative' phase of the menstrual cycle, wherein vascular and endometrial tissues proliferate extensively to prepare the uterus to support a pregnancy. This proliferative phase of the endometrial cycle has its counterpart in the ovarian 'follicular' phase, and

culminates in the release of a secondary oocyte (ovulation) and the formation of a *corpus luteum* from the ovarian follicle remnants (Corner and Allen, 1929).

1.1.2 Secretory Phase & Decidualisation

Following ovulation, during the 'secretory' phase of the endometrial cycle (whose ovarian counterpart is the 'luteal' phase), the *corpus luteum* effects a substantial increase in progesterone, required for establishing and maintaining pregnancy in the oestradiol-primed endometrium (Corner and Allen, 1929; Csapo and Pulkkinen, 1978).

Under the action of progesterone, the endometrium undergoes differentiation ('decidualisation'), wherein epithelial glands develop and become functional (Noyes *et al*., 1950; Csapo and Pulkkinen, 1978). Endometrial stromal cells are acted upon directly by progesterone to induce their decidualisation, transforming them from an elongated to a spherical morphology and inducing their expression of prolactin, glycogen and insulin-like growth factor-binding protein 1 (IGFBP1; Brosens *et al*., 1999; Dunn *et al*., 2003).

The endometrial decidualisation response is initiated intracellularly by the production of cyclic adenosine monophosphate (cAMP; Brosens *et al*., 1999), occurring first in perivascular stromal cells before emanating outward through the endometrial stroma. Failure to successfully decidualise is thought to be an important contributor in some menstrual disorders and causes of infertility (*ibid.*).

In humans, decidualisation occurs independently of embryonic/endometrial contact ('implantation'), and is therefore said to occur 'spontaneously'. Humans moreover display the most extensive decidualisation response of any menstruating species studied (Ramsey *et al*., 1976), likely in order to mitigate the considerable trophoblast invasion seen at implantation (Finn, 1996).

During implantation, extravillous trophoblast (EVT) cells, derived from embryonic trophectoderm, invade the maternal decidual tissue ('decidua') and mediate early placentation (Aplin, 1991; Burrows *et al*., 1993). This involves, primarily, the remodelling of maternal spiral arterioles ('haemochorial placentation'; thereby ensuring the foetus has adequate blood flow; Pijnenborg *et al*., 1983) and of the extracellular matrix (regulating trophoblast invasion; (Burrows *et al*., 1993; Damsky *et al*., 1994). Decidual regulation of the extent of trophoblast invasion is crucial: if trophoblast invasion is too vigorous, complications such as *placenta accreta*, *increta* or *percreta* (attachment of the placenta to, into or through the myometrium, respectively) may arise; conversely, insufficient invasion may give rise to a number of different complications, including pre-eclampsia, foetal growth restriction and recurrent miscarriage (Ball *et al*., 2006; Pijnenborg *et al*., 1991).

Oestradiol and its actions are also decreased during the late secretory phase in part by the actions of progesterone. Progesterone promotes the conversion of oestradiol to its less biologically-active form (oestrone; E_1) via the induction of the steroid-metabolising 17β-hydroxysteroid dehydrogenase enzymes (Tseng and Gurpide, 1974, 1975a; Polow *et al*., 1975; Isomaa *et al*., 1993), regulating the availability of oestrogen ligands. Progesterone also reportedly reduces expression of the oestrogen receptor (ER; Tseng and Gurpide, 1975b), thereby furthering inhibiting the actions of oestradiol.

Concentrations of ER decline in the endometrium through the secretory phase of the menstrual cycle, while progesterone receptor (PR) concentrations are maintained in the endometrial stroma, but decrease in the glandular epithelium (Lessey *et al*., 1988).

1.1.3 Progesterone Withdrawal & Menstruation

The absence of an implanting conceptus leads to the regression of the corpus luteum (forming a *corpus albicans*) and a sharp decline in progesterone and oestradiol concentrations consequent thereupon (Csapo and Resch, 1979). Sex steroid withdrawal triggers the onset of menstruation (**Figure 1**), in which the upper, functional layer of the endometrium ('zona functionalis') is broken down, shed and subsequently restored. Withdrawal of progesterone in particular, unable to act either directly via its cognate receptor (progesterone receptor; PR) or indirectly via intermediate factors, effects a number of histological changes in the endometrium, including tissue oedema and the recruitment of myriad circulating leucocytes (Finn, 1986), breakdown of the basal lamina supporting endothelial cells (Roberts *et al*., 1992), and augmented blood vessel permeability and fragility (Noyes *et al.*, 1950; Garry *et al*., 2010). Important molecular events accompany these histological changes, such as the focal activation of matrix metalloproteinases (MMPs) in regions of menstrual lysis (Marbaix *et al*., 1996; Vassilev *et al*., 2005; Gaide Chevronnay *et al*., 2009) and the increased expression of cyclooxygenase-2 (COX-2; (Jones *et al*., 1997a; Critchley *et al*., 1999) and consequent increase in prostaglandins (Sugino *et al*., 2004).

It was on the basis of these observations that menstruation was first hypothesised an inflammatory event by Finn (1986), sharing, as the menstrual endometrium did, so many of the classical features of inflammation.

Local hypoxia is also thought to be an important contributor to menstruation and to post-menstrual repair in the endometrium, acting as a potent angiogenic stimulus. *In vitro* experiments have demonstrated that the production of the angiogenic vascular

endothelial growth factor (VEGF) is increased 10-fold in decidualised endometrial stromal cells under hypoxic (2% pO_2) conditions (Popovici *et al*., 1999).

Endometrial expression of a key transcription factor sub-unit in the regulation of hypoxic response, hypoxia inducible factor-1α (HIF-1α), occurs exclusively in the secretory and menstrual phases, and maximally during progesterone withdrawal in the late secretory and menstrual phases (Critchley *et al*., 2006).

Menstruation only occurs in species whose endometria spontaneously decidualise prior to implantation, whereas in species whose endometria do not decidualise until embryonic/endometrial contact is established (Finn, 1998), the withdrawal of progesterone does not effect endometrial breakdown or bleeding. Menstruating species appear limited to old world primates (including humans), elephant shrews (*Elephantulus myuras jamesoni*; van der Horst and Gillman, 1941) and some species of fruit bat (e.g. *Glossophaga soricina*; Hamlett, 1934).

1.1.4 Perimenstrual Window

Following menstruation, endometrial inflammation must be resolved alongside cellular proliferation and angiogenesis in order to regenerate the functional endometrium from its underlying basal layer ('zona basalis'; Noyes *et al*., 1950; Garry *et al*., 2010).

The span of events from the regression of the corpus luteum in the late secretory phase through menstruation and culminating in the post-menstrual repair of the endometrium in the proliferative phase is termed herein the 'perimenstrual' window (i.e. endocrine 'luteo-follicular' transition), and is depicted in **Figure 2**.

Figure 1. Cyclical changes in ovarian sex steroid concentrations through the menstrual cycle effect changes in endometrial morphology, culminating in menstruation in the absence of successful implantation. The human endometrium undergoes extensive proliferation under the oestradiol-dominant proliferative phase and differentiation under the progesterone-dominant secretory phase. Withdrawal of progesterone in the absence of implantation triggers menstruation. *E_2 = oestradiol (green), P_4 = progesterone (blue).*

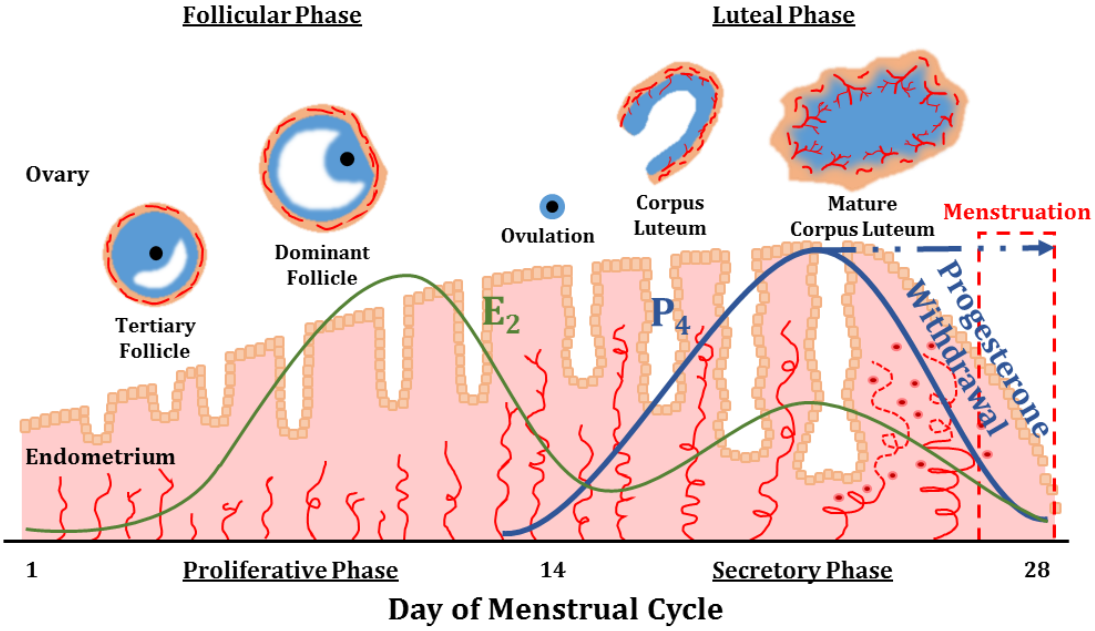

Figure 2. The 'perimenstrual' window comprises the transition from late secretory phase (ovarian luteal) to early proliferative phase (ovarian follicular), wherein the endometrium is shed and subsequently restored. Regression of the corpus luteum and the consequent decline in progesterone concentration effects breakdown of the basal lamina, increased blood vessel permeability and fragility and menstrual shedding; the 'perimenstrual' window in the endometrium is equivalent to the luteo-follicular transition in the ovary.
E_2 = oestradiol (green), P_4 = progesterone (blue).

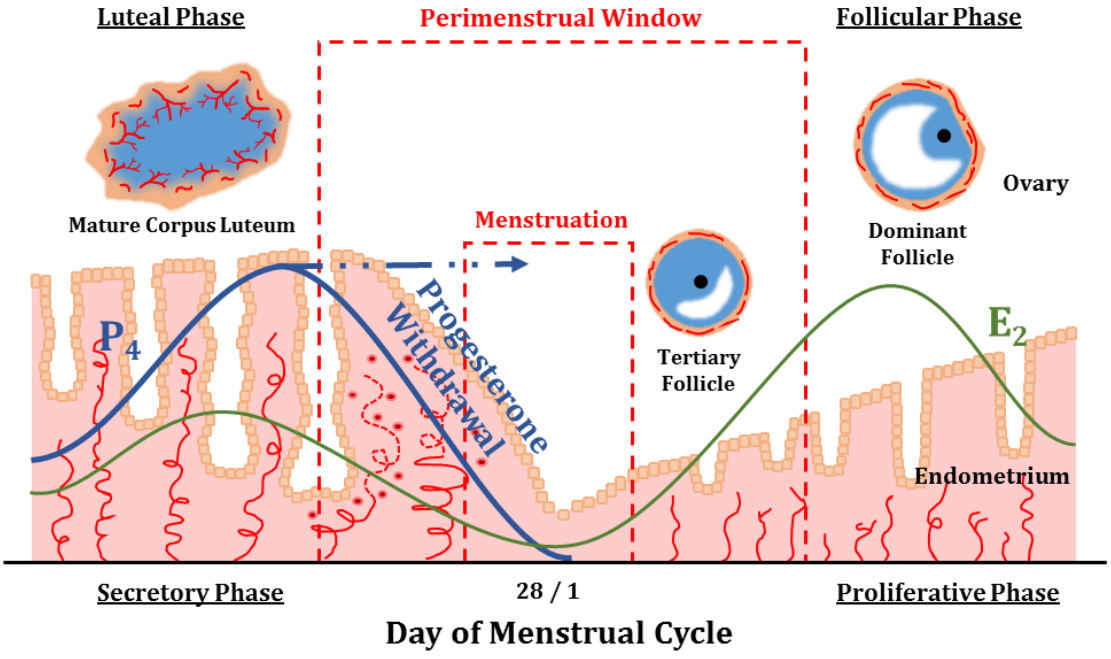

1.2 Inflammation

Inflammation is a generic response mounted by the immune system to noxious stimuli in order to eliminate infection, regenerate injured tissue and restore physiological function.

Very generally, inflammation is classified into 'acute' and 'chronic' responses, with the former characterised by a short-lived, intial response to injurious stimuli and the latter by a prolonged response lasting for many months or years, involving the persistence of certain immune cells at the site of inflammation alongside host-mediated tissue destruction and/or fibrosis, ultimately risking loss of function (see review by Buckley *et al*., 2014). It is critical therefore that inflammation be efficiently resolved upon successful elimination of the noxious stimulus, in order to limit damage and restore tissue integrity.

1.2.1 Acute Inflammation

Acute inflammation is characterised by four cardinal features, first defined by the Roman encyclopaedist Aulus Celsus in the early 1st century, AD: *calor* (heat), *rubor* (redness), *tumor* (swelling) and *dolor* (pain). Heat and redness can be principally attributed to the increased blood flow (hyperaemia) at the site of inflammation; swelling to increased fluid accumulation (oedema); and pain to the stimulation of nerve endings by released inflammatory mediators, such as bradykinin and histamine (Maling *et al*., 1974; Johnston *et al*., 1976).

At a cellular level, acute inflammation unfolds through the rapid recruitment of neutrophil granulocytes, followed shortly thereafter by inflammatory monocytes which

differentiate into macrophages, proliferate *in situ* and orchestrate the continuing inflammatory response and its resolution (see review by Gilroy and De Maeyer, 2015).

Molecular mediators of acute inflammation produced locally and by recruited leucocytes include prostanoids (prostaglandins and prostacyclins), lipid mediators, complement, cytokines and chemokines, all acting individually and in concert to shape the inflammatory response by inducing vasodilation, modifying cell adhesion molecule expression and ultimately recruiting leucocytes (see review by Serhan *et al*., 2007).

1.2.2 Resolution of Inflammation

Resolution of inflammation, not merely the passive cessation of a continued inflammatory response, is an active process no less tightly coordinated than the initiation of the inflammatory response itself.

Pro-inflammatory mediator synthesis must be abrogated and existing inflammatory mediators must be degraded in order to curtail further leucocyte recruitment, restore vascular integrity and tissue oedema. Prostanoids are catabolised via a series of oxidation and reduction reactions (Anggård, 1966; Ensor and Tai, 1995), whereas clearance of chemokines can occur through chemokine receptor-dependent scavenging by apoptotic leucocytes (Ariel *et al*., 2006).

As the acute inflammatory response matures, the recruitment of monocytes is favoured over that of neutrophils, a switch suggested to be mediated in part by the neutrophil-expressed soluble interleukin-6 (IL-6) receptor (sIL-6R). Once complexed with IL-6, sIL-6R is thought to inhibit IL-1- and TNFα-induced CXC chemokine synthesis (such as the neutrophil chemokine CXCL8) and to potentiate CC chemokine expression (such as the monocyte chemokine CCL2; Hurst *et al*., 2001; McLoughlin *et al*., 2003).

To resolve inflammation, recruited inflammatory leucocytes remaining in the tissue must either re-enter circulation, undergo cell death locally and be engulfed by phagocytic cells, or drain from the tissue via the lymphatics. An increase in monocytes and the macrophages into which they differentiate is thought to increase the capacity for neutrophils and debris to be eliminated and engulfed (see reviews by Buckley *et al*., 2013; Gilroy and De Maeyer, 2015).

Phagocytosis of apoptotic neutrophils is currently understood to play an important, two-fold contribution to the resolution of inflammation: first, the deactivation of neutrophils protects the tissue from any further release of neutrophil-derived inflammatory mediators; second, the recognition of apoptotic cells by macrophages during phagocytosis modulates macrophage phenotype and promotes the release of anti-inflammatory and pro-resolution cytokines, such as IL-10 and TGF-β (Huynh *et al*., 2002), and lipid mediators, such as lipoxins and resolvins (see review by Buckley *et al*., 2014).

1.2.3 Menstruation as Inflammation

The demise of the corpus luteum and the consequent decline in endometrial progesterone concentrations effect a host of histological changes in the menstrual endometrium, analogous to those seen in classical inflammation: tissue oedema (Finn, 1986), increased endometrial blood flow and vessel permeability (Noyes *et al*., 1950; Finn, 1986; Garry *et al*., 2010) and the recruitment of large numbers of leucocytes (Finn, 1986; King *et al*., 1996; Hiby *et al*., 1997; Moffett-King, 2002; Evans and Salamonsen, 2012).

These histological changes led Finn (1986) to propose menstruation an inflammatory phenomenon, a hypothesis further supported by subsequent discoveries of important

molecular changes occuring alongside these: focal activation of matrix metalloproteinases (MMPs; Marbaix *et al*., 1996; Vassilev *et al*., 2005; Gaide Chevronnay *et al*., 2009), increased cyclooxygenase-2 (COX-2) expression (Jones et al., 1997a; Critchley et al., 1999) and prostaglandin concentrations in consequence (Sugino *et al*., 2004).

The precise timing of the onset of menstrual inflammation is not completely understood, though the earliest stages are likely to involve the release of inhibition of the transcription factor NF-κB: progesterone withdrawal allows the dissociation of its inhibitory sub-unit IκB, freeing NF-κB to facilitate the transcription of COX-2 and various inflammatory cytokines and chemokines (see review by Evans and Salamonsen, 2012).

Artificially-decidualised human endometrial stromal cells have been shown to produce a wide variety of inflammatory mediators *in vitro* upon withdrawal of oestradiol and progesterone, including the chemokines CCL2, 5 and 11, and CXCL8 and 10, and the cytokines IL-1RA, -6, -12 and -15 and GM-CSF (Evans and Salamonsen, 2014). This response was found orchestrated by the transcription factor NF-κB, also responsible for the endometrial transcription of the adhesion molecules ICAM and VCAM (Kayisli *et al*., 2004).

Although critical for the destruction of the endometrial tissue, many of these inflammatory features are also critical to its subsequent successful repair.

Leucocytes recruited at menstruation are integral in the process of endometrial repair, as demonstrated by the depletion of neutrophil granulocytes – impeding and retarding endometrial repair in a mouse model of menses (Kaitu'u-Lino *et al*., 2006) – and

inferred from the depletion of macrophages – hampering wound healing in a mouse model of myocardial injury (van Amerongen *et al.*, 2007).

Chemokines maximally produced at menses also appear to perform a range of functions, both recruiting leucocytes and facilitating angiogenesis. A prime example of this can be found in CXCL8 (IL-8): in addition to its well-documented chemotactic properties with respect to neutrophils, CXCL8 is reportedly active in angiogenesis (Koch *et al.*, 1992) and the induction of chemotaxis and proliferation in vascular smooth muscle cells (Yue *et al.*, 1994).

1.3 Endometrial Leucocytes

Populations of endometrial leucocytes fluctuate in number along with the menstrual cycle, constituting between 8.2% (Bulmer *et al*., 1991) and 10 – 15% (Kamat and Isaacson, 1987) of the endometrial stromal compartment during the proliferative phase when their numbers are lowest, and up to 20 – 25% (Kamat and Isaacson, 1987) to 40 – 45% immediately prior to menstruation (Bonatz *et al*., 1992; Salamonsen and Woolley, 1999) at their most abundant.

Leucocytes have been suggested to play an important role not only in the breakdown of endometrial tissue, but in its concurrent repair (Salamonsen and Lathbury, 2000).

1.3.1 Neutrophil Granulocytes

Neutrophils are the most abundant leucocyte of the human immune system, exhibiting limited phagocytic activity and containing a variety of pre-formed microbicidal molecules, latent matrix metalloproteinases (pro-MMPs) and cytotoxic and inflammatory mediators packaged in cytoplasmic granules.

During acute inflammation, neutrophils are rapidly recruited in response to a range of chemotactic factors including CXCL8, whereupon they phagoyctose any bacteria they encounter or release the contents of their granules ('degranulate') in the event that they do not encounter pathogens (Nathan, 1987). Contained in peroxidase-positive primary granules (also called 'azurophilic' granules) are α-defensins, myeloperoxidase (MPO) and neutrophil elastase enzymes, released in response to activating stimuli such as CXCL8 and TNF-α (Nathan, 1987; Nathan *et al*., 1989).

The haeme-group-containing MPO is capable of converting hydrogen peroxide into various potent derivatives, including hypobromous, hypoiodous and hypochlorous

acids (HOBr, HOI and HOCl respectively), the last of which further reacts with amines to produce longer-lived, anti-bacterial chloramines (Harrison and Schultz, 1976).

Neutrophil elastase is a serine protease which in addition to its antimicrobial and proteolytic activities, plays a role in NETosis, a phenomenon whereby neutrophils extrude their nuclear DNA in neutrophil extracellular traps (NETs) to ensnare and destroy bacterial pathogens (Brinkmann *et al*., 2004). Elastase exhibits an unusual affinity for DNA, and upon neutrophil activation, translocates to the nucleus to degrade histone proteins (Papayannopoulos *et al*., 2010) and initiate the extrusion of nuclear DNA and NET formation. DNA released via NETosis is subsequently coated with elastase proteins (Urban *et al*., 2009).

Neutrophil granulocytes are recruited to the endometrium in substantial numbers immediately prior to menstruation (Poropatich *et al*., 1987), coincident with declining progesterone concentrations, whereupon they are estimated to comprise between 6 – 15% of the total endometrial cell numbers (Salamonsen and Woolley, 1999). In addition to containing high levels of MMPs, endometrial neutrophils are suggested to activate MMPs *in situ* (Gaide Chevronnay *et al*., 2012), thereby furthering endometrial breakdown at menstruation.

1.3.2 Macrophages

Macrophages, prolific mononuclear phagocytes of the immune system, are present throughout the menstrual cycle, though do show a modest increase in number at the advent of menstruation (Salamonsen and Woolley, 1999; Thiruchelvam *et al*., 2012). Phagocytic clearance of apoptotic cells by macrophages appears critical to the successful, spontaneous resolution of inflammation in other tissues (Savill *et al*.,

1989a), and is thus likely important to resolution of menstrual inflammation in the endometrium as well.

Macrophages are suggested to fulfil a diverse set of functions in the endometrium, in keeping with their tremendous versatility and plasticity elsewhere. In preparing the endometrium for its role as the primary interface with a potential implanting conceptus, macrophages are thought to be important (Lea and Clark, 1991; Kats *et al*., 2005), constituting as much as 27 – 32% of the maternal decidua in early pregnancy (Lessin *et al*., 1988); in the absence of the above, however, macrophages are thought to be involved in initiating menstruation (Critchley *et al*., 2002; Thiruchelvam *et al*., 2012). Post-menses, macrophages phagocytose cellular debris (Garry *et al*., 2010) and contribute to the remodelling of the endometrium as the tissue is restored (Maybin *et al*., 2012).

1.3.3 Uterine Natural Killer (uNK) Cells

NK cells of the endometrium and decidua have a distinct phenotype from their peripheral blood NK cell counterparts, and are therefore referred to as uterine NK (uNK) cells. uNK cells are the predominant lymphocytes of the decidua, wherein they comprise some 70% of the leucocyte population (Spornitz, 1992), though they are also present in fluctuating numbers through the menstrual cycle in the non-pregnant endometrium.

Fewest in number during the proliferative phase, uNK cells are small and lack visible granules; during the secretory phase, uNK cells proliferate and differentiate in response to stromal-cell-derived IL-15 and prolactin, becoming larger and granulated (Spornitz,

1992; Verma *et al*., 2000; Wilkens *et al*., 2013). Progesterone, required for stromal cell decidualisation and IL-15 and prolactin production (Dunn *et al*., 2002; Gubbay *et al*., 2002), is therefore critical to the survival and differentiation of uNK cells – uNK cells are moreover only found in the endometria of ovariectomised women subsequent to oestrogen and progesterone treatment (King *et al.*, 1996).

The primary physiological role of uNK cells in the decidua is thought to be in facilitating the proper remodelling of spiral arterioles by the trophoblast during implantation and placentation (see reviews by Moffett and Loke, 2006; Moffett and Colucci, 2014), though their role in the non-pregnant endometrium is not as clear. It is known, however, that during the secretory phase, uNK cells produce a number of angiogenic cytokines, such as VEGF and angiopoietin 2 (ANG2; Li *et al*., 2001) – it is on this basis surmised that uNK cells may also participate in post-menstrual repair.

1.4 Apoptosis

Apoptosis is a form of programmed cell death in which cells are induced to condense and fragment their nuclear material ('pyknosis' and 'karyorrhexis', respectively), condense their cytoplasmic material, and then release their contents in membrane-bound apoptotic bodies ('blebbing'). The process was first described by Kerr *et al*. (1972), who noted that the majority of resultant apoptotic bodies were observed in the cytoplasm of intact, neighbouring cells, having likely been rapidly phagocytosed and cleared from tissues. These bodies, once engulfed, were seen to undergo phagosomal degradation (Wyllie *et al*., 1972) in a process not dissimilar to autolysis (Trump *et al*., 1965).

1.4.1 Cysteine-Aspartic Acid Proteases (Caspases)

Cells are induced to undergo apoptosis through either extrinsic or intrinsic pathways, both of which converge on the cleavage of inactive pro-caspase-3 to active, cleaved caspase-3 (**Figure 3**), an 'executioner' cysteine-aspartic acid protease (caspase) whose activation irreversibly initiates the cascade of apoptotic events (Slee *et al*., 2001). Extrinsic induction of apoptosis occurs in response to secreted factors such as TNF-α, TRAIL and Fas (CD95L) ligands which activate so-called death receptors (Ward *et al*., 1999; Witko-Sarsat *et al*., 2011), while intrinsically-mediated apoptosis takes place in response to the release of mitochondrially-derived factors such as cytochrome c and SMAC (Second mitochondria-derived activator of caspases; Witko-Sarsat *et al*., 2011). Extrinsic apoptotic pathways lead to pro-caspase-3 cleavage by the 'initiator' caspase-8 (Li *et al*., 1998), while intrinsic apoptotic pathways lead to pro-caspase-3 cleavage by the initiator caspase-9 (Li *et al*., 1997).

Figure 3. Intrinsic and extrinsic apoptotic pathways converging on caspase-3 cleavage. Diagrammatic representation of intrinsic and extrinsic apoptosis pathways, showing cleaved-caspase-9-mediated caspase-3 cleavage (intrinsic, red) and cleaved-caspase-8-mediated caspase-3 cleavage (extrinsic, blue). NB: simplified diagram omits many participants in the apoptosis pathway (see review by Danial and Korsmeyer, 2004).

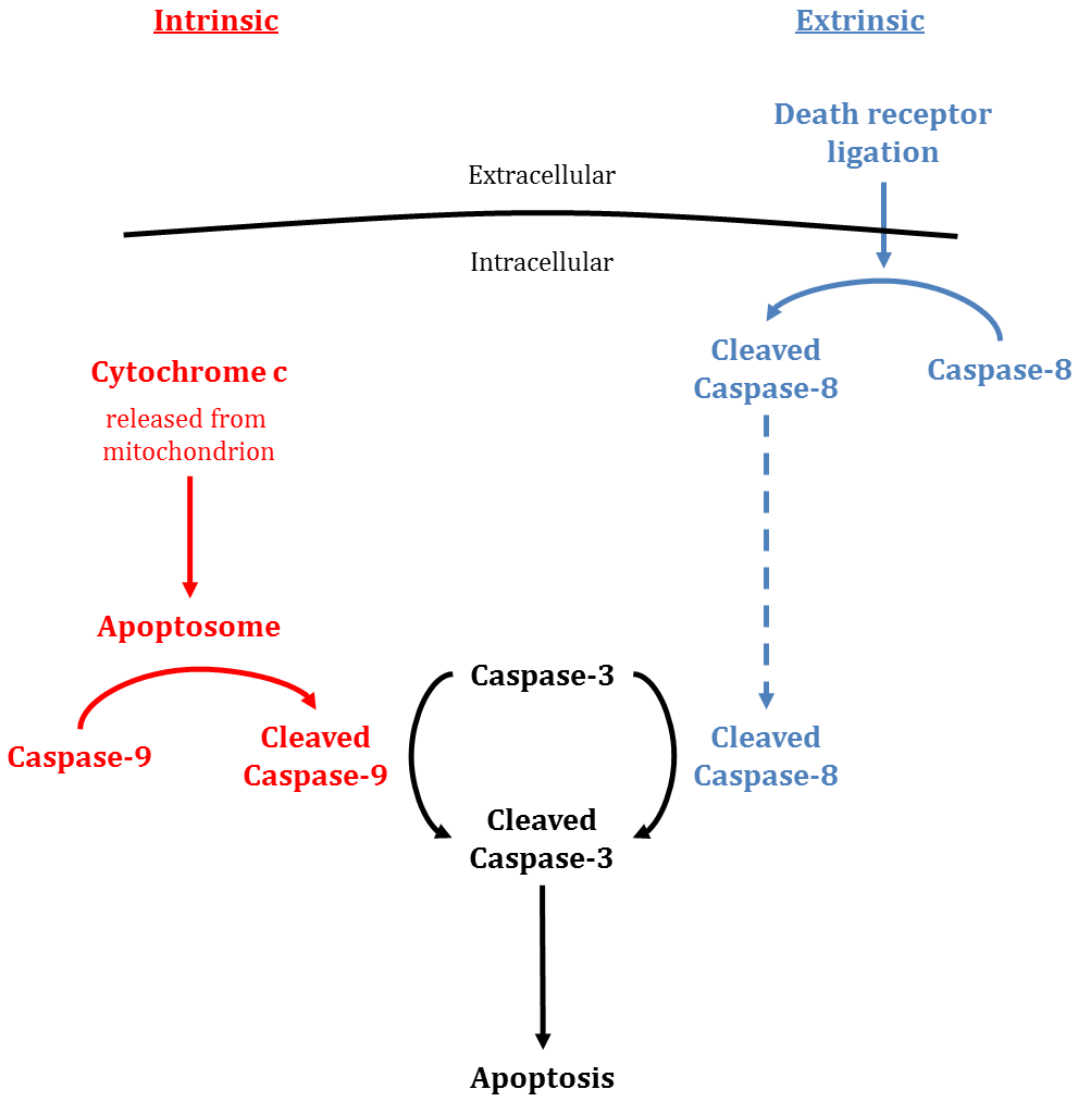

1.4.2 Phagocytic Clearance

The clearance of apoptotic cells by resident phagocytes (typically macrophages and dendritic cells) represents a critical juncture in the transition from inflammation to its resolution, acting to both deplete inflammatory cells from the site and to skew phagocytes to an anti-inflammatory phenotype.

Apoptotic cells express a range of so-called 'eat me' signals, for example the externalisation of ordinarily inner-membrane-restricted phosphatidylserine (Fadok *et al*., 1998; Henson *et al*., 2001); their recognition via the phagocyte-expressed G-protein-coupled receptor, brain-specific angiogenesis inhibitor 1 (BAI1; Park *et al*., 2007), allows phagocytes to engulf and degrade these apoptotic bodies (Fadok *et al*., 2001).

In most acute inflammatory contexts, short-lived neutrophils represent the major infiltrating leucocyte constituent, and are therefore among the more abundant apoptotic cells to be encountered by professional phagocytes in the resolving inflammatory environment. Apoptotic neutrophils have vastly diminished sensitivity to otherwise potent external stimuli (Dransfield *et al*., 1995), retaining their cytotoxic contents within their plasma membranes, sequestered from the external environment. Macrophages recognise and phagocytose apoptotic cells (Savill et al., 1989a), instigating a series of intracellular events inhibitory to pro-inflammatory cytokine production (Fadok *et al*., 1998; Stern *et al*., 1996) and stimulatory to anti-inflammatory cytokine production (Savill *et al*., 2002).

Macrophage phagocytic capacity is enhanced by a variety of factors: cytokines (Ren *et al*., 1995), prostaglandins (Rossi *et al*., 1998) and glucocorticoids (Liu *et al*., 1999) notable amongst them.

1.5 Heavy Menstrual Bleeding (HMB)

Heavy menstrual bleeding (HMB) is a disorder of menstruation which represents a significant obstacle to quality of life in otherwise healthy women (NICE Clinical Guideline 44 on HMB, 2007). Medical treatment options are available, but their costs are significant. Treatment failure will impel a significant proportion of women to proceed to surgical management of the complaint. Hysterectomy, for which HMB is the commonest indication, carries risk of serious complications and necessarily spells the end of a patient's fertility.

A better understanding of the pathophysiology of HMB is therefore of great importance to improve medical treatment options and to limit the necessity for surgical intervention.

1.5.1 Subjective and Objective Clinical Definitions of HMB

'Heavy menstrual bleeding' is the term currently accepted and recommended by the Fédération Internationale de Gynécologie et d'Obstétrique (FIGO), supplanting the previously-used and ambiguously-defined terms of 'menorrhagia', 'metrorrhagia' and 'dysfunctional uterine bleeding' (Fraser *et al*., 2011; Munro *et al*., 2012).

The subjective definition for HMB has been established by the National Institute for Health and Care Excellence (NICE) in the UK as 'excessive menstrual blood loss that interferes with a woman's physical, social, emotional and/or material quality of life' (NICE Clinical Guideline 44 on HMB, 2007), recognising the importance of the patient's own perception of her menstrual bleeding and its impact in the determination treatment options.

Some of the earliest studies into menstrual blood loss (MBL) in women's menstrual cycles, conducted 50 years ago in Sweden, found a mean MBL volume of 40 mL and noted that volumes of greater than 63 mL were associated with iron deficiency anaemia (Hallberg and Nilsson, 1964; Hallberg *et al*., 1966a, 1966b). Based on the 95th percentile MBL volume calculated from these early studies (76 mL), a more objective definition for HMB of ≥80 mL per cycle was established by NICE (Clinical Guideline 44 on HMB, 2007).

Objective measurements of MBL volumes are typically extrapolated from menstrual haemoglobin content, estimating only the volume of blood lost (Warner *et al*., 2004); though in practice menstrual fluid is further comprised by extravascular fluid, transudate and shed endometrium.

Of some concern in comparing the subjective and objective definitions for HMB, less than 50% of women referred to gynaecological services for the complaint of HMB were found to have an MBL of greater than 80 mL upon objective measurement (Fraser *et al*., 1984; Bonnar and Sheppard, 1996; Gannon *et al*., 1996; Irvine *et al*., 1998). More recent studies have moreover found the 80-mL threshold criterion not predictive of iron deficiency, adverse menstrual outcome or disease (Warner *et al*., 2004).

1.5.2 Significance of HMB

In the UK and elsewhere, HMB is a very common condition with a not insignificant impact on health-related quality of life (Shapley *et al*., 2002; Shankar *et al*., 2008). Estimates of its incidence in the population range from 9 – 14% of pre-menopausal women (Fraser *et al*., 2009) to 25% in the UK (Shapley *et al*., 2004), depending on whether objective or subjective criteria were used to establish HMB; subjectively-

defined HMB in some developing countries is estimated at 25 – 35% (Harlow and Campbell, 2004; Santos *et al*., 2011). In the UK, the incidence of self-reported HMB increases from one in three to one in two as menopause becomes imminent (Prentice, 1999), consistent with what is observed in developing countries (Khatri and Gupta, 1978).

More than 800,000 British women seek help for HMB each year (NICE Clinical Guideline 44 on HMB, 2007). In a national audit to assess patient outcomes of women with HMB in England and Wales, 75% of women reported having had their symptoms for over a year, and over half reported 'severe' or 'very severe' pain alongside their symptoms (RCOG National Heavy Menstrual Bleeding Audit, 2012). In the hypothetical event that their symptoms were to persist for a further 5 years, over 80% of the patients asked said that they would feel 'unhappy' or 'terrible' (RCOG National Heavy Menstrual Bleeding Audit, 2012).

NICE estimate that 3.5 million work days are lost each year in the UK as a result of HMB and its treatment (NICE Clinical Guideline 44 on HMB, 2007) – this figure is likely to increase with employment rates, which reached 66% for women aged 16 – 64 in 2013 (Office for National Statistics UK, 2013). In the United States, a study by Frick *et al*. (2009) calculated a financial burden for HMB of greater than $2000 per patient each year, due to the combined costs of home management and work absences.

Referrals concerning women with HMB constitute some 20% of the 1.2 million referrals to specialist gynaecologist services each year in England and Wales (NICE Draft Scope for Hysterectomy Consultation, 2004), making it the fourth commonest indication for gynaecological services referrals (RCOG National Heavy Menstrual Bleeding Audit, 2012): some 30,000 English and Welsh women elect to undergo surgical treatment each year.

Half of the 47,000 hysterectomies carried out in the NHS in England in 2000 and 2001 were for the complaint of HMB – half of the women undergoing HMB-related hysterectomies are thought to have had 'normal' uteri (i.e. with no recognised pathology; NICE Draft Scope for Hysterectomy Consultation, 2004).

Amongst women attending outpatient gynaecology clinics with HMB symptoms, just under half had fibroids, endometriosis and/or uterine polyps – over half, therefore, had no structural origin for their symptoms (RCOG National Heavy Menstrual Bleeding Audit, 2012).

1.5.3 Structural and Non-Structural Classification of HMB

HMB aetiology is divided into nine structural and non-structural categories in the 'PALM-COEIN' classification system outlined by FIGO (Munro *et al*., 2011a, 2011b). In the PALM-COEIN acronym, 'PALM' represents the visually-objective, structural criteria: polyp (P), adenomyosis (A), leiomyoma (L; uterine fibroids) and malignancy/hyperplasia (M); 'COEIN' represents non-structural abnormalities: coagulopathy (C), ovulatory dysfunction (O), endometrial (E), iatrogenic (I) and not otherwise classified (N). Fibroids are present in between 10 – 40% of women with HMB, but approximately 50% of women with HMB have no recognised pathology (Duckitt and Collins, 2008; RCOG National Heavy Menstrual Bleeding Audit, 2012).

In the absence of recognised pathologies outlined in the PALM-COEIN classification system, HMB is suggested to have its origin in disturbed local inflammatory events and in the disruption of vascular factors leading to increased and/or prolonged bleeding (Critchley and Maybin, 2011).

1.5.4 Pathophysiology of HMB

Menstruation, consequent upon the withdrawal of progesterone from the endometrium, involves the expression of a diverse range of inflammatory mediators. These inflammatory molecules, produced by and acting on endometrial and recruited immune cells, influence a variety of functions: chemotaxis, tissue destruction, wound healing, apoptosis and haemostasis, to name only a few. The importance of the tightly-regulated expression of such inflammatory mediators in the endometrium therefore cannot be overstated.

Inflammatory molecules and enzymes of considerable importance with respect to menstruation and its successful resolution are: (1) the prostaglandin- (PG-) synthesising enzyme cyclooxygenase-2 (COX-2), upregulated at menses (Critchley *et al*., 1999; Hapangama *et al*., 2002); (2) the vasodilatory molecule prostaglandin E_2 (PGE_2), synthesised from the COX-2-catalysed prostaglandin H_2 (PGH_2) by PGE synthase; (3) the vasoconstrictive molecule prostaglandin $F_{2\alpha}$ ($PGF_{2\alpha}$), synthesised from PGH_2 by PGF synthase; (4) chemokines, including CXCL8 (IL-8) and CCL2 (MCP-1), acting principally on neutrophil granulocytes and monocytes respectively to recruit them from circulation (Jones et al., 1997a; Milne et al., 1999); and (5) the extracellular-matrix-degrading enzymes, matrix metalloproteinases (MMPs), upregulated and activated at menses (Marbaix *et al*., 1996; Salamonsen and Woolley, 1999; Salamonsen *et al*., 2000; Galant *et al*., 2004; Gaide Chevronnay *et al*., 2009).

Vascular tone in the human endometrium is heavily dependent on the regulated expression of the vasoactive prostaglandins, PGE_2 and $PGF_{2\alpha}$, the most abundant two prostaglandins found in the endometrium (Smith *et al*., 1981a; Lumsden *et al*., 1983; **Figure 4**). PGE_2 and $PGF_{2\alpha}$ exert their actions through the binding of EP and FP

receptors respectively, both of which are expressed in endometrial perivascular cells (Milne *et al*., 2001; Milne and Jabbour, 2003). Genes downstream of EP and FP receptor activation regulate tissue remodelling and vascular function and, as well as leucocyte recruitment/trafficking; FP receptor signalling in particular is important in the regulation of basic fibroblast growth factor (bFGF; Keightley *et al*., 2010), CXCL8 (Sales *et al*., 2009) and vascular endothelial growth factor (VEGF; Sales *et al*., 2005).

Figure 4. Prostaglandin biosynthesis pathway. Prostaglandins E_2 and $F_{2\alpha}$ are synthesised from a prostaglandin H_2 precursor, its own production catalysed by cyclooxygenase (COX) enzymes from arachidonic acid. PGE_2 (orange) is an important endometrial vasodilator, whereas $PGF_{2\alpha}$ (blue) regulates endometrial vasoconstriction; the ratio of $PGF_{2\alpha}$:PGE_2 is decreased in the endometrium of women with objectively-verified HMB (Smith *et al*., 1981a). *PTGDS = prostaglandin D_2 synthase, PTGES = prostaglandin E_2 synthase, PTGFS = prostaglandin $F_{2\alpha}$ synthase, PTGIS = prostaglandin I_2 synthase (prostacyclin synthase).*

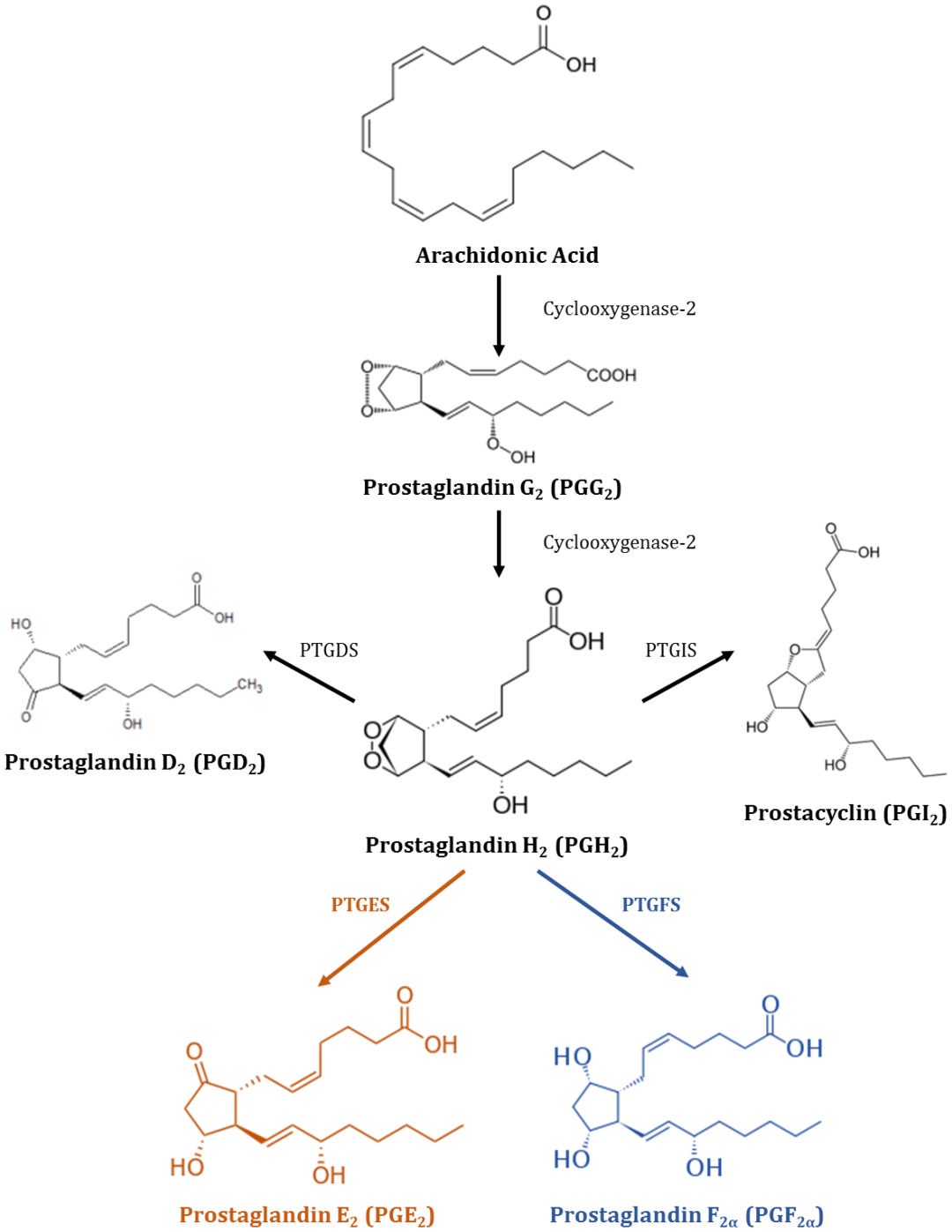

PGE_2 appears more highly synthesised in the endometrium of women with HMB than is $PGF_{2\alpha}$ (Smith *et al*., 1981a), leading to a significantly decreased $PGF_{2\alpha}$:PGE_2 ratio in the late-secretory-phase endometrium in these women; exacerbating this is the observation that women with objectively-measured HMB have greater endometrial *PTGS1* and *PTGS2* (COX-1 and -2) transcription and augmented EP receptor functionality than do women without HMB (Smith *et al*., 2007). The endometrium of women with HMB is known moreover to express more total prostaglandins in general (Smith *et al*., 1981a, 1981b). The success of COX-2-inhibiting, non-steroidal anti-inflammatory drugs (NSAIDs) such as mefenamic acid in the treatment of HMB (Duckitt and Collins, 2008; Jabbour *et al*., 2006; NICE Clinical Guideline 44 on HMB, 2007) lend further credence to the above.

1.5.5 Medical and Surgical Treatments for HMB

The main objectives of HMB treatments are to reduce menstrual blood loss and/or improve the quality of patient life. Treatments may be divided into non-surgical and surgical options, stratified by the recommendations of NICE as follows (NICE Clinical Guideline 44 on HMB, 2007). Medical treatments are first recommended:

1. The levonorgestrel-releasing intrauterine system (LNG-IUS)
2. Anti-fibrinolytic drugs (e.g. tranexamic acid), non-steroidal anti-inflammatory drugs (NSAIDs; e.g. mefenamic acid), or the combined oral contraceptive pill (COCP)
3. Progestogens (e.g. norethisterone)

Amongst the medical treatments available, the LNG-IUS is considered the most effective, providing long-term treatment for upwards of 5 years, as effective as endometrial ablation and improving most health-related quality of life outcomes (Kaunitz *et al*., 2009; Endrikat *et al*., 2011; Kaunitz and Inki, 2012).

Surgical treatments, offered to patients for whom all the above medical treatments have failed or produced unacceptable side-effects, include the following:

1. Endometrial ablation, either by trans-cervical resection with loop diathermy and roller-ball ablation, by fluid-filled thermal balloon or by microwave ablation
2. Hysterectomy, removing part of or the entire uterus

Though endometrial ablation is less invasive than hysterectomy, it does not guarantee complete amenorrhoea, and uterine perforation, hysterectomy and death are still potential complications (NICE Draft Scope for Hysterectomy Consultation, 2004).
One in thirty women undergoing hysterectomy will experience a 'major adverse event' during or after the operation, including but not limited to bladder or bowel damage, infection and heavy bleeding requiring blood transfusion; the mortality rate of hysterectomy is 0.4 – 1.1 per 1000 operations (NICE Draft Scope for Hysterectomy Consultation, 2004). Surgery is nevertheless considered the preferred option for women with 'severe' HMB (Coulter *et al*., 1994; Cromwell *et al*., 2009; Roberts *et al*., 2011), and is the only treatment assuring complete amenorrhoea.

1.6 Modelling Menstruation

Menstruation only occurs in mammals whose endometria spontaneously decidualise prior to implantation, such as humans and old world primates. In other mammalian species, like the mouse, the endometrium does not decidualise until embryonic/endometrial contact is established (Finn, 1998), and therefore the decline in progesterone in the absence of pregnancy does not trigger endometrial shedding and bleeding.

1.6.1 Non-Human Primate Models

Given that non-human primates undergo spontaneous endometrial decidualisation, some researchers have made use of species like the rhesus macaque as a model for human menstruation, uncovering a great many other molecular and histological similarities to the human endometrium and menstruation. Both species express increased levels of MMPs (Brenner *et al*., 1996; Rudolph-Owen *et al*., 1998) and VEGF during the menstrual phase (Nayak *et al*., 2000), necessarily preceded by a withdrawal of progesterone to effect these changes (Slayden and Brenner, 2006).

Despite the similarities between humans and macaques, ethical considerations regarding the use of primates for research and great expense in their maintenance limit the macaque's utility as a model. A mouse model of human menstruation therefore remains an attractive prospect in the pursuit of a relatively inexpensive means of modelling and experimentally manipulating the events of menstruation.

1.6.2 Mouse Models of Menstruation

The first model of mouse menses was developed by Finn and Pope (1984), with an important refinement in the model's reproducibility following some 20 years later. Finn and Pope's prototype mouse model employed sequential oestradiol and progesterone injections in ovariectomised mice, priming the endometrium for decidualisation, and pioneered the use of intrauterine arachis oil injections to stimulate endometrial decidualisation. In terms of overall decidualisation rates, Finn and Pope's model was remarkably successful, with only approximately one mouse in six failing to exhibit a decidualisation response at the end of the protocol. Despite this success, however, tremendous variability and poor reproducibility in the timing of the decidualisation responses discouraged further pursuit of the model for the better part of the next two decades.

Twenty years later, Brasted *et al*. (2003) introduced subcutaneously-implanted, progesterone-releasing Silastic pumps, as developed by Cohen and Milligan (1993), in place of progesterone injections. The use of Silastic implants to control the release of progesterone allowed for the rapid withdrawal of progesterone from the uterus via the pump's surgical removal, vastly improving the reproducibility of the timings of menstrual events which follow progesterone withdrawal in the model.

In the twelve years that followed Brasted *et al.*'s study, the mouse model of menses has enjoyed considerable success in modelling important features of human menstruation, including factors influencing endometrial repair, expression of inflammatory mediators and factors influencing menstrual bleeding (Kaitu'u *et al*., 2005; Kaitu'u-Lino *et al*., 2006; Cheng *et al*., 2007; Kaitu'u-Lino *et al*., 2007; Xu *et al*., 2007; Menning *et al*., 2012; Rudolph *et al*., 2012; Cousins *et al*., 2014). Specific contributions of these studies will be discussed in further detail in Chapter 4 and Chapter 6.

1.7 Hypotheses

Menstruation, triggered in the human endometrium by the withdrawal of progesterone, effects a host of well-recognised inflammatory features, such as the expression of inflammatory cytokines and the recruitment of inflammatory leucocytes. These features can be simulated and studied in an established mouse model of menses, amenable to experimental manipulation.

Inasmuch as menstruation can be compared to inflammation, apoptosis and phagocytic clearance are likely involved in its resolution, as indeed they are in the resolution of inflammation in other contexts.

The particulars of (1) the extent to which leucocyte influx and apoptosis occur, (2) the timing with which they occur and (3) their importance across the perimenstrual window in humans and after progesterone withdrawal in the mouse are yet to be fully characterised.

1. Menstruation is an inflammatory event, involving the recruitment of neutrophils. Resolving menstruation will involve, in part, resolving inflammation – a process which the phagocytosis of apoptotic cells by recruited and resident macrophages positively influences. Endometrial apoptosis may be integral to both the destruction of tissue at menses, and to the resolution of endometrial inflammation.

Hypothesis: Coordinated apoptosis and neutrophil recruitment are components of the menstrual event and precede menstrual shedding in the normal human endometrium.

2. Mice do not ordinarily menstruate, but the phenomenon can be simulated in a well-established mouse model of menses. Mice are ovariectomised and human endocrine regulation is simulated by the sequential introduction of oestradiol and progesterone; progesterone withdrawal effects menstrual-like changes.

Hypothesis: Apoptosis and neutrophil recruitment are recapitulated in the endometrium of a mouse model of induced menstruation, and are components of the menstrual event which precede overt menstrual shedding.

3. Heavy menstrual bleeding is a common, benign gynaecological complaint, negatively impacting quality of life. Menstruation is disordered in these women, such that they bleed more and/or longer per menstrual cycle. What role apoptosis plays in this is as yet unclear.

Hypothesis: Apoptosis is dysregulated in the endometrium of women who suffer heavy menstrual bleeding.

4. Apoptosis is an important feature of the decidualised mouse endometrium in the mouse model of menses. Apoptosis can be abrogated with pharmacological inhibitors of apoptosis-mediating caspases. The introduction of a caspase inhibitor at the time of progesterone withdrawal may dysregulate menses and repair, perhaps representing a valuable model for heavy menstrual bleeding.

Hypothesis: Experimental inhibition of apoptosis in a mouse model of induced menstruation will delay endometrial repair, delay the resolution of inflammation and lead to dysregulated proliferation.

1.8 Aims & Research Questions

During the 'perimenstrual' window of the human menstrual cycle, to determine…

1. When and where apoptosis occurs in the human endometrium
2. When and in what numbers neutrophils are recruited to the human endometrium
3. Where macrophages are localised in the human endometrium

Following progesterone withdrawal in a mouse model of menstruation, to delineate…

4. When and where apoptosis occurs in the mouse endometrium
5. When and in what numbers neutrophils are recruited
6. What changes occur in glucocorticoid receptor target gene transcription

During the perimenstrual window of the human menstrual cycle, compared to the endometrium of women with normal menstrual bleeding, to determine…

7. Whether the endometrium of women suffering heavy menstrual bleeding exhibits differential transcription of apoptotic genes
8. Whether the endometrium of women suffering heavy menstrual bleeding shows differences in the intensity or localisation of apoptosis
9. Whether the endometrium of women suffering heavy menstrual bleeding exhibits differential transcription of inflammatory cytokines and chemokines

Following progesterone withdrawal in a mouse model of menstruation, to determine…

10. Whether inhibition of apoptosis delays endometrial repair
11. Whether inhibition of apoptosis modulates the inflammatory environment of the endometrium
12. Whether inhibition of apoptosis affects the intensity or distribution of proliferation and/or hypoxia in the endometrium

2. General Materials & Methods

2.1 Patient Sample Collection

2.1.1 Human Endometrial Tissue Collection

Full-thickness endometrial tissue biopsies (i.e. from luminal epithelium, through functional and basal endometrial layers, to endometrial/myometrial junction; **Figure 5**) were obtained from the uterine cavities of healthy women, who were selected on the basis of menstrual cycles of reasonable and predictable length (21 – 35 days in length), the absence of reports of heavy menstrual bleeding (HMB), no recent exogenous hormones, no known endometriosis or large fibroids (>3 cm) and no previous endometrial ablation.

Samples for histological comparisons between the endometria of women with and without objectively-measured HMB and for RT-qPCR-based studies were obtained by endometrial suction curettage (Pipelle, Laboratorie CCD, Paris, France) from healthy women selected on the basis of the same criteria detailed above and in whom menstrual blood loss (MBL) had been objectively measured by alkaline haematin method (Warner *et al*., 2004). Samples were divided by MBL volume into either <80 mL (NMB) or ≥80 mL (HMB; (National Collaborating Centre for Women's and Children's Health and National Institute for Health and Care Excellence (NICE), 2007).

Endometrial tissues were processed either by fixation in 4% neutral-buffered formalin (NBF) for 24 hours and transferred to 50% ethanol prior to paraffin embedding for use in immunohistochemistry studies, or by immediate storage in RNAlater (Ambion Europe Ltd., Warrington, UK), an RNA stabilisation reagent, then stored at -80°C for RNA extraction.

Samples were collected with permission from the Lothian Research Ethics Committee, held by Professor HOD Critchley (1994/6/17; 05/S1103/14; 10/S1402/59), and informed, written consent was obtained from all patients.

Figure 5. Endometrial/myometrial junction in full-thickness human endometrial biopsies. Photomicrograph represents haematoxylin-stained, 'full-thickness' human endometrial tissue from luminal epithelium (right-most in photomicrograph), through functional and basal endometrial layers to endometrial/myometrial junction (left-most in photomicrograph). *Endo = endometrium, µm = micrometre, myo = myometrium; diagram of uterus adapted from MediVisuals Inc.* (© 2007).

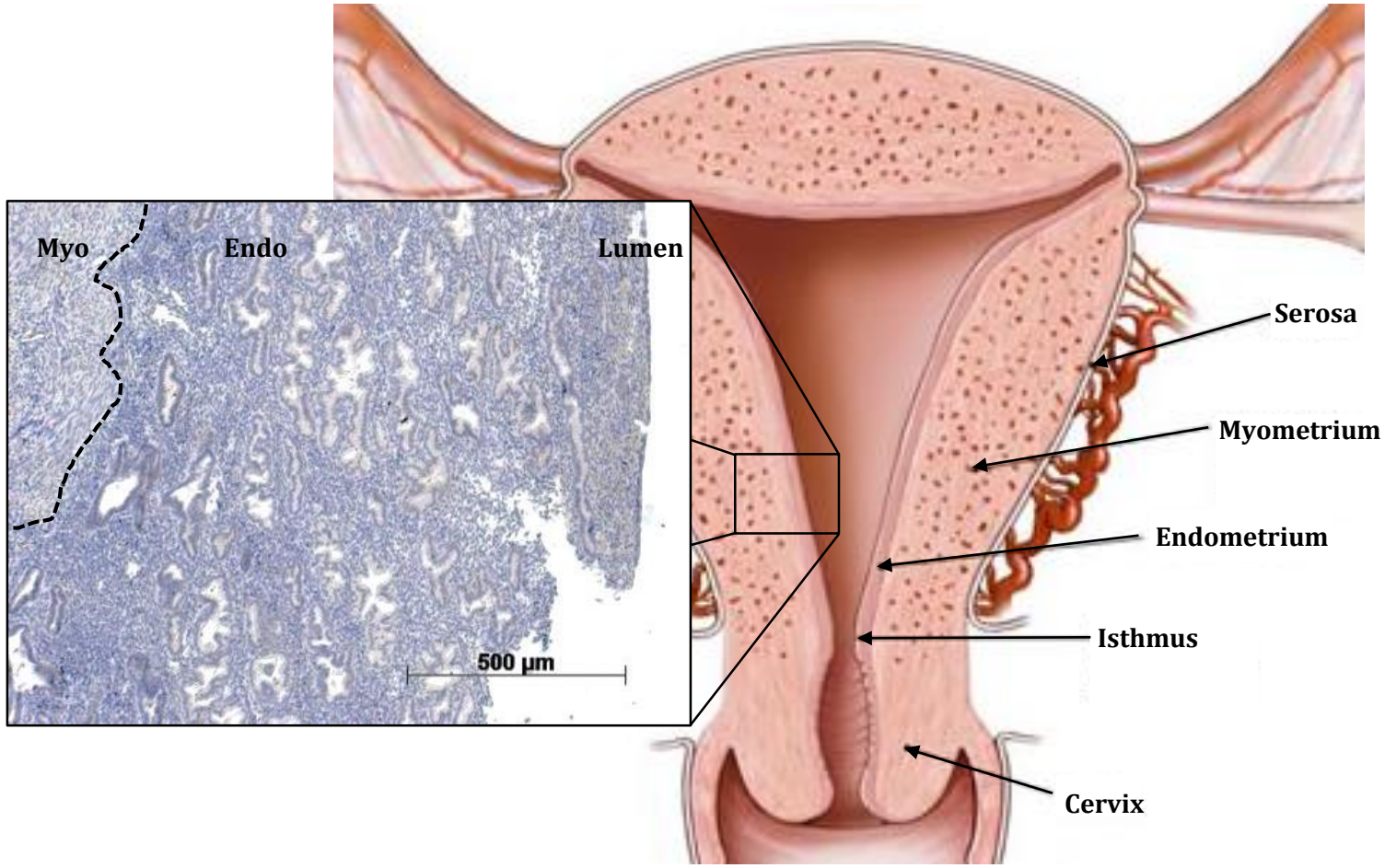

2.1.2 Dating of Endometrial Biopsies

Endometrial biopsies were dated according to the three following criteria:

1. **Histological appearance**: as assessed by consultant pathologist (Professor Alistair Williams), based on criteria described by Noyes *et al.* (1950)
2. **Last menstrual period (LMP)**, as reported by patient
3. **Serum progesterone and oestradiol concentrations**: measured from serum samples collected from patients at the time of their endometrial biopsy and determined by radioimmunoassay

2.1.3 Perimenstrual Window (Luteo-Follicular Transition)

Patient endometrial samples were selected according to the exclusion criteria detailed in 2.1.1 Human Endometrial Tissue Collection, then grouped according to their menstrual cycle stage (**Table 1**) in order to span the late secretory to the proliferative phase of the endometrial cycle (corresponding to the luteal and follicular phases, respectively, in the ovarian cycle). This span is hereafter termed the 'perimenstrual window', or luteo-follicular transition (**Figure 2**).

Patient menstrual cycle day is presented either as the number of days following the onset of menses (for menstrual and proliferative phase samples), or as the number of days prior to the likely onset of menses (for late secretory phase samples), which is calculated by subtracting the cycle day from the mean of the maximum and minimum patient-reported menstrual cycle lengths.

Relevant patient sample details for full-thickness endometrial biopsies are given in **Table 1** and sample details for RT-qPCR studies are given in **Table 2**.

Table 1. Patient sample details for full-thickness endometrial biopsies used for immunohistochemical and immunofluorescent studies, from women not complaining of heavy menstrual bleeding. Cycle day determined from last menstrual period reported by patient, or by subtracting from the mean of reported cycle minima/maxima (given in parentheses); histological stage determined by pathologist. *E_2 = oestradiol, nM = nanomolar, pM = picomolar, P_4 = progesterone.*

Laboratory Code	Cycle Day	Cycle Min./Max. (days)	Histological Stage	Serum [E_2] (pM)	Serum [P_4] (nM)
AR169	21 (-5)	21/28	Late Secretory	819	6.37
AR172	24 (-5)	28/28	Mid Secretory	1949	94.25
AR103	25 (-4)	28/28	Late Secretory	467	17.6
AR189	26 (-3)	28/28	Late Secretory	176	11.29
AR218	29 (-2)	28/32	Late Secretory	168	4.44
AR180	28 (-1)	28/28	Late Secretory	275	5.3
AR104	33 (-1/0)	30/31	Late Secretory	495	22
AR196	1	-	Late Secretory/Menstrual	392	3.06
AR129	1	-	Menstrual	151	4.31
AR211	2	-	Menstrual	153	1.61
AR214	2	-	Menstrual	176	2.55
CT1185EM	3	-	Menstrual	242	<3

Table 1 continued.

Laboratory Code	Cycle Day	Cycle Min./Max. (days)	Histological Stage	Serum [E_2] (pM)	Serum [P_4] (nM)
AR212	5	-	Weakly Proliferative	104	2.47
AR161	6	-	Proliferative	318	2.6
AR223	7	-	Late Proliferative	340	6.38
CT892EM	7	-	Proliferative	424	<3
CT2015EM	8	-	Proliferative	607	<3
CT787EM2	8	-	Proliferative	928	<3
CA748EM	8	-	Proliferative	215	<3
AR136	9	-	Mid Proliferative	1002	13.68
CT1215EM	10	-	Proliferative	275	<3
AR118	10	-	Mid Proliferative	311	1.4
CT1148EM	11	-	Proliferative	372	<3
AR125	11	-	Mid Proliferative	842	7.1

Table 2. Sample details for endometrial biopsies from women with objectively-measured normal and heavy menstrual bleeding used in RT-qPCR studies. Histological stage determined by pathologist; menstrual blood loss measured by alkaline-haematin method (2.1.1 Human Endometrial Tissue Collection), where heavy menstrual bleeding is defined as a menstrual blood loss of greater than or equal to 80 mL. *E_2 = oestradiol, HMB = heavy menstrual bleeding, MBL = menstrual blood loss, mL = microlitre, nM = nanomolar, NMB = normal menstrual bleeding, pM = picomolar, P_4 = progesterone.*

Laboratory Code	Cycle Day	Histological Stage	Serum [E_2] (pM)	Serum [P_4] (nM)	NMB MBL (mL)
CA85E	23	Late Secretory	90.6	11.51	35
CH325E	28	Late Secretory	427.6	19.84	21
CH315E	2	Menstrual	108	3.16	42
CT1142E	2	Menstrual	129	<3	66
CT1185E	3	Menstrual	242	<3	70
CH1004E	5	Menstrual	140	<3	38
CT1370E	6	Proliferative	260.11	<3	78
CT1070E	7	Proliferative	270	<3	14
CT1114E	7	Proliferative	215	<3	64
CH996E	8	Proliferative	672	<3	48
CT1384E	11	Proliferative	879.31	<3	68

Table 2 continued.

Laboratory Code	Cycle Day	Histological Stage	Serum [E_2] (pM)	Serum [P_4] (nM)	HMB MBL (mL)
CT1373E	1	Late Secretory	242.31	8.54	348
CH481E	2	Late Secretory	91	<3	127
CT1221E	24	Late Secretory	154	10.6	221
CT1215E	25	Late Secretory	118	3.4	175
CT1188E	26	Late Secretory	368	16.5	212
CH359E	26	Late Secretory	220	14.76	138
CH540E2	27	Late Secretory	320.8	18.92	85
CT1119E	27	Late Secretory	239	16.5	125
CH393E	28	Late Secretory	71	9.6	114
CH133E	2	Menstrual	144.3	18.44	287
CT1339E	3	Menstrual	107.2	<3	228
CT1374E	4	Menstrual	208.77	<3	80
CT1044E	6	Proliferative	256	<3	305
CT1052E2	7	Proliferative	872	<3	161
CH998E	9	Proliferative	142	<3	107
CT1162E	9	Proliferative	300.9	<3	83
CH330E	10	Proliferative	243	<3	91
CH96E2	11	Proliferative	1135.8	9.7	184
CT1318E	11	Proliferative	463.8	<3	129

2.1.4 Additional Tissue Usage

Colon 'pinch' sections, used as positive controls for leucocyte staining, were provided by Dr. Gwo-Tzer Ho, and were collected under ethical approval obtained from the Lothian Research Ethics Committee.

Peripheral blood monocytes and neutrophils were collected from healthy volunteer blood donations under ethical approval obtained by the Lothian Research Ethics Committee, held by Professor HOD Critchley (08/S1103/38), with informed, written consent obtained from all donors.

2.1.5 Isolation of Leucocytes from Peripheral Blood & Cell Culture

Peripheral monocytes and neutrophil granulocytes for use as positive immunohistochemistry controls were obtained and isolated from blood donated from healthy volunteers (collected with permission from the Lothian Research Ethics Committee; 08/S1103/38), with informed, written consent obtained from all volunteers.

Blood was collected in 50-mL plastic tubes (BD Biosciences, Oxford, UK) containing 4 mL 3.8% sodium citrate per 40 mL of blood collected, and polymorphonuclear (PMN) and peripheral blood mononuclear cells (PBMCs) were isolated using a dextran sedimentation and Percoll gradient method (Pertoft *et al*., 1978; Marwick *et al*., 2013).

Monocytes were enriched from the PBMC fraction by incubating in 12-well culture plates (Corning, New York, USA) at a concentration of 5.0×10^5 mL^{-1} for 1 hour at 37°C, 5% CO_2 and 100% humidity, after which all non-adherent cells were discarded. Fresh, 10% charcoal-stripped foetal calf serum (CS-FCS)-containing, 2 mM L-glutamine-, 200 U/mL penicillin-, 100 µg/mL streptomycin- and 2.5 µg/mL fungizone-supplemented

Roswell Park Memorial Institute (RPMI)-1640 medium (Life Technologies, Carlsbad, USA) was then added to the wells, and the cells were kept at 37°C, 5% CO2 and 100% humidity until preparation of cytocentrifuge slides on the same day.

PMN cells were likewise suspended at a concentration of 5.0×10^5 mL^{-1} and kept at 37°C, 5% CO_2 and 100% humidity until cytocentrifugation.

2.1.6 Generation of Monocyte-Derived Macrophages

A fraction of the monocyte population was retained to differentiate into monocyte-derived macrophages (MDMs), using medium (supplemented as above) containing 5 µL M-CSF (Sigma-Aldrich Ltd., Dorset, UK) per mL RPMI, replaced every 24 hours for a period of 5 days. MDMs were incubated at 37°C, 5% CO2 and 100% humidity until sufficiently differentiated.

2.1.7 Cytocentrifugation & Fixation of Leucocytes for Immunocytochemistry

Neutrophils, monocytes and monocyte-derived macrophages were cytocentrifuged at 300 rpm for 3 minutes at volumes of 200 µL, allowed to air dry, then fixed with either cold methanol (-20°C) for 10 minutes, or with 10% NBF and washed in 0.5% Tween 20-containing (Sigma-Aldrich Ltd.) 0.01 M phosphate-buffered saline (PBS; pH 7.4) for a further 10 minutes. All slides were subsequently stored in PBS (without Tween 20 detergent) at 4°C until used for immunocytochemistry.

2.2 Immunohistochemistry

2.2.1 Dewaxing & Rehydration

Immunohistochemical staining was performed on NBF-fixed, paraffin-embedded tissue samples, cut into 5-µm sections on a HM 325 rotary microtome (Thermo Fisher Scientific, Loughborough, UK) and mounted on electrostatically-charged glass slides. After mounting on slides, the tissue sections were kept overnight in a 50°C oven to ensure proper adherence of the tissue to the glass slide.

Tissue sections were subjected to dewaxing in xylene for 10 minutes, then rehydration in decreasing concentrations of ethanol (100% twice, 95%, 80% and 70%) for 20 seconds each.

2.2.2 Heat-Induced Epitope Retrieval (HIER)

Tissue sections underwent heat-induced epitope retrieval (HIER) in 0.01 M sodium citrate buffer (pH 6.0) (unless otherwise indicated; **Table 3**) to break formalin-induced cross-linking and increase the availability of antigenic sites. HIER was performed with the use of a 'decloaking' chamber (Biocare Medical, Concord, USA), bringing the slides and buffer to 127°C for 10 seconds. Following heating, sections were allowed to cool for 20 minutes, then washed in phosphate-buffered saline (PBS) for 10 minutes.

2.2.3 Blocking

To quench endogenous peroxidase activity, sections were incubated with 3% H_2O_2/methanol (Sigma-Aldrich Ltd., Dorset, UK; Thermo Fisher Scientific Ltd.) at room temperature for a period of 10 minutes, then washed in PBS for 10 minutes. Non-

specific binding of the secondary antibody (and associated background staining) was discouraged by incubation of tissue sections with a non-immune block consisting of serum from the species in which the secondary antibody was raised (Biosera, Boussens, France), diluted 1 in 5 in 5% w/v bovine serum albumin (BSA; Sigma-Aldrich Ltd.) in PBS (**Table 3**).

2.2.4 Primary Antibodies & Controls

Tissue sections were incubated in a humidified chamber overnight at 4°C with 50 μL of primary antibody diluted to the appropriate concentration in the 20% serum/BSA/PBS solution (**Table 3**). Confirmation of staining specificity was achieved using equimolar concentrations of generic immunoglobulins from the same species in which the primary monoclonal antibodies were raised or the immunoglobulin fraction of serum from non-immunised animals in which polyclonal antibodies were raised in place of the primary antibodies. Sections from tissues known to express high levels of proteins of interest were used as positive controls. After incubation, tissue sections were washed for 10 minutes in PBS.

Table 3. Details for primary and secondary antibodies and negative controls used in immunohistochemical studies. *BrdU = 5-bromo-2'-deoxyuridine CD = cluster of differentiation, dig. = digoxigenin, GARP = goat anti-rat (peroxidase) 2°, HAMP = horse anti-mouse (peroxidase) 2°, HARabP = horse anti-rabbit (peroxidase) 2°, HIER = heat-induced epitope retrieval, mAb = monoclonal antibody, NaCitrate = sodium citrate, pAb = polyclonal antibody, RabASP= rabbit anti-sheep (peroxidase) 2°. * denotes secondary antibody was contained as a part of an ImmPress peroxidase-labelling secondary antibody kit (Vector Labs, Peterborough, UK).*

Primary Antibody	Dilution / Concentration (µg/mL)	Species Raised & Clone	Supplier	Secondary Antibody	Negative Control	HIER
BrdU	1:600 / 4.33	Sheep pAb	Fitzgerald Ind.	RabASP	Sheep anti-dig.	NaCitrate (pH 6)
CD45 (Human)	1:400 / 1.25	Mouse mAb (HI30)	BD Biosciences	HAMP *	Mouse IgG1 κ	NaCitrate (pH 6)
CD45 (Mouse)	1:1000 / 0.50	Rat mAb (30-F11)	BioLegend	GARP *	Rat IgG2b κ	NaCitrate (pH 6)
CD68 (Human)	1:200 / 2.05	Mouse mAb (KP1)	Dako	HAMP *	Mouse IgG1 κ	NaCitrate (pH 6)
Cleaved Caspase-3	1:400 / *Unspec.*	Rabbit pAb	Cell Signaling Tech.	HARabP *	Rabbit Normal Ig	NaCitrate (pH 6)
Elastase (Human)	1:500 / 0.22	Mouse mAb (NP57)	Dako	HAMP *	Mouse IgG1 κ	-
Gr-1 (Mouse)	1:1000 / 0.50	Rat mAb (RB6-8C5)	R&D Systems	GARP *	Rat IgG2b κ	-
Pimonidazole	1:200 / 0.30	Mouse mAb (4.3.11.3)	Hypoxyprobe Inc.	HAMP *	Mouse IgG1 κ	NaCitrate (pH 6)
Ly6G (Mouse)	1:1000 / 0.50	Rat mAb (1A8)	BioLegend	GARP *	Rat IgG2a κ	NaCitrate (pH 6)
Myeloperoxidase	1:1250 / 1.60	Rabbit pAb	Dako	HARabP *	Rabbit Normal Ig	NaCitrate (pH 6)

2.2.5 Peroxidase-Labelled Secondary Antibodies (3,3'-Diaminobenzidine; DAB)

Tissue sections were incubated in a humidified chamber with secondary antibody added by drop (~30 μL) using the ImmPRESS peroxidase-labelled anti-mouse, -rabbit or -rat Ig systems (Vector Labs, Peterborough, UK). Secondary antibodies were raised against immunoglobulins of the species in which the primary antibodies were raised (**Table 3**), and incubation took place at room temperature for a period of 30 minutes. After incubation, tissue sections were washed for 10 minutes in PBS.

2.2.6 Detection (DAB)

Staining was developed and visualised with the chromogenic peroxidase substrate 3,3'-diaminobenzidine (DAB; Zymed Laboratories Inc., San Francisco, USA). Oxidisation of DAB by peroxidase enzymes yields a brown precipitate, indicating the presence of antibody-antigen complex ('positive immunoreactivity'). Tissue sections were rinsed in water after 2 minutes of exposure to DAB to terminate the reaction.

2.2.7 Dehydration, Counterstaining & Mounting (DAB)

Tissues were counterstained with Harris' haematoxylin, briefly rinsed in 1% acid alcohol (70% EtOH containing 1% concentrated hydrochloric acid) and immersed in Scott's tap water (distilled water with 20 g/L sodium bicarbonate, 3.5 g/L magnesium sulphate) for 25 seconds, then taken through a series of increasing concentrations of ethanol (70%, 80%, 95%, and 100% twice) for 20 seconds each. Finally, tissues were immersed in xylene for 10 minutes and mounted with PERTEX mounting solution (Histolab Products AB, Gothenburg, Sweden) and plastic coverslips.

2.2.8 Biotinylated Secondary Antibodies & Fluorescent Labelling (Immunofluorescence)

Tissue sections were incubated in a humidified chamber with biotinylated secondary antibody raised against immunoglobulins of the species in which the primary antibodies were raised. Secondary antibodies were diluted 1:200 in the 20% serum/BSA/PBS solution (in which the serum species is matched to the species in which the secondary antibodies were raised), and incubation took place at room temperature for a period of 30 minutes. After incubation, tissue sections were washed for 10 minutes in PBS.

Fluorescent labelling was achieved by incubation with Tyramide Signal Amplification (TSA; PerkinElmer, Waltham, USA) reagent, which uses horseradish peroxidase (HRP) to catalyse the covalent attachment of fluorescent labels (**Table 4**) for detection of the protein of interest. Incubation took place at room temperature, and the TSA reagent was diluted 1:50 in amplification diluent. After incubation, tissue sections were washed for 10 minutes in PBS.

Table 4. List of fluorophores used in immunofluorescent labelling, with excitation and emission peak wavelengths, colour and associated counterstain. *DAPI = 4',6-diamidino-2-phenylindole, nm = nanometre.*

Fluorophore		Excitation Peak Wavelength	Emission Peak Wavelength	Colour	Counterstain
		358 nm	461 nm	Blue	DAPI
Cy2	Fluorescein	489 nm	506 nm	Green	SYTOX Green
Cy3	Indocarbocyanine	550 nm	570 nm	Orange	Propidium iodide
Cy5	Indodicarbocyanine	650 nm	670 nm	Far Red	TO-PRO-3

2.2.9 Counterstaining & Mounting (Immunofluorescence)

Tissue sections were counterstained with SYTOX Green (Thermo Fisher Scientific) or 4',6-diamidino-2-phenylindole (DAPI; Sigma-Aldrich Ltd.) nucleic acid stains, diluted 1:1000 in PBS and with 10 minutes' incubation. After incubation, tissue sections were washed for 10 minutes in PBS, then mounted with PermaFluor aqueous mounting solution (PerkinElmer) and plastic coverslips.

2.2.10 Bright-Field Microscopy

Bright-field photomicrographs of DAB-visualised tissue sections were captured by means of a Provis AX70 microscope (Olympus, Center Valley, USA) fitted with a QICAM Fast 1394 camera (QImaging, Surrey, Canada), and with the use of AxioVision 4.8 software (Carl Zeiss Ltd., Cambridge, UK).

2.2.11 Confocal Microscopy

Photomicrographs of immunofluorescently-labelled tissue sections were captured by means of an LSM710 confocal microscope (Carl Zeiss Ltd.) and with the use of ZEN 2012 software (Carl Zeiss Ltd.).

2.3 Semi-Quantitative Histoscoring

To determine immunohistochemical staining intensity and localisation in human and mouse tissues, a semi-quantitative histoscoring strategy was employed. A histoscore of 0 – 300 was determined by multiplying a staining intensity grade of 0 – 3 (where 0 = no staining, 1 = weak staining, 2 = moderate staining and 3 = strong staining) by an estimation of the percentage of tissue staining positive within each cellular compartment (to the nearest 10%). This semi-quantitative histoscoring strategy is a standard method, and has been used in several previous studies (Aasmundstad *et al.*, 1992; Wang *et al.*, 1998; Critchley *et al.*, 2006). Scores obtained with this method have been found comparable to those obtained by a computerised image analysis system, with a strong correlation found between the two methods (Wang *et al.*, 1998).

In human 'full thickness' endometrial tissue sections (detailed in **Figure 5**, 2.1.1 Human Endometrial Tissue Collection), the tissue was divided into the following cellular compartments: surface epithelium, glandular epithelium, stroma, and perivascular/endothelial cells.

In mouse uterine tissue sections, the tissue was divided into the following cellular compartments: surface epithelium, glandular epithelium, decidual mass/stroma, basal stroma and perivascular cells/endothelium.

Each sample histoscore represents the average from three different tissue sections.

2.4 Histological Assessment of Endometrial Repair

The mouse endometrium proliferates and differentiates under the actions of oestradiol and progesterone (termed 'decidualisation'), and the subsequent withdrawal of progesterone triggers menstrual-like features in the tissue, including a loss of structural integrity between decidualised cells, complete tissue destruction and finally separation of necrotic endometrium from the underlying myometrium. Subsequent to (and alongside) this tissue breakdown, the endometrium undergoes re-epithelialisation and stromal restoration. This process is termed 'endometrial repair'.

To determine the stage of endometrial repair in progesterone-withdrawn mouse uterine tissue, haematoxylin- and eosin- (H&E) stained tissue sections were scored according to a set of morphological features of endometrial breakdown and repair (**Table 5**) developed by Kaitu'u-Lino *et al*. (2006).

Each sample's 'endometrial repair score' was obtained by taking an average of three different 'complete' cross-sections through the tissue (wherein all cellular compartments were present, and the endometrium was fully encircled by smooth muscle).

Table 5. Morphological features used in the determination of endometrial repair stage in the progesterone-withdrawn mouse uterus. As previously described in a study of endometrial repair in a mouse model of induced menstruation (Kaitu'u-Lino *et al*., 2006).

Repair Score	Morphological Features
1	Decidualised tissue • Expansion of stromal compartment • Glands pushed toward myometrium • Presence of decidual cells
2	Early breakdown • Some loss of structural integrity between decidual cells • Most decidua still intact
3	Complete breakdown • Some sloughing of endometrium from myometrium • Complete tissue destruction in decidual zone • No intact decidual tissue
4	Early repair • Beginnings of re-epithelialisation • Dissociation of necrotic tissue from myometrium
5	Complete repair • Complete re-epithelialisation • Stromal restoration • Some luminal debris

2.5 Cell Counting & Stereology

To obtain an estimate of the numbers of cells of interest present in human and mouse tissues, a combination of cell-counting strategies was employed: stereological microscopy (manual counting), and ImageJ1 software-assisted cell counting (semi-automated) using stereology microscopy or AxioScan slide scanner image captures.

2.5.1 Stereological Microscopy

Manual cell counting by means of stereological microscopy was undertaken using a Leica DMRB stereology microscope (Leica Microsystems, Milton Keynes, UK) with Prior automatic stage (Prior Scientific Instruments Ltd., Cambridge, UK), on a computer equipped with Image-Pro Plus 7.0 software (Media Cybernetics UK, Wokingham, UK).

The area comprised by endometrium in each section was delineated, from which random fields were chosen for counting. Over each of these fields, a grid of 500 points (6.4 μm x 6.0 μm) was superimposed at a magnification of 400x, and points were counted depending on whether they fell over cells of interest (i.e. immunopositive cells), unstained tissue (immunonegative cells) or luminal and interstitial space (**Figure 6**). The number of cells and fields counted was calculated according to the equations below:

Standard error (SE):

$$(1) \quad SE = \sqrt{\left[\frac{P_{pi}(100-P_{pi})}{P_T}\right]}$$

P_{pi} represents the percentage of points occupied by the cells of interest, and P_T represents the total number of points that fall on any tissue, stained or unstained.

The sparser the cells of interest, therefore, the more points must be counted to minimise SE and **percentage standard error (%SE)**:

$$(2) \quad \%SE = 100\%(\frac{SE}{P_{pi}})$$

Optimally, *%SE* should be equal to or less than 5%, allowing the calculation of a **minimum P_T value** for such a *%SE* value:

$$(3) \quad P_T \geq 400(100{P_{pi}}^{-1} - 1)$$

If a cell of interest were to comprise 2.5% of the total points within a tissue (P_{pi} = 2.5%), then 15,600 points (or 32 fields of 500 points each) per section would need to be counted to ensure *%SE* ≤ 5%.

Figure 6. Example image of grid used in stereological cell counting in endometrial tissue. Late secretory phase human endometrium stained with an antibody against the human neutrophil marker myeloperoxidase (MPO; brown) and the nuclear counterstain, haematoxylin (blue); photomicrograph is taken at 400x magnification.

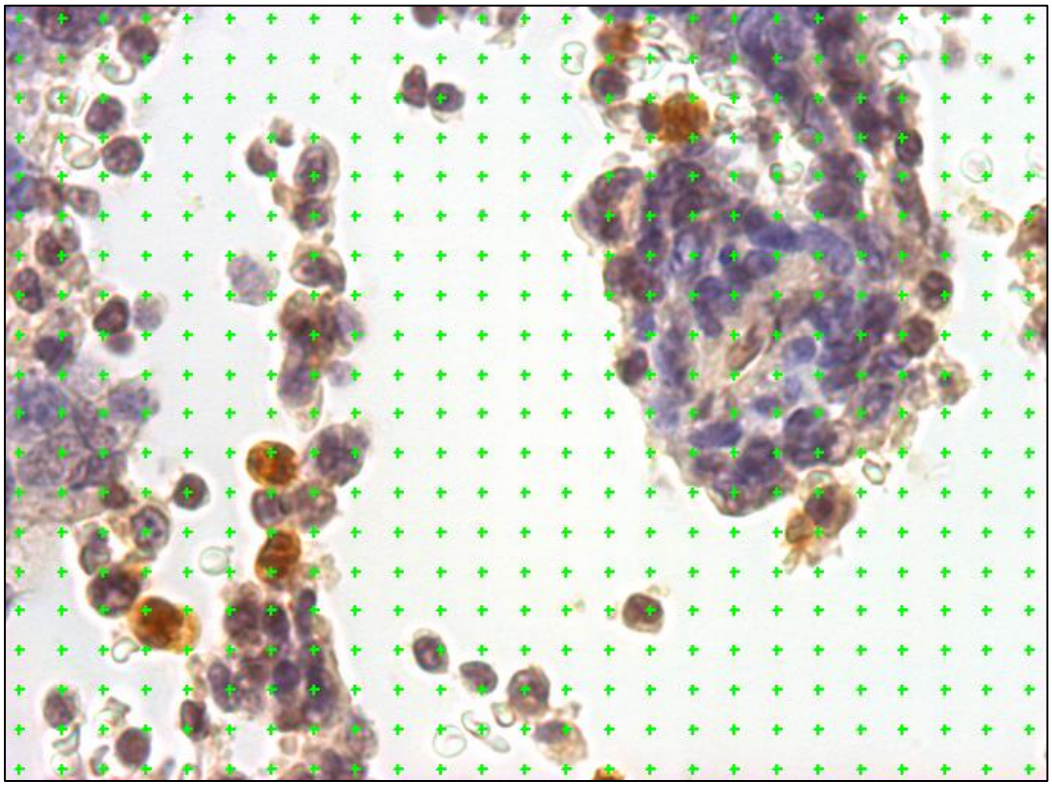

2.5.2 ImageJ1-Assisted Neutrophil Quantification

A semi-automated strategy was also employed for cell counting, using a combination of stereological microscopy and software and the open-source image manipulation software, ImageJ1 (Schneider *et al.*, 2012), modified for use in the detection of fluorescently- and conventionally-stained nuclei.

As with conventional stereological microscopy, a Leica DMRB stereology microscope (Leica Microsystems) with Prior automatic stage (Prior Scientific Instruments Ltd.) was used in conjunction with Image-Pro Plus 7.0 software (Media Cybernetics UK) to delineate the area comprised by the endometrium in tissue sections and to select a number of random fields therein for cell counting. Images were taken from these random fields at 400x magnification and exported as .jpeg files for use with ImageJ1.

As an additional means of generating images for subsequent ImageJ1 analysis, whole-tissue tiled images were captured using an AxioScan (Carl Zeiss Ltd.) slide scanner, saved in compressed, ZEN Software native .czi file-type format and exported as .jpeg files for use with ImageJ1. Whole-tissue tiled images captured in this way comprise a superposition of tiled images generated from 20x, 50x, 100x, 200x and 400x magnifications, and were amenable to easy navigation to re-visit areas of interest in the context of the larger tissue.

A macro written by Abigail Dobyns (Yellon *et al.*, 2013) for use with ImageJ1 software allows the discrimination of cell nuclei on the basis of colour threshold: pixels representing haematoxylin nuclear stain have a unique RGB (red, green and blue light) value which can be used to discriminate them from other pixels. Establishing minimum and maximum size criteria corresponding to likely nuclear dimensions then allows the software to identify putative nuclei and to assign numbers (tagging) for counting purposes. User intervention is required prior to finalising nuclear counts in order to

eliminate false positives (i.e. to remove objects misidentified as nuclei) and to manually tag false negatives (i.e. nuclei which have escaped detection). Subsets of nucleated cells may then be designated either positive or negative for a marker of interest on the basis of DAB-visualised immunoreactivity, and the number of immunopositive cells can be normalised to the total number of nuclei.

2.6 RNA Extraction & Reverse Transcription Quantitative Polymerase Chain Reaction (RT-qPCR)

The reverse transcription quantitative polymerase chain reaction (RT-qPCR) experiments described herein strove to comply with the Minimum Information for publication of Quantitative real-time PCR Experiments (MIQE) guidelines (Bustin *et al*., 2009).

2.6.1 RNA Extraction

Total RNA from human endometrial tissue and mouse uterine tissue was extracted using reagents and materials from commercially available RNeasy Mini Kits (QIAGEN Ltd., Sussex, UK) and according to the manufacturer's instructions, with additional DNA digestion treatment of samples performed by 10-minute incubation with RNase-free DNase I (QIAGEN Ltd.) during RNA purification. Subsequent to RNA extraction, RNA concentrations were quantified and purities were verified by means of a Nanodrop 1000 spectrophotometer v3.7 (Thermo Fisher Scientific) and stored at -80°C.

2.6.2 RNA Quality Validation

For RNA used in gene array studies, quality was additionally ensured using an Agilent 2100 Bioanalyser system in conjunction with 2100 Expert analysis software (Agilent Technologies, Cheshire, UK). RNA samples were loaded into RNA6000 Nano chips (Agilent Technologies) and run according to the manufacturer's instructions, allowing the visualisation of 18S and 28S rRNA (ribosomal RNA) fluorescence peaks. The ratio of 28S to 18S fluorescence peaks allows the calculation of an RNA integrity number (RIN), which if below 7.5, is indicative of RNA degradation.

Only samples with RINs > 7.5 were reverse-transcribed to cDNA and used in gene array studies.

2.6.3 Reverse Transcription

Complementary DNA (cDNA) was generated from RNA samples by reverse transcription, using 1.25 U/µL multiscribe reverse transcriptase, 0.5 mM each deoxynucleotide triphosphates (dATP, dCTP, dGTP, dTTP), 0.4 U/µL ribonuclease inhibitor and 5.5 mM $MgCl_2$ (PE Biosystems, Warrington, UK). A summary of the reagents in this mixture can be found in **Table 6**.

Nineteen µL of this mixture was aliquoted into individual tubes with 1 µL of 100-ng/µL RNA (100 ng). As controls for DNA contamination, one tube was included with no reverse transcriptase and one tube was included with no RNA (both replaced with water). Following mixing of the samples, an incubation programme was run on a Bioer GenePro PCR Cycler (Hangzhou Bioer Ltd., Binjiang, China) for 20 minutes at 25°C, 60 minutes at 42°C and 5 minutes at 95°C. cDNA samples were stored at -20°C.

Table 6. Summary of reagents and concentrations in reverse transcription mixtures. *RNA = ribonucleic acid, µL = microliter, ng = nanogram.*

Reagent	Stock Concentration	20-µL Reaction Volume (µL)	Final Concentration
Vilo Reaction Mix	5x	4	1x
Superscript Enzyme	10x	0.25	0.125x
Nuclease-free H_2O	-	14.75	-
RNA (100 ng/µL)	-	1	-

2.6.4 Reverse Transcription Quantitative Polymerase Chain Reaction (RT-qPCR)

Levels of gene-specific sequences in reverse transcription-generated cDNA were measured by a TaqMan- (hydrolysis probe) based RT-qPCR assay (**Figure 7**). Forward and reverse primers specific to either end of a target sequence of cDNA were designed and used in conjunction with a dual fluorescently-labelled probe which specifically hybridises to a region of cDNA in between the two primer annealing sites. The probe's two fluorescent dyes consist of a 'reporter' label at the 5' end (6-carboxyfluorescein; FAM) and a 'quencher' label at the 3' end (6-carboxytetramethylrhodamine; TAMRA). In an intact probe, the TAMRA quencher label suppresses fluorescence from the FAM reporter label via fluorescence resonance energy transfer (FRET; Bustin, 2000). During the amplification stage of RT-qPCR, however, the probe is cleaved by the 5'-to-3' exonuclease activity of the *Taq* polymerase, separating the FAM reporter from the TAMRA quencher and allowing fluorescent signal emission proportional to the amount of PCR product generated (**Figure 7**). The specificity of the probe to the target sequence ensures that the probe will only be cleaved and signal will only be emitted if the target sequence has been amplified.

Two internal controls were used to normalise signal to the amount of cDNA present in the samples: 18S ribosomal RNA (amplified with a probe conjugated to the reporter label VIC, which emits fluorescence at a different wavelength from the FAM reporter on probes for amplification of target sequences on genes of interest), and *ATP5B* (amplified with a probe conjugated to the FAM reporter label, as with the genes of interest). TaqMan Supermix (Thermo Fisher Scientific) used to prepare RT-qPCR reaction mixtures also contains ROX, a passive dye used by ABI 7900HT Fast Real-Time PCR System cyclers (Applied Biosystems, Warrington, UK) to additionally normalise transcript levels to the volume of Supermix present (and hence loading volume).

Figure 7. TaqMan- (hydrolysis probe) based RT-qPCR assay principles. Hydrolysis probes incorporate a 5'-conjugated 'reporter' label and a 3'-conjugated 'quencher' molecule (1). Reporter fluorescence is suppressed by the quencher molecule via fluorescence energy transfer (FRET; Bustin, 2000) in intact probes. Subsequent to probe and primer annealing (2 and 3), *Taq* DNA polymerase amplification of the target sequence allows its 5'-to-3' exonuclease activity to cleave the hydrolysis probe, liberating the reporter from the quencher molecule (4). Free reporter molecule fluorescence emission is unhindered after polymerase cleavage (5) and is proportional to the amount of PCR product generated. *dNTP = deoxyribonucleotide triphosphate, PCR = polymerase chain reaction. Diagram adapted from da Silva and Pieniazek (2003).*

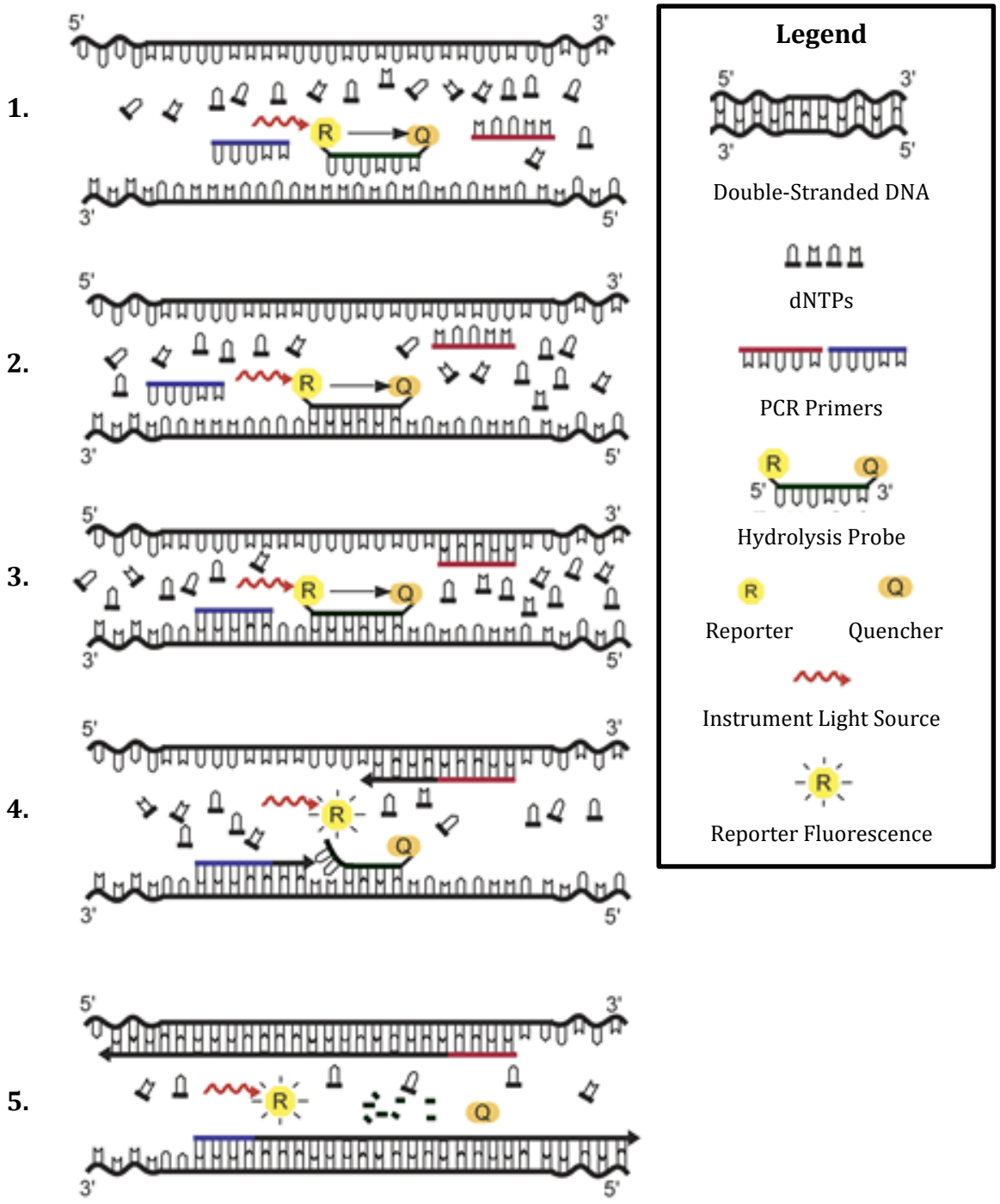

Primers and probes were designed with the aid of the Universal Probe Library Assay Design Centre (Roche Diagnostics Ltd., Burgess Hill, UK), and a basic local alignment search tool (BLAST) was used to verify specificity and ensure no sequence homology to other sequences in scientific databases. Primers were synthesised by Eurofins MWG Operon (Ebersberg, Germany) and probes were obtained from Roche Diagnostics Ltd. All primer/probe sets designed for use in this thesis were determined to be unlikely to amplify non-specific templates.

RT-qPCR reaction mixtures were each prepared according to the following reagent concentrations: TaqMan Supermix (Thermo Fisher Scientific) buffer containing 200 µM each of deoxyadenosine triphosphate (dATP), deoxycytidine triphosphate (dCTP) and deoxyguanosine triphosphate (dGTP), 400 µM deoxyuridine triphosphate (dUTP) and 5.5 mM $MgCl_2$. Gene-specific reaction mixtures were then prepared from these, containing either ribosomal 18S primers and probe (200 nM and 100 nM, respectively; Applied Biosystems) or specific forward and reverse primers and probe (200 nM and 100 nM, respectively) for the target sequence of the gene of interest (**Table 8** and **Table 9**). A summary of the reagents contained in these mixtures and their concentrations can be found in **Table 7**.

Nine µL of these mixtures were aliquoted into the appropriate wells of 384-well RT-qPCR plates (Applied Biosystems) along with 1 µL of cDNA into each well. As negative controls, triplicate wells were included with no cDNA template (replaced with water), the product of the reverse transcription reaction negative control without the reverse transcriptase enzyme, and the reverse transcription reaction negative control with water in place of RNA. As positive controls, cDNA generated from tissues known to express genes of interest, such as mouse liver, was used.

Each sample was run in triplicate technical replicates. RT-qPCR was performed using an Applied Biosystems 7900HT Fast Real-Time PCR System (Applied Biosystems) with

samples initially heated to 95°C for 2 minutes, then run for 40 cycles of 95°C for 15 seconds and 60°C for 60 seconds. Data were analysed and processed by means of Sequence Detection System v2.3 software (PE Biosystems).

Data from RT-qPCR experiments were analysed by the $\Delta\Delta C_q$ (quantification cycle) method, as described by Applied Biosystems: target mRNA-derived cDNA levels were normalised to cDNA loading for each sample using the internal controls described prior (*Actb* and *ATP5B*), and then related to an internal control. Primer/probe sets were validated for linearity of response to specific cDNA sequences by serial 2-fold dilution of cDNA (1/2 to 1/64) produced from a pooled set of RNA samples. Log[RNA] was plotted against ΔC_q values to determine the slope of the line through the x, y coordinates. All primer/probe sets designed for use in this thesis yielded absolute slope values of <0.1.

Table 7. Summary of reagents and concentrations in RT-qPCR reaction mixtures. *cDNA = complementary deoxyribonucleotide, µL = microlitre, µM = micromolar, nM = nanomolar, UPL = universal probe library (Roche Diagnostics Ltd., Burgess Hill, UK).*

Reagent	Stock Concentration	10-µL Reaction Volume (µL; 384-well plate)	Final Concentration
TaqMan Supermix	2x	5	1x
Forward Primer	20 µM	0.1	200 nM
Reverse Primer	20 µM	0.1	200 nM
Specific UPL Probe	10 µM	0.1	100 nM
Nuclease-free H_2O	-	3.7	-
cDNA	-	1	-

Table 8. Primer and probe sequences for human genes of interest examined in TaqMan-based RT-qPCR studies. All primers were designed with the aid of the Universal Probe Library (UPL) Assay Design Centre (Roche Diagnostics Ltd., Burgess Hill, UK). *ATP5B = adenosine triphosphate synthase subunit beta, CCL2 = C-C motif chemokine ligand 2, CTTN = cortactin, CXCL8 = C-X-C motif chemokine ligand 8, DIABLO = direct IAP-binding protein, low pI, HSPA5 = heat shock 70 kDa protein 5, IL6 = interleukin-6, nM = nanomolar, NOS3 = endothelial nitric oxide synthase, TBX2 = T-box transcription factor 2, THRA = thyroid hormone receptor alpha, TNFA = tumour necrosis factor alpha.*

Gene	Accession Number	Forward Primer Sequence	Reverse Primer Sequence	Primer Conc. (nM)	Probe	Probe Conc. (nM)
CCL2	NM_002982.3	tcaaactgaagctcgcactc	gtgactggggcattgattg	200	UPL Probe 67	100
CTTN	ENST00000346329.3	tcggaaccggaagtagagc	aggcattggggactgattc	200	UPL Probe 28	100
CXCL8	NM_000584.3	gagcactccataaggcacaaa	atggttccttccggtggt	200	UPL Probe 72	100
DIABLO	ENST00000413918.1	tgactgcagttggtctttcag	gcggttatagaggcctgatct	200	UPL Probe 74	100
HSPA5	NM_005347.4	agctgtagcgtatggtgctg	aaggggacatacatcaagcagt	200	UPL Probe 64	100
IL6	NM_000600.2	gatgagtacaaaagtcctgatcca	ctgcagccactggttctgt	200	UPL Probe 40	100
NOS3	NM_000603.4	gatcccccagaactcttcct	cagggctgcaaaccactc	200	UPL Probe 1	100
TBX2	NM_005994.3	cacaagctaggcacggagat	cagcaggatatacttggccttc	200	UPL Probe 9	100
THRA	ENST00000264637.4	ggctgtgctgctaatgtcaa	tgactcttctcgatcttgtcca	200	UPL Probe 40	100
TNFA	NM_000594.2	tccagacttccttgagacacg	cccggtctcccaaataaatac	200	UPL Probe 36	100
ATP5B	NM_001686.3	agaggtcccatcaaaaccaa	tcctgctcaacactcatttcc	200	UPL Probe 50	100

Table 9. Primer and probe sequences for mouse genes of interest examined in TaqMan-based RT-qPCR studies. All primers were designed with the aid of the Universal Probe Library (UPL) Assay Design Centre (Roche Diagnostics Ltd., Burgess Hill, UK). *Actb = beta actin, Cxcl1 = C-X-C motif chemokine ligand 1, Il6 = interleukin-6, nM = nanomolar, Tnfa = tumour necrosis factor alpha.*

Gene	Accession Number	Forward Primer Sequence	Reverse Primer Sequence	Primer Conc. (nM)	Probe	Probe Conc. (nM)
Cxcl1	NM_008176.3	actccaacacagcaccatga	tggtctgcaggcactgac	200	UPL Probe 49	100
Il6	NM_031168.1	gctaccaaactggatataatcagga	ccaggtagctatggtactccagaa	200	UPL Probe 6	100
Tnfa	NM_013693.2	ctgtagcccacgtcgtagc	ttgagatccatgccgttg	200	UPL Probe 25	100
Actb	ENSMUST00000100497.4	ctaaggccaaccgtgaaaag	accagaggcatacagggaca	200	UPL Probe 64	100

2.6.5 Mouse Glucocorticoid Signalling PCR Array

To investigate the transcriptional profiles of various genes involved in glucocorticoid receptor-mediated signalling in the mouse endometrium following progesterone withdrawal, a Mouse Glucocorticoid Signalling RT^2 Profiler SYBR Green-based PCR Array (QIAGEN Ltd.) was performed.

Whole tissue RNA was extracted from mouse endometrial samples from mice sacrificed at various time-points following progesterone withdrawal (see 2.7 Mouse Model of Induced Menstruation) using commercially available RNeasy Mini Kits (QIAGEN Ltd.) according to the manufacturer's instructions (see 2.6.1 RNA Extraction), after which the RNA quality was verified by means of an Agilent 2100 Bioanalyser system (Agilent Technologies; see 2.6.2 RNA Quality Validation). cDNA was synthesised using an RT^2 First Strand cDNA synthesis kit with additional genomic DNA elimination (QIAGEN Ltd.): RNA samples were diluted to 0.125 μg/μL (1 μg per 8 μL) in RNase-free water, added to 2 μL of genomic elimination buffer and incubated at 42°C for 5 minutes (step 1, **Table 10**). Reverse transcription reagents and enzymes were added to each reaction mixture and mixed by gentle pipetting, then incubated at 42°C for 15 minutes followed by 95°C for 5 minutes (step 2, **Table 10**). Ninety-one microlitres of RNase-free water was added to each reaction mixture (step 3, **Table 10**) after which the samples were stored at -20°C.

cDNA synthesis mixtures were loaded into 384-well Mouse Glucocorticoid Signalling RT^2 Profiler PCR Array plates with the aid of an 10-μL, 8-channel pipettor according to the following reaction mixtures: 650 μL RT^2 SYBR Green mastermix, 102 μL cDNA and 548 μL RNase-free water. After brief centrifugation, each PCR array plate was run on an Applied Biosystems 7900HT Fast Real-Time PCR System (Applied Biosystems) with samples initially heated to 95°C for 10 minutes, then run for 40 cycles of 95°C for

15 seconds and 60°C for 60 seconds. Data were analysed and processed by means of Sequence Detection System v2.3 software (PE Biosystems).

A dissociation (melt) curve analysis was performed after each experiment to verify the specificity of the assay, wherein a first derivative dissociation curve was produced for each well – a single peak appearing at a temperature of greater than 80°C indicates high PCR specificity.

Data from PCR array experiments were analysed by the $\Delta\Delta C_q$ (quantification cycle) method, as described by Applied Biosystems: target mRNA-derived cDNA levels (**Table 11**) were normalised to the geometric mean of a panel of internal, housekeeping controls included in the plates (*Actb*, *B2m*, *Gapdh*, *Gusb* and *Hsp90ab1*), then related to an internal control. Normalised data were subsequently analysed by 2-way ANOVA with Dunnett's multiple comparisons tests, with all comparisons made to 0 hours progesterone withdrawal.

Table 10. Summary of reagents and concentrations in RT² First Strand (QIAGEN Ltd.) reverse transcription and genomic DNA elimination mixtures. *µg = microgram, µL = microlitre, RNA = ribonucleic acid, RT = reverse transcriptase.*

Reagent	111-µL Reaction Volume (µL)	Step
RNA (100 µg)	x	1
Nuclease-free H_2O	8 – x	1
GE Buffer	2	1
BC3 Buffer	4	2
Control P2	1	2
RE3 RT Mix	2	2
Nuclease-free H_2O	3	2
Nuclease-free H_2O	91	3

Table 11. List of gene transcripts examined by Mouse Glucocorticoid Signalling RT^2 Profiler PCR Array (QIAGEN Ltd.).

Gene Symbol	Full Gene Name
Adarb1	Adenosine deaminase, RNA-specific, B1
Aff1	AF4/FMR2 family, member 1
Ak2	Adenylate kinase 2
Ampd3	Adenosine monophosphate deaminase 3
Angptl4	Angiopoietin-like 4
Anxa4	Annexin A4
Aqp1	Aquaporin 1
Arid5b	AT rich interactive domain 5B (MRF1-like)
Asph	Aspartate-beta-hydroxylase
Atf4	Activating transcription factor 4
Bcl6	B-cell leukaemia/lymphoma 6
Bmper	BMP-binding endothelial regulator
Calcr	Calcitonin receptor
Cebpa	CCAAT/enhancer binding protein (C/EBP), alpha
Cebpb	CCAAT/enhancer binding protein (C/EBP), beta
Col4a2	Collagen, type IV, alpha 2
Creb1	CAMP responsive element binding protein 1
Creb3	CAMP responsive element binding protein 3
Creb3l4	CAMP responsive element binding protein 3-like 4
Ctgf	Connective tissue growth factor
Cyb561	Cytochrome b-561
Ddit4	DNA-damage-inducible transcript 4
Diras2	DIRAS family, GTP-binding RAS-like 2
Dusp1	Dual specificity phosphatase 1
Edn1	Endothelin 1
Ehd3	EH-domain containing 3
Errfi1	ERBB receptor feedback inhibitor 1
Fkbp5	FK506 binding protein 5
Fosl2	Fos-like antigen 2
Gdpd1	Glycerophosphodiester phosphodiesterase domain containing 1
Ghrhr	Growth hormone releasing hormone receptor
Glul	Glutamate-ammonia ligase (glutamine synthetase)
Got1	Glutamate oxaloacetate transaminase 1, soluble
H6pd	Hexose-6-phosphate dehydrogenase (glucose 1-dehydrogenase)
Has2	Hyaluronan synthase 2
Hnrpll	Heterogeneous nuclear ribonucleoprotein L-like
Il10	Interleukin-10
Il1rn	Interleukin-1 receptor antagonist
Il6	Interleukin-6
Il6ra	Interleukin-6 receptor, alpha

Klf13	Kruppel-like factor 13
Klf9	Kruppel-like factor 9
Lox	Lysyl oxidase
Mertk	C-mer proto-oncogene tyrosine kinase
Mt1	Metallothionein 1
Mt2	Metallothionein 2
Nfkbia	Nuclear factor of kappa light polypeptide gene enhancer in B-cells inhibitor alpha
Nr3c1	Nuclear receptor subfamily 3, group C, member 1
Pdcd7	Programmed cell death 7
Pdgfrb	Platelet derived growth factor receptor, beta polypeptide
Pdp1	Pyruvate dehydrogenase phosphatase catalytic subunit 1
Per1	Period homolog 1 (Drosophila)
Per2	Period homolog 2 (Drosophila)
Pik3r1	Phosphatidylinositol 3-kinase, regulatory subunit, polypeptide 1 (p85 alpha)
Pld1	Phospholipase D1
Plekhf1	Pleckstrin homology domain containing, family F (with FYVE domain) member 1
Pou2f1	POU domain, class 2, transcription factor 1
Pou2f2	POU domain, class 2, transcription factor 2
Rasa3	RAS p21 protein activator 3
Rgs2	Regulator of G-protein signalling 2
Rhob	Ras homolog gene family, member B
Rhoj	Ras homolog gene family, member J
Sesn1	Sestrin 1
Sgk1	Serum/glucocorticoid regulated kinase 1
Slc10a6	Solute carrier family 10 (sodium/bile acid co-transporter family), member 6
Slc19a2	Solute carrier family 19 (thiamine transporter), member 2
Slc22a5	Solute carrier family 22 (organic cation transporter), member 5
Snta1	Syntrophin, acidic 1
Sphk1	Sphingosine kinase 1
Spsb1	SplA/ryanodine receptor domain and SOCS box containing 1
Stat5a	Signal transducer and activator of transcription 5A
Stat5b	Signal transducer and activator of transcription 5B
Tbl1xr1	Transducin (beta)-like 1X-linked receptor 1
Tnf	Tumour necrosis factor
Tnfaip3	Tumour necrosis factor, alpha-induced protein 3
Tsc22d3	TSC22 domain family, member 3
Usp2	Ubiquitin specific peptidase 2
Usp54	Ubiquitin specific peptidase 54
Vdr	Vitamin D receptor
Vldlr	Very low density lipoprotein receptor
Xdh	Xanthine dehydrogenase
Zfp281	Zinc finger protein 281
Zfp36	Zinc finger protein 36
Zhx3	Zinc fingers and homeoboxes 3

2.7 Mouse Model of Induced Menstruation

Mice do not ordinarily menstruate, but a mouse model of simulated menses has been optimised in which mice are ovariectomised to eliminate circulating endogenous hormones and oestradiol and progesterone are administered to mimic human endocrine regulation of the uterus through the menstrual cycle (Finn and Pope, 1984; Brasted *et al.*, 2003; Cousins *et al.*, 2014; **Figure 8**). Decidualisation of the endometrium is initiated by injection of oil into the lumen of the uterus. Upon withdrawal of progesterone, the endometrial environment is subject to a host of histological and molecular changes analogous to those seen in the human endometrium during menstruation: the decidualised endometrium is shed, leucocytes are recruited (Menning *et al.*, 2012) and menstrual-like bleeding occurs (Cousins *et al.*, 2014; Rudolph *et al.*, 2012). Subsequently, the tissue is repaired and restored.

Figure 8. Mouse model of induced menstruation protocol. Ovariectomised C57Bl/6 mice were administered oestradiol and progesterone to mimic human endocrine regulation of the endometrium through the menstrual cycle, with decidualisation induced via injection of oil into the lumen of the uterus; withdrawal of progesterone induced bleeding and menstrual-like endometrial changes (Finn and Pope, 1984; Brasted *et al.*, 2003; Cousins *et al.*, 2014). *E_2 = oestradiol, ng = nanogram, P_4 = progesterone; ovex = ovariectomy, i.u. = intrauterine, s.c. = subcutaneous.*

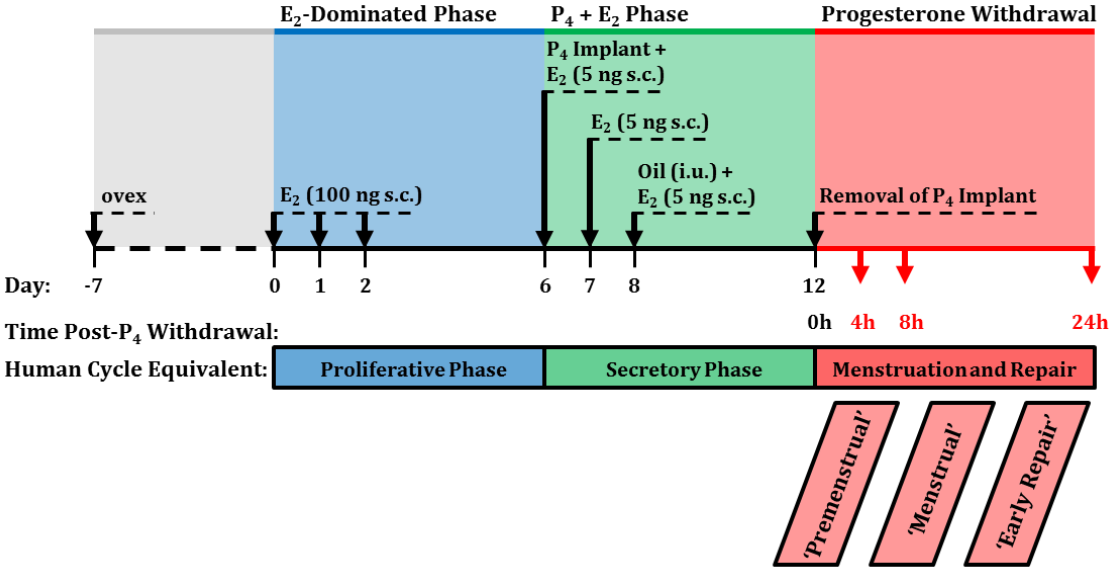

2.7.1 Surgical Ovariectomy

Female C57Bl/6 mice of 8 – 12 weeks of age (Harlan Laboratories, Indianapolis, USA), housed in groups of four, were ovariectomised under inhaled isoflurane-induced (Abbott Laboratories, Abbott Park, USA) anaesthesia, with buprenorphine hydrochloride (0.03 mg/kg; Ceva Animal Health Ltd., Amersham, UK) analgesic administered subcutaneously upon induction of anaesthesia.

A small area of the mouse's lower back was shaved and disinfected with povidone-iodide surgical scrub (Animalcare Ltd., Dunnington, UK), and a small incision was made in the skin. Two small incisions were made, one on each side of the body wall, to facilitate manipulation of the ovary and uterine horn out of the body wall and subsequent excision of the whole ovary with as little removal of the uterus as possible. Incisions made in the body wall were typically small enough to heal without intervention, but were sutured if felt to be too large to do so.

Following bilateral ovariectomy, the incision was closed and held together with surgical clips (BD Biosciences), whereupon the mouse was allowed to recover from anaesthesia, singly-housed in a heat-pad-warmed cage. After recovering consciousness and showing signs of alertness and activity, the mouse was returned to group-housing.

Mice were monitored for post-operative pain for several days following surgery and administered additional buprenorphine hydrochloride (0.03 mL) if exhibiting signs of pain or distress: un-groomed fur, ears flattened against body, narrowed or squinting eyes, limping or limb-favouring, and/or the absence of typical exploratory behaviour (e.g. rearing up, climbing on cage).

Mice were allowed to recover for a minimum of 7 days following ovariectomy before continuing with induced menses protocol.

2.7.2 Subcutaneous Administration of Oestradiol

A 1 mg/mL stock oestradiol solution (in 100% EtOH; Sigma-Aldrich Ltd., Dorset, UK) was diluted 1:1000 in peanut oil (Sigma-Aldrich Ltd.) to prepare a 1 μg/mL solution of oestradiol (in 0.1% EtOH/peanut oil), to be administered subcutaneously at a dose of 100 ng (100 μL).

The same stock oestradiol solution was diluted 1:20 in 100% EtOH, then 1:1000 in peanut oil (Sigma-Aldrich Ltd.) to prepare a 50 ng/mL solution of oestradiol (in 0.1% EtOH/peanut oil), to be administered subcutaneously at a dose of 5 ng (100 μL).

Mice were injected with 100 ng of oestradiol (100 μL; 4 μg/kg body weight) on three consecutive mornings (days 0, 1 and 2 of the protocol; **Figure 8**), then injected with 5 ng of oestradiol (100 μL; 200 ng/kg body weight) on three later consecutive mornings (days 6, 7 and 8 of the protocol; **Figure 8**).

2.7.3 Subcutaneous Implantation of Progesterone-Releasing Silastic Pump

Progesterone-releasing Silastic pumps, similar to those described by Cohen and Milligan (1993), were constructed by cutting 1.4-cm lengths of Silastic tubing (Dow Corning Co., Midland, US), then sealing one end with siloxane resin (Dow Corning Co.) to a depth of 0.2 cm and allowing the resin to dry. The tube segments were then packed with progesterone (Sigma-Aldrich Ltd.) to a depth of 1 cm, leaving a 0.2-cm space to be sealed with siloxane resin.

After filling and sealing the Silastic pumps, they were cleaned with 70% EtOH, taken through 6 rinses with sterile PBS, then immersed in a 1% carbon-stripped foetal calf serum (CS-FCS)/PBS solution and incubated for a minimum of 24 hours at 37°C,

5% CO_2 and 100% humidity to prime the pumps and begin diffusion of the progesterone out of the devices.

Silastic pumps were implanted subcutaneously through a small incision in the back into the mice on day 6 of the protocol (**Figure 8**) under inhaled isoflurane-induced anaesthesia and with buprenorphine hydrochloride (0.03 mg/kg) analgesic administered subcutaneously upon induction of anaesthesia. The incision was closed and held together with surgical clips, whereupon the mouse was allowed to recover from anaesthesia, singly-housed in a heat-pad-warmed cage. After recovering consciousness and showing signs of alertness and activity, the mouse was returned to group-housing.

2.7.4 Intrauterine Decidualisation of Endometrium

As mice normally undergo an oestrous reproductive cycle, in which stromal cells do not undergo differentiation ('decidualisation') in the absence of a blastocyst, decidualisation must be artificially induced in the mouse (Finn and Keen, 1963).

Decidualisation of the endometrium was performed on day 8 of the protocol (**Figure 8**) by the introduction of peanut oil (Sigma-Aldrich Ltd.) stimulus into the uterus via the cervix, using non-surgical embryo transfer (NSET) devices (ParaTechs Corporation, Lexington, USA). Eighteen μL of oil were pipetted into one uterine horn, using a flexible Teflon tip and plastic speculum, leaving the other uterine horn without oil stimulus to act as a non-decidualised control.

Oil stimulus was introduced under inhaled isoflurane-induced anaesthesia, after which the mouse was allowed to recover, singly-housed, in a heat-pad-warmed cage. Subsequent to recovery of consciousness, alertness and activity, the mouse was returned to group-housing.

2.7.5 Withdrawal of Progesterone

Progesterone-releasing Silastic pumps were surgically removed on day 12 of the protocol (**Figure 8**), under isoflurane-induced anaesthesia and with buprenorphine hydrochloride (0.03 mg/kg) analgesic administered subcutaneously upon induction of anaesthesia.

Pumps were removed via a small incision in the skin next to where the pumps were inserted, after which the incision was held together with surgical clips, then the mouse was allowed to recover, singly-housed, in a heat-pad-warmed cage. After recovering consciousness and showing signs of alertness and activity, the mouse was returned to group-housing.

2.7.6 Intraperitoneal Administration of Caspase Inhibitor

In a caspase-inhibition model of mouse menses (**Figure 9**), mice were administered the pan-caspase inhibitor quinolyl-valyl-O-methylaspartyl-[2,6-difluorophenoxy]-methyl ketone (Q-VD-OPh; Sigma-Aldrich Ltd., Dorset, UK) while under isoflurane-induced anaesthesia for the removal of the progesterone-releasing Silastic pumps, on day 12 of the protocol.

Q-VD-OPh is a potent, non-cytotoxic inhibitor of the three major caspase-dependent apoptotic pathways (caspase-9/-3, caspase-8/-10 and caspase-12; Caserta *et al*., 2003) and is functional in different species (mouse and human) and cell types, preventing the caspase activation, caspase substrate cleavage and DNA fragmentation that are characteristic of apoptosis.

Q-VD-OPh was dissolved in dimethyl sulphoxide (DMSO), then diluted 1:10 in sterile PBS to prepare a 3.33 mg/mL solution for injection (in 10% DMSO/PBS) to be

administered intraperitoneally at a dose of 500 µg (150 µL; 25 mg/kg body weight). A lower dose was also prepared by further diluting the DMSO-dissolved Q-VD-OPh in DMSO 2:5 before diluting 1:10 in sterile PBS, yielding a 1.33 mg/mL solution (in 10% DMSO/PBS) for intraperitoneal injection at a dose of 200 µg (150 µL; 10 mg/kg body weight). Q-VD-OPh has been administered to ovariectomised mice at a dose of 25 mg/kg body weight with no adverse effects reported (Liu *et al.*, 2011).

Vehicle control was prepared by diluting DMSO 1:10 in sterile PBS, i.e. 10% DMSO/PBS, and was also injected intraperitoneally at a dose of 150 µL.

Figure 9. Mouse model of induced menstruation protocol with Q-VD-OPh caspase inhibition. Ovariectomised C57Bl/6 mice were administered oestradiol and progesterone to mimic human endocrine regulation of the endometrium through the menstrual cycle, with decidualisation induced via injection of oil into the lumen of the uterus; withdrawal of progesterone induced bleeding and menstrual-like endometrial changes (Finn and Pope, 1984; Brasted *et al.*, 2003; Cousins *et al.*, 2014). The pan-caspase inhibitor Q-VD-OPh is administered intraperitoneally concomitant with progesterone withdrawal. *E_2 = oestradiol, i.p. = intraperitoneal, i.u. = intrauterine, kg = kilogram, mg = microgram, ng = nanogram, ovex = ovariectomy, P_4 = progesterone, Q-VD-OPh = quinolyl-valyl-O-methylaspartyl-[2,6-difluorophenoxy]-methyl ketone, s.c. = subcutaneous.*

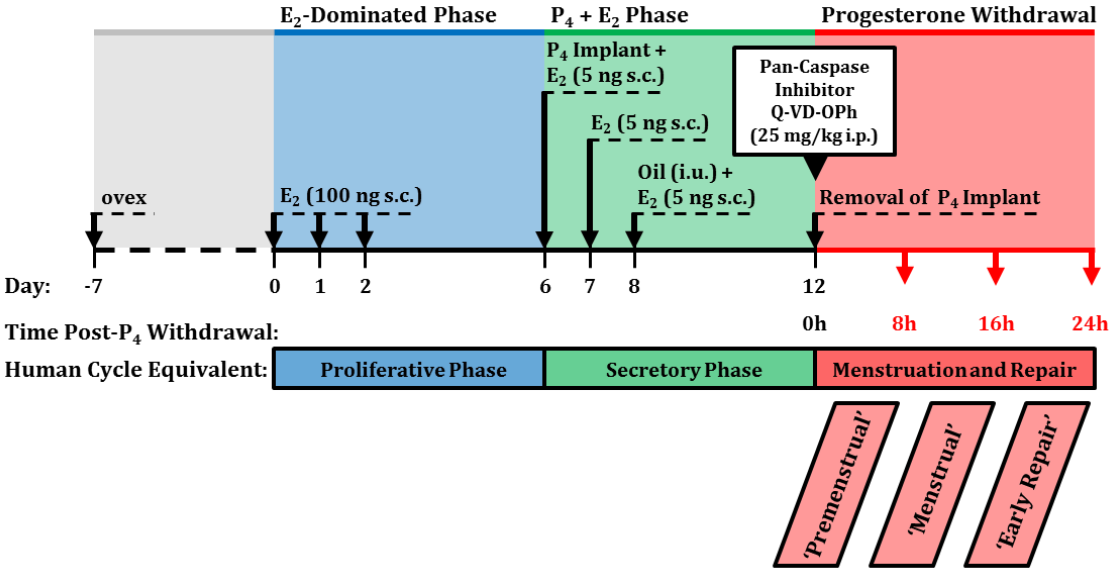

2.7.7 Intraperitoneal Administration of BrdU & Hypoxyprobe

To facilitate immunohistochemical staining for markers of proliferation and hypoxia, mice were administered the compounds 5'-bromo-2'-deoxyuridine (BrdU; BD Biosciences) and pimonidazole hydrochloride ('Hypoxyprobe'; Hypoxyprobe Inc., Burlington, USA), respectively, 1.5 hours prior to culling and collection of tissues.

BrdU is a brominated analogue of deoxythymidine which is incorporated into replicating DNA during the S phase of the cell cycle, allowing its immunohistochemical detection with BrdU-specific antibodies and thereby indicating which cells are actively proliferating (Gratzner, 1982).

Pimonidazole hydrochloride is a 2-nitroimidazole compound which forms adducts with thiol-containing amino acids at partial oxygen pressures (pO_2) of less than 10 mmHg *in vitro* and *in vivo*, occurring only in the presence of certain redox enzymes found in hypoxic cells (Varghese *et al*., 1976; Raleigh *et al*., 1985). These adducts can be detected immunohistochemically with pimonidazole-specific antibodies, indicating hypoxic cells.

BrdU was dissolved in sterile PBS at a concentration of 12.5 mg/mL and administered intraperitoneally at a dose of 1.5 mg (120 µL; 60 mg/kg body weight); Hypoxyprobe was dissolved in sterile PBS at a concentration of 50 mg/mL and administered intraperitoneally at a dose of 1.5 mg (30 µL; 60 mg/kg body weight). Both substances were administered simultaneously in a single, 150-µL dose to minimise the number of injections.

2.7.8 Tissue Collection

Mice were sacrificed and tissues were collected at various time-points after progesterone withdrawal (**Figure 8** and **Figure 9**). Schedule 1 termination of the mice was performed by rising concentration of CO_2 and cervical dislocation, after which the mice were dissected, the uterine horns were removed and their weights recorded.

Uterine horns were split, with half of the horn processed by fixation in 4% NBF for 24 hours and transferred into 50% ethanol for paraffin embedding and use in immunohistochemistry studies, and the other half of the horn stored in RNAlater (Ambion Europe Ltd.), an RNA stabilisation reagent, then stored at -80°C for RNA extraction.

2.7.9 Ethical Approvals & Severity Recording

Severity of each surgical procedure was subjectively determined on the basis of observable pain symptoms and recorded as 'mild', 'moderate' or 'severe', and the maximum severity experienced for each mouse throughout the entire protocol was also recorded. Body weights were recorded at three points in the protocol: at ovariectomy, at insertion of the progesterone-releasing implant and at removal of the implant.

No mouse experienced a maximum severity of greater than 'moderate', nor experienced a decrease in body weight of greater than 10%.

All mouse experiments were performed under a Home Office-issued Personal Licence (Gregory Armstrong, PIL: I00B1A8F3) and Project Licence (Professor PTK Saunders, PPL: 60/4208).

3. Neutrophil Recruitment and Apoptosis in the Normal Human Endometrium

3.1 Introduction

The human endometrium is subject to sex-steroid-driven cycles of proliferation, differentiation, shedding and repair throughout a woman's reproductive years (**Figure 1**): it undergoes extensive proliferation in the oestrogen-dominated proliferative phase (Corner and Allen, 1929), followed by progesterone-driven proliferation in the secretory phase (Csapo and Pulkkinen, 1978). In the absence of pregnancy, a decline in progesterone concentrations triggers menstruation.

Restoration of the endometrium from its underlying basal layer must occur subsequent to menstruation in order to prepare the endometrium for the next cycle. The transition from late secretory phase, through menstruation, to early proliferative phase is herein termed the 'perimenstrual' window (**Figure 2**).

Human menstruation entails a number of changes analogous to the stages of acute inflammation, and has long therefore been regarded an inflammatory phenomenon (Finn, 1986).

Endometrial leucocytes are comprised by a diverse range of resident mononuclear cells, as well as recruited granulocytes and mononuclear cells. Chief amongst those cells recruited to the human endometrium at menses is the neutrophil granulocyte, the most abundant leucocyte of the human immune system. Macrophages are present throughout the menstrual cycle, though their numbers are increased at menses by differentiation of recruited inflammatory monocytes (Salamonsen and Woolley, 1999; Thiruchelvam *et al*., 2012).

Apoptosis is a specialised form of programmed cell death, critical to remodelling of tissue, disposal of aged and infected cells and resolution of inflammation (Kerr *et al*.,

1972; Savill *et al*., 2002). Cells are induced to undergo apoptosis through a number of intrinsic and extrinsic pathways, all of which converge on the activation of a cysteine-aspartic acid protease (caspase) called caspase-3 (Slee *et al*., 2001; **Figure 3**).

Resolving inflammation is an active, regulated process by which inflammatory response is blunted and a pro-resolution response is mounted. Apoptosis is critical in this process, eliminating remaining inflammatory leucocytes and sequestering their cytotoxic contents, and reversing the inflammatory profile of the phagocytes who engulf them (Savill *et al*., 2002). Limiting and resolving endometrial inflammation post-menses is likely an important component to the repair process.

3.1.1 Hypothesis & Research Questions

Hypothesis: Coordinated apoptosis and neutrophil recruitment are components of the menstrual event and precede menstrual shedding in the human endometrium.

During the 'perimenstrual' window of the human menstrual cycle…

1. When and where does apoptosis occur in the human endometrium?
2. When and in what numbers are neutrophils recruited into the human endometrium?
3. Where are macrophages localised in the human endometrium?

3.2 Materials & Methods

3.2.1 Human Endometrial Tissue Collection

Full-thickness endometrial tissue biopsies (described in 2.1.1 Human Endometrial Tissue Collection) used for immunohistochemical and immunofluorescent studies were obtained from the uterine cavities of healthy women with informed, written consent and grouped by menstrual cycle phase (see 2.1.2 Dating of Endometrial Biopsies). Patient biopsies were selected to span the 'perimenstrual window', from the late secretory phase of the endometrial cycle to the early proliferative phase (see **Table 2** in 2.1.3 Perimenstrual Window (Luteo-Follicular Transition) for full details on patient endometrial sample selection).

Patient menstrual cycle day was presented either as the number of days following the onset of menses (for menstrual and proliferative phase samples) or as the number of days prior to the likely onset of menses (for late secretory phase samples), which was calculated by subtracting the cycle day from the mean of the minimum and maximum patient-reported menstrual cycle lengths.

Samples for RT-qPCR-based studies were obtained by endometrial suction curettage (Pipelle, Laboratorie CCD, Paris, France) of uterine cavities of healthy women as described above and further categorised by menstrual blood loss (MBL) as determined by alkaline haematin method (Warner *et al*., 2004; see **Table 2** in 2.1.3 Perimenstrual Window (Luteo-Follicular Transition) for full details on patient endometrial samples selected for RT-qPCR studies).

3.2.2 Immunohistochemistry & Immunofluorescence

Cleaved caspase-3, neutrophil elastase, myeloperoxidase (MPO) and CD68 protein localisation was examined in full-thickness human endometrial tissues across the perimenstrual window (see 2.1.1 Human Endometrial Tissue Collection and 2.1.3 Perimenstrual Window (Luteo-Follicular Transition)), according to the immunohistochemical and immunofluorescent protocols described in 2.2 Immunohistochemistry.

The co-localisation of CD68 and neutrophil elastase and of CD68 and cleaved caspase-3 was also examined by double immunofluorescence, using the protocols described in 2.2.8 Biotinylated Secondary Antibodies & Fluorescent Labelling (Immunofluorescence).

3.2.3 Semi-Quantitative Histoscoring

To further determine cleaved caspase-3 localisation and expression intensity in full-thickness human endometrial tissues across the perimenstrual window (n = 22; see 2.1.1 Human Endometrial Tissue Collection and 2.1.3 Perimenstrual Window (Luteo-Follicular Transition)), a semi-quantitative histoscoring method was used (Aasmundstad *et al*., 1992; Wang *et al*., 1998; Critchley *et al*., 2006): tissue sections were divided into cellular compartments (surface epithelium, glandular epithelium, stroma and perivascular/endothelial cells), with each compartment assigned a staining intensity grade of 0 – 3 (where 0 = no staining, 1 = weak staining, 2 = moderate staining and 3 = strong staining). Each staining intensity was then multiplied by the estimated percentage of tissue staining positive (to the nearest 10%), yielding a histoscore for each tissue compartment of 0 – 300.

Full details of semi-quantitative histoscoring protocol can be found in 2.3 Semi-Quantitative Histoscoring.

3.2.4 Cell-Counting & Stereology

A combination of stereological microscopy and ImageJ1 software-assisted (Schneider *et al*., 2012) cell-counting strategies were employed to investigate neutrophil abundance in full-thickness human endometrial tissue sections across the perimenstrual window (n = 20; see 2.1.1 Human Endometrial Tissue Collection and 2.1.3 Perimenstrual Window (Luteo-Follicular Transition)) immunohistochemically stained for neutrophil elastase.

'Manual' cell counting by stereological microscopy was undertaken according to the protocols described in 2.5.1 Stereological Microscopy, using a Leica DMRB stereology microscope (Leica Microsystems, Milton Keynes, UK) and Image-Pro Plus 7.0 software (Media Cybernetics UK, Wokingham, UK). Elastase-immunopositive cells were counted from random fields selected from an area of the sections manually delineated as endometrium by means of a counting grid system: each randomly-selected 400x-magnification field had a grid of 500 points (6.4 μm x 6.0 μm) superimposed over it, and these points were counted depending on whether they lay over immunopositive cells, immunonegative cells (unstained tissue) or luminal/interstitial space. Full details of stereology microscopy protocols and standard error calculations can be found in 2.5.1 Stereological Microscopy.

'Semi-automated' cell counting was undertaken as described in 2.5.2 ImageJ1-Assisted Neutrophil Quantification, using first either a Leica DMRB stereology microscope (Leica Microsystems) or an AxioScan slide scanner (Carl Zeiss Ltd., Cambridge, UK) to capture images for analysis. Using the former, 400x magnification fields randomly selected

from the endometrium by Image-Pro Plus 7.0 software were exported as .jpeg image files; using the latter, whole-tissue tiled images were captured using ZEN software (Carl Zeiss Ltd.) and exported as .jpeg image files. Elastase-immunopositive cells were counted and normalised to total number of cells using open-source image manipulation software ImageJ1 (Schneider *et al*., 2012) modified to detect fluorescently- and immunohistochemically-stained nuclei (Abigail Dobyns; Yellon *et al*., 2013) on the basis of colour threshold and size discrimination.

Full details of ImageJ1-assisted, semi-automated cell counting protocols can be found in 2.5.2 ImageJ1-Assisted Neutrophil Quantification.

3.2.5 RNA Extraction & RT-qPCR

Total RNA from human endometrial tissues across the perimenstrual window from women with objectively-measured 'normal' menstrual bleeding (menstrual blood loss < 80 mL; n = 10 – 12), details of which are described in **Table 2**, 2.1.3 Perimenstrual Window (Luteo-Follicular Transition), was extracted and cDNA synthesised according to the protocols described in 2.6 RNA Extraction & Reverse Transcription Quantitative Polymerase Chain Reaction (RT-qPCR).

Levels of *CCL2* (*MCP1*), *CXCL8* (*IL8*), *IL6* and *TNFA* mRNA transcripts (see **Table 8**) were measured by TaqMan- (hydrolysis probe) based RT-qPCR assay in triplicate technical replicates and normalised to *ATP5B* mRNA levels as a housekeeping control; human liver cDNA was included as a positive control and appropriate negative controls were also included. Data were analysed by $\Delta\Delta C_q$ (quantification cycle) method as described by Applied Biosystems (Warrington, UK).

Full details of RT-qPCR and data analysis protocols can be found in 2.6 RNA Extraction & Reverse Transcription Quantitative Polymerase Chain Reaction (RT-qPCR).

3.3 Results

3.3.1 Localisation & Intensity of Apoptosis across the Perimenstrual Window

Apoptosis was extensive throughout the late secretory and menstrual phase human endometrium (**Figure 10, Figure 11**): peak cleaved caspase-3 expression was observed in the glandular epithelium in the late secretory phase persisting into the menstrual phase, while cleaved caspase-3 was not substantially expressed in the endometrial stroma until the menstrual phase (**Figure 10**). Cleaved caspase-3 expression decreased dramatically in all tissue compartments by the proliferative phase.

In the glandular epithelium, the mean cleaved caspase-3 histoscores of late secretory and menstrual phase endometrial samples were significantly higher than those of the early proliferative phase ($p < 0.05$; **Figure 10B**).

In the endometrial stroma, the mean cleaved caspase-3 mean histoscore was significantly higher in the menstrual phase than in the early proliferative phase ($p < 0.01$; **Figure 10C**).

Negligible cleaved caspase-3 expression was found in endothelial and perivascular cells of the human endometrium throughout the perimenstrual window, never amounting to more than 10% tissue coverage (and therefore a positive histoscore); these data have not been shown.

A panel of representative photomicrographs taken from endometrial tissues immunohistochemically-stained for cleaved caspase-3 is shown in **Figure 11**.

Immunofluorescent co-localisation of cleaved caspase-3 with the nuclear counterstain Sytox Green revealed the presence of 'double-positive' apoptotic bodies within the glandular epithelium of the late secretory phase endometrium (**Figure 12**): small

bodies can be seen within cleaved caspase-3 immunopositive cells, representing the condensation and fragmentation of nuclear material in cells undergoing apoptosis.

Figure 10. Peak apoptosis (cleaved caspase-3^{+}) is observed in the glands of the late-secretory-phase human endometrium, preceding menstrual shedding, and in the stroma of the menstrual-phase endometrium. Semi-quantitative immunoreactivity histoscoring (staining intensity multiplied by percentage of tissue staining positive) for cleaved caspase-3 (1:400, Cell Signalling Tech.) in the human endometrium across the perimenstrual window revealed extensive apoptosis in the glandular epithelium in late secretory phase (n = 5), preceding overt menstrual bleeding and shedding, and continuing into the menstrual phase (n = 6); apoptosis in the endometrial stroma did not increase appreciably until the menstrual phase. Cleaved caspase-3 expression decreased markedly in both the glandular epithelium and endometrial stroma by early proliferative phase (n = 11). A) Each x-value represents data from one individual patient sample. *Day of patient menstrual cycle is presented as the number of days following menses (positive values) or as the numer of days prior to the onset of menses (negative values; see 3.2.1 Human Endometrial Tissue Collection).* B, C) Data grouped by menstrual phase for glandular epithelium (B) and stroma (C). * $p < 0.05$, ** $p < 0.01$; *error bars represent SEM; significance determined by 1-way ANOVA and Tukey's multiple comparisons test.* E_2 *= oestradiol,* P_4 *= progesterone.*

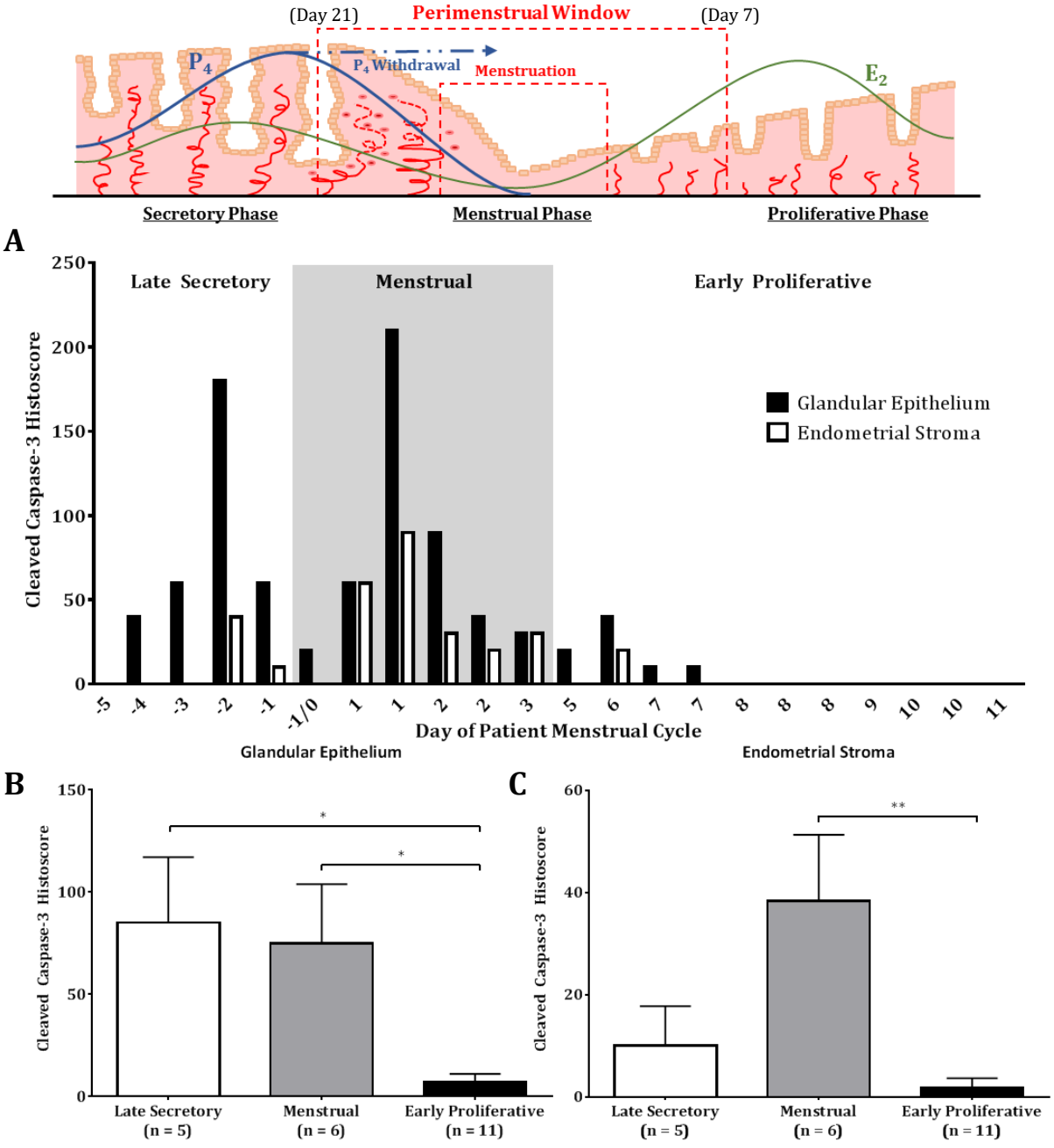

Figure 11. Cleaved caspase-3 localisation in the human endometrium across the perimenstrual window. Representative photomicrographs of cleaved caspase-3 (1:400, Cell Signalling Tech.) staining in serial sections of human endometrium through the perimenstrual window (late secretory phase, n = 5; menstrual phase, n = 6; early proliferative phase, n = 11). Brown-filled triangles indicate cleaved caspase-3 immunoreactivity. *Isotype control: non-immunised rabbit serum Ig fraction (Dako); nuclear counterstain: haematoxylin. Scale bars (500 µm, 100 µm) in image.* E_2 *= oestradiol,* P_4 *= progesterone.*

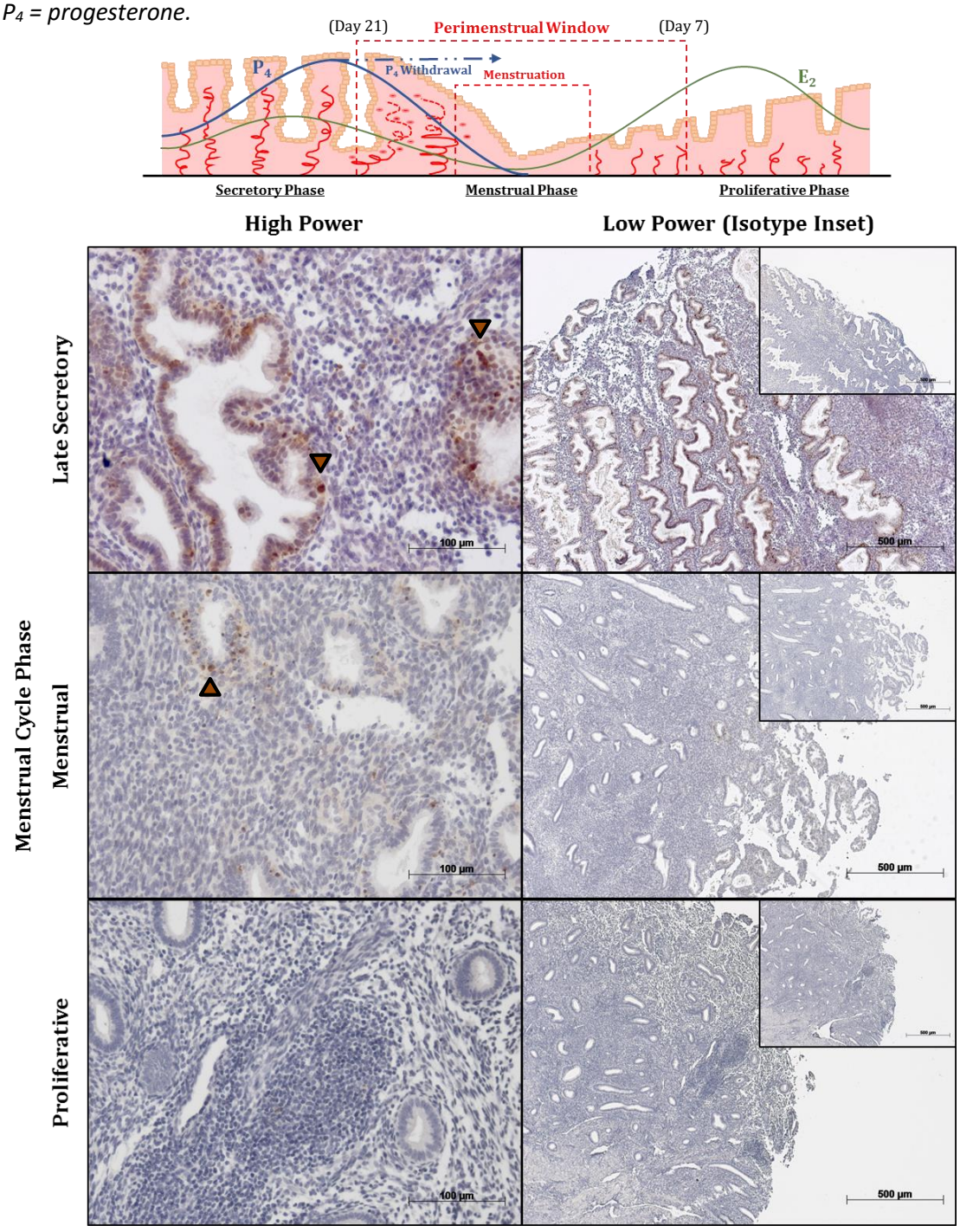

Figure 12. Apoptosis (cleaved caspase-3^{+}) precedes menstrual shedding in the glands and stroma of the late-secretory-phase human endometrium. Representative immunofluorescent photomicrograph of cleaved caspase-3 (red; 1:500, Cell Signalling Tech.) staining in late secretory phase human endometrium (menstrual day 29/-2); yellow represents co-localisation of cleaved caspase-3 and nuclear counterstain. *Menstrual day presented as days post-menses (positive)/days pre-menses (negative; see 3.2.1 Human Endometrial Tissue Collection). Blue box in diagram depicts late secretory phase. Nuclear counterstain: Sytox Green (green; Molecular Probes Inc.). Scale bar (20 µm) in image. E_2 = oestradiol, P_4 = progesterone.*

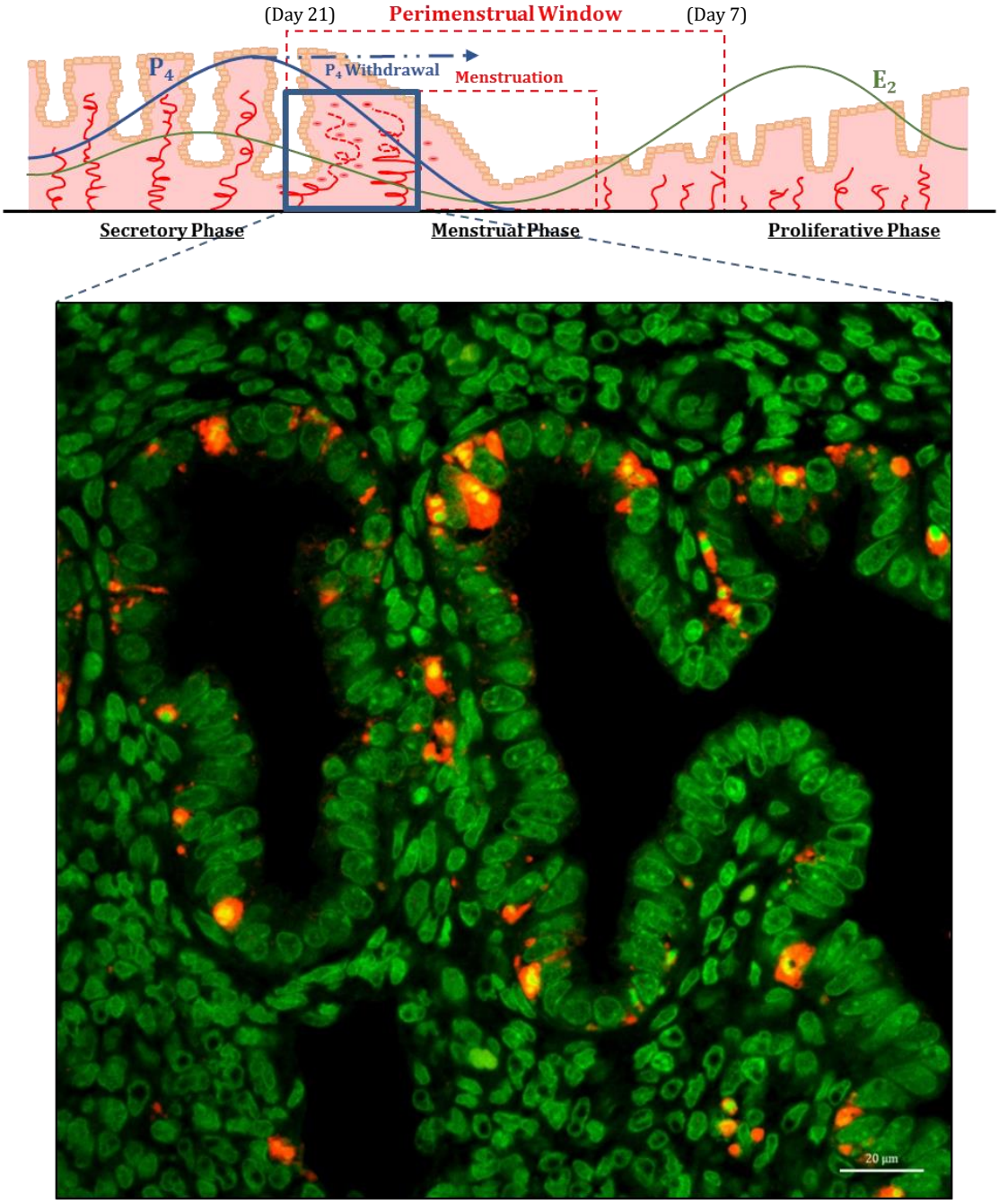

3.3.2 Neutrophil Recruitment across the Perimenstrual Window

Investigation into neutrophil abundance in endometrial tissues across the perimenstrual window revealed a precipitous increase in neutrophil elastase-immunopositive cells at the advent of the menstrual phase (**Figure 13**), with numbers decreasing to pre-menstrual levels by the early proliferative phase.

Mean neutrophil abundance was statistically significantly greater in menstrual phase endometrium than in late secretory phase ($p < 0.01$; **Figure 13B**) and early proliferative phase endometrium ($p < 0.001$; **Figure 13B**).

Immunohistochemical staining of endometrial tissues across the perimenstrual window was undertaken with both elastase- and myeloperoxidase- (MPO)-specific antibodies (panels of representative photomicrographs of which are shown in **Figure 14** and **Figure 15**, respectively), however elastase-stained tissues allowed for better discrimination of immunopositive cells from surrounding immunonegative cells, and were therefore used for quantification of neutrophils in the endometrial stroma (**Figure 13**).

Figure 16 depicts a representative immunofluorescent photomicrograph taken from menstrual phase endometrial tissues stained for neutrophil elastase.

Figure 13. Neutrophil abundance (elastase$^+$) peaks at the advent of menstruation in the human endometrium, whereas neutrophils are virtually non-existent in the late secretory and proliferative phases. Percentage of endometrial stroma comprised by neutrophils, as determined by ImageJ-assisted, stereological elastase-positive (1:500, Dako) cell counting of late secretory (n = 5), menstrual (n = 6) and early proliferative (n = 9) phase human endometrial tissues. A) Each x-value represents data from one individual patient sample. *%SE indicated above bars (%SE > 5 where unstated; see* 2.5.1 Stereological Microscopy*). Day of patient menstrual cycle presented as the number of days following menses (positive) and as the numer of days prior to the onset of menses (negative; see 3.2.1 Human Endometrial Tissue Collection).* B) Data grouped by menstrual phase. ** p < 0.01, *** p < 0.001; *error bars represent SEM; significance determined by 1-way ANOVA and Tukey's multiple comparisons test. E_2 = oestradiol, P_4 = progesterone.*

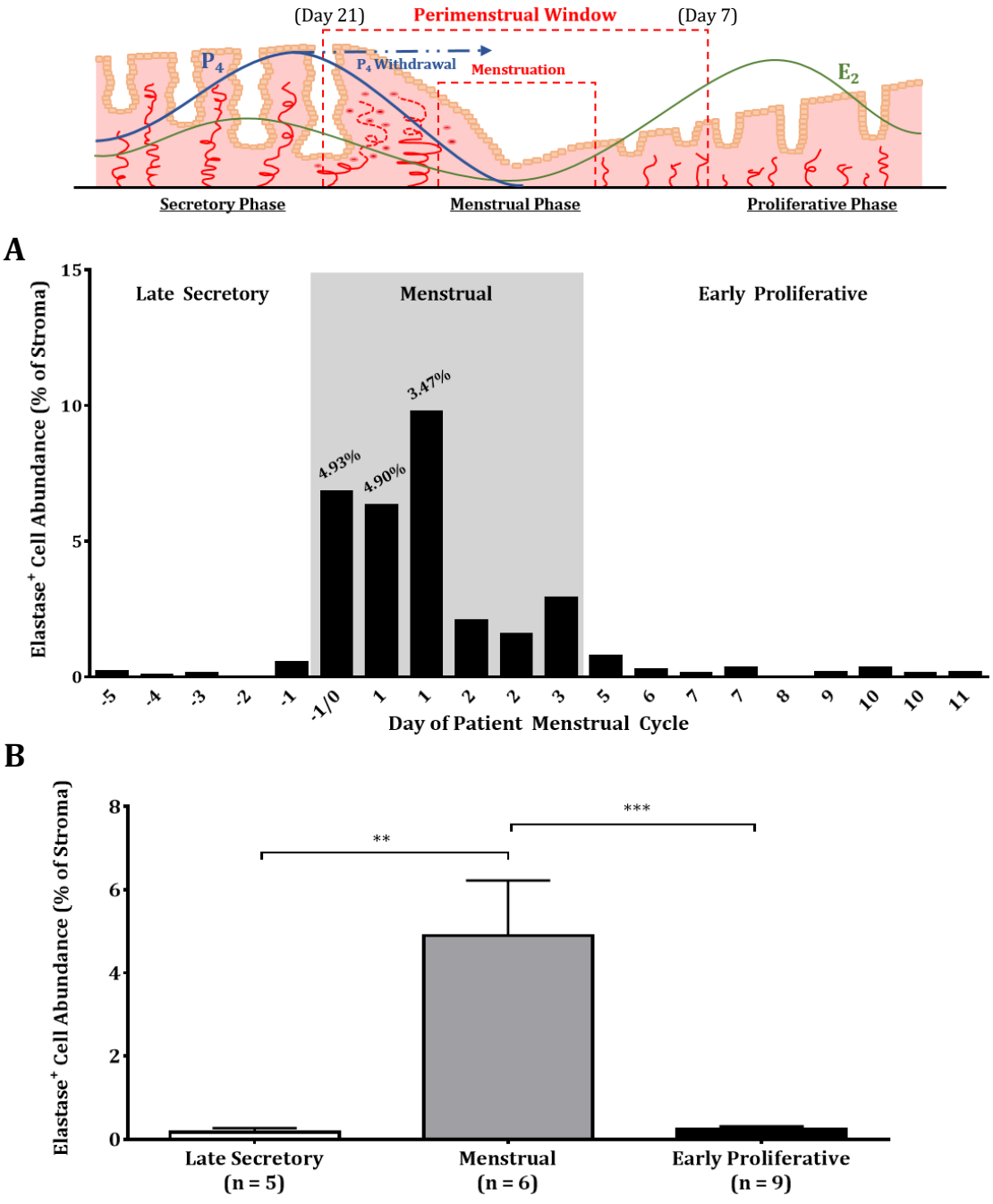

Figure 14. Neutrophil elastase localisation in the human endometrium across the perimenstrual window. Representative photomicrographs of immunohistochemical staining for the human neutrophil marker, elastase (1:500, Dako), in serial sections of human endometrium through the perimenstrual window (late secretory phase, n = 5; menstrual phase, n = 6; early proliferative phase, n = 9). Brown-filled triangles indicate elastase immunoreactivity. *Isotype control: mouse IgG1κ (Sigma-Aldrich); nuclear counterstain: haematoxylin. Scale bars (500 µm, 100 µm) in image.* *E_2 = oestradiol, P_4 = progesterone.*

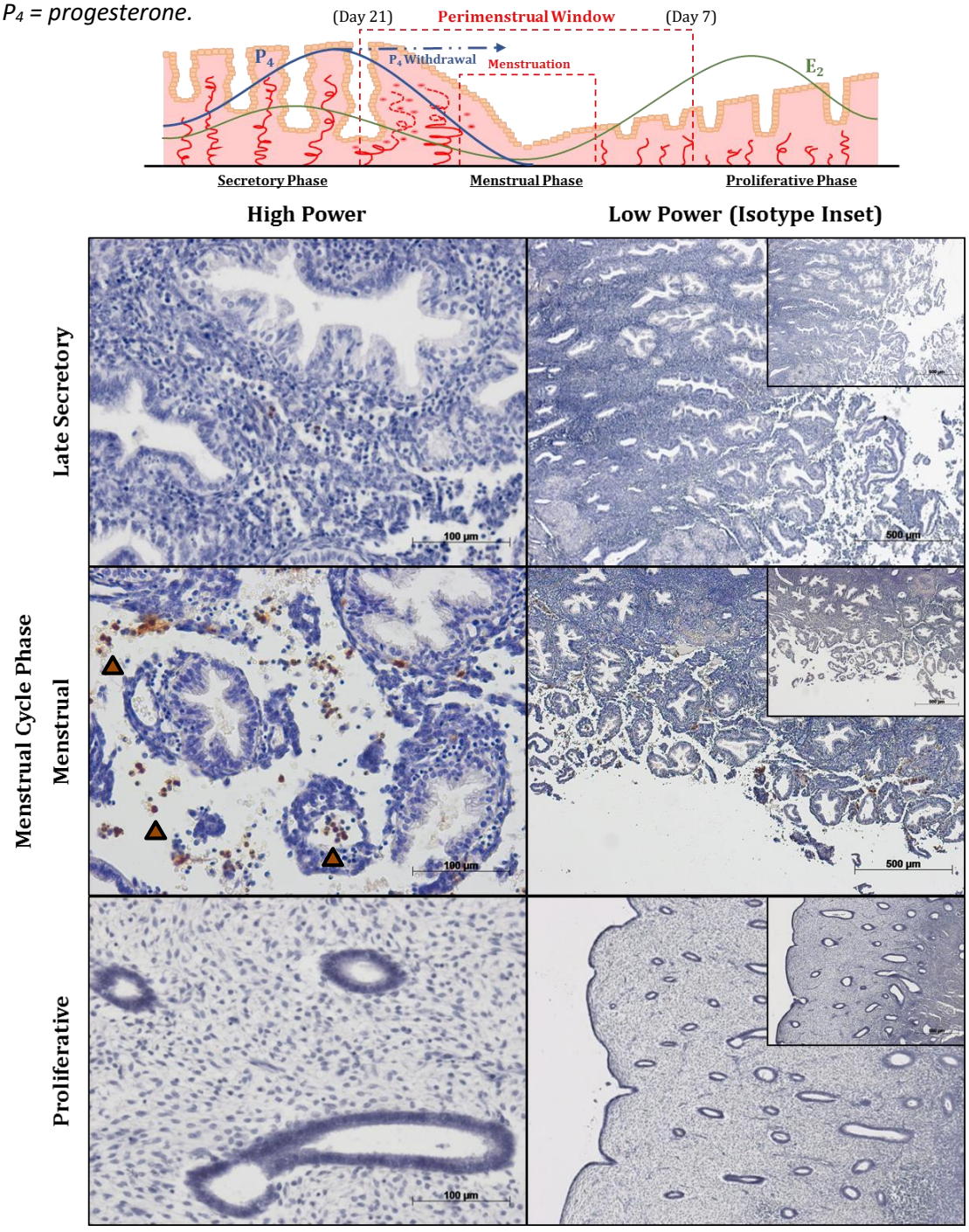

Figure 15. Neutrophil myeloperoxidase (MPO) localisation in the human endometrium across the perimenstrual window. Representative photomicrographs of immunohistochemical staining for the neutrophil marker, myeloperoxidase (MPO; 1:1250, Dako), in serial sections of human endometrium through the perimenstrual window (late secretory phase, n = 5; menstrual phase, n = 6; early proliferative phase, n = 9). Brown-filled triangles indicate MPO immunoreactivity. *Isotype control: non-immunised rabbit serum Ig fraction (Dako); nuclear counterstain: haematoxylin. Scale bars (500 µm, 100 µm) in image. E_2 = oestradiol, P_4 = progesterone.*

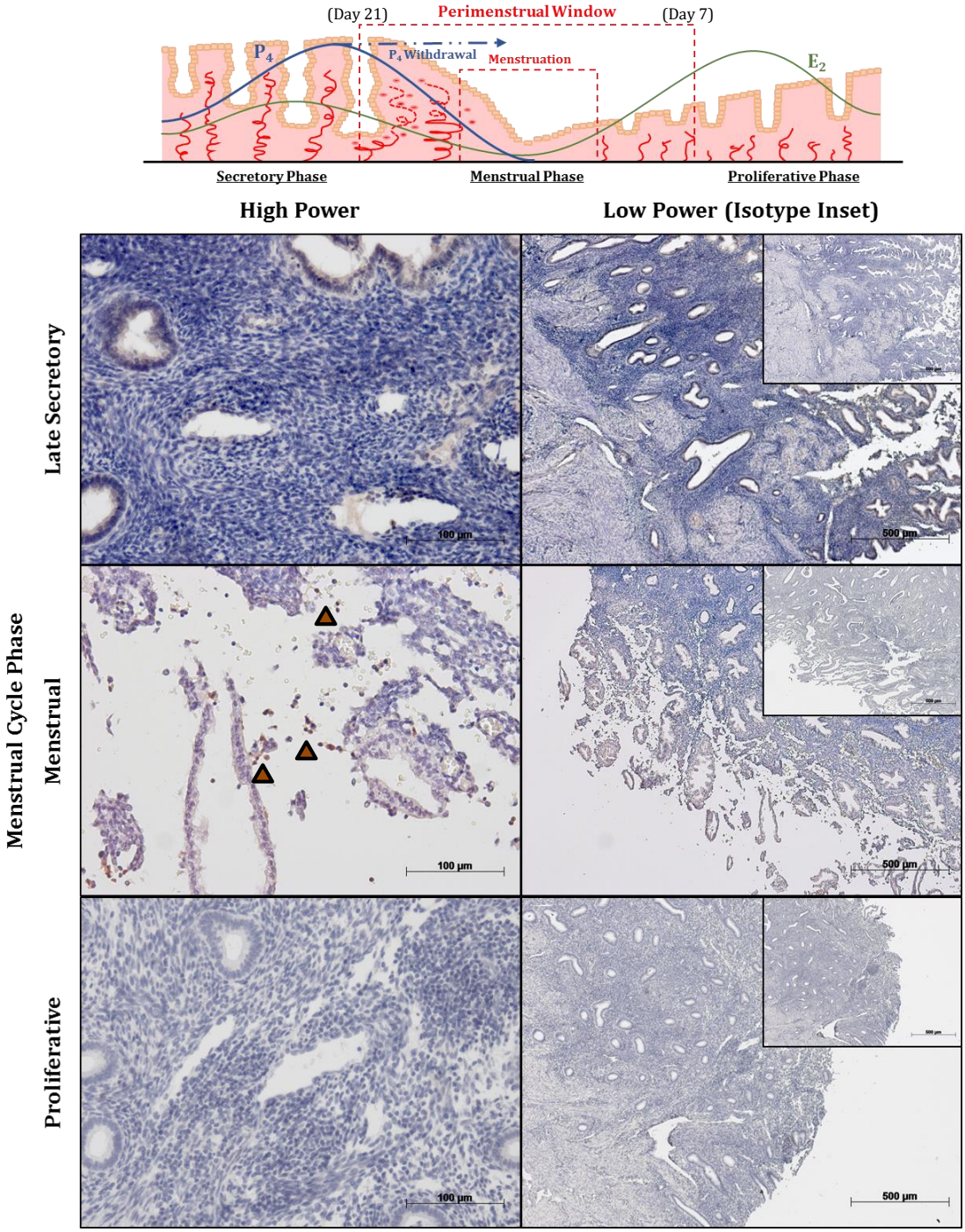

Figure 16. Neutrophil elastase$^+$ cells are abundant in the menstrual-phase human endometrium. Representative immunofluorescent photomicrograph of elastase (red; 1:1000, Dako) staining in menstrual phase human endometrium (menstrual day 1). *Blue box in diagram depicts menstrual phase. Nuclear counterstain: Sytox Green (green; Molecular Probes Inc.). Scale bar (20 µm) in image. E_2 = oestradiol, P_4 = progesterone.*

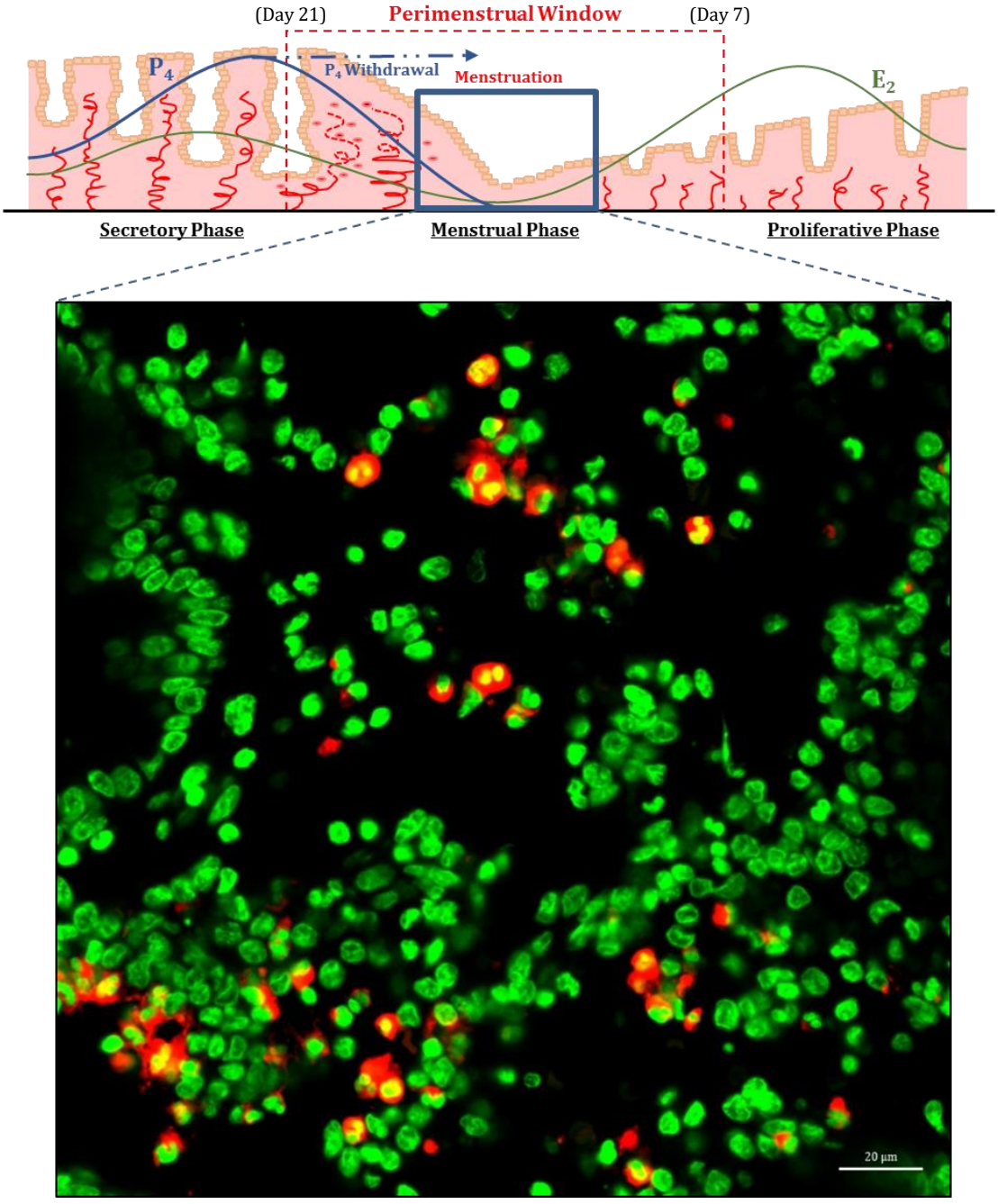

3.3.3 *CCL2*, *CXCL8, IL6* & *TNFA* Transcription across the Perimenstrual Window

Transcription of the leucocyte chemokine *CCL2* (*MCP1*) was significantly increased in menstrual-phase endometrium of women with objectively-measured 'normal' menstrual bleeding (NMB) compared to late secretory phase ($p < 0.05$) and early proliferative phase endometrium ($p < 0.01$; **Figure 17A**). The chemokine *CXCL8* (*IL8*) showed very highly significantly increased transcription in the endometrium at menstrual phase compared to late secretory and early proliferative phases ($p < 0.0001$; **Figure 17B**).

The cytokine *IL6* showed increased transcription in the endometrium of women with objectively-measured NMB at menstrual phase compared to late secretory and early proliferative phases ($p < 0.01$ and 0.001; **Figure 17C**), as did transcription of the inflammatory cytokine *TNFA* at menstrual phase compared to late secretory ($p < 0.05$) and proliferative ($p < 0.01$) phases (**Figure 17D**).

Figure 17. Transcription of leucocyte chemokines and of inflammatory cytokines is increased in the menstrual-phase endometrium of women with objectively-measured 'normal' menstrual bleeding. RT-qPCR quantification of chemokine *CCL2* and *CXCL8* (A, B) and of inflammatory cytokine *IL6* and *TNFA* (C, D) mRNA levels in the endometrium of women with objectively-measured normal menstrual bleeding (MBL < 80 mL), with data analysed by $\Delta\Delta C_q$ method and normalised to *ATP5B* mRNA levels. * $p < 0.05$, *** p < 0.01, *** p < 0.001, **** p < 0.0001; significance determined 2-way ANOVA with Tukey's multiple comparisons test. ATP5B = adenosine triphosphate synthase subunit beta, mitochondrial, CCL2 = C-C motif chemokine ligand 2, C_q = quantification cycle, CXCL8 = C-X-C chemokine ligand 8, E_2 = oestradiol, IL6 = interleukin-6, MBL = menstrual blood loss, mL = microlitre, P_4 = progesterone TNFA = tumour necrosis factor alpha.*

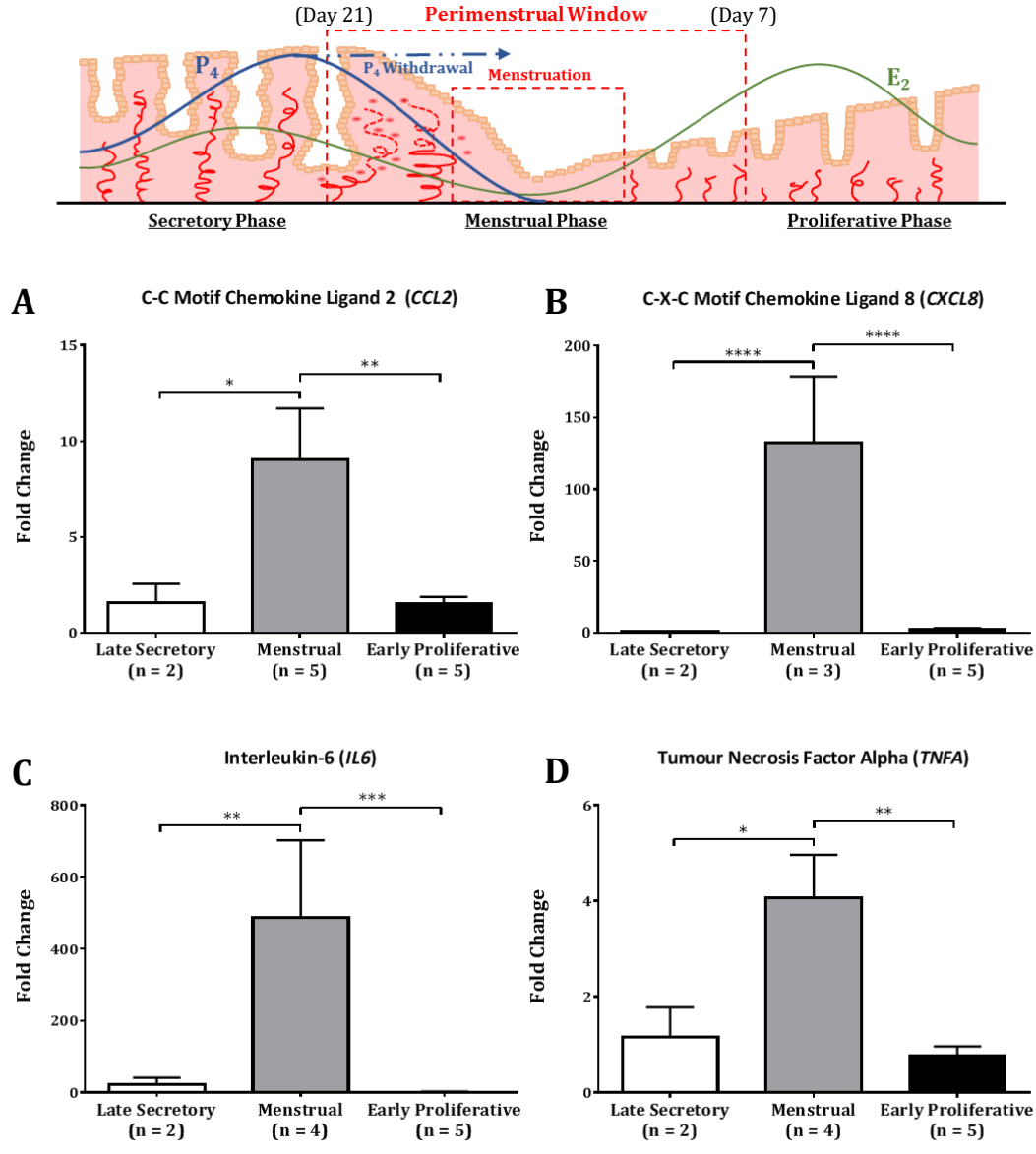

3.3.4 Neutrophil & Macrophage Co-localisation in Menstrual-Phase Endometrium

Neutrophils and macrophages, immunopositive for neutrophil elastase and CD68 respectively, were both found in abundance in menstrual phase human endometrium (**Figure 18A**), but were not observed in close association with one another. Elastase-immunopositive neutrophils were most often observed close to the surface epithelium and within areas of the stroma with particularly disturbed structural integrity (**Figure 18C**), while CD68-immunopositive macrophages were more often observed in association with glands and adjacent to areas of disturbed structural integrity (**Figure 18B**).

Figure 18. Neutrophils (elastase$^+$) and macrophages (CD68$^+$) are abundant in the shedding menstrual-phase human endometrium. A) Representative immunofluorescent photomicrograph of CD68 (blue; 1:200, Dako) and elastase (red; 1:1000, Dako) staining in menstrual phase human endometrium (menstrual day 1). B, C) Higher power photomicrographs. Blue-outlined arrows indicate CD68$^+$ cells; red-outlined arrows indicate elastase$^+$ cells. *Blue box in diagram depicts menstrual phase. Nuclear counterstain: Sytox Green (green; Molecular Probes Inc.). Scale bars (50 µm, 10 µm) in image.*

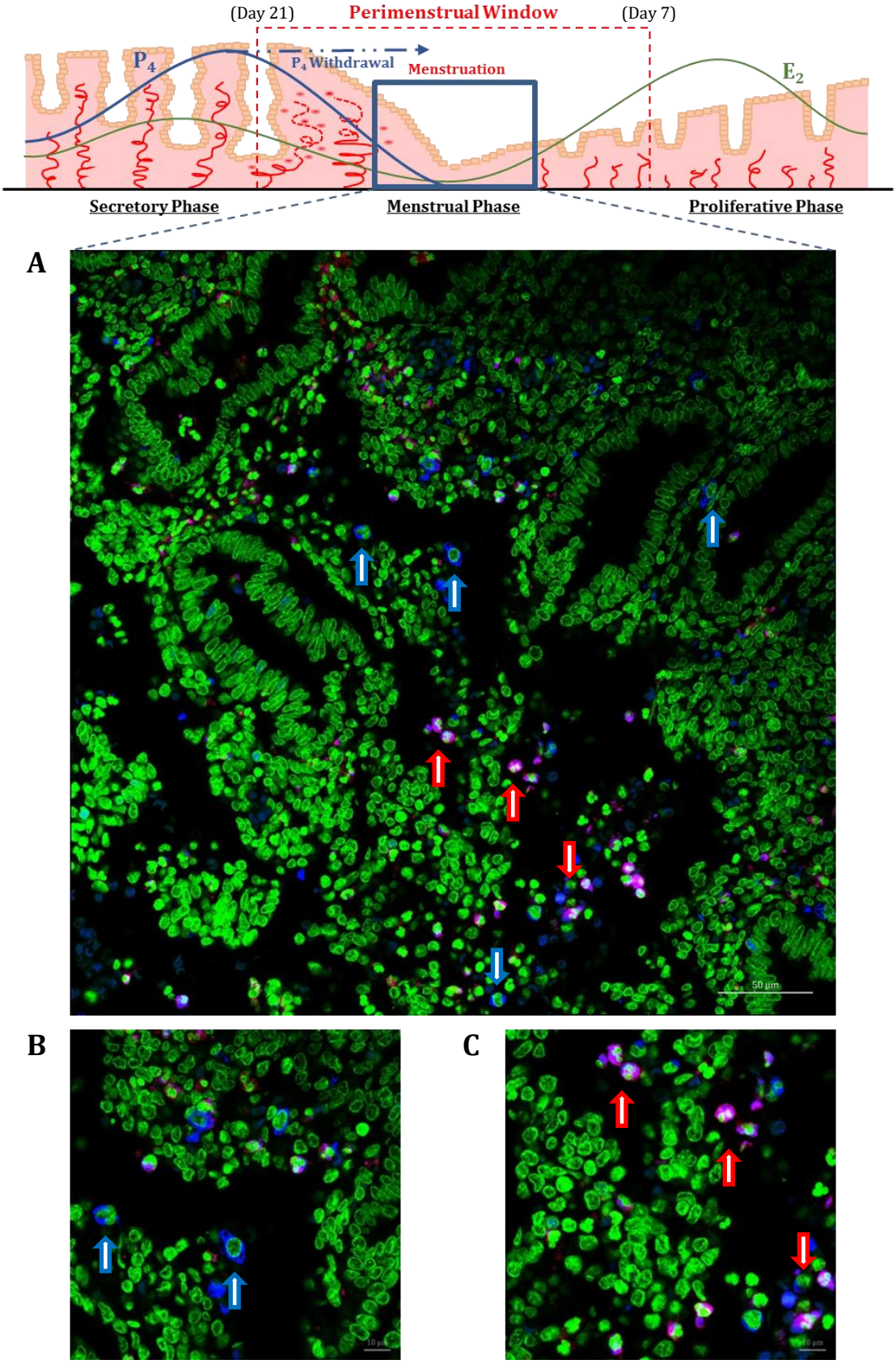

3.3.5 Macrophage & Apoptosis Co-localisation across the Perimenstrual Window

Macrophage ($CD68^+$) co-localisation with the apoptosis marker, cleaved caspase-3, was investigated in endometrial tissues across the perimenstrual window, revealing apoptotic cells within (and immediately basal to) the endometrial glands of late secretory phase tissues (**Figure 19**, **Figure 20**), and revealing macrophages in close association therewith (**Figure 19C**, **Figure 20C**) and actively phagocytosing apoptotic bodies (**Figure 19B**, **Figure 20B**).

Menstrual phase endometrial tissues continued to show frequent incidence of apoptotic bodies found in and around endometrial glands – basally in particular (**Figure 22B**, **C**) – and while macrophages continued to be observed phagocytosing apoptotic material (**Figure 21B**), double-positive macrophages ($CD68^+$, cleaved caspase-3^+) began to be found in the stroma of the endometrium as well (**Figure 21C**), away from the glands. These double-positive macrophages seemed to show more uniform expression of cleaved caspase-3, rather than the discrete cleaved caspase-3^+ bodies seen in actively-phagocytosing macrophages adjacent to glands.

A very different pattern of macrophage and cleaved caspase-3 localisation and expression emerged from the investigation of early proliferative phase endometrial tissues, with apoptosis no longer detectable in the (now less tortuous) glands, and macrophages much more seldom found in association therewith (**Figure 23B**). Macrophages were still reasonably abundant, though far more often found in the endometrial stroma distant from glands, and often immunopositive for cleaved caspase-3 (**Figure 24B**). Cleaved caspase-3 expression, when found in macrophages, was uniform across the cells; never in discrete intracellular bodies.

Figure 19. Apoptotic bodies (cleaved caspase-3^{+}) pushed basally from the glands of the late-secretory-phase human endometrium, nearer to macrophages (CD68^{+}). A) Representative immunofluorescent photomicrograph of CD68 (blue; 1:200, Dako) and cleaved caspase-3 (red; 1:500, Cell Signalling Tech.) staining in late secretory phase human endometrium (menstrual day 28/-1). B and C) Higher power photomicrographs. *Menstrual day presented as days post-menses (positive)/days pre-menses (negative; see 3.2.1 Human Endometrial Tissue Collection). Blue box in diagram depicts late secretory phase. Nuclear counterstain: Sytox Green (green; Molecular Probes Inc.). Scale bars (50 µm, 10 µm) in image.*

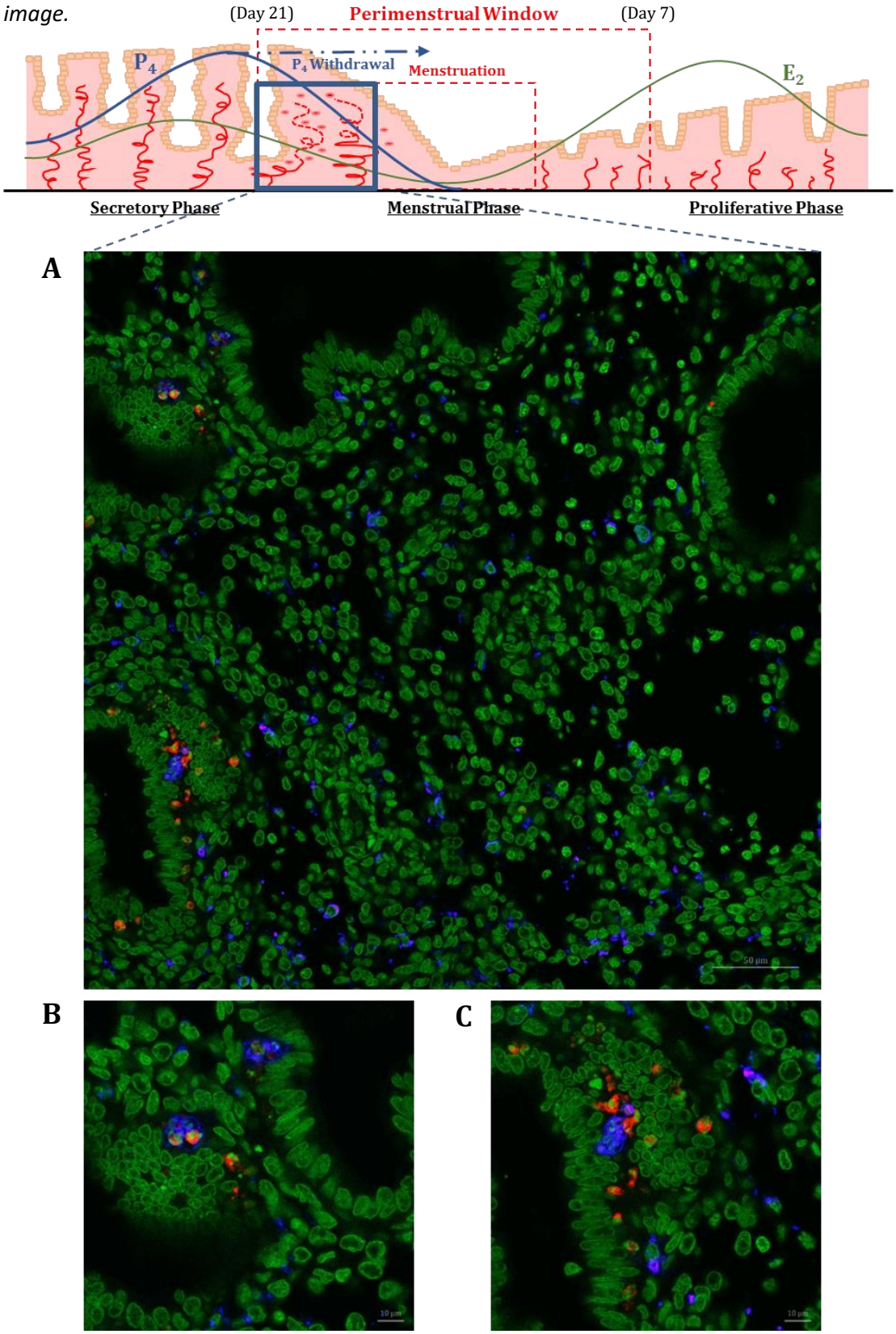

Figure 20. Macrophages (CD68^{+}) adjacent to endometrial glands in the late secretory phase, phagocytosing apoptotic bodies (cleaved caspase-3^{+}). A) Representative immunofluorescent photomicrograph of CD68 (blue; 1:200, Dako) and cleaved caspase-3 (red; 1:500, Cell Signalling Tech.) staining in late secretory phase human endometrium (menstrual day 28/-1). B and C) Higher power photomicrographs. *Menstrual day presented as days post-menses (positive)/days pre-menses (negative; see 3.2.1 Human Endometrial Tissue Collection). Blue box in diagram depicts late secretory phase. Nuclear counterstain: Sytox Green (green; Molecular Probes Inc.). Scale bars (50 µm, 10 µm) in image.*

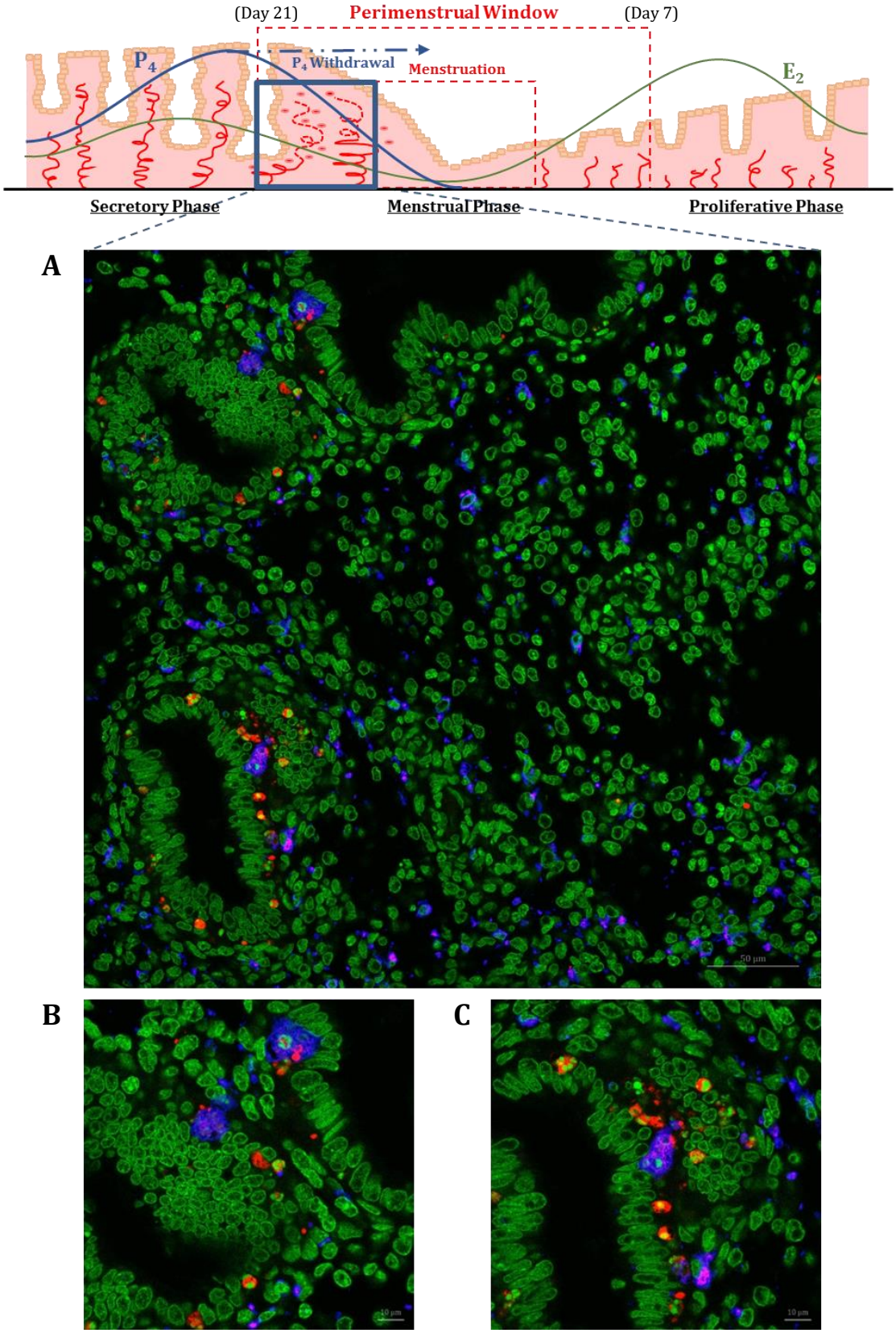

Figure 21. Co-localisation of macrophage (CD68) and apoptotic (cleaved caspase-3) markers found in endometrial stroma at menses. A) Representative immunofluorescent photomicrograph of CD68 (blue; 1:200, Dako) and cleaved caspase-3 (red; 1:500, Cell Signalling Tech.) staining in menstrual phase human endometrium (menstrual day 1). B and C) Higher power photomicrographs. *Blue box in diagram depicts menstrual phase. Nuclear counterstain: Sytox Green (green; Molecular Probes Inc.). Scale bars (50 µm, 10 µm) in image.*

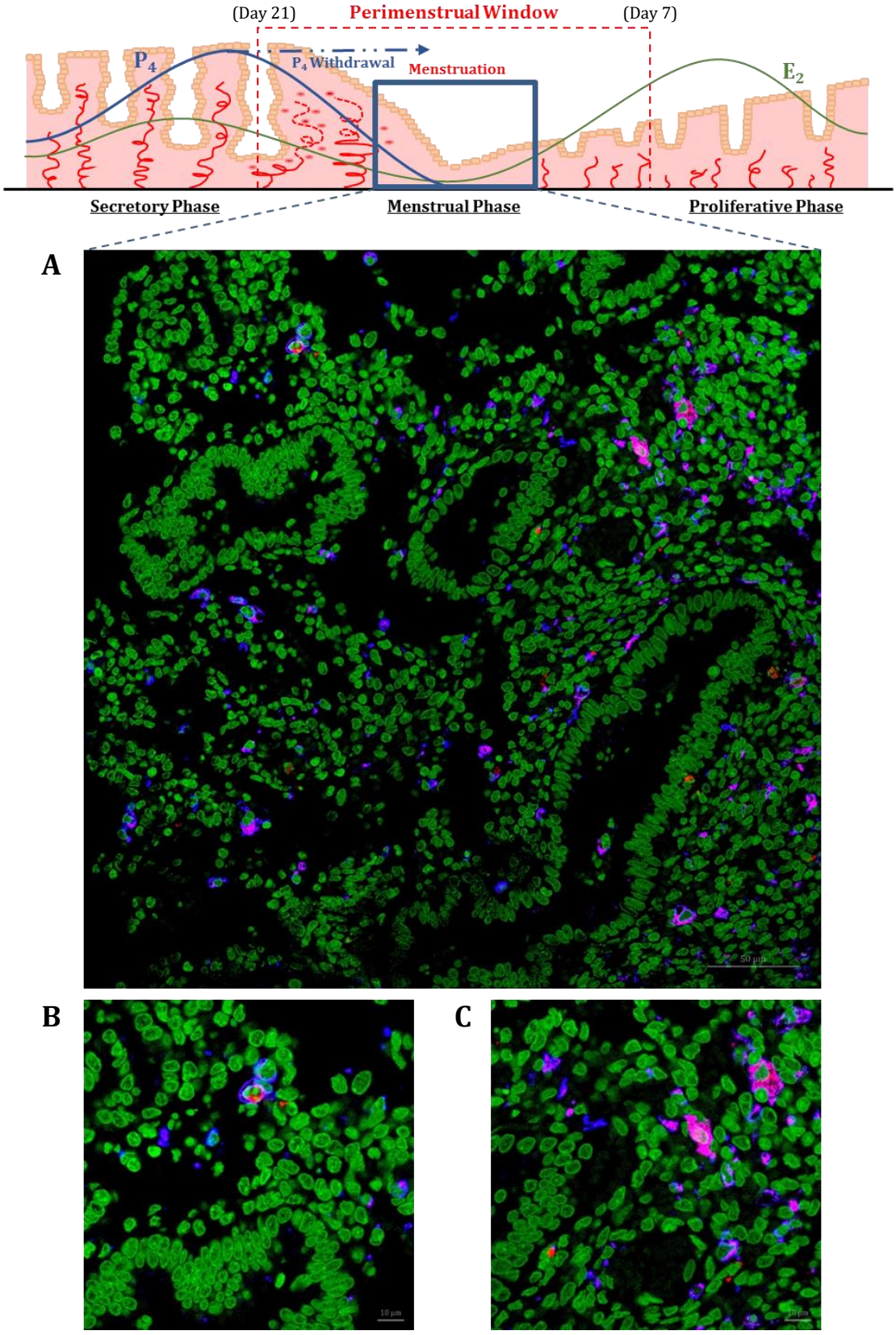

Figure 22. Apoptotic bodies (cleaved caspase-3^{+}) continue to be pushed basally from endometrial glands at menses. A) Representative immunofluorescent photomicrograph of CD68 (blue; 1:200, Dako) and cleaved caspase-3 (red; 1:500, Cell Signalling Tech.) staining in menstrual phase human endometrium (menstrual day 2). B and C) Higher power photomicrographs. *Blue box in diagram depicts menstrual phase. Nuclear counterstain: Sytox Green (green; Molecular Probes Inc.). Scale bars (50 µm, 10 µm) in image.*

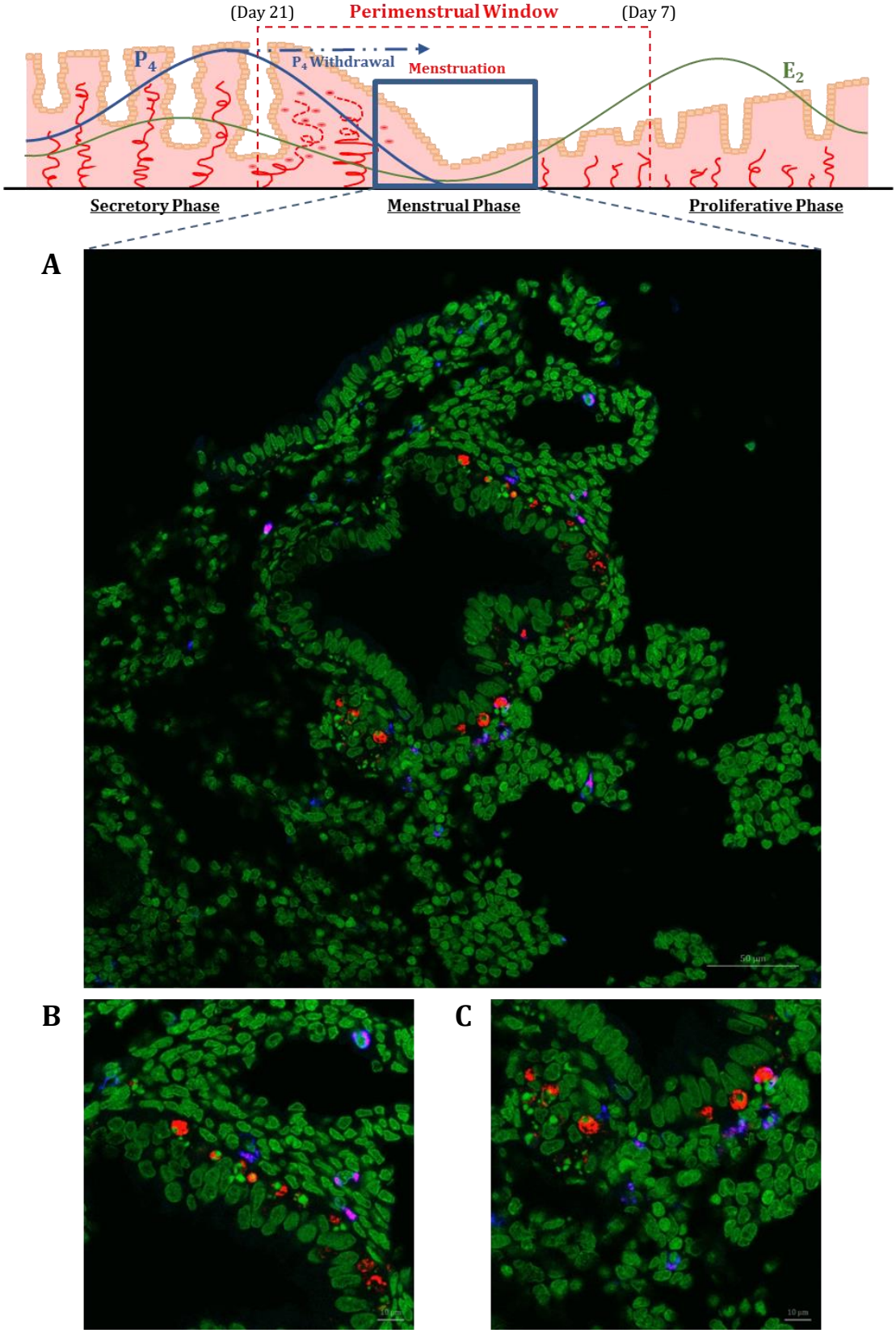

Figure 23. Double-positive macrophages (CD68^{+}, cleaved caspase-3^{+}) only seldom adjacent to glands and apoptotic bodies (cleaved caspase-3^{+}) no longer found in endometrial glands of the early proliferative phase. A) Representative immunofluorescent photomicrograph of CD68 (blue; 1:200, Dako) and cleaved caspase-3 (red; 1:500, Cell Signalling Tech.) staining in proliferative phase human endometrium (menstrual day 7). B) Higher power photomicrograph. *Blue box in diagram depicts early proliferative phase. Nuclear counterstain: Sytox Green (green; Molecular Probes Inc.). Scale bars (50 µm, 10 µm) in image.*

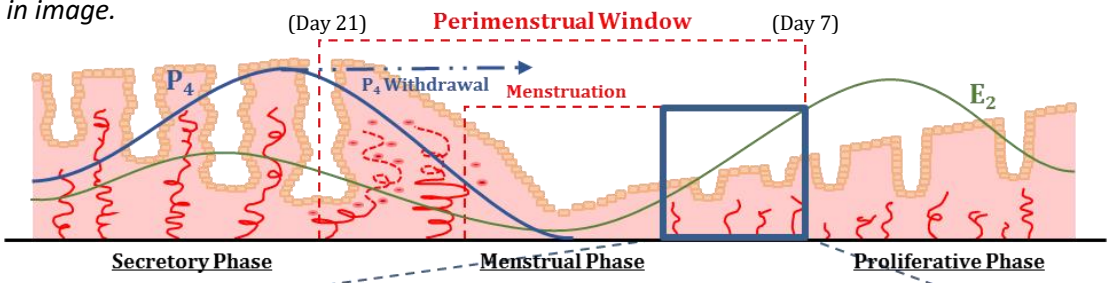

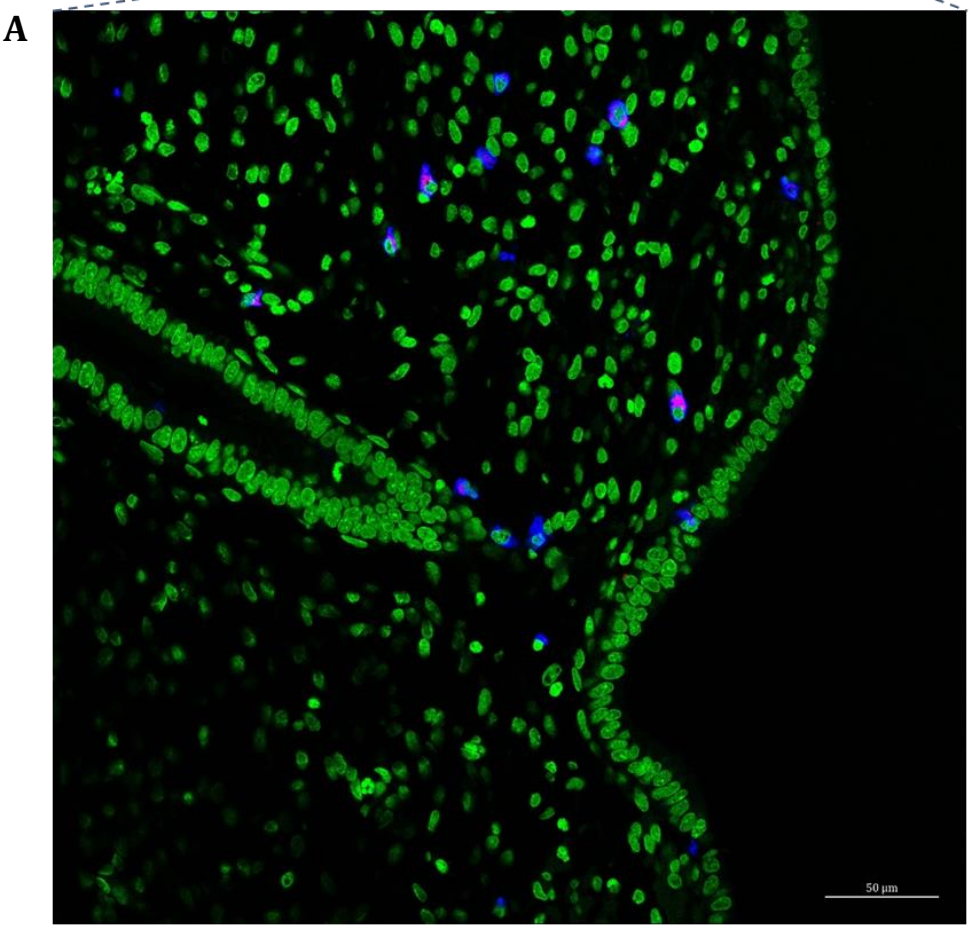

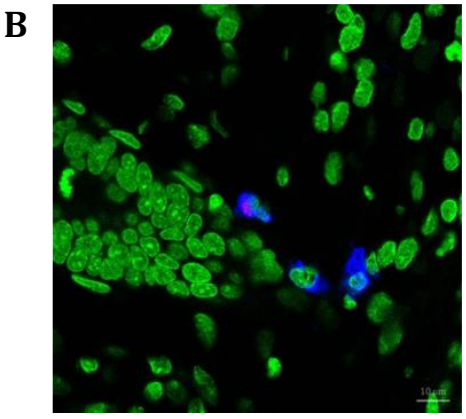

Figure 24. Macrophages double-positive for CD68 and cleaved caspase-3 are abundant in the endometrial stroma of early proliferative phase. A) Representative immunofluorescent photomicrograph of CD68 (blue; 1:200, Dako) and cleaved caspase-3 (red; 1:500, Cell Signalling Tech.) staining in proliferative phase human endometrium (menstrual day 7). B) Higher power photomicrograph. *Blue box in diagram depicts early proliferative phase. Nuclear counterstain: Sytox Green (green; Molecular Probes Inc.). Scale bars (50 µm, 10 µm) in image.*

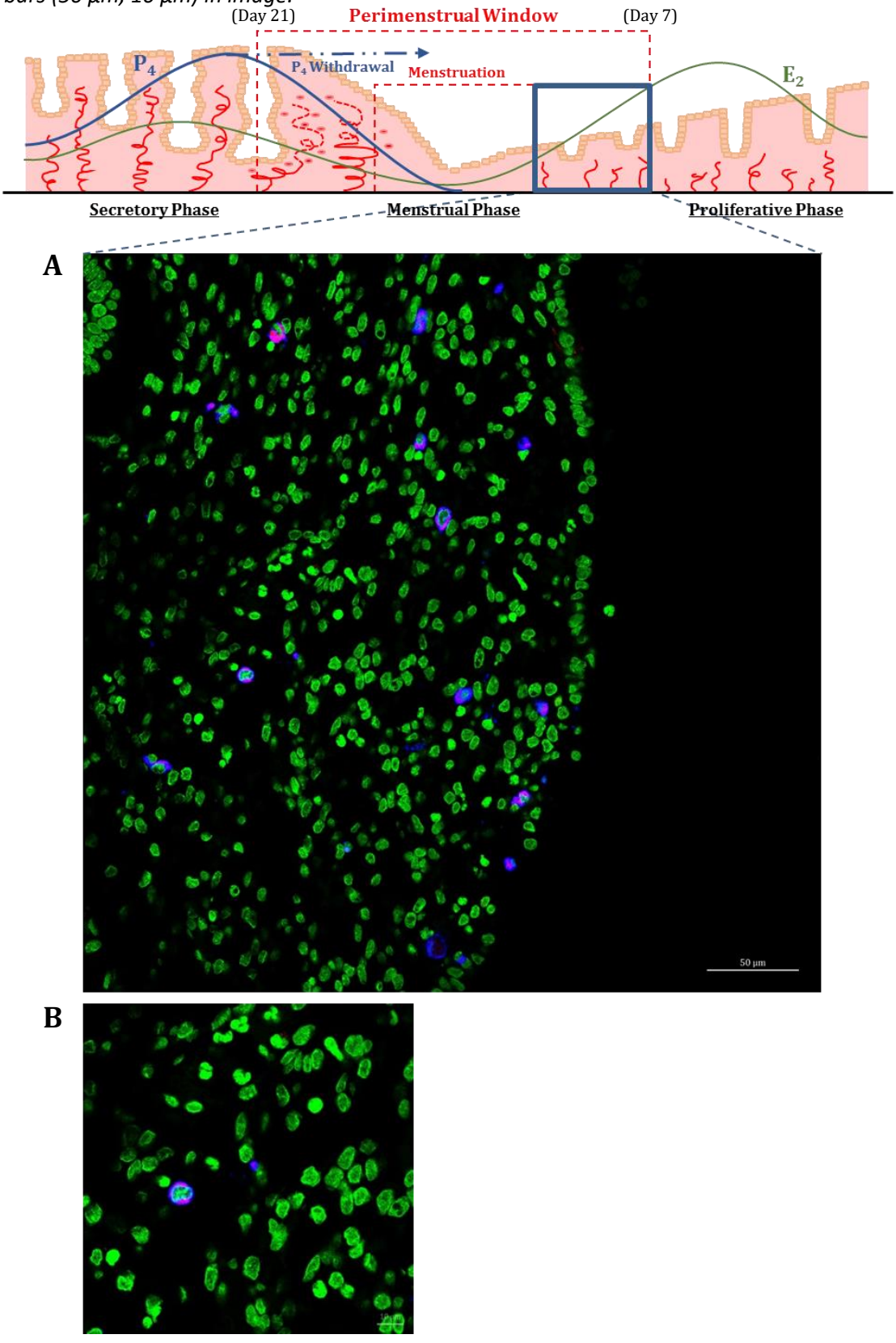

3.4 Discussion

3.4.1 Cleaved Caspase-3 & Apoptosis

The immunohistochemical and semi-quantitative histoscoring data of this chapter describe significant increases in apoptosis in the human endometrium across the perimenstrual window, preceding cessation of menstruation and restoration of tissue in the proliferative phase. Mean menstrual cycle phase cleaved caspase-3 immunoreactivity histoscores were significantly higher in the glands of the late secretory menstrual phases than in the glands of the proliferative phase, and significantly higher in the endometrial stroma in the menstrual phase than in the proliferative phase.

Data plotted from individual patient samples, meticulously characterised and selected to span the days preceding, during and following menstruation, revealed subtleties to the expression profile of cleaved caspase-3 in proliferative-phase endometrial tissues: far from exhibiting uniform levels of apoptosis throughout the phase, all measureable cleaved caspase-3 expression occurred in samples taken at days earliest in the phase (menstrual cycle days 5 – 7) with expression undetectable thereafter (days 8 – 11). This is of particular interest, given that these 'very early proliferative' phase samples were otherwise histologically indistinguishable from their 'late-early proliferative' phase counterparts, yet were clearly still engaged in the process of apoptotic remodelling.

The data presented in this chapter were all generated from 'full-thickness' endometrial tissue biopsies (described in 2.1.1 Human Endometrial Tissue Collection), and thus gave what were felt to be reliable and complete measurements of apoptosis through

the entirety of the endometrium – estimates that might otherwise have been incomplete had the tissue samples been derived by endometrial sampling (e.g. 'Pipelle' tissue biopsies).

To better compare endometrial samples derived from the late secretory phase, menstrual cycle days were presented both conventionally (as days following the last menstrual period) and as days until the likely onset of menses, determined by subtracting the menstrual cycle day from the average of the patient's reported minimum and maximum cycle lengths in days (described in further detail in 2.1.3 Perimenstrual Window (Luteo-Follicular Transition)). Presenting patient menstrual cycle day as 'days until menses', even if only as an estimate, gave what was felt to be a better indication of the timing of events leading up to menstruation.

Previous studies have undertaken to investigate apoptosis in the endometrial glands (Stewart *et al*., 1999), though only in proliferative-phase samples (where they describe apoptosis as present). The authors sought to determine levels of apoptosis by broad agreement of terminal deoxynucleotidyl transferase (TdT)-mediated dUTP-biotin nick end labelling (TUNEL) staining with morphological assessment of apoptotic criteria (namely a clearly-defined, rounded intraepithelial structure containing basophilic, pyknotic chromatin material; Kerr *et al*., 1972). The investigations into apoptosis described in this chapter used tissues spanning the perimenstrual window (late secretory, menstrual and early proliferative phases), and employed cleaved caspase-3 immunostaining a method of apoptosis detection superior to TUNEL staining (Duan *et al*., 2003). TUNEL staining, unlike cleaved caspase-3 staining, suffers a number of false-negative- and -positive-generating pitfalls: apoptotic cells which have not yet undergone chromatin fragmentation (Wyllie *et al*., 1984) will fail to be detected, whereas cells undergoing active gene transcription (Kockx *et al*., 1998), autolysis

(Grasl-Kraupp *et al*., 1995) or in tissues which have been exposed to certain tissue fixation and processing techniques (Baron *et al*., 2000) will be inappropriately labelled.

Other studies previously conducted which concern apoptosis in the human endometrium have investigated ectopic endometrial apoptosis as a potential discriminator of ovarian endometriosis from adenomyosis (Suganuma *et al*., 1997), or have looked at the effects of levonorgestrel-releasing intrauterine systems (LNG-IUS) on endometrial apoptosis (Maia *et al*., 2005; Maruo *et al*., 2001), but have not sought to carefully delineate the dynamics of apoptosis across menstruation in the normal human endometrium.

One difficulty encountered in the experiments of this chapter was the characterisation of cleaved caspase-3 immunoreactivity in the surface epithelium – tissues which were often lost to menstrual shedding. The expression profile of cleaved caspase-3 in the surface epithelium of the endometrium is likely to follow a similar course to that of the glandular epithelium, though it proved difficult to obtain reliable measurements for this due to its shedding in the menstrual phase. When present, as in the early-proliferative-phase endometrium, the surface epithelium showed no appreciable cleaved caspase-3 expression; but the underrepresentation of the surface epithelium at menstruation too much hampered a reliable comparison between menstrual phases, therefore these data were not shown.

3.4.2 Neutrophil Recruitment

Further described in this chapter were significant increases in neutrophil abundance in the menstrual-phase endometrium relative to both late-secretory- and proliferative-

phase endometrium, as determined by immunostaining for neutrophil elastase and myeloperoxidase (MPO) and stereological cell counting.

As with the cleaved caspase-3 immunoreactivity data, the neutrophil quantification data presented in this chapter made exclusive use of 'full-thickness' endometrial tissue biopsies (described in 2.1.1 Human Endometrial Tissue Collection), facilitating more reliable and complete measurements through the entire endometrium. In tissues otherwise derived, for instance by endometrial suction curettage ('Pipelle' biopsies), these quantification data might have overrepresented neutrophil numbers.

Of particular interest in this dataset, when histoscores were plotted from individual patient samples by menstrual cycle day, was that the most significant increases in elastase$^+$ neutrophil abundance were observed early in the menstrual phase (menstrual cycle days -1/0 to 1), after which neutrophil abundance decreased steadily from menstrual cycle day 2 onward.

In contrast to the cleaved caspase-3 immunoreactivity profile, neutrophils were not present in the endometrium to any appreciable extent before the advent of overt menstruation, but exhibited a precipitous increase in number thereafter.

The neutrophil abundance data generated in this chapter conflict with data reported by Salamonsen and Woolley (1999; courtesy of Maria Jeziorska), which showed elastase$^+$ neutrophils comprising some 6 – 15% of the endometrial stroma on menstrual days 26 – 28 (which the authors designate 'menses'). The data presented in this chapter show a stromal neutrophil (elastase$^+$) abundance of never more than 1% in samples from these menstrual cycle days, and even in tissue samples more properly designated 'menstrual phase', not more than 1 – 10% of the total endometrial stroma (mean ± SEM = 4.902 ± 1.321%). It is likely that the data presented by Salamonsen and Woolley (1999) represent a less-complete picture of neutrophil abundance in the human endometrium

perimenstrually, having not utilised exclusively 'full-thickness' endometrial samples as these studies have done, nor having characterised samples by all three criteria of (1) histological appearance first detailed by Noyes *et al.* (1950), (2) last menstrual period (LMP) and (3) serum progesterone and oestradiol concentrations (see 2.1.2 Dating of Endometrial Biopsies). For these reasons, the data presented herein are felt likelier to represent true neutrophil population dynamics in the human endometrium across the perimenstrual window.

A difficulty encountered in quantifying perimenstrual neutrophil numbers in the endometrium was one of statistical concern: the total number of cells which must be counted to achieve a given percent standard error (%SE) value increases in linear proportion with the decrease in immunopositive cell abundance (see 2.5.1 Stereological Microscopy). The less abundant a cell is, the more total cells must be counted to achieve the same certainty in the measurement; and as cell abundance approaches zero, the total cell count required approaches infinity.

What in a tissue of modest cell abundance is an issue of impracticality is therefore in a tissue of very meagre cell abundance an issue of outright impossibility – tissue samples with low neutrophil abundance may simply not contain enough total endometrial cells to support counting sufficient to achieve a percent standard error of less than 5%.

In all but three patient samples examined herein, neutrophil abundance was too low to count cells sufficient to achieve a standard error of less than 5% (see 2.5.1 Stereological Microscopy for %SE calculations); this is indicated by bars without explicitly-stated %SE values appearing above them (**Figure 13A**).

Though these studies demonstrate neutrophil abundance decreasing through the menstrual and proliferative phases of the menstrual cycle, a mechanism for this

decrease has not been investigated. Neutrophils, once recruited to sites of inflammation and activated (often by the same chemokines), largely do not re-enter circulation, with the exception of those from 'marginated pools' found intravascularly in the spleen, liver, bone marrow and lung (Peters *et al*., 1985; Ussov *et al*., 1995). It may therefore be supposed that infiltrating endometrial neutrophils are cleared from the endometrium by one or several of the following means:

1. Menstrual shedding – neutrophils may be lost alongside shedding endometrial tissue
2. Lymphatic drainage – neutrophils may exit the tissue via the lymphatic system
3. NETosis – neutrophils may be eliminated from the tissue by forming neutrophil extracellular traps (Brinkmann *et al*., 2004)
4. Apoptotic cell death – neutrophils may undergo apoptosis and be subsequently cleared by resident phagocytic cells

That neutrophils may be lost 'passively' by menstrual shedding is a hypothesis testable by fluorescence-activating cell sorting (FACS) analysis of menstrual eluent for elastase-immunopositive cells – it seems implausible that at least some neutrophils are not lost in this manner.

Neutrophil migration to lymph nodes following infection is well described (Abadie *et al*., 2005; Chtanova *et al*., 2008; Maletto *et al*., 2006), therefore it is not unlikely that this occurs subsequent to 'physiological' neutrophil recruitment in the endometrium.

If endometrial neutrophils undergo NETosis to any significant extent in the endometrium, they would likely still be immunoreactive for neutrophil elastase, given that NETs are typically impregnated with neutrophil elastase subsequent to their formation (Urban *et al*., 2009), and therefore detectable immunohistochemically.

With respect to apoptosis and phagocytic clearance, there is considerable basis upon which to advance such a hypothesis. Firstly, neutrophils are thought to be among the shortest-lived of any leucocyte, with a lifespan in circulation previously estimated at less than 8 hours (Dancey *et al*., 1976; though more recent *in vivo* work suggests the neutrophil's 'circulating lifespan' in humans may be as much as 5.4 days; Pillay *et al*., 2010). Secondly, neutrophils readily undergo apoptosis in order to help terminate inflammatory response and progress tissue repair (Savill *et al*., 1989a; Grigg *et al*., 1991), with apoptosis being the major means of neutrophil disposal in animal models of inflammation (Sanui *et al*., 1982; Savill *et al*., 1992; Cox *et al*., 1995).

Neutrophil apoptosis contributes to the resolution of inflammation by rendering neutrophils unable to respond to extracellular, degranulation-inducing stimuli and thereby decreasing inflammatory mediator secretion (Whyte *et al*., 1993). It also allows them to be recognised by phagocytic macrophages via the expression of so-called 'eat me' signals and subsequently engulfed and degraded (Savill *et al*., 1989b; Fadok *et al*., 1998).

In the work detailed in this chapter, macrophages were observed in some abundance across the perimenstrual window, often immunopositive for cleaved caspase-3 and in some cases visibly engaged in the process of engulfing apoptotic cells and debris (see 3.4.4 Macrophage Localisation).

The majority of apoptosis taking place in the endometrium in the late secretory and menstrual phases appears to be constrained to the glandular epithelium, but apoptosis is also significantly increased in the endometrial stroma of the menstrual phase. At least some of these stromal cells undergoing apoptosis may be comprised by neutrophils.

Taken together, these data are not inconsistent with the hypothesis that neutrophil apoptosis and phagocytic clearance are a mechanism for the elimination of neutrophils

from the endometrium. Further work investigating immunofluorescent co-localisation of apoptosis and neutrophil markers across the perimenstrual window could shed light on the fate of endometrial neutrophils, though this may underrepresent the number of apoptotic neutrophils present in the tissue: apoptotic neutrophils are rapidly engulfed and degraded by macrophages, therefore their immunoreactivity to neutrophil-specific antibodies is likely unreliable.

3.4.3 Inflammatory Gene Transcription & Expression

Transcriptional changes in the inflammatory chemokines and cytokines investigated in this chapter revealed statistically significant increases in *CCL2* (*MCP1*), *CXCL8* (*IL8*), *IL6* and *TNFA* at menstruation relative to the late secretory and early proliferative phases. These findings corroborate some of the existing literature regarding chemokine transcription in the endometrium across the menstrual cycle (Jones *et al*., 1997a; Milne *et al*., 1999; Maybin *et al*., 2011), though are the first to do so in endometrial tissues so carefully characterised for menstrual cycle staging (see 2.1.2 Dating of Endometrial Biopsies) and for 'normal' menstrual blood loss (see 2.1.1 Human Endometrial Tissue Collection). This chapter's findings regarding *IL6* and *TNFA* transcription are the first to demonstrate its upregulation at menstruation.

C-C motif chemokine ligand 2 (CCL2, also known as MCP-1) is a potent chemoattractive and activating molecule which acts primarily on monocytes, and to a lesser extent on NK cells and basophil granulocytes (Allavena *et al*., 1994; Hartmann *et al*., 1995). It is reportedly expressed and secreted by certain lymphocytes (Yoshimura *et al*., 1989a), fibroblasts (Yoshimura and Leonard, 1990), endothelial cells (Sica et al., 1990a) as well

as by monocytes themselves (Yoshimura *et al*., 1989b), with its expression increased in response to pro-inflammatory stimuli such as TNFα and IL-1β (Baggiolini *et al*., 1994). Chemotaxis and activation are induced in monocytes and macrophages through the binding of CCL2 to its high-affinity receptor CCR2 (Charo *et al*., 1994; Graves *et al*., 1999). CCR2 has been reported to be expressed by neutrophils (Iida *et al*., 2005), apparently inducing their transmigration into tissues *in vivo* (Reichel *et al*., 2009)

Endometrial CCL2 immunoreactivity has been reported as highest in the late secretory phase relative to the early secretory phase (Jones *et al*., 1997a), but no description was made of *CCL2* transcription.

The data presented in this chapter found significantly higher transcription of *CCL2* in the menstrual phase relative to the late secretory phase, though this is not necessarily in conflict with Jones *et al*.'s findings – posttranscriptional regulation may prevent the increased levels of *CCL2* mRNA transcript observed in these studies from being translated into equivalently increased quantities of CCL2 protein.

CXCL8 (also known as IL-8), a chemokine belonging to the C-X-C motif family of chemokines, is a very potent neutrophil chemoattractant and activator, inducing mobilisation from bone marrow, adhesion to endothelial cells, extravasation from peripheral blood into tissues and degranulation in tissues (Zhang *et al*., 2001). Binding of CXCL8 is mediated by its cognate receptors, CXCR1 and CXCR2 (Huber *et al*., 1991; Jones *et al*., 1997b), which are highly expressed by neutrophils. CXCR1 and 2 are also expressed by endothelial cells (Murdoch *et al*., 1999), for which they also reportedly act as a chemotactic factor, mediating CXCL8's role in angiogenesis (Koch *et al*., 1992; Strieter *et al*., 1995a, 1995b).

CXCL8 production is described in fibroblasts, endothelial cells, epithelial cells and monocytes (Baggiolini *et al*., 1994) and is stimulated in neutrophils by adherence to

endothelium (Strieter *et al*., 1990) and various toll-like receptor (TLR) agonists, including the bacterial product lipopolysaccharide (LPS; Bazzoni *et al*., 1991; Strieter *et al*., 1990) and the fungal product zymosan (Schröder *et al*., 2006). TNFα, in concert with LPS and/or interferon gamma (IFNγ), is also reportedly able to stimulate the production of CXCL8 in neutrophils (Scapini *et al*., 2000).

Neutrophil apoptosis is reportedly inhibited by CXCL8 *in vitro* (Colotta *et al*., 1992; Dunican *et al*., 2000), though in other studies, CXCL8 failed to suppress neutrophil apoptosis (Ottonello *et al*., 2002); there is little evidence for its inhibition of neutrophil apoptosis *in vivo* (Ertel *et al*., 1998).

In the normal human endometrium, CXCL8 expression has been described across the menstrual cycle (Jones *et al*., 1997a; Maybin *et al*., 2011) in stromal cells (Arici *et al*., 1993, 1996) as well as in blood vessel perivascular cells (Critchley et al., 1994a; Milne et al., 1999). Maybin *et al*. (2011) reported significant increases in *CXCL8* transcription and protein expression in the menstrual phase, wherein it has been suggested to play a role in menstrual repair.

Data presented in this chapter closely corroborate the findings of previous studies regarding *CXCL8* transcription, finding significantly higher levels of *CXCL8* mRNA in endometrial samples of the menstrual phase relative to those of the late secretory and early proliferative phases.

IL-6 is a pleiotropic immunoregulatory cytokine which orchestrates a number of pro- and anti-inflammatory effects. Early studies into IL-6 uncovered its pro-inflammatory functions, namely its regulation of the production of hepatic acute phase proteins such as C-reactive protein and complement factors (Akira and Kishimoto, 1992). IL-6 was also found to suppress neutrophil apoptosis through Bax downregulation, as well as to inhibit the spontaneous activity of caspase-3 (Ottonello *et al*., 2002).

More recent studies, however, suggest a more complex role for IL-6: in healthy humans, lipopolysaccharide (LPS) induction of TNFα expression is inhibited by the co-administration of recombinant IL-6 (Starkie *et al*., 2003); and in mice, staphylococcal enterotoxin B (SEB) induction of TNFα and interferon gamma (IFNγ) expression is increased with the co-administration of IL-6-neutralising antibodies (Matthys *et al*., 1995). This concept of IL-6 as an inflammation-limiting molecule has been furthered by still more recent studies undertaken by Mauer *et al*. (2014), in which IL-6 is implicated in the induction of alternative macrophage activation. IL-6 seems capable therefore of bridging pro- and anti-inflammatory responses, facilitating the resolution of inflammation rather than simply potentiating inflammation.

Dynamic endometrial transcription of *IL6* across the menstrual cycle has been reported, with peak transcription found in the late secretory phase (von Wolff et al., 2000); studies undertaken by these authors however failed to investigate transcription in menstrual-phase samples. Further work corroborated these transcriptional data with protein expression data, demonstrating peak IL-6 expression in the late secretory phase, localised to the endometrial glands and its secretions (von Wolff et al., 2002). As before, however, the authors did not investigate its expression in menstrual-phase samples.

The *IL6* transcriptional data presented in this chapter demonstrate a significant increase in *IL6* mRNA transcript at menses relative to the late secretory and early proliferative phases, as yet undescribed in the literature.

Tumour necrosis factor alpha (TNFα) is an inflammatory cytokine produced principally by activated macrophages and T-cells (Black *et al*., 1997), as well as by neutrophil granulocytes (Bennouna *et al*., 2003; Denkers *et al*., 2003). It was first discovered in the serum of bacillus-Calmette-Guérin- (BCG)-infected mice following LPS

administration (Carswell *et al*., 1975), and was quickly appreciated for its myriad inflammatory activities: it is the central regulator of LPS-induced endotoxic shock (Beutler *et al*., 1985; Tracey *et al*., 1986), it mediates neutrophil adherence to endothelial cells (Gamble *et al*., 1985), induces apoptosis in endothelial cells *in vitro* (Robaye *et al*., 1991), accelerates constitutive neutrophil apoptosis (Murray *et al*., 1997), and potentiates the expression of CXCL8 and CCL2 chemokines in endothelial cells (Sica *et al*., 1990a, 1990b).

In the endometrium, TNFα expression has been described in some detail (Hunt *et al*., 1992), thought to be expressed in endometrial stromal and epithelial cells (Tabibzadeh, 1991) and implicated in menstrual tissue shedding (Tabibzadeh *et al*., 1995). *TNFA* mRNA levels are reportedly increased in the late-secretory-phase endometrium (von Wolff et al., 2000), though as with the authors' investigation of *IL6* transcription, no menstrual-phase samples were included in the sample cohort.

The data in this chapter demonstrate that *TNFA* is subject to significant transcriptional upregulation at menses, with menstrual-phase levels of *TNFA* mRNA higher than those of both the late secretory and early proliferative phases.

The RT-qPCR and Western blotting data presented in this chapter were obtained from a mixture of 'full-thickness' and 'Pipelle' tissue samples, fragments of which were taken to generate whole-tissue RNA and protein extracts. This being the case, it is possible that the upper layer of the endometrium ('zona functionalis') was overrepresented in comparison to the basal layer ('zona basalis').

Despite the great efforts taken in carefully characterising the menstrual phase and menstrual bleeding status of the endometrial tissue biopsies used in these experiments, the work suffered limited tissue availability and sample sizes, particularly for samples derived from biopsies of the late secretory and menstrual phases.

Augmented sample sizes would have been of great benefit to the transcriptional data and the analysis thereof, as well as to the Western blotting experiments to corroborate the transcriptional differences uncovered.

3.4.4 Macrophage Localisation

The immunofluorescent co-localisation data in this chapter present an interesting narrative with respect to the phagocytic clearance of apoptotic cells across the perimenstrual window, showing macrophages localising to endometrial glands almost as soon as apoptotic cells first begin to appear.

A number of double-positive stromal macrophages were observed ($CD68^{+}$/cleaved caspase-3^{+}) which could indicate macrophages in the process of undergoing apoptosis themselves. The absence of corroborating morphological changes, such as nuclear or cytoplasmic condensation or nuclear fragmentation, suggests that they are likely macrophages which contain considerable cleaved caspase-3 rather than macrophages expressing it themselves.

The principal interest of the work detailed herein was to determine where macrophages were (particularly in relation to apoptotic cells); not, as was the case with neutrophils, to quantify macrophage numbers present in the tissue. Endometrial macrophage dynamics have already been adequately described in the literature:

Macrophage populations in the endometrium are thought to represent contributions from two distinct sources: *in situ* proliferation of resident macrophages (Daems and De Bakker, 1982; Merad *et al*., 2002; Jenkins *et al*., 2011) and macrophages derived from monocytes recruited into the tissue (Doulatov *et al*., 2010; Schulz *et al*., 2012). Among the chemotactic stimuli by which monocytes are brought into the endometrium is CCL2

(MCP-1), which is highly expressed in the late-secretory-phase endometrium (Jones *et al*., 1997a).

Endometrial macrophage populations have been reported to be relatively stable across the menstrual cycle, increasing only in the late secretory/menstrual phase and early proliferative phase (Braun *et al*., 2002), though the authors of this study combined samples of the late secretory and menstrual phases into one group; a more recent study by Cominelli *et al*. (2014) described macrophage abundance as significantly increased only in the menstrual phase, relative to the proliferative and secretory phases.

Although macrophages have been described in the endometrium, these data are the first to demonstrate macrophages phagocytosing apoptotic bodies in the glands of the endometrium and to carefully characterise changes in their localisation across the perimenstrual window.

3.4.5 Summary & Conclusions

The data presented in this chapter show that apoptosis is extensive in the human endometrium from the late secretory phase, well in advance of overt menstrual shedding, and may be among the earliest detectable histological changes leading up to menses.

Further to this, this chapter's data expand upon and clarify existing literature regarding dynamic neutrophil populations across the perimenstrual window, showing them to be less numerous than previously supposed, though still among the most abundant non-resident cells of the endometrial stroma at menstruation. Macrophage localisation before, during and following menstruation was carefully delineated, demonstrating their trafficking to apoptotic glands and their subsequent movement into the stroma.

RT-qPCR experiments detailed in this chapter corroborated existing literature regarding the menstrual increases in transcription of *CCL2* and *CXCL8*, and uncovered similar increases in the transcription of *IL6* and *TNFA*. None of the above had previously been confirmed in the endometrium of women with objectively-verified 'normal' menstrual bleeding.

The novelty of these observational studies undertaken here lies in the use of exquisitely-characterised tissues, allowing accurate subdivision of menstrual cycle day and even 'premenstrual cycle day' for tissue samples. This improved 'resolution' allows for a better understanding of the dynamics of apoptosis and neutrophil recruitment across the perimenstrual window.

A summary of the observations detailed in this chapter is given in **Table 12**.

Table 12. Summary of observations in the human endometrium across the late secretory, menstrual and early proliferative phases of the menstrual cycle. Upward-facing arrows (↑) and shades of orange reflect increases in the observed quantity described in this chapter. White boxes without symbols reflect the absence of observation (cleaved caspase-3, CD68, Elastase, MPO) or 'baseline' for transcriptional changes. Novel data to which the summary table refer can be found on the pages listed in the right-most column. *LS = late secretory phase, M = menstrual phase, EP = early proliferative phase. * denotes statistical significance (p < 0.05 – 0.0001) for the observations described.*

Menstrual Phase	LS	M	EP	Pages
Apoptosis (cleaved caspase-3) in glandular epithelium	↑↑↑/*	↑↑↑/*		88, 89, 90
Apoptosis (cleaved caspase-3) in endometrial stroma		↑↑/*		88, 89, 90
Neutrophil infiltration (Elastase, MPO)		↑↑↑/*		92, 93, 94, 95
CCL2, *CXCL8*, *IL6*, *TNFA* transcription		↑↑↑/*		97
Macrophage (CD68) localisation proximal to endometrial glands	↑↑↑	↑↑↑	↑	101, 102
Double-positive macrophage (CD68/ cleaved caspase-3) localisation in endometrial stroma		↑	↑↑	103, 106

4. Neutrophil Recruitment and Apoptosis in a Mouse Model of Induced Menstruation

4.1 Introduction

In response to increased progesterone, the oestrogen-primed human endometrium undergoes extensive differentiation (termed 'decidualisation'), with endometrial stromal cells changing morphology and expressing a range of decidualisation factors such as prolactin and insulin-like growth factor-binding protein 1 (Brosens *et al*., 1999; Dunn *et al*., 2003). In humans, decidualisation occurs irrespective of embryonic/endometrial contact (i.e. implantation), and is therefore termed 'spontaneous decidualisation' (Finn, 1998). Should implantation fail to occur, however, the corpus luteum regresses and ceases to produce progesterone, triggering menstruation (Csapo and Resch, 1979).

Mice, along with other mammalian species whose endometria do not undergo spontaneous decidualisation (Finn, 1998), do not menstruate. In the absence of implantation in these species, withdrawal of progesterone alone does not initiate endometrial breakdown. Nevertheless, menstruation can be simulated in mice, the first foray into which was conducted more than 30 years ago (Finn and Pope, 1984): ovariectomised mice were administered sequential oestradiol and progesterone injections to mimic human endocrine regulation, and the endometrium was stimulated to undergo decidualisation with the intrauterine injection of oil. A significant refinement to this model was introduced more recently, substituting subcutaneously-implanted progesterone-releasing implants in place of progesterone injections (Brasted *et al*., 2003). Removal of the progesterone implant simulates corpus luteum regression, triggering menstrual-like molecular and histological changes. The studies described herein employ a modified version of this model (**Figure 8**).

In humans, menstruation is regarded an inflammatory phenomenon (Finn, 1986), exhibiting a range of inflammatory features such as leucocyte recruitment (King *et al*., 1996; Evans and Salamonsen, 2012) and leucocyte chemokine expression (Jones *et al*., 1997a; Milne *et al*., 1999). In studies undertaken in mouse models of menstruation, these features have also been shown to occur (Cheng *et al*., 2007; Menning *et al*., 2012).

Apoptosis acts generally to facilitate remodelling of tissue and the disposal of aged and infected cells; and more specifically to inflammation, to deactivate and eliminate infiltrating leucocytes and to influence phagocytic cell behaviour (Savill *et al*., 1989a, 2002). Cysteine-aspartic acid proteases (caspases) are critical effectors of apoptosis, with both intrinsically- and extrinsically-mediated apoptotic pathways converging on the cleavage and activation of caspase-3 (Slee *et al*., 2001; **Figure 3**).

4.1.1 Hypothesis & Research Questions

Hypothesis: Apoptosis and neutrophil recruitment are recapitulated in the endometrium of a mouse model of induced menstruation, and are components of the menstrual event which precede overt endometrial shedding.

Following progesterone withdrawal in a mouse model of induced menstruation…

1. When and where does apoptosis occur in the mouse endometrium?
2. When and in what numbers are neutrophils recruited to the mouse endometrium?
3. What changes occur in endometrial glucocorticoid receptor target gene transcription?

4.2 Materials & Methods

4.2.1 Mouse Model of Induced Menstruation

A mouse model of simulated menses has been optimised in which mice are ovariectomised and administered oestradiol and progesterone subcutaneously to mimic human menstrual endocrine regulation of the uterus (Finn and Pope, 1984; Brasted *et al*., 2003; Cheng *et al*., 2007; Cousins *et al*., 2014; see 2.7 Mouse Model of Induced Menstruation). Oil injection into the lumen of the uterus stimulates decidualisation, and upon withdrawal of progesterone, the endometrium exhibits a number of menstrual-like features. The tissue is subsequently repaired and restored.

Mice were sacrificed at 0, 4, 8 and 24 hours following progesterone withdrawal (**Figure 8**), and uterine horns were removed and weighed. Each uterine horn was split into two parts, one of which was processed by 4% NBF fixation and embedded in paraffin for immunohistochemistry studies, and the other of which was stored in RNA-stabilising reagent and stored at -80°C for RNA extraction.

Progesterone withdrawal periods are defined herein as:

- 0 – 8 hours post-progesterone withdrawal = simulated 'premenstrual' phase
- 8 – 16 hours post-progesterone withdrawal = simulated 'menstrual' phase
- 16 – 24 hours post-progesterone withdrawal = simulated 'early repair' phase

4.2.2 Immunohistochemistry

Cleaved caspase-3 and Ly6G (a neutrophil marker) localisation and immunostaining intensity were examined in mouse endometrial tissues following progesterone

withdrawal (n = 29; see 2.7 Mouse Model of Induced Menstruation), according to the immunohistochemical protocols described in 2.2 Immunohistochemistry. Progesterone withdrawal time-points of 0 hours (n = 9), 4 hours (n = 7), 8 hours (n = 6) and 24 hours (n = 7) were examined.

4.2.3 Semi-Quantitative Histoscoring

Localisation and expression intensity of cleaved caspase-3 in mouse endometrial tissues following progesterone withdrawal (n = 29; see 2.7 Mouse Model of Induced Menstruation) was investigated using a method of semi-quantitative histoscoring was employed (Aasmundstad *et al*., 1992; Wang *et al*., 1998; Critchley *et al*., 2006).

Each sample histoscore represents the average of histoscores from three 'complete' cross-sections through the tissue (in which the tissue was fully encircled by smooth muscle and all cellular compartments were present).

Full details of semi-quantitative histoscoring protocol can be found in 2.3 Semi-Quantitative Histoscoring.

4.2.4 Cell-Counting & Stereology

Stereological microscopy and ImageJ1 software-assisted (Schneider *et al*., 2012) cell-counting strategies were employed in combination to determine neutrophil abundance in mouse endometrial tissues following progesterone withdrawal (n = 29; see 2.7 Mouse Model of Induced Menstruation) immunostained for the neutrophil marker Ly6G.

A Leica DMRB stereology microscope (Leica Microsystems, Milton Keynes, UK) and Image-Pro Plus 7.0 software (Media Cybernetics UK, Wokingham, UK) were used for

'manual' cell counting. Full details of stereology microscopy protocols and standard error calculations can be found in 2.5.1 Stereological Microscopy.

'Semi-automated' cell counting was undertaken using a Leica DMRB stereology microscope (Leica Microsystems) or AxioScan slide scanner (Carl Zeiss Ltd.) to capture images for analysis. Ly6G-immunopositive cells were counted and normalised to the total number of cells using ImageJ1 software (Schneider *et al*., 2012) modified to detect immunohistochemically-stained nuclei by colour threshold and size discrimination criteria (Abigail Dobyns; Yellon *et al*., 2013). Full details of ImageJ1-assisted, semi-automated cell counting protocols can be found in 2.5.2 ImageJ1-Assisted Neutrophil Quantification.

4.2.5 RNA Extraction & RT-qPCR

Total RNA was extracted from mouse uterine tissues following progesterone withdrawal (n = 20 – 21; see 2.7 Mouse Model of Induced Menstruation) and cDNA was synthesised according to the protocols described in 2.6 RNA Extraction & Reverse Transcription Quantitative Polymerase Chain Reaction (RT-qPCR). Progesterone withdrawal time-points of 0 hours (n = 3), 8 hours (n = 9) and 24 hours (n = 8 – 9) were examined.

Levels of *Cxcl1* and *Tnfa* mRNA transcripts (see **Table 9**) were measured by TaqMan-(hydrolysis probe) based RT-qPCR assay in triplicate technical replicates and normalised to *Actb* mRNA levels as a housekeeping control: mouse liver cDNA was included as a positive control and appropriate negative controls were also included. Data were analysed $\Delta\Delta C_q$ (quantification cycle) method as described by Applied Biosystems (Warrington, UK).

Full details of RT-qPCR and data analysis protocols can be found in 2.6 RNA Extraction & Reverse Transcription Quantitative Polymerase Chain Reaction (RT-qPCR).

4.2.6 Glucocorticoid Receptor Target Gene Array

Differential transcription of glucocorticoid receptor target genes was investigated in the mouse endometrium following progesterone withdrawal (n = 24; see 2.7 Mouse Model of Induced Menstruation) by means of a Mouse Glucocorticoid Signalling RT^2 Profiler SYBR Green-based PCR Array (QIAGEN Ltd., Sussex, UK; see 2.6.5 Mouse Glucocorticoid Signalling PCR Array). Progesterone withdrawal time-points of 0 hours (n = 7), 8 hours (n = 7), 16 hours (n = 3) and 24 hours (n = 7) were examined.

Total RNA was extracted from mouse uterine tissues as described in 2.6 RNA Extraction & Reverse Transcription Quantitative Polymerase Chain Reaction (RT-qPCR), its quality was verified by means of an Agilent 2100 Bioanalyser system (Agilent Technologies, Cheshire, UK; see 2.6.2 RNA Quality Validation) and diluted to 0.125 μg/μL, then cDNA was synthesised using the commercially available RT^2 First Strand cDNA synthesis kit (QIAGEN Ltd.).

Levels of 84 gene transcripts involved in glucocorticoid receptor-mediated transcription (see **Table 10**) were measured by SYBR-Green-based PCR array, normalised to the geometric mean of a panel of internal, housekeeping controls included in the plates (*Actb*, *B2m*, *Gapdh*, *Gusb* and *Hsp90ab1*), then related to an internal control. Normalised data were subsequently analysed by 2-way ANOVA with Dunnett's multiple comparisons tests, with all comparisons made to pre-progesterone-withdrawal time-points (0h post-progesterone withdrawal).

4.3 Results

4.3.1 Localisation & Intensity of Apoptosis in the Mouse Endometrium at 0, 4, 8 & 24 Hours Post-Progesterone Withdrawal

Apoptosis was found extensive throughout the mouse endometrium from 8 hours following progesterone withdrawal (simulated 'premenstrual' phase; **Figure 25A**), where peak cleaved caspase-3 expression was observed in the decidualised stroma and surface epithelium ($p < 0.0001$; **Figure 25B**, **C**) as revealed by immunohistochemistry and semi-quantitative histoscoring. By 24 hours after withdrawal of progesterone (simulated 'early repair' phase), apoptosis had decreased substantially in the surface epithelium to levels not significantly higher than pre-withdrawal (0 hours), while apoptosis was still significantly increased in the decidualised stroma ($p < 0.0001$; **Figure 25C**).

The basal stroma of the mouse endometrium showed significant increases in the expression of cleaved caspase-3 from 8 hours post-progesterone withdrawal (simulated 'premenstrual' phase; $p < 0.05$; **Figure 25D**) and persisting until 24 hours' withdrawal (simulated 'early repair' phase; $p < 0.01$).

Semi-quantitative histoscoring of cleaved caspase-3-immunostained mouse endometrium revealed no statistically significant increases in apoptosis in the glandular epithelium or perivascular and endothelial cells following progesterone withdrawal.

A panel of representative photomicrographs taken from endometrial tissues immunohistochemically-stained for cleaved caspase-3 is shown in **Figure 26**.

Figure 25. Cleaved caspase-3 expression peaks in the surface epithelium, decidualised stroma and basal stroma of the mouse endometrium from 8 hours post-progesterone withdrawal, preceding overt menstrual bleeding. Semi-quantitative immunoreactivity histoscoring (staining intensity multiplied by percentage of tissue staining positive) for cleaved caspase-3 (1:400, Cell Signalling Tech.) in the mouse endometrium at 0 (n = 9), 4 (n = 7), 8 (n = 6) and 24 (n = 7) hours following progesterone withdrawal. A) Individual data points plotted vs. histoscore, B, C, D) mean histoscores in surface epithelium, decidualised stroma and basal stroma. * p < 0.05, ** p < 0.01, ***** p < 0.0001; lines represent group mean and error bars represent SEM; significance determined by 1-way ANOVA and Dunnett's multiple comparisons test (to 0h post-progesterone withdrawal). E_2 = oestradiol, P_4 = progesterone.*

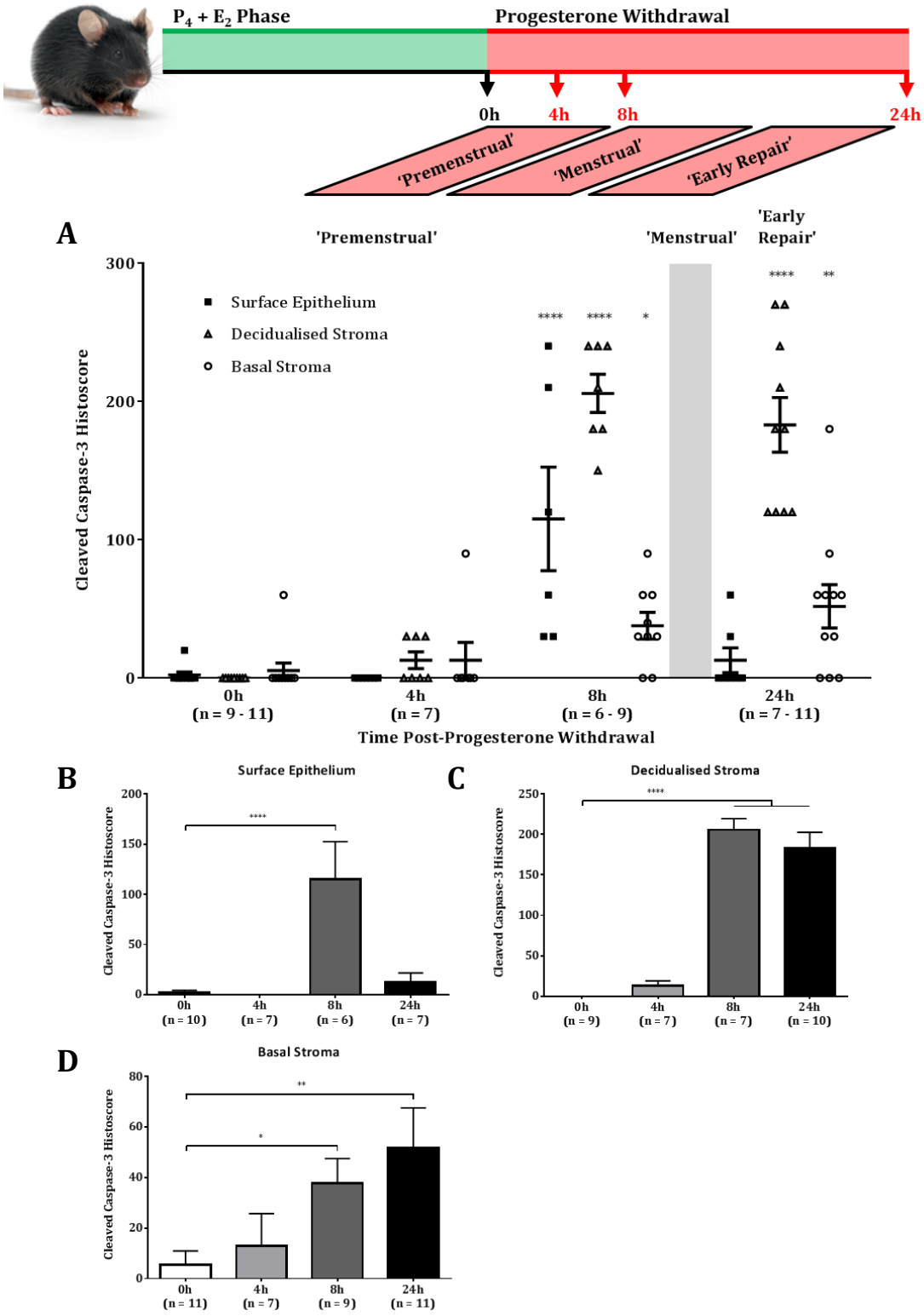

Figure 26. Extensive apoptosis (cleaved caspase-3^{+}) is observed in the surface epithelium and decidualised and basal stroma of the mouse endometrium at 8 and 24 hours post-progesterone withdrawal. Representative photomicrographs of cleaved caspase-3 (1:400, Cell Signalling Tech.) staining in serial sections of mouse endometrium at 0 (n = 9), 4 (n = 7), 8 (n = 6) and 24 (n = 7) hours following progesterone withdrawal revealed extensive apoptosis from 8 hours onward. Decidualised stroma comprises the entirety of the stroma containing decidual cells; basal stroma is defined as any stroma without decidual cells between the underlying myometrial smooth muscle and the overlying decidualised stroma and/or epithelium. Brown-filled triangles indicate cleaved caspase-3 immunoreactivity. *Isotype control: non-immunised rabbit serum Ig fraction (Dako); nuclear counterstain: haematoxylin. Scale bars (500 µm, 50 µm) in image.* *E_2 = oestradiol, P_4 = progesterone.*

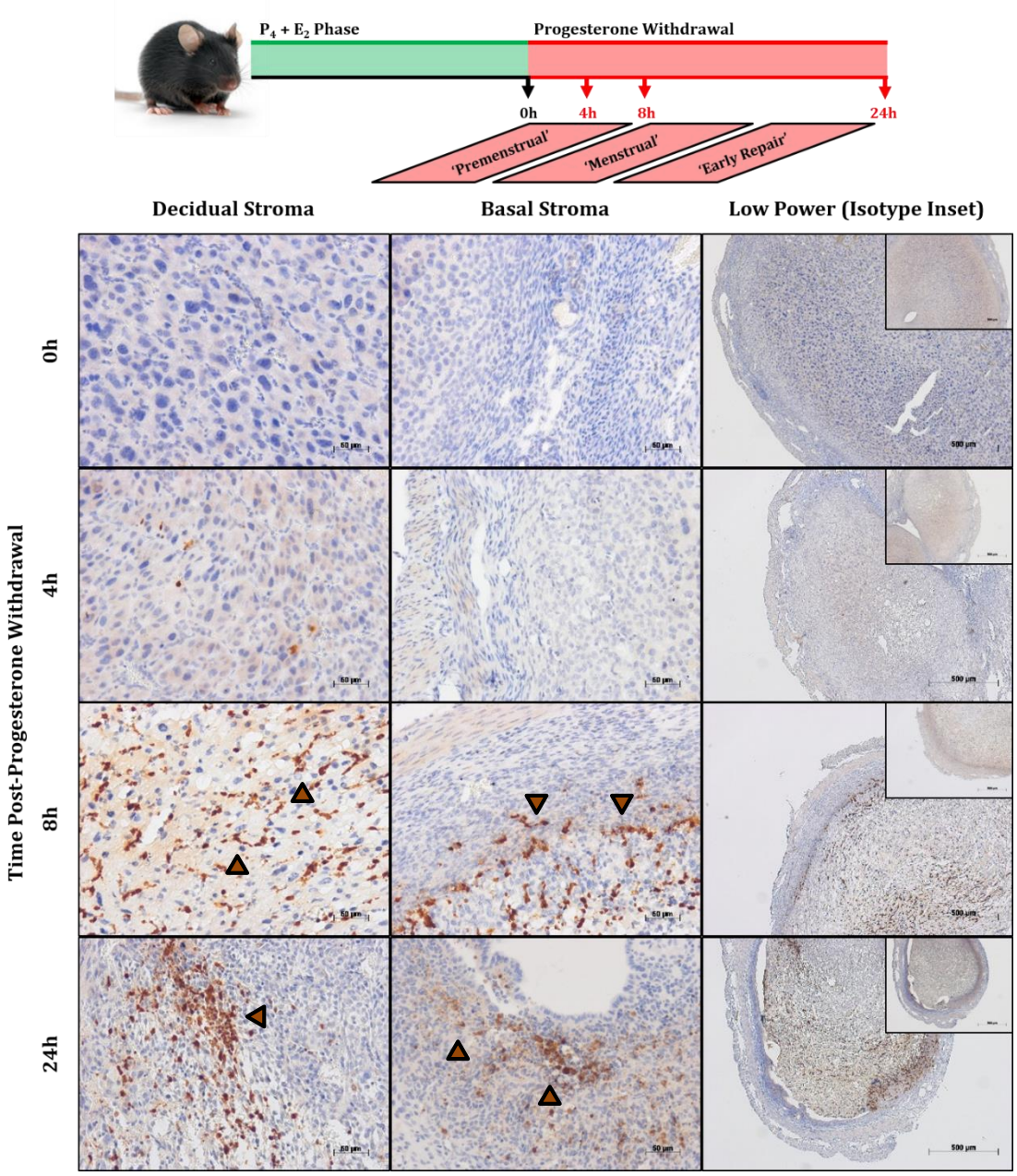

4.3.2 Neutrophil Recruitment in the Mouse Endometrium at 0, 4, 8 & 24 Hours Post-Progesterone Withdrawal

The mouse endometrium was revealed to be subject to significant increases in $Ly6G^+$ neutrophil abundance following withdrawal of progesterone (**Figure 27**, **Figure 28**), with modest increases found at 8 hours (simulated 'premenstrual' phase; $p < 0.05$) and more substantial increases found at 24 hours (simulated 'early repair' phase; $p < 0.001$).

Figure 28 depicts a panel of representative photomicrographs of mouse endometrial tissues immunohistochemically-stained for Ly6G. At 8 hours post-progesterone withdrawal, neutrophils are found amongst the decidual stromal cells of the endometrium; they show no particular propensity to aggregate or cluster, instead showing roughly uniform distribution through the decidua. By 24 hours post-progesterone withdrawal, neutrophils were more often found proximal to the newly epithelialising luminal surface, in small clustered groups of cells.

Figure 27. Neutrophil abundance is significantly increased in the mouse endometrium at 8 hours post-progesterone withdrawal and peaks at 24 hours post-progesterone withdrawal. Percentage of endometrial stroma comprised by neutrophils, as determined by ImageJ-assisted stereological Ly6G-positive (1:1000, BioLegend) cell counting in mouse endometrial tissues at 0 (n = 9), 4 (n = 6), 8 (n = 9) and 24 (n = 12) hours following progesterone withdrawal. *Box plot denotes group median and 25th and 75th percentiles, with individual data points superimposed; bars represent minimum and maximum values. * p < 0.05, *** p < 0.001; significance determined by 1-way ANOVA and Dunnett's multiple comparisons test (to 0h post-progesterone withdrawal). E_2 = oestradiol, P_4 = progesterone.*

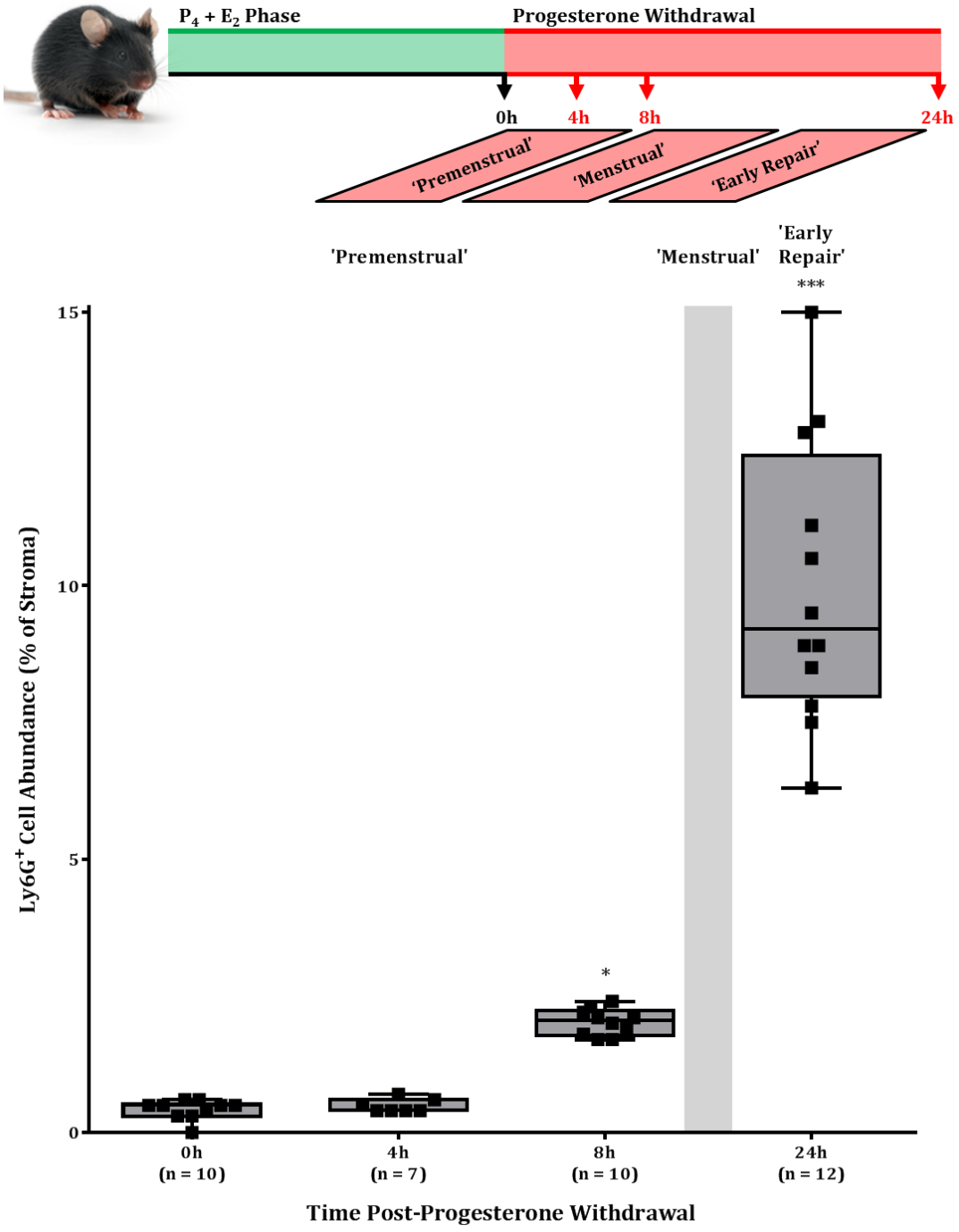

Figure 28. Neutrophil infiltration (Ly6G^{+}) is observed in the mouse endometrium at 8 and 24 hours post-progesterone withdrawal. Representative photomicrographs of Ly6G (1:1000, BioLegend) staining in serial sections of mouse endometrium at 0 (n = 9), 4 (n = 7), 8 (n = 6) and 24 (n = 7) hours following progesterone withdrawal showed abundant neutrophils at 8 and 24 hours post-progesterone withdrawal. Brown-filled triangles indicate Ly6G immunoreactivity. *Isotype control: rat IgG2a (BioLegend); nuclear counterstain: haematoxylin. Scale bars (500 µm, 100 µm) in image. E_2 = oestradiol, P_4 = progesterone.*

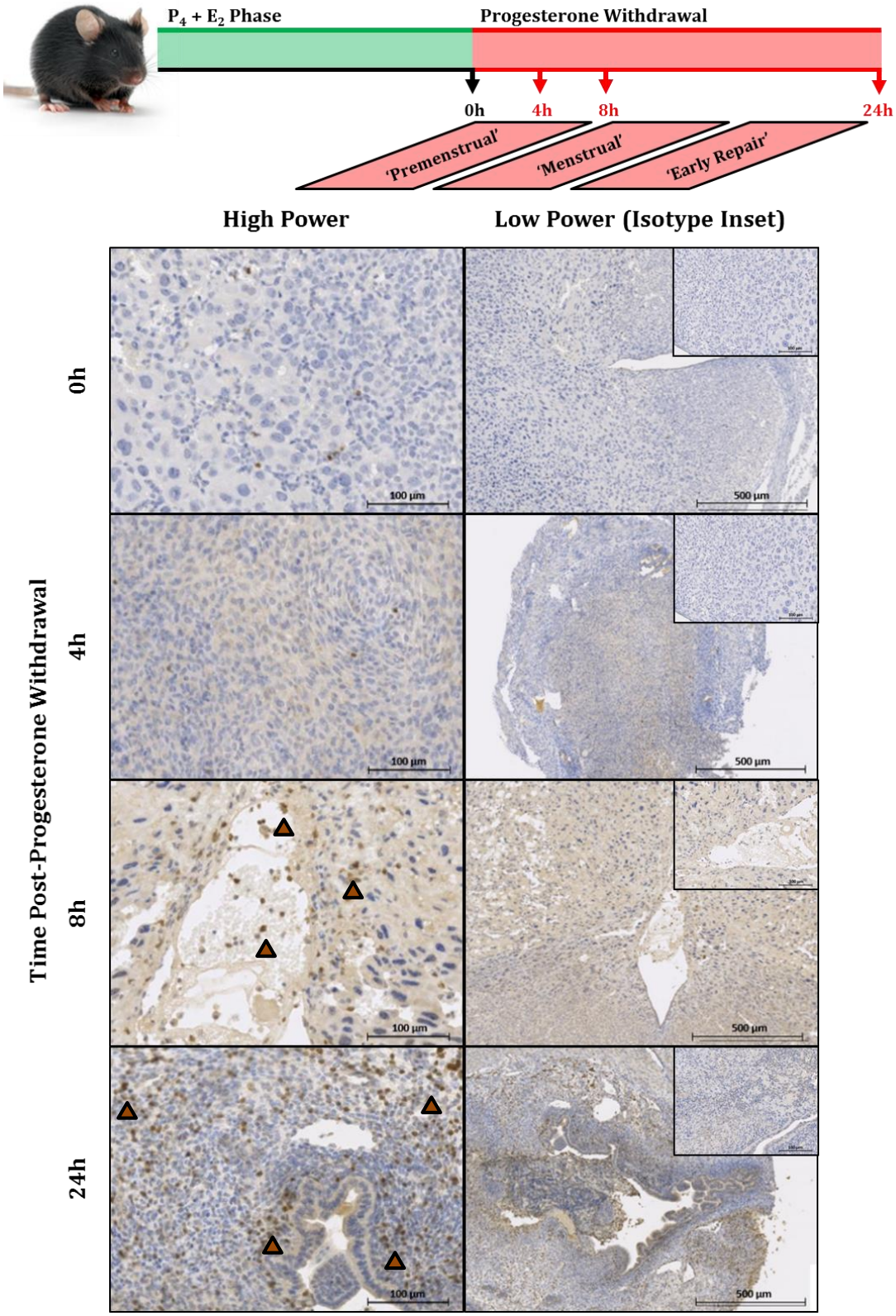

4.3.3 *Cxcl1* & *Tnfa* Transcription in the Mouse Endometrium at 0, 8 & 24 Hours Post-Progesterone Withdrawal

Transcription of the neutrophil chemokine *Cxcl1* (mouse homologue of human *CXCL8*/*IL8*) showed a significant increase of several orders of magnitude in the mouse endometrium at 24 hours following progesterone withdrawal (simulated 'early repair' phase; $p < 0.05$; **Figure 29A**) compared to pre-withdrawal levels (0 hours). While there was a modest increase found in *Cxcl1* transcription at 8 hours post-progesterone withdrawal (simulated 'premenstrual' phase), this result was not statistically significant.

The inflammatory cytokine, tumour necrosis factor alpha (*Tnfa*), showed a substantial increase in its transcription in the mouse endometrium at 24 hours post-progesterone withdrawal (simulated 'early repair' phase; $p < 0.05$; **Figure 29B**) compared to pre-withdrawal levels.

Figure 29. Transcription of the neutrophil chemokine *Cxcl1* and the inflammatory cytokine *Tnfa* is highest in the mouse endometrium at 24 hours following progesterone withdrawal. RT-qPCR quantification of *Cxcl1* (mouse homologue of human *CXCL8*/*IL8*; A) and *Tnfa* (B) mRNA levels in whole uterus RNA extracts, with data analysed by $\Delta\Delta C_q$ method and normalised to *Actb* (β-actin) mRNA levels. ** p < 0.05; error bars represent SEM; significance determined by 1-way ANOVA and Dunnett's multiple comparisons test (to 0h post-progesterone withdrawal).* *Cxcl1 = C-X-C chemokine ligand 1, E_2 = oestradiol, P_4 = progesterone, Tnfa = tumour necrosis factor alpha.*

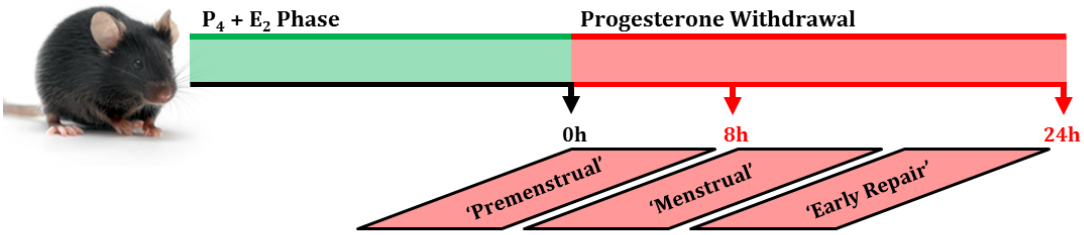

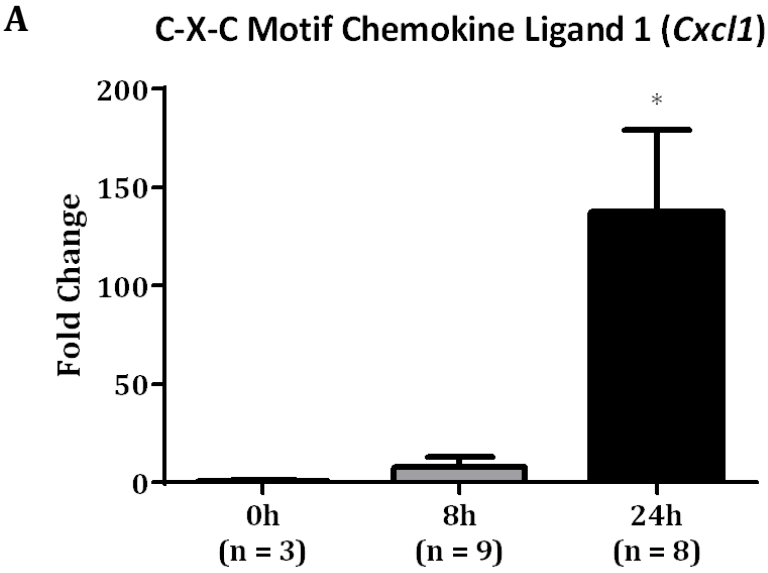

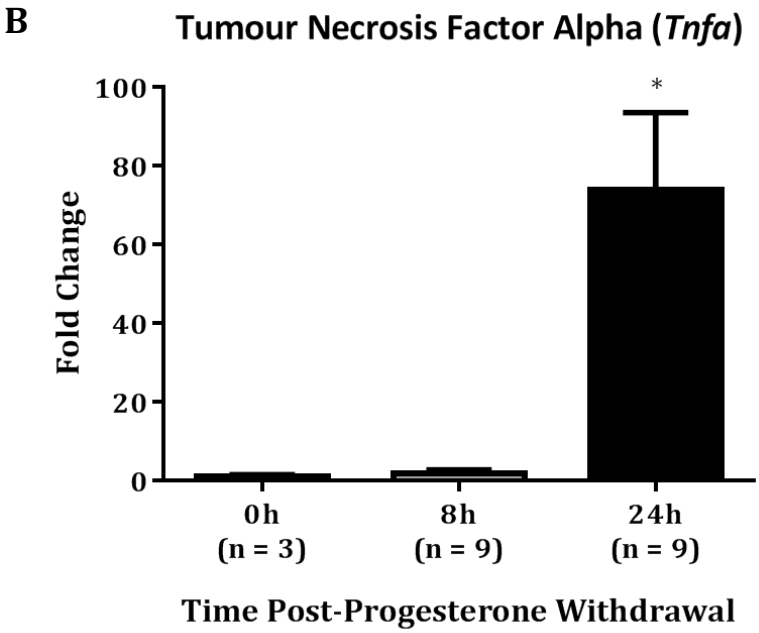

4.3.4 Glucocorticoid Receptor Target Gene Transcription in the Mouse Endometrium at 0, 8, 16 & 24 Hours Post-Progesterone Withdrawal

Investigation into the transcription of a number of glucocorticoid receptor target genes by PCR array revealed several differentially-transcribed genes in the mouse endometrium across progesterone withdrawal time-points (**Figure 30A**, **B**).

The majority of the transcriptional increases were observed at 24 hours post-progesterone withdrawal (simulated 'early repair' phase) relative to pre-withdrawal levels (0 hours): these included connective tissue growth factor (*Ctgf*), lysyl oxidase (*Lox*) and nuclear factor of kappa light polypeptide gene enhancer in B-cells inhibitor alpha (*Nfkbia*), all of which showed increased transcription at 24 hours ($p < 0.001$, 0.01 and 0.05, respectively; **Figure 30A**).

Transcription of ERBB receptor feedback inhibitor 1 (*Errfi1*) showed a significant increase at 16 hours after progesterone withdrawal (simulated 'menstrual' phase; $p < 0.05$) which then decreased to pre-withdrawal levels by 24 hours (simulated 'early repair' phase; **Figure 30A**).

Highly significant decreases in transcription were found in metallothionein 1 (*Mt1*) at all time-points ($p < 0.0001$; **Figure 30B**): 8 hours (simulated 'premenstrual' phase), 16 hours (simulated 'menstrual' phase) and 24 hours (simulated 'early repair' phase). Regulator of G-protein signalling 2 (*Rgs2*) also showed decreased transcription at 8 hours ($p < 0.01$), 16 hours ($p < 0.05$) and 24 hours ($p < 0.001$) after progesterone withdrawal.

Transcription of EH-domain containing 3 (*Ehd3*), FK506 binding protein 5 (*Fkbp5*) and serum/glucocorticoid regulated kinase 1 (*Sgk1*) were significantly decreased at 24 hours ($p < 0.05$ for each; **Figure 30B**), and the transcription of glutamate-ammonia

ligase (*Glul*) was very highly significantly decreased at 24 hours ($p < 0.0001$; **Figure 30B**).

Figure 30. Differential transcription of glucocorticoid receptor target genes following progesterone withdrawal in the mouse endometrium. Targeted gene array RT-qPCR assay, revealing increased (A) and decreased (B) transcription of genes downstream of the glucocorticoid receptor in whole uterus RNA extracts following the withdrawal of progesterone (0h, n = 7; 8h, n = 7; 16h, n = 3; 24h, n = 7), with data analysed by $\Delta\Delta C_q$ method and normalised to the geometric mean of five housekeeping gene mRNA levels (*Actb*, *B2m*, *Gapdh*, *Gusb* and *Hsp90ab1*). ** p < 0.05, ** p < 0.01, *** p < 0.001, **** p < 0.0001, # denotes ** (8h vs. 0h), * (16h vs. 0h) and *** (24h vs. 0h); error bars represent SEM; significance determined by 2-way ANOVA and Dunnett's multiple comparisons test for all PCR array genes (to 0h post-progesterone withdrawal). Actb = beta-actin, B2m = beta-2 microglobulin, Ctgf = connective tissue growth factor, E_2 = oestradiol, Ehdf = EH domain-containing 3, Fkbp5 = FK506 binding protein 5, Errfi1 = ERBB receptor feedback inhibitor 1, Gapdh = glyceraldehyde 3-phosphate dehydrogenase, Glul = glutamate-ammonia ligase, Gusb = ß-glucuronidase, Hsp90ab1 = heat shock protein HSP 90-beta, Lox = lysyl oxidase, Mt1 = metallothionein 1, Nfkbia = nuclear factor of kappa light polypeptide gene enhancer in B-cells inhibitor alpha, P_4 = progesterone, Rgs2 = regulator of G-protein signalling 2, Sgk1 = Serum-/glucocorticoid-regulated kinase 1.*

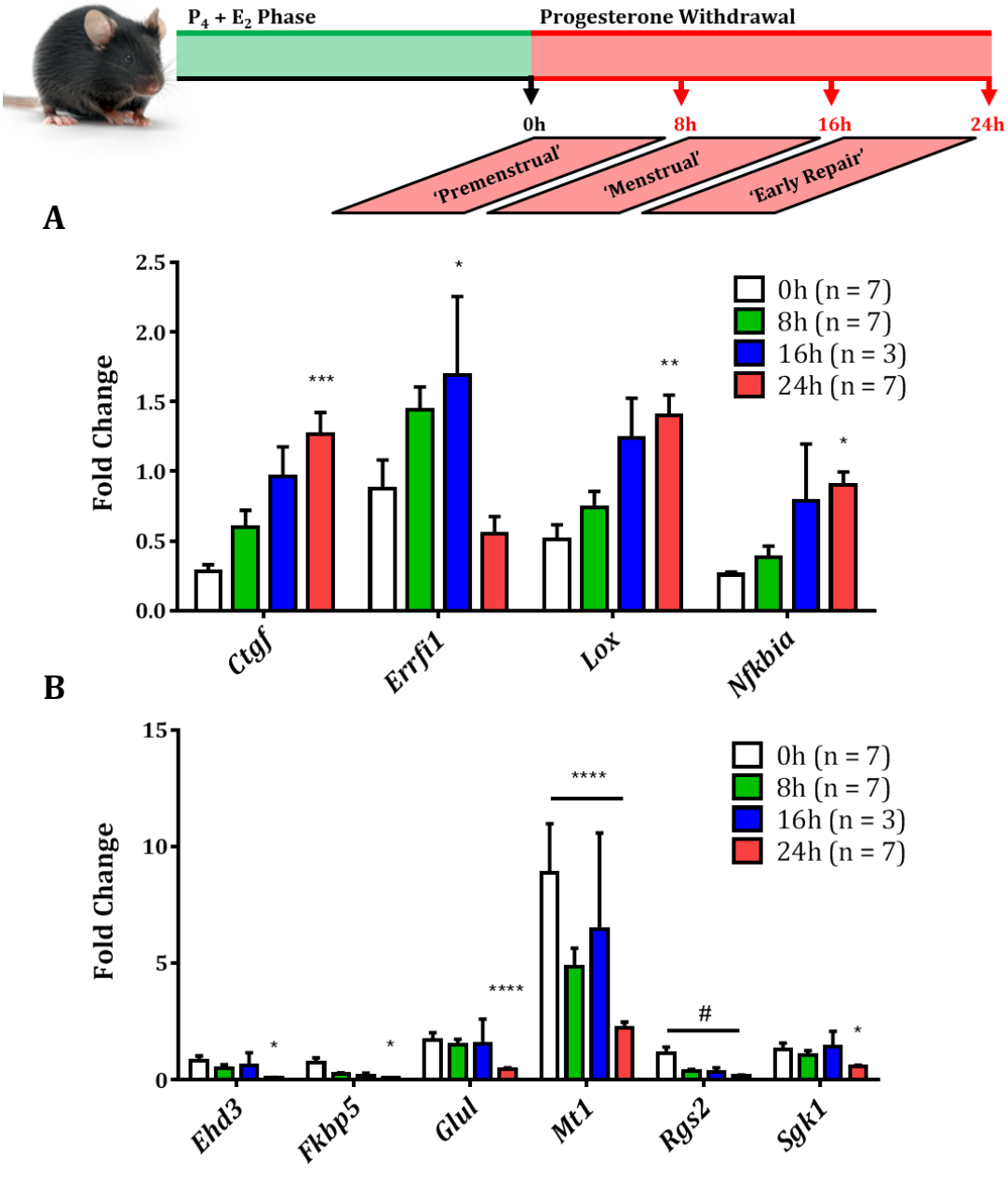

4.4 Discussion

4.4.1 Cleaved Caspase-3 & Apoptosis

Immunohistochemical and semi-quantitative experiments undertaken in this chapter describe a pattern of apoptosis in the mouse endometrium initiating sometime between 4 and 8 hours after the withdrawal of progesterone, such that by 8 hours apoptosis is tremendously widespread in the surface epithelium and decidualised stroma, extending down into the basal stroma.

This level of apoptosis seems to be maintained in what remains of the decidualised stroma for some time, being still significantly increased at 24 hours post-progesterone. This very likely still represents 'new' and ongoing apoptosis, rather than the continued presence of apoptotic cells from earlier progesterone withdrawal time-points, as apoptotic bodies only remain for a few hours before their phagocytosis (Wyllie, 1980). Extensive re-epithelialisation at 24 hours post-progesterone withdrawal seems to reduce the proportion of epithelial cells which are apoptotic to not significantly higher levels than pre-progesterone withdrawal levels.

Taken together, these cleaved caspase-3 expression and localisation experiments and their data represent a novel investigation into apoptosis in the mouse endometrium, differing from previous studies undertaking to do the same (Brasted *et al*., 2003; Xu *et al*., 2007) which did not strive to discriminate the localisation of apoptosis within the endometrium to specific tissue compartments (as these experiments did), and which made use of terminal deoxynucleotidyl transferase (TdT)-mediated dUTP-biotin nick end labelling (TUNEL) staining as a means of detecting apoptosis (whereas these

experiments used the more sensitive method of cleaved caspase-3 immunohistochemistry).

TUNEL staining has been a standard immunohistochemical technique for the detection of DNA fragmentation in tissue sections as a proxy for apoptosis for decades (Gavrieli *et al*., 1992), and still enjoys wide use. As late-stage apoptosis necessarily exhibits the feature of chromatin cleavage (Wyllie *et al*., 1984; Gavrieli *et al*., 1992), TUNEL staining relies on the binding of terminal deoxynucleotidyl transferase (TdT) to the nicked ends of cleaved nuclear material (specifically the 3'-OH ends) and its subsequent catalysis of a biotinylated poly-deoxyuridine polymer to these ends. The immunohistochemical detection of these polymers (indicating 'nicked DNA ends') allows the discrimination of cells whose nuclear material is fragmenting and thus are likely undergoing apoptosis (Gavrieli *et al*., 1992). TUNEL staining, however, is not without its limitations: non-apoptotic nuclei undergoing active gene transcription are known false positives (Kockx *et al*., 1998; Duan *et al*., 2003), as are cells undergoing the autolysis (Grasl-Kraupp *et al*., 1995; Duan *et al*., 2003), a related but distinct form of cell death. Moreover a wide variety of tissue fixation, processing and pre-treatment protocol can inappropriately introduce non-apoptotic DNA strand breaks (Baron *et al*., 2000; Duan *et al*., 2003), further compounding the possibility of false positives identified by TUNEL staining.

Cleaved caspase-3 staining, the method undertaken by the experiments described in this chapter, is a highly specific indicator of apoptosis, relying on the detection of the cleaved (active) form of caspase-3, a primary 'executioner' caspase involved in apoptosis. Caspase-3 effects the proteolytic degradation of numerous proteins, as well as the fragmentation of nuclear material during apoptosis (Slee *et al*., 2001). Thus apoptosis may be detected by the activation of caspase-3 before apoptotic cell nuclei are morphologically detectable and before apoptotic cell nuclear material is detectably

degraded, thereby eliminating many of the false negatives that would otherwise be missed by TUNEL staining methods. Studies undertaken by Duan *et al*. (2003) comparing TUNEL staining to cleaved caspase-3 immunohistochemistry showed cleaved caspase-3 to be a reliable method for detecting cells morphologically consistent with apoptosis as well as cells morphologically indistinguishable from healthy ones (i.e. early-stage apoptosis), concluding that cleaved caspase-3 was a superior method for the detection of apoptosis.

Brasted *et al*. (2003) describe a pattern of apoptosis in the mouse endometrium after the withdrawal of progesterone in which $TUNEL^{+}$ cells are abundant from '0 hours' (preceding the withdrawal of progesterone). These data are in conflict with the data presented in this chapter, in which apoptosis was not detectable until 8 hours after progesterone withdrawal. The work done by Brasted *et al*. (2003) goes on to show that levels of apoptosis are high at 12 hours, then somewhat decreased (but still reasonably high) at 16, 20 and 24 hours after progesterone withdrawal; these data are in rough agreement with the data presented herein, where apoptosis was found to be decreased (but still high) at 24 hours.

While Brasted *et al.* examined apoptosis only within the decidualised stroma (as opposed to the experiments in this chapter, which sought to investigate apoptosis across various tissue compartments), this does not explain the over-representation of apoptosis in the mouse endometrium at 0 hours. Rather, this discrepancy is likeliest explained by their use of the more highly false-positive-prone TUNEL staining methodology – perhaps non-apoptotic DNA strand breaks were introduced by particulars of the fixation, processing and pre-treatment to which their tissue sections were subjected (Baron *et al*., 2000). Brasted *et al.* moreover do not show any photomicrographs of TUNEL-stained decidual cells, which may have helped

corroborate their observation of substantial apoptotic cell abundance pre-progesterone withdrawal.

Studies undertaken by Xu *et al*. (2007) also describe apoptosis in the mouse endometrium by TUNEL staining, though their work describes these features following the administration of the progesterone receptor antagonist mifepristone (RU486) rather than the physiological withdrawal of progesterone. This pharmacological withdrawal of progesterone via antiprogestin administration has its roots in studies in the human endometrium, and has previously been proposed a means for menstrual induction (Bygdeman, 2003; Xiao *et al*., 2003). The administration of mifepristone in mice produced a pattern of endometrial apoptosis very similar to that seen in the experiments detailed in this chapter's work: low/undetectable apoptosis at 0 hours, a peak in apoptosis prior to 24 hours and mid- to high levels at 24 hours. Xu *et al.* showed low levels of apoptosis at 8 hours, in contradiction with the high levels of apoptosis uncovered by cleaved caspase-3 expression in this chapter's experiments, but this is likely explained by the inability of TUNEL staining to identify early, pre-DNA-fragmentation stages of apoptosis (which cleaved caspase-3 immunohistochemistry may still detect). The work described by Xu *et al.* also has some limitations in their quantification of apoptosis, relying on absolute numbers of $TUNEL^{+}$ cells discovered (rather than a proportion normalised to total cells) and examining apoptosis across whole sections of endometrium (rather than subdividing by tissue compartment) – aspects which the work undertaken in this chapter strove to refine.

While the characterisation of apoptosis given in these experiments was felt to be more rigorous than had been previously described in the literature, it is worth noting the relative paucity of time-points which were investigated in this work – further work

determining when beyond 24 hours post-progesterone withdrawal apoptosis resolves would be of not inconsiderable interest.

4.4.2 Neutrophil Recruitment

Stereological investigation into the numbers and timings of neutrophil infiltration in the mouse endometrium, described in the experiments of this chapter, revealed a baseline of negligible neutrophil abundance from 0 to 4 hours after the withdrawal of progesterone, which increased modestly at 8 hours. By 24 hours, the proportion of the endometrial stroma comprised by neutrophils had risen to approximately 10%, the highest abundance of any of the time-points examined. These stereological data represent what is felt to be a much more sensitive characterisation and accurate reflection of neutrophil abundance than has been undertaken in previous published works, owing to the use of the highly neutrophil-specific antibody against the Ly6G antigen (clone 1A8) as a means of detecting neutrophils. Other work describing neutrophils in the mouse endometrium following the withdrawal of progesterone use a range of less-specific anti-neutrophil antibodies, both for the detection and the depletion of neutrophils (Kaitu'u-Lino *et al*., 2006; Cheng *et al*., 2007; Menning *et al*., 2012).

To detect neutrophils in tissues, the experiments undertaken by Kaitu'u-Lino *et al*. (2006) employed an antibody recognising the Ly6B.2 antigen (clone 7/4) which, while expressed by neutrophils, is also expressed by inflammatory monocytes and a subset of activated macrophages (Rosas *et al*., 2010). The numbers of neutrophils Kaitu'u-Lino *et al*. show in their immunostained mouse endometrial tissues are therefore likely an over-representation, though the authors did not endeavour to quantify them.

In defence of the work described by Kaitu'u-Lino *et al.*, it should be noted that the authors were ostensibly demonstrating that neutrophils were absent from the tissue after neutralising-antibody-mediated depletion, therefore the fact that anti-Ly6B.2 antibodies likely overestimates neutrophil numbers did not undermine their premise.

Studies undertaken by Cheng *et al*. (2007) strove to describe changes in leucocyte populations after progesterone withdrawal in a related (but not identical) model of mouse decidualisation. The principal difference between the models used by Cheng *et al.* and that used by Brasted *et al*., Kaitu'u-Lino *et al.*, Menning *et al*., Cousins *et al.* and the studies described herein, lies in the method of progesterone withdrawal. Whereas the Brasted model administers progesterone via a subcutaneously-implanted progesterone-releasing Silastic implant (whose subsequent removal effects progesterone withdrawal), the Cheng model administers progesterone via subcutaneous injections alongside oestradiol. Progesterone withdrawal subsequent to termination of injections is much less acute and the timings of 'menstrual' events is much more variable in consequence – a problem which dissuaded Finn and Pope (1984) from pursuit of this model some 30 years ago.

Cheng *et al*. (2007) nevertheless describe an abundance of neutrophils in the volume fractions from the progesterone-withdrawn mouse uterus, though as with the work by Kaitu'u-Lino *et al*. (2006), employing an antibody against the neutrophil-, monocyte- and macrophage-expressed Ly6B.2 antigen (clone 7/4; Rosas *et al*., 2010) to do so.

Menning *et al*. (2012), in their work investigating the role of neutrophils and vascularisation in the regulation of menstrual bleeding in a mouse model, also made use of a not-entirely neutrophil-specific antibody (clone RB6-8C5), recognising granulocyte receptor 1 (Gr-1). Expression of the Gr-1 antigen was originally thought to

be restricted to mature murine granulocytes (hence its name; Tepper *et al*., 1992), but Gr-1 was later discovered to belong to the gene family, lymphocyte antigen complex 6 (Ly6), and to comprise two sets of antigens: the granulocyte-restricted antigen Ly6G and the neutrophil-, dendritic-cell-, monocyte-, macrophage- and lymphocyte-expressed antigen Ly6C (Jutila *et al*., 1988, 1994). The anti-Gr-1 antibody RB6-8C5 used by Menning *et al*. recognises both Ly6G and Ly6C antigens (Fleming *et al*., 1993; Ribechini *et al*., 2009). Since Menning *et al*. employed this antibody only to verify neutrophil depletion following the administration of a neutralising antibody (also Gr-1/clone RB6-8C5), this lack of specificity is unlikely to have undermined the premise of their work: neutrophils will certainly have been depleted, but it is worth noting that a broad range of other leucocytes will also have been depleted by this method.

All immunohistochemical and stereological characterisations of neutrophil numbers and their localisation undertaken in the work of this chapter have employed a Ly6G-specific antibody (clone 1A8) which demonstrates no cross-reactivity with the more broadly leucocyte-expressed Ly6C (Fleming *et al*., 1993; Daley *et al*., 2007).

Despite the rigor with which these neutrophil abundance characterisations have been undertaken, it would be of great interest to determine when after progesterone withdrawal neutrophils are fully cleared from the tissue. Further work with later progesterone withdrawal time-points (e.g. 32 and 40 hours post-progesterone withdrawal) would help fully delineate the dynamics of neutrophil recruitment and clearance in the menses-simulated mouse endometrium.

4.4.3 Inflammatory Gene Transcription

Transcriptional changes in the neutrophil chemokine gene *Cxcl1* (KC; GRO-α) and in the inflammatory cytokine gene *Tnfa* investigated in this chapter revealed relatively modest (and not statistically significant) increases at 8 hours after progesterone withdrawal, and drastic, significant increases at 24 hours. These data corroborate existing literature concerning the transcription of *Tnfa* and other C-X-C motif chemokines, and are the first to demonstrate transcriptional increases in *Cxcl1*.

Transcription of *Cxcl1*, a homologue of the human neutrophil chemokine *CXCL8*/*IL8* (Oquendo *et al*., 1989; Scholten and Al-samman, 2012), has not previously been shown in the mouse endometrium post-progesterone withdrawal, though the transcription of *Cxcl2* (GRO-β), another mouse neutrophil chemokine and *CXCL8*/*IL8* homologue, has been demonstrated massively upregulated at 24 hours post-progesterone withdrawal in work undertaken by Menning *et al*. (2012).

CXCL1 is of considerable interest in the repairing, 'menstrual' endometrium from several angles, exhibiting a functional pleiotropy not dissimilar to that of human CXCL8. With respect to angiogenesis, CXCL1 is reportedly chemoattractive for endothelial cells and serves an angiogenic function (Koch *et al*., 1992; Strieter *et al*., 1995a, 1995b), though a conflicting study by Cao *et al*. (1995) found it to be anti-angiogenic *in vivo* and inhibitory to endothelial cell proliferation *in vitro*.

In the context of apoptosis and neutrophil recruitment/clearance dynamics, CXCL1 was found to suppress neutrophil apoptosis (Dunican *et al*., 2000), inhibiting both TUNEL immunoreactivity and caspase-3-mediated cleavage of certain specific colorimetric substrates.

CXCL1 appears to be a reliable indicator of inflammation, with its production in neutrophils stimulated by the fungal product and toll-like receptor (TLR) agonist, zymosan (Schröder *et al*., 2006). Neutrophil CXCL1 production is also stimulated by the TLR agonist, lipopolysaccharide (LPS) in conjunction with TNFα (Scapini *et al*., 2000).

The demonstration by the experiments undertaken in this chapter that *Cxcl1* transcription is increased at 24 hours post-progesterone withdrawal is in keeping with the neutrophil abundance data presented alongside, which showed substantial increases in neutrophil numbers at 24 hours. This strengthens the argument that the infiltration of large numbers of neutrophils is a 'deliberate', coordinated response, and lending credence to the assertion that neutrophils are important to the breakdown and repair of the mouse endometrium following progesterone withdrawal (Kaitu'u-Lino *et al*., 2006).

Studies undertaken by Menning *et al*. (2012) demonstrated a significant increase in the transcription of *Tnfa* at 24 hours post-progesterone withdrawal – a finding corroborated by the data presented in this chapter. Increased TNFα at 24 hours post-progesterone withdrawal is moreover in line with the finding by Menning *et al.* that transcription of the prostanoid synthesis pathway gatekeeper enzyme *Ptgs2* (cyclooxgenase-2; COX-2) is also increased at 24 hours, as TNFα is a known inducer of *Ptgs2* transcription (Chen *et al*., 2000; Nakao *et al*., 2002).

Increased transcription of two inflammatory factors (*Cxcl1* and *Tnfa*) was described in this chapter, but in the absence of sufficient tissue, it was not possible to corroborate these data with the accompanying protein expression data which could verify increases

in the expression of these cytokines. Further work, either by means of Western blotting or enzyme-linked immunosorbent assay (ELISA), could satisfactorily demonstrate this aspect. In the absence of these data, it cannot necessarily be concluded that levels of CXCL1 and TNFα proteins are increased in the mouse endometrium.

4.4.4 Glucocorticoid Receptor Target Gene Transcription

Targeted PCR array studies described in this chapter revealed a number of significant transcriptional changes in glucocorticoid receptor target genes in the mouse endometrium after the withdrawal of progesterone. By 8 hours post-progesterone withdrawal, significant decreases were observed in endometrial levels of metallothionein 1 (*Mt1*) and regulator of G-protein signalling 2 (*Rgs2*) mRNA. Sixteen hours following progesterone withdrawal saw continued, statistically significant decreases in *Mt1* and *Rgs2* transcription, as well as significant increases in ERBB receptor feedback inhibitor 1 (*Errfi1*) transcription.

Many transcriptional differences described in this work, however, were only observed at 24 hours post-progesterone withdrawal: transcription of connective tissue growth factor (*Ctgf*), lysyl oxidase (*Lox*) and nuclear factor of kappa light polypeptide gene enhancer in B-cells inhibitor alpha (*Nfkbia*) was significantly increased at this time, whereas the transcription of EH domain-containing 3 (*Ehd3*), FK506 binding protein (*Fkbp5*), glutamate-ammonia ligase (*Glul*) and serum-/glucocorticoid-regulated kinase 1 (*Sgk1*) was decreased.

Taken together, these investigations into glucocorticoid receptor target gene transcription in a mouse model of menstruation are an entirely novel contribution to the current understanding of how glucocorticoids function in the endometrium at the time of menstruation.

Glucocorticoids are potent anti-inflammatory steroid hormones whose availability is controlled by activating and inactivating enzymes of the 11β-hydroxysteroid dehydrogenase (11β-HSD) family. Glucocorticoids exist in an active form (cortisol in humans, corticosterone in the mouse) and an inactive form (cortisone and dehydrocorticosterone, respectively). 11β-HSD-1 catalyses the conversion of inactive cortisone/dehydrocorticosterone to cortisol/corticosterone, while 11β-HSD-2 catalyses the inverse inter-conversion reaction. The 11β-HSD enzymes are reportedly dynamically expressed through the menstrual cycle in humans and in endometrial stromal cells *in vitro* in response to changing steroid environments (Arcuri *et al*., 1996; Smith *et al*., 1997), and *Hsd11b1* and *Hsd11b2* transcription in the mouse uterus have also been described (Thompson *et al*., 2002).

Glucocorticoids exert their effects primarily through the binding of their cognate receptor, the glucocorticoid receptor (GR), expression of which in the human endometrium has previously been described (Bamberger *et al*., 2001; Henderson *et al*., 2003).

Although only significant transcriptional changes uncovered by the gene array were presented in this chapter, it is worth noting that the *Nr3c1* (GR) was amongst the genes investigated which did not show any differential transcription across progesterone withdrawal time-points investigated. Any differences therefore in GR transcriptional activities will likely be due to changes in glucocorticoid concentrations and activation, and due to GR co-activator/-repressor expression.

Metallothionein 1 (MT1) belongs to the metallothionein family of metal-binding enzymes, which reportedly mediate zinc homeostasis and heavy metal sequestration (Kägi and Kojima, 1987). Metallothioneins are acutely induced by inflammation (Lee *et al*., 1999) and somewhat counter-intuitively, by the anti-inflammatory glucocorticoids

(Kelly *et al*., 1997). In a study undertaken with gene knockouts of *Mt1* and *Mt2* in mice, embryonic and fibroblast cells treated with cisplatin were more susceptible to apoptosis (Kondo *et al*., 1997), as were mouse lung fibroblasts to copper-dependent apoptosis (Kawai *et al*., 2000).

Expression of metallothioneins has been described in the mouse maternal deciduum, where their expression varies considerably (Liang *et al*., 1996), and have more recently been described in a mouse model of decidualisation and progesterone withdrawal (Cheng *et al*., 2007), in which the authors found decreased *Mt1* transcription at all time-points examined after termination of progesterone injections.

The most plausible hypothesis for the highly significant decreases in *Mt1* transcription uncovered in the mouse endometrium at 8, 16 and 24 hours post-progesterone withdrawal in these studies is that *Mt1* downregulation is to facilitate apoptosis as endometrial breakdown and repair occurs.

Regulator of G-protein signalling 2 (RGS2) is a ubiquitously-expressed member of the RGS family of proteins, which reportedly inhibit the mitogenic activities of various G-protein-coupled-receptor- (GPCR)-binding cytokines via the attenuation of GPCR signalling (Siderovski *et al*., 1994; Heximer *et al*., 1997). More recently, RGS2 has been suggested to play a role in the negative regulation of hypertrophy (Nunn *et al*., 2010).

Rgs2 mRNA has been localised to the decidual zone of the pregnant mouse endometrium by *in situ* hybridisation and was found highly transcribed in artificially-decidualised endometrial stromal cells of a pseudo-pregnant mouse model (Huang *et al*., 2003), where the authors suggest a role for RGS2 in embryo implantation.

It is possible that RGS2 represents an important 'self-limiting' aspect to decidualisation, highly expressed in the decidualised endometrium and drastically reduced upon the

withdrawal of progesterone – consistent with the decrease in *Rgs2* mRNA observed in these studies at 8, 16 and 24 hours post-progesterone withdrawal.

ERBB receptor feedback inhibitor 1 (ERRFI1) is a fibroblast-expressed adaptor protein, induced by mitogenic stimulation (hence its alternative name, mitogen inducible gene-6; MIG-6; Wick *et al*., 1995) which exhibits increased transcription during normal cell cycle progression (*ibid.*). ERRFI1 contains a number of binding domains, including a Cdc-43- and Rac-interactive-binding (CRIB) domain, epidermal-growth-factor-receptor- (EGFR)-binding domain, 14-3-3-binding domain and SRC-homology-3- (SH3)-binding domain (Burbelo *et al*., 1995; Pirone *et al*., 2001). Steroid receptor co-activator (SRC) family proteins augment nuclear receptor transcriptional activities, enhancing the actions of the oestrogen receptors ERα and ERβ, the progesterone receptor (PR) and the glucocorticoid receptor (GR; Oñate *et al*., 1995; Anzick *et al*., 1997; Wong *et al*., 2001).

ERRFI1 has been identified as a downstream target of SRC-1 in the mouse uterus (Jeong *et al*., 2009), and is suggested to regulate the response of the endometrium to oestrogen in establishing tissue homeostasis. ERRFI1's well established role in interacting indirectly with various steroid hormones and their cognate receptors is consistent with the finding herein that *Errfi1* transcription is dynamically regulated in the progesterone-withdrawn mouse endometrium – increased significantly at 16 hours post-progesterone withdrawal, and decreased to pre-withdrawal levels by 24 hours.

Connective tissue growth factor (CTGF) is a pleiotropic growth factor whose activities influence a wide range of biological processes, including wound repair, angiogenesis, stromal proliferation and extracellular matrix (ECM) production (Frazier *et al*., 1996; Hishikawa *et al*., 2000; Igarashi *et al*., 1993; Ivkovic *et al*., 2003).

Its presence, both as mRNA transcript and expressed protein, has been previously demonstrated in the human endometrium (Uzumcu *et al*., 2000), though not in the menstrual phase until some years later (Maybin *et al*., 2012). Investigation into *CTGF* transcription and expression in the human endometrium across the menstrual cycle revealed statistically significant increases in mRNA transcript in the menstrual phase, and peak protein expression in the proliferative phase, localised to the epithelial and stromal cell compartments (Maybin *et al*., 2012).

The finding of increased *Ctgf* transcription in the mouse endometrium at 24 hours post-progesterone withdrawal is consistent with the literature concerning CTGF expression in the human endometrium, and supports a role for repair in the progesterone-withdrawn mouse endometrium.

Lysyl oxidase (LOX) is a copper-dependent, ECM-modifying enzyme responsible for cross-linking and stabilising collagen and elastin (Lucero and Kagan, 2006); it and related LOX family proteins are further implicated in functions relating to cell growth regulation, monocyte motility induction (Lazarus *et al*., 1995; Li *et al*., 2000) and to the promotion of epithelial-to-mesenchymal transition (EMT; Peinado *et al*., 2005; Moreno-Bueno *et al*., 2011). In the human endometrium, LOX expression has not been described, though LOXL1 (LOX-like 1, a LOX family protein) is reportedly downregulated during the window of implantation (Talbi *et al*., 2006).

In a mouse model of menses, Cousins *et al*. (2014) have recently demonstrated the importance of epithelial-to-mesenchymal transition in the repair of the endometrium, which the finding of increased *Lox* transcription is likely to support.

Nuclear factor of kappa light polypeptide gene enhancer in B-cells inhibitor alpha (NFKBIA; also termed IκBα) is an inhibitor of NF-κB, a family of transcription factors

considered pivotal mediators of inflammatory immune response. NF-κB regulates the transcription of countless inflammatory cytokines and chemokines, including *CXCL1* (Ohmori *et al*., 1995), *CXCL8* (Kunsch and Rosen, 1993) and *TNFA* (Collart *et al*., 1990; Shakhov *et al*., 1990), as well as enzymes such as *PTGS2* (COX-2; Yamamoto *et al*., 1995). Some NF-κB-induced cytokines, like TNFα, activate NF-κB in a positive feedback loop (Blackwell *et al*., 2013). Transcription of the NF-κB inhibitor, *NFKBIA*/IκBα, is also induced by NF-κB however, acting as a self-limiting, negative-feedback control mechanism (Haskill *et al*., 1991; Sun *et al*., 1993).

The increased *Nfkbia* transcription in the mouse endometrium at 24 hours post-progesterone withdrawal described by these studies, along with the increases in *Cxcl1* and *Tnfa* transcription, may all be mediated by NF-κB – the subsequent expression of NFKBIA/IκBα is therefore likely a means by which to curtail further *Cxcl1* and *Tnfa* transcription (amongst other NF-κB-transcribed inflammatory mediators) as inflammation is resolved and the endometrium is restored.

Comparatively understudied amongst the glucocorticoid receptor target genes investigated is Eps15 homology (EH) domain-containing 3 (EHD3), a protein localised to endocytic vesicles and surmised to play a role in their trafficking (Galperin *et al*., 2002). More recent studies undertaken by Naslavsky *et al*. (2009) have supported a role for EHD3 in endosomal trafficking, demonstrating impaired endosome sorting with the experimental abrogation of *Ehd3*. Very little is known about EHD3 in the context of menstruation or the endometrium, though quite recent work has implicated it more generally as a tumour suppressor, with restoration of its expression inducing cell cycle arrest and apoptosis in glioma cancer cell lines *in vitro* (Chukkapalli *et al*., 2014). Chukkapalli *et al.* further note that experimental silencing of *Ehd3* in glioma cells increases cell growth – it is plausible that the decrease in *Ehd3* transcription observed

in the mouse uterus at 24 hours post-progesterone withdrawal is to facilitate cell growth and tissue restoration.

FK506-binding protein 5 (FKBP5) is a heat-shock protein 90 (HSP90) co-chaperone protein which acts to inhibit the ligand-activated transcriptional activities of steroid hormone receptors such as GR and PR (Lydon *et al*., 1995; Cheung-Flynn *et al*., 2005; Yang *et al*., 2006), whereas its counterpart FKBP4 enhances these transcriptional activities. *Fkbp4*$^{-/-}$ mice reportedly demonstrate impaired implantation and decidualisation (Tranguch *et al*., 2005). FKBP4 and 5 are believed to have opposing functions, though in the human endometrium *FKBP5* transcription is reportedly low and unvarying across the menstrual cycle and does not affect the transcription of decidualisation factors *in vitro* (Yang *et al*., 2012), whereas *FKBP4* transcription varied according to menstrual phase and its experimental abrogation decreased decidualisation factor transcription (*ibid.*).

Thus, despite a well-described role for FKBP4 in the endometrium, much less is known about FKBP5. The decrease in *Fkbp5* transcription described in the mouse endometrium at 24 hours post-progesterone withdrawal herein is likely, nevertheless, to effect reduced inhibition of steroid hormone receptor transcriptional activity. It is plausible that this is to facilitate oestrogen-mediated proliferative effects as the endometrium is repaired.

Glutamate-ammonia ligase (GLUL) is an enzyme responsible for catalysing the synthesis of glutamine from glutamate and ammonia (Liaw *et al*., 1995), though whose endometrial-specific actions remain as yet unknown. Interestingly, however, *Glul* transcription and expression have been reported recently to be induced by the transcription factor, forkhead box protein O1 (FOXO1; Kamei *et al*., 2014). FOXO1 is up-regulated by progesterone, and in turn induces the transcription of insulin-like

growth factor-binding protein 1 (*Igfbp1*; Nakamura *et al*., 2013), which acts to inhibit endometrial epithelial cell proliferation (*ibid.*).

Thus, the decrease in *Glul* mRNA transcript described in the mouse endometrium at 24 hours post-progesterone withdrawal may reflect the loss of FOXO1 (due to decreased progesterone), and is associated with increased endometrial epithelial cell proliferation only indirectly via the loss of IGFBP1 (due to decreased FOXO1).

Serum-/glucocorticoid-regulated kinase 1 (SGK1) is a serine/threonine kinase involved in endometrial epithelial cell survival, and induced and phosphorylated in endometrial stromal cells during decidualisation (Feroze-Zaidi *et al*., 2007), where it is suggested to interact with the transcription factor FOXO1. Studies conducted in the mouse, in which SGK1 was experimentally manipulated to be constitutively expressed, saw the abrogation of certain endometrial receptivity genes' expression and a decrease in embryo implantation (Salker *et al*., 2011). SGK1 is also reported to induce apoptosis via the phosphorylation of the transcription factor FOXO3a (You *et al*., 2004).

The decrease in endometrial *Sgk1* transcription at 24 hours post-progesterone withdrawal described in these studies likely reflects a role in the re-establishment of endometrial receptivity post-menses, and perhaps in the inhibition of apoptosis as endometrial repair progresses.

Somewhat disconcertingly, tumour necrosis factor alpha (*Tnfa*) was amongst the genes comprising the panel of glucocorticoid receptor target genes investigated in the gene array, though no statistically significant differences were uncovered in its transcription between 0 hours post-progesterone withdrawal and 8, 16 or 24 hours. This is in disagreement with the RT-qPCR-identified, statistically significant increase in *Tnfa* transcription described at 24 hours in the mouse endometrium in work of this chapter

(**Figure 29B**) and in studies undertaken by Menning *et al*. (2012). Although the gene array employed a SYBR-Green-based amplification/detection strategy whereas the RT-qPCR experiments of this chapter and of Menning *et al.* employed a TaqMan-(hydrolysis probe)-based strategy, *Tnfa* was amplified in all three cases with primers (and probes, where applicable) designed to the same *Tnfa* NCBI accession number (NM_013693.2). No compelling explanation for the discrepancy is therefore immediately apparent.

Studies undertaken in this chapter detailed a number of transcriptional changes in glucocorticoid receptor target genes by PCR array, but many of these changes identified require further RT-qPCR validation to confirm the findings.

Of additional benefit to the corroboration of the findings detailed herein would be protein expression data as determined either by immunohistochemistry or Western blotting. Without these supporting data, again, the conclusion cannot necessarily be drawn that the expression of these gene products is increased or decreased in the mouse endometrium.

4.4.5 Parallels to Human Menstruation

An important aspect to the work detailed in this chapter is the parallel which can be drawn between the observations made in the progesterone-withdrawn mouse endometrium in the menses model and those made in the 'perimenstrual' human endometrium (Chapter 3). In the mouse, 'menses' occurs due to the removal of the progesterone-releasing Silastic implant; in the human, menses occurs due to the regression of the progesterone-producing corpus luteum.

Features common to both the mouse and human endometrium include:

- Early endometrial apoptosis preceding overt menstrual bleeding and tissue destruction
    - 8 hours post-progesterone withdrawal in the mouse
    - Late secretory phase in the human
- Tremendous increases in infiltrating neutrophil granulocyte abundance
    - 8 – 24 hours post-progesterone withdrawal in the mouse
    - Menstrual phase in the human
- Increased transcription of inflammatory chemokines and cytokines (*Tnfa*/*TNFA*, *Cxcl1*/*CXCL8*)
    - 24 hours post-progesterone withdrawal in the mouse
    - Menstrual phase in the human

Though not investigated in the work comprising these studies, glucocorticoids and their actions have been demonstrated to be dynamically regulated in the human endometrium across the menstrual cycle, with significantly increased transcription of the cortisol-activating enzyme *HSD11B1* (11β-HSD-1) and of the glucocorticoid receptor *NR3C1* (GR) in the menstrual phase (McDonald *et al*., 2006). The differential transcription of various glucocorticoid receptor target genes identified in this chapter support a role for glucocorticoids in the progesterone-withdrawn mouse endometrium. All these aspects taken together strengthen the legitimacy of this mouse model in recapitulating the events of human menstruation.

Despite the many similarities between the mouse model of menstruation and its human phenomenon counterpart, there were some notable differences observed.

With respect to the timings and extent of apoptosis in the mouse endometrium post-progesterone withdrawal, one important difference was in the relative absence of apoptosis in the endometrial glands of the mouse endometrium. Whereas the human endometrium exhibited tremendous apoptosis in the glandular epithelium (constituting the majority of the apoptosis observed in the human endometrium), the mouse endometrium did not.

This difference is likely explained by the localisation of these structures: in the decidualised human endometrium, glands remain amongst the decidual stroma and are shed alongside it upon the advent of menstruation; in the decidualised mouse endometrium, glands are pushed basally toward the myometrium, and seem rarely (if ever) to be shed following progesterone withdrawal – thus they are likely 'exempt' from 'menstrual' tissue injury.

4.4.6 Summary & Conclusions

The results of this chapter depict a progesterone-depleted endometrial environment in the mouse with remarkable similarities to the human endometrium as progesterone concentrations decline into and through menses. Apoptosis is shown to be a tightly coordinated process, progressing from virtual non-existence during early progesterone withdrawal (0 – 4 hours) to tremendous levels of expression throughout the endometrium by 8 hours.

The chemoattraction of neutrophils after progesterone withdrawal, at least partly via the induction of *Cxcl1*, culminated in substantial increases in endometrial neutrophil numbers by 24 hours post-progesterone withdrawal; here, at their most abundant, they constitute as much as 10% of the stroma.

Broad transcriptional changes in glucocorticoid receptor target genes take place from 8 hours after progesterone withdrawal, many of which mirror transcriptional changes seen in the human endometrium across the perimenstrual window.

The mouse model of induced menses is therefore an invaluable tool in modelling the events of human menstruation.

A summary of the observations detailed in this chapter is given in **Table 13**.

Table 13. Summary of observations in the mouse endometrium subsequent to the withdrawal of progesterone. Upward-facing arrows (↑) and shades of orange reflect increases in the observed quantity described in this chapter; downward-facing arrows (↓) and shades of blue reflect decreases. White boxes without symbols reflect the absence of observation (cleaved caspase-3, Ly6G) or 'baseline' for transcriptional changes. 'N/A' and grey-shaded boxes represent time-points for which no data were available. Novel data to which the summary table refers can be found on the pages listed in the right-most column. ** denotes statistical significance (p < 0.05 – 0.0001) for the observations described.*

Hours Post-Progesterone Withdrawal	**0**	**4**	**8**	**16**	**24**	**Page**
Apoptosis (cleaved caspase-3)			↑↑↑/*	*N/A*	↑↑/*	131
Neutrophil infiltration (Ly6G)			↑/*	*N/A*	↑↑↑/*	134
Cxcl1 and *Tnfa* transcription		*N/A*	↑	*N/A*	↑↑↑/*	137
Ctgf, *Lox* and *Nfkbia* transcription		*N/A*	↑	↑↑	↑↑↑/*	140
Errfi1 transcription		*N/A*	↑	↑↑/*		140
Ehd3, *Fkbp5*, *Glul* and *Sgk1* transcription		*N/A*			↓↓/*	140
Mt1 and *Rgs2* transcription		*N/A*	↓↓/*	↓↓/*	↓↓↓/*	140

5. Dysregulation of Apoptosis in the Endometrium from Women with Heavy Menstrual Bleeding (HMB)

5.1 Introduction

Each menstrual cycle of a woman's reproductive life sees her endometrium subjected to growth, differentiation, injury and repair under the influence of ovarian sex steroids (see **Figure 1,** 1.1 Hormonal Regulation of the Human Endometrium & the Menstrual Cycle). Following menstruation, the endometrium must restore itself from the underlying basal layer. The period of the menstrual cycle comprised by the late secretory phase (prior to menstruation), menstrual phase and early proliferative phase (post-menstruation) is herein termed the 'perimenstrual' window (**Figure 2**).

Many of the features which characterise menstruation are analogous to features observed in acute inflammation, such as leucocyte recruitment (King *et al*., 1996; Evans and Salamonsen, 2012) and coordinated chemokine expression (Jones *et al*., 1997a; Milne *et al*., 1999).

Heavy menstrual bleeding (HMB) is a common disorder of menstruation affecting up to 25% of pre-menopausal women in the UK (Shapley *et al*., 2004), subjectively defined by the National Institute for Health and Care Excellence (NICE) as 'excessive menstrual blood loss that interferes with a woman's physical, social, emotional and/or material quality of life' (NICE Clinical Guideline 44 on HMB, 2007). Objectively, HMB is defined by a menstrual blood loss (MBL) of ≥80 mL per cycle (NICE Clinical Guideline 44 on HMB, 2007), as measured by alkaline haematin method (Warner *et al*., 2004).

Medical treatment options are available, but they are costly – and many women will still require surgical management of the complaint (Roberts *et al*., 2011). Half of the hysterectomies carried out in the NHS in England between the years of 2000 and 2001 were for HMB, and half of the women undergoing hysterectomies for HMB had no recognised pathology (NICE Draft Scope for Hysterectomy Consultation, 2004).

A whole genome array analysis of gene transcription in menstrual-phase endometrial biopsies from women with objectively-verified normal and heavy menstrual bleeding was performed by Dr. JA Maybin with the assistance of Dr. E Marshall, uncovering 259 differentially-transcribed genes (**Figure 31A**, **B**). 'Apoptotic regulation' was the most represented process network amongst the genes identified (**Figure 32**). These data were published previously in JA Maybin's 2011 PhD thesis. A number of the targets identified were pursued for validation in the studies described herein.

Apoptotic cell death is critical to the maintenance of tissue homeostasis, allowing for the disposal of aged and infected cells, as well as facilitating the successful, spontaneous resolution of acute inflammation (Kerr *et al*., 1972; Savill *et al*., 2002). Cells can be induced to undergo apoptosis through either intrinsic or extrinsic pathways, with both mediated the actions of caspases and converging on the activation of caspase-3 (Slee *et al*., 2001; **Figure 3**). In its capacity for resolving acute inflammation, the contributions of apoptosis are two-fold: (1) apoptotic cell death eliminates inflammatory leucocytes, safely sequestering their cytotoxic granule contents; and (2) resident phagocytes are induced to adopt pro-resolution phenotypes by engulfing apoptotic bodies (Savill and Haslett, 1995; Savill *et al*., 2002). Resolving the inflammation that characterises menstruation is likely a component to the successful repair of the endometrium post-menses.

Figure 31. Whole genome array and *in silico* analysis of menstrual-phase endometrium of women with heavy menstrual bleeding (HMB) versus normal menstrual bleeding controls (NMB) revealed a number of differentially-transcribed genes. RNA was extracted from menstrual-phase whole endometrial biopsies from women with objectively-confirmed heavy menstrual bleeding (n = 4) and normal menstrual bleeding (n = 4). Illumina HumanHT-12 Expression BeadChip microarray analysis was performed by the Finnish DNA Microarray Centre (FDMC) in Turku, and GeneGo *in silico* analysis was undertaken using the gene ontology (GO) and GeneGo projects, with differentially-transcribed genes uploaded to MetaCore v5.4 software. Green numbers and points indicate up-regulated gene transcripts; red indicates down-regulated gene transcripts. A) Thresholds used in filtering differentially-transcribed genes and corresponding numbers of results. B) Volcano plot (fold change vs. significance); dots above the horizontal dashed line are statistically significant by t-test. C) Top five GeneGo process networks from above. *FC = fold change, HMB = heavy menstrual bleeding, mRNA = messenger ribonucleic acid, NMB = normal menstrual bleeding. Work undertaken by JA Maybin, E Marshall, HOD Critchley; published previously in JA Maybin 2011 University of Edinburgh PhD thesis.*

A

	FC	log(FC)	*p*	Up	Down	Total
NMB vs. HMB	1.2	0.260	0.05	88	171	259

B

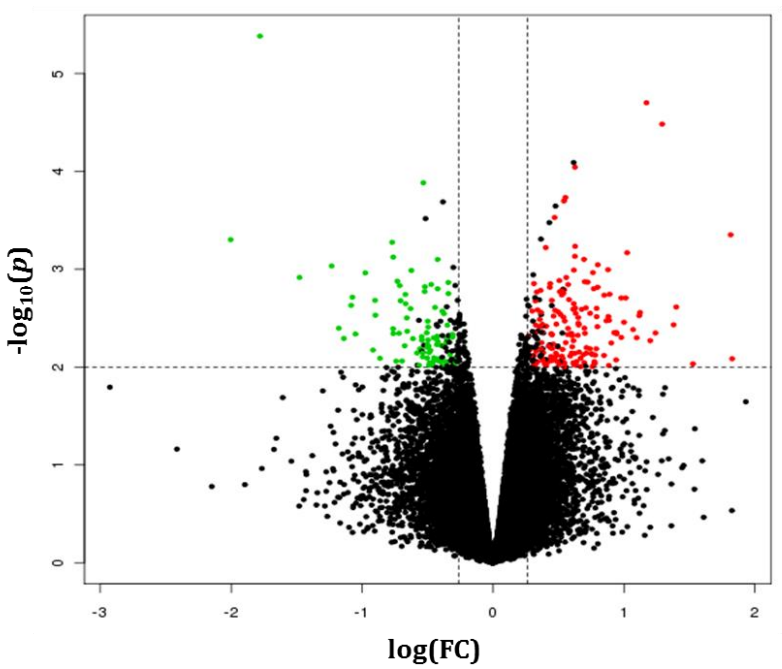

C

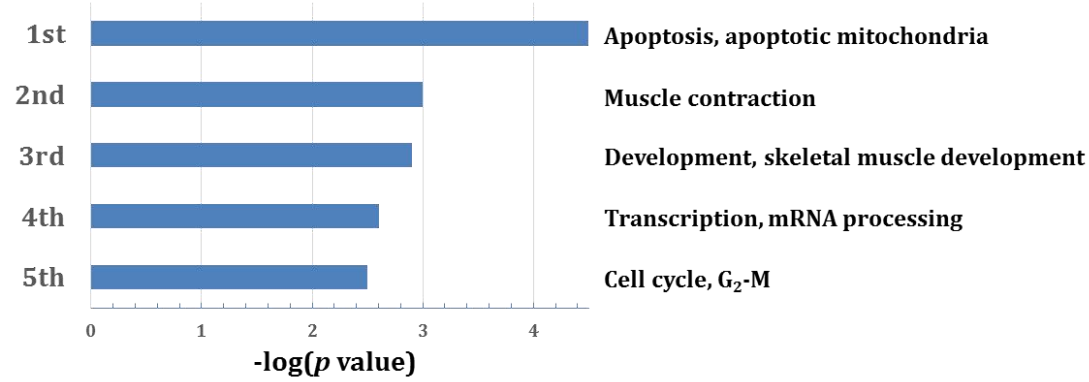

Figure 32. Interactions between gene transcripts involved in apoptotic regulation, programmed cell death and positive regulation of biological processes in the menstrual-phase endometrium of women with HMB versus NMB. Red circles indicate transcripts up-regulated and blue circles indicate transcripts down-regulated in the menstrual-phase endometrium of women with heavy menstrual bleeding vs. normal menstrual bleeding controls. Red arrows indicate positive regulation and blue arrows indicate negative regulation; grey arrows indicate an unknown regulatory relationship. Gene transcripts enclosed by **black boxes** indicate genes pursued for validation in this chapter. *Interaction network adapted from JA Maybin, E Marshall, HOD Critchley; published previously in JA Maybin 2011 University of Edinburgh PhD thesis.*

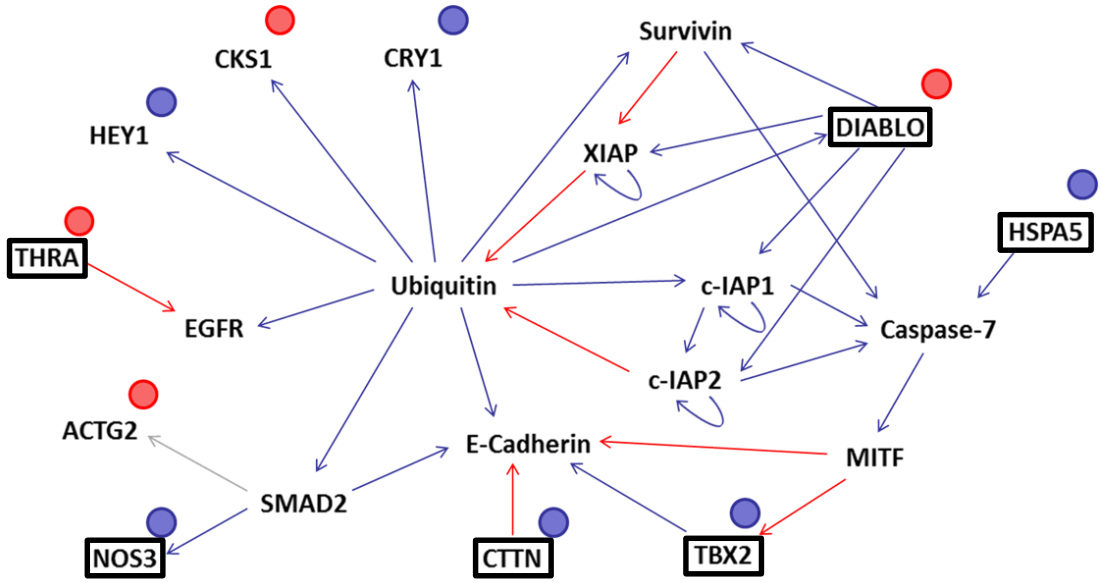

5.1.1 Hypothesis & Research Questions

Hypothesis: Apoptosis is dysregulated in the endometrium of women who suffer heavy menstrual bleeding.

During the perimenstrual window of the human menstrual cycle, compared to the endometrium of women with normal menstrual bleeding…

1. Does the endometrium of women suffering heavy menstrual bleeding exhibit differential transcription of apoptotic genes?
2. Does the endometrium of women suffering heavy menstrual bleeding show differences in the intensity or localisation of apoptosis?
3. Does the endometrium of women suffering heavy menstrual bleeding exhibit differential transcription of inflammatory cytokines and chemokines?

5.2 Materials and Methods

5.2.1 Human Endometrial Tissue Collection

Endometrial biopsies used for immunoreactivity and histological comparisons were obtained by endometrial suction curette sampling ('Pipelle' tissue biopsies; Laboratorie CCD, Paris, France) from the uterine cavities of healthy women with informed, written consent (described in 2.1.1 Human Endometrial Tissue Collection) and grouped by menstrual cycle phase on their characterisation by (i) histological dating (based on the criteria described by Noyes *et al*. (1950)), (ii) last menstrual period (LMP) reported by the patient and (iii) serum oestradiol and progesterone concentrations at the time of biopsy (see 2.1.2 Dating of Endometrial Biopsies).

Samples were selected from the menstrual and proliferative phases of the endometrial cycle, full details of which can be found in 2.1.3 Perimenstrual Window (Luteo-Follicular Transition)), and categorised by menstrual blood loss (MBL) as determined by alkaline haematin method (Warner *et al*., 2004): patients with normal menstrual bleeding (NMB) had losses of <80 mL per cycle and patients with heavy menstrual bleeding (HMB) had losses of ≥80 mL (NICE Clinical Guideline 44 on HMB, 2007).

Samples for RT-qPCR-based studies were also categorised by menstrual blood loss, and chosen to span the 'perimenstrual window' (from late secretory phase to early proliferative phase of the menstrual cycle).

5.2.2 Immunohistochemistry

Localisation of cleaved caspase-3 was examined in tissue samples derived from endometrial sampling ('Pipelle' tissue biopsies) from the menstrual and proliferative

phases (see 2.1.1 Human Endometrial Tissue Collection), and was performed according to the immunohistochemical protocols described in 2.2 Immunohistochemistry.

5.2.3 Semi-Quantitative Histoscoring

Cleaved caspase-3 localisation and staining intensity was further determined in menstrual- and proliferative-phase 'Pipelle' tissue samples in women with objectively-measured NMB and HMB (Menstrual: NMB, n = 7, HMB, n = 5; Proliferative: NMB, n = 8, HMB, n = 6) by employing a semi-quantitative histoscoring method (Aasmundstad *et al*., 1992; Wang *et al*., 1998; Critchley *et al*., 2006). Tissue sections were first divided into cellular compartments comprising surface epithelium, glandular epithelium, stroma and perivascular/endothelial cells. Each compartment was then assigned a staining intensity grade of 0 – 3 based on the cleaved caspase-3 immunoreactivity observed, where '0' represented no staining, '1' was weak staining, '2' was moderate staining and '3' was strong staining. A histoscore of 0 – 300 for each tissue compartment was then calculated by multiplying the staining intensity by the estimated percentage of tissue staining positive (to the nearest 10%) within that compartment.

Each sample histoscore represents the average from three different tissue sections.

Full details of semi-quantitative histoscoring protocols are described in 2.3 Semi-Quantitative Histoscoring.

5.2.4 Whole Genome Array & Functional *in Silico* Analysis

A whole genome array analysis of gene transcription in menstrual-phase endometrial biopsies from women with objectively-verified NMB and HMB was undertaken by

Dr. JA Maybin with the assistance of Dr. E Marshall, published previously in JA Maybin's 2011 University of Edinburgh PhD thesis:

Quality of RNA from menstrual-phase endometrial biopsies (NMB, n = 4; HMB, n = 4) was assessed by means of an Agilent 2100 Bioanalyser system (Agilent Technologies, Cheshire, UK; see 2.6.2 RNA Quality Validation), diluted to 0.150 μg/μL and sent to the Finnish DNA Microarray Centre (FDMC; Turku Centre for Biotechnology) for analysis by 'HumanHT-12 v3 Expression BeadChip' (BD-103-0603; Illumina Inc., San Diego, USA). BeadChip arrays target >25,000 annotated genes using 48,804 RefSeq- (Build 36.2, Release 22) and UniGene- (Build 199) database-designed probes, with each probe's expression value then calculated from approximately 15 measurements.

The FDMC confirmed RNA quality by Nanodrop 1000 spectrophotometer v3.7 (Thermo Fisher Scientific, Loughborough, UK) and Experion Automated Electrophoresis Station (Bio-Rad Laboratories Ltd., Hemel Hempstead, UK). Amplification of RNA was undertaken on 300 ng total RNA using the Illumina TotalPrep RNA Amplification kit (Life Technologies, Carlsbad, USA), and complementary RNA (cRNA) quality was again confirmed as above.

Seven hundred and fifty nanograms of biotin-labelled cRNA from each sample was hybridised to Beadchip arrays for 18 hours at 58°C, as specified in the Illumina Whole Genome Gene Expression Direct Hybridisation protocol (revision A), after which hybridisation was detected with 1 μg/mL streptavidin-Cy3 (GE Healthcare Ltd., Little Chalfont, UK). BeadChip arrays were scanned by means of an Illumina BeadArray Reader (Illumina Inc.), using BeadScan v3.5 software (Illumina Inc.), and numerical results were presented extracted with GenomeStudio 2008 v1 software (Illumina Inc.). Quantile normalisation method was employed to eliminate non-biological variation between samples and biotin labelling homogeneity was confirmed for all samples.

Correlation and cluster analysis by Pearson's metrics and principal component analysis (PCA) were employed to examine sample relations, and the R statistical computing software package 'LIMMA' (Smyth, 2005; Smyth, Gordon K. *et al*., 2003) was employed to test changes in endometrial gene expression between samples from women with NMB and HMB. Thresholds for filtering differentially-transcribed genes are given in **Figure 31A**, based on statistical significance and magnitude of mean inter-group expression difference.

Functional and clinical significance of differentially-transcribed genes identified by the analysis were assessed by the FDMC using the R package 'globaltest' (Goeman *et al*., 2004) and the Gene Ontology (GO) project. Functional processes and gene networks were determined with the use of MetaCore v5.4 software (build 19940; GeneGo Inc., St. Joseph, USA), a data-mining tool used to predict relationships between gene products from public-domain, peer-reviewed literature.

5.2.5 RNA Extraction & RT-qPCR

Total RNA was extracted from human endometrial tissues across the perimenstrual window from women with objectively-measured NMB and HMB (NMB, n = 10 – 12; HMB, n = 15 - 18), details of which are described in **Table 2**. After extracting RNA, cDNA was synthesised according to protocols described in 2.6 RNA Extraction & Reverse Transcription Quantitative Polymerase Chain Reaction (RT-qPCR).

Levels of *CTTN*, *DIABLO* (*SMAC*), *HSPA5* (*GRP78*), *NOS3* (*eNOS*), *TBX2* and *THRA* mRNA transcripts (see **Table 8**), identified as differentially-regulated by whole genome array (**Figure 31**, **Figure 32**), were measured in menstrual-phase endometrium of women with NMB and HMB; levels of *CCL2* (*MCP1*), *CXCL8* (*IL8*), *IL6* and *TNFA* mRNA transcripts were measured in late-secretory-, menstrual- and early-proliferative-phase

endometrium of women with NMB and HMB. All measurements were performed by TaqMan- (hydrolysis probe) based RT-qPCR assay in triplicate technical replicates and normalised to *ATP5B* mRNA levels as a housekeeping control. Samples of human liver cDNA were included as a positive control and appropriate negative controls were also included. Data were analysed by $\Delta\Delta C_q$ (quantification cycle) method as described by Applied Biosystems (Warrington, UK).

Full details of RT-qPCR protocols and data analysis methodology are described in 2.6 RNA Extraction & Reverse Transcription Quantitative Polymerase Chain Reaction (RT-qPCR).

5.3 Results

5.3.1 Differential Transcription of Apoptotic Genes in the Menstrual-Phase Endometrium of Women with Heavy Menstrual Bleeding

Transcription of the T-box 2 transcription factor (*TBX2*) was significantly decreased in the menstrual-phase endometrium of women with objectively-measured heavy menstrual bleeding in comparison to that of women with normal menstrual bleeding ($p < 0.01$; **Figure 33**).

While transcriptional decreases were uncovered in thyroid hormone receptor alpha (*THRA*), direct IAP-binding protein, low pI (*DIABLO*) and cortactin (*CTTN*), these decreases did not attain statistical significance ($p = 0.0599$, 0.0705 and 0.0903, respectively).

Modest (but not statistically significant) decreases were also found in the transcription of heat shock 70 kDa protein 5 (*HSPA5*; $p = 0.1447$) and endothelial nitric oxide synthase (*NOS3*; $p = 0.3324$).

Figure 33. Decreased *TBX2* transcription observed in the menstrual-phase endometrium of women with HMB, validated from microarray-identified differentially-regulated apoptotic gene transcripts in menstrual-phase endometrial biopsies. RT-qPCR quantification of mRNA levels of microarray-identified transcripts differentially-regulated in the endometrium of women with objectively-verified 'normal' (n = 3 – 4) vs. heavy menstrual bleeding (n = 3); data were analysed by $\Delta\Delta C_q$ method and normalised to *ATP5B* mRNA levels. *HMB = heavy menstrual bleeding, NMB = normal menstrual bleeding. ** p < 0.01; n.s. = not significant (p values stated at lower right of each graph); error bars represent SEM; significance determined by unpaired t-tests. ATP5B = adenosine triphosphate synthase subunit beta, mitochondrial, CTTN = cortactin, DIABLO = direct IAP-binding protein, low pI, E_2 = oestradiol, HSPA5 = heat shock 70 kDa protein 5, NOS3 = endothelial nitric oxide synthase, P_4 = progesterone, TBX2 = T-box 2, THRA = thyroid hormone receptor alpha.*

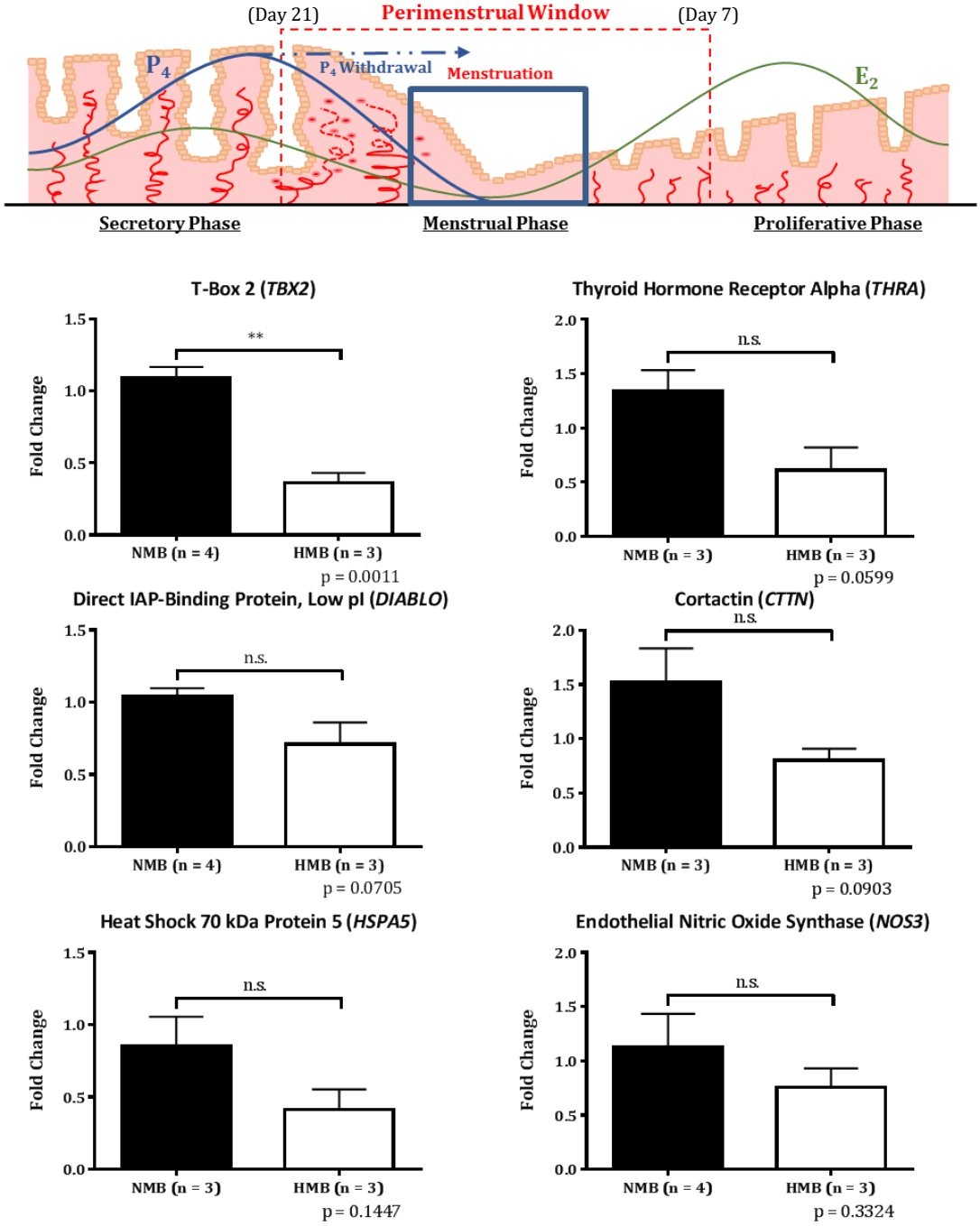

5.3.2 Dysregulated Apoptosis in the Endometrium of Women with Heavy Menstrual Bleeding

Comparisons in the localisation and staining intensity of cleaved caspase-3 between menstrual-phase endometrial biopsies from women with and without heavy menstrual bleeding revealed no significant differences in mean histoscores (**Figure 34A**), even in the glandular epithelium where cleaved caspase-3 expression differences were most pronounced ($p = 0.1360$; **Figure 34B**). A panel of representative tiled and high power photomicrographs of these immunostained endometrial biopsies is given in **Figure 35**. No significant differences were found between the histoscores of proliferative-phase endometrial biopsies from women with and without heavy menstrual bleeding (**Figure 36A**), at which time the differences in glandular epithelial cleaved caspase-3 expression where virtually non-existent ($p = 0.6894$; **Figure 36B**). Representative tiled and high power photomicrographs of these tissues are shown in a panel in **Figure 37**.

Figure 34. No significant differences identified in apoptosis between menstrual-phase endometrial biopsies of women with HMB and NMB controls. Semi-quantitative immunoreactivity histoscoring (staining intensity multiplied by percentage of tissue staining positive) for cleaved caspase-3 (1:400, Cell Signalling Tech.) in menstrual-phase endometrial biopsies of women with objectively-confirmed 'normal' (n = 5) and heavy menstrual bleeding (n = 7). A) Individual data points plotted vs. histoscore, B) mean histoscore in the glandular epithelium. *n.s. = not significant; lines represent mean, error bars represent SEM; significance determined by unpaired t-test.* E_2 *= oestradiol, HMB = heavy menstrual bleeding, NMB = normal menstrual bleeding,* P_4 *= progesterone.*

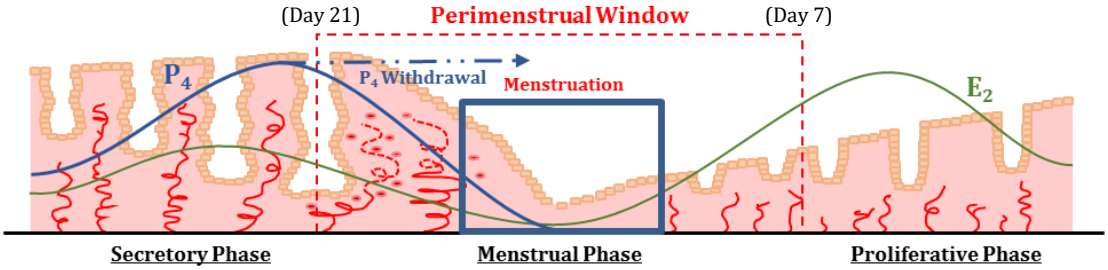

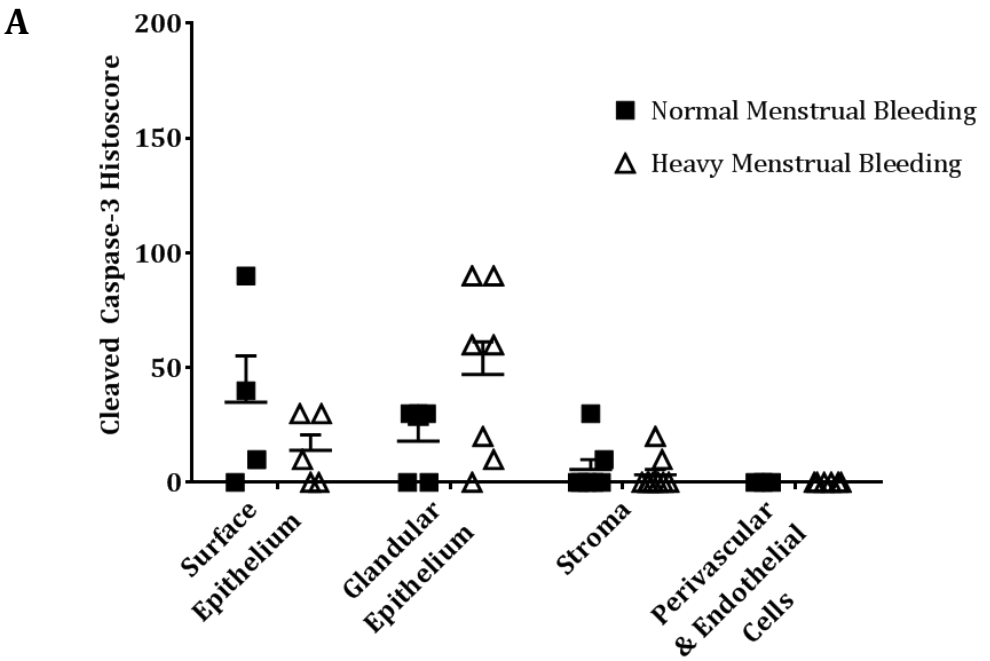

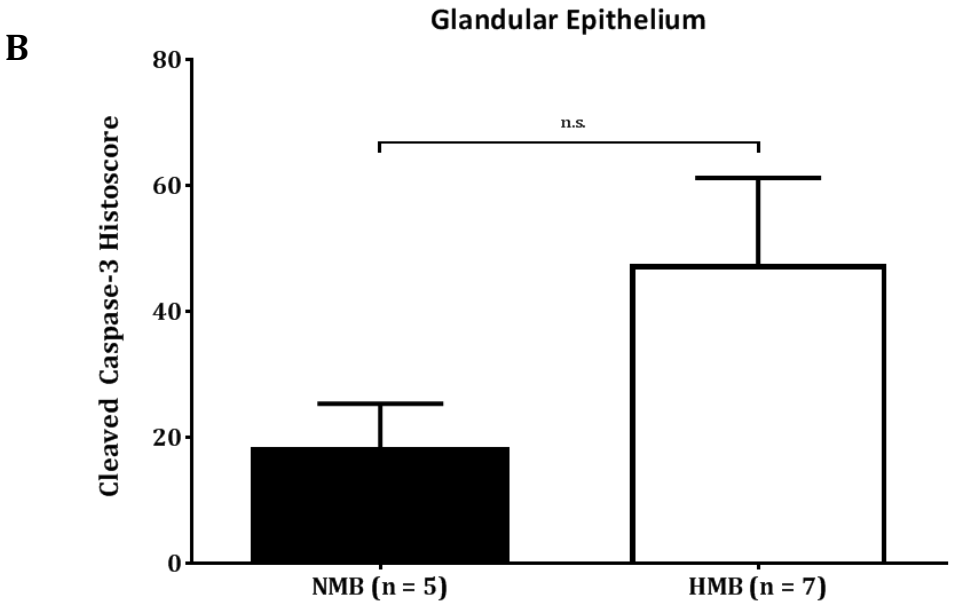

Figure 35. Apoptosis (cleaved caspase-3^{+}) in the endometrial glands and stroma of menstrual-phase biopsies from women with HMB and NMB. Representative photomicrographs of cleaved caspase-3 (1:400, Cell Signalling Tech.) staining in in menstrual-phase endometrial biopsies of women with objectively-confirmed 'normal' (n = 5) and heavy menstrual bleeding (n = 7). Brown-filled triangles indicate cleaved caspase-3 immunoreactivity. *Isotype control: non-immunised rabbit serum Ig fraction (Dako); nuclear counterstain: haematoxylin. Scale bars (500 µm, 100 µm) in image. E_2 = oestradiol, HMB = heavy menstrual bleeding, NMB = normal menstrual bleeding, P_4 = progesterone.*

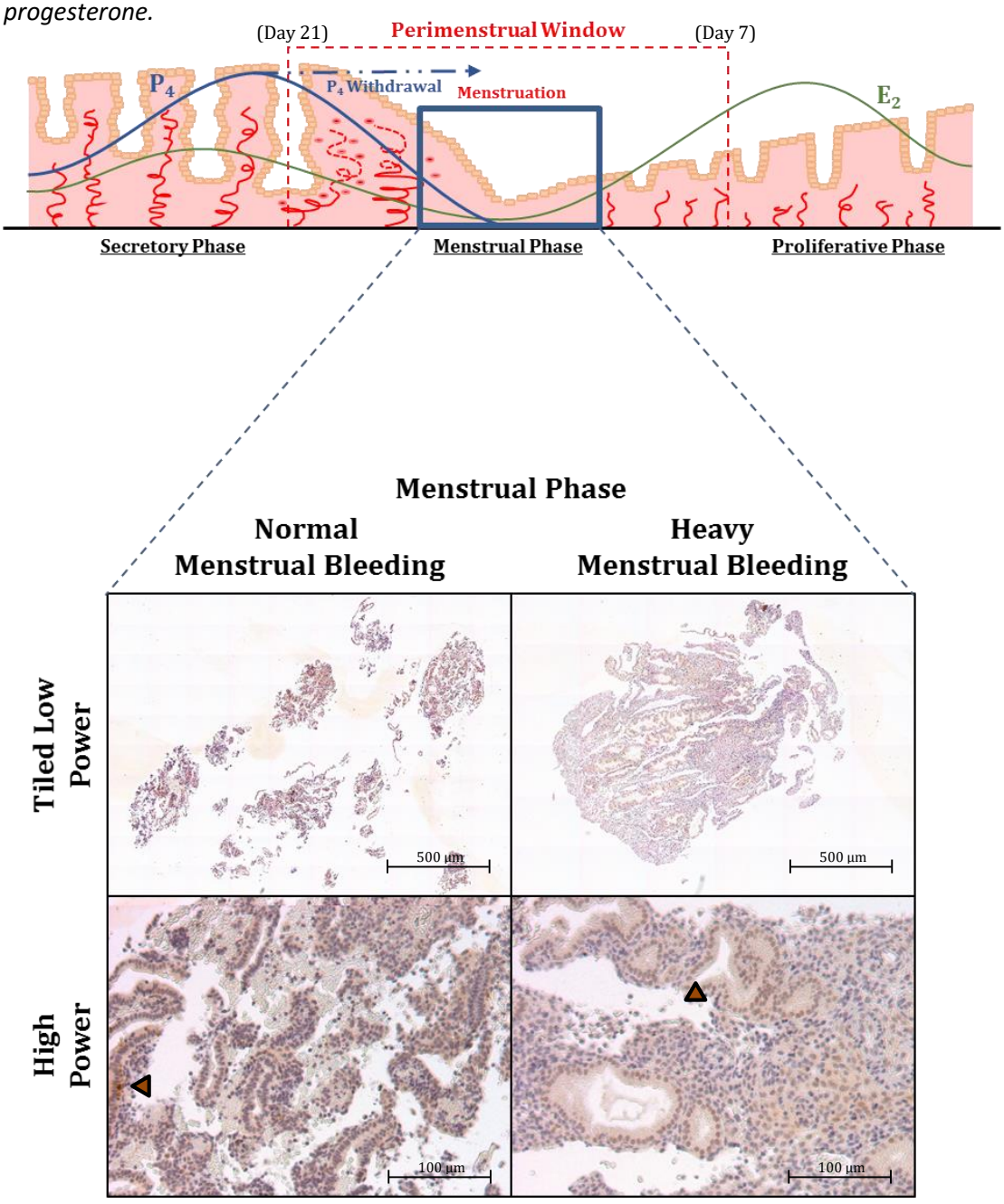

Figure 36. No significant differences identified in apoptosis between proliferative-phase endometrial biopsies of women with HMB and NMB controls. Semi-quantitative immunoreactivity histoscoring (staining intensity multiplied by percentage of tissue staining positive) for cleaved caspase-3 (1:400, Cell Signalling Tech.) in proliferative-phase endometrial biopsies of women with objectively-confirmed 'normal' (n = 8) and heavy menstrual bleeding (n = 6). A) Individual data points plotted vs. histoscore, B) mean histoscore in the glandular epithelium. *n.s. = not significant; lines represent mean, error bars represent SEM; significance determined by unpaired t-test. E_2 = oestradiol, HMB = heavy menstrual bleeding, NMB = normal menstrual bleeding, P_4 = progesterone.*

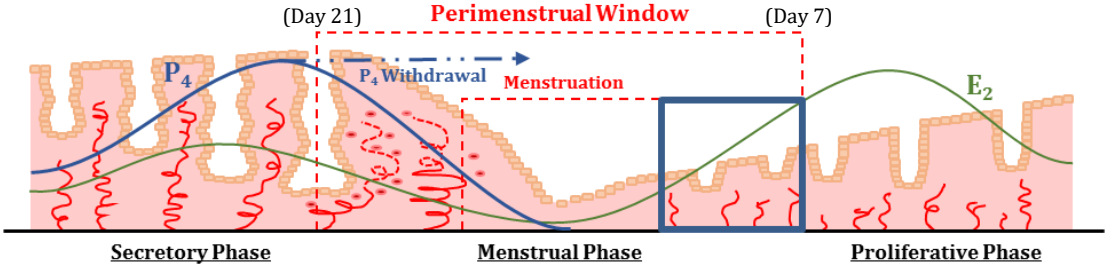

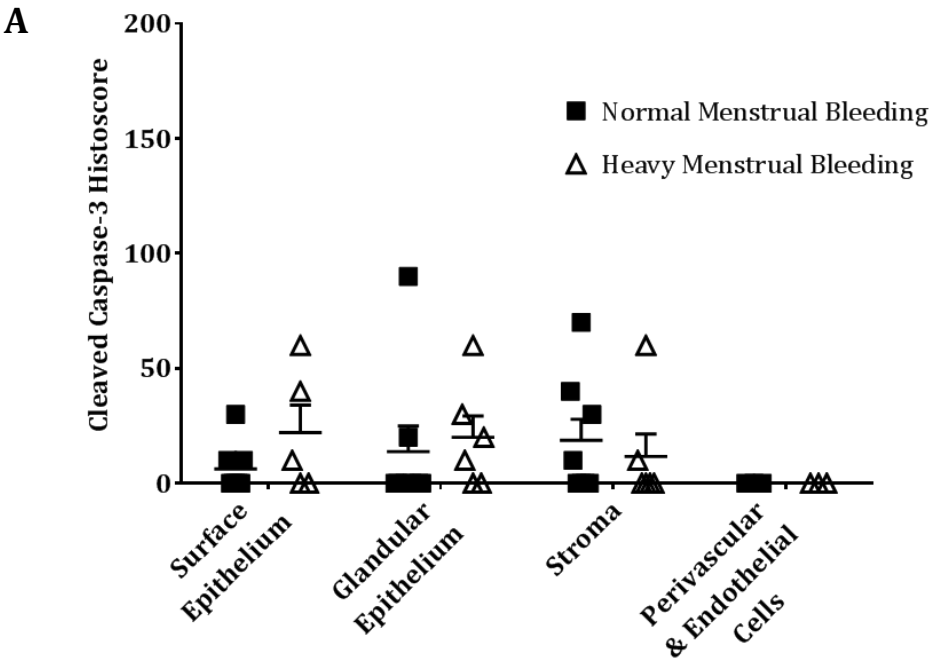

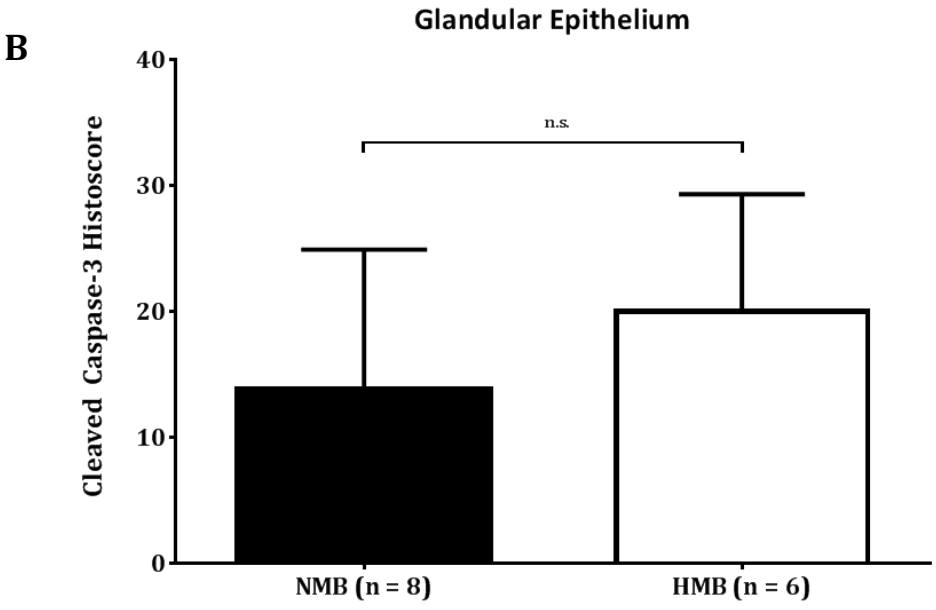

Figure 37. Apoptosis (cleaved caspase-3^{+}) is sparse in proliferative-phase endometrial biopsies from both women with HMB and from women with NMB. Representative tiled photomicrographs of cleaved caspase-3 (1:400, Cell Signalling Tech.) staining in proliferative-phase endometrial biopsies of women with objectively-confirmed 'normal' (n = 8) and heavy menstrual bleeding (n = 6). *Isotype control: non-immunised rabbit serum Ig fraction (Dako); nuclear counterstain: haematoxylin. Scale bars (500 µm, 100 µm) in image. E_2 = oestradiol, HMB = heavy menstrual bleeding, NMB = normal menstrual bleeding, P_4 = progesterone.*

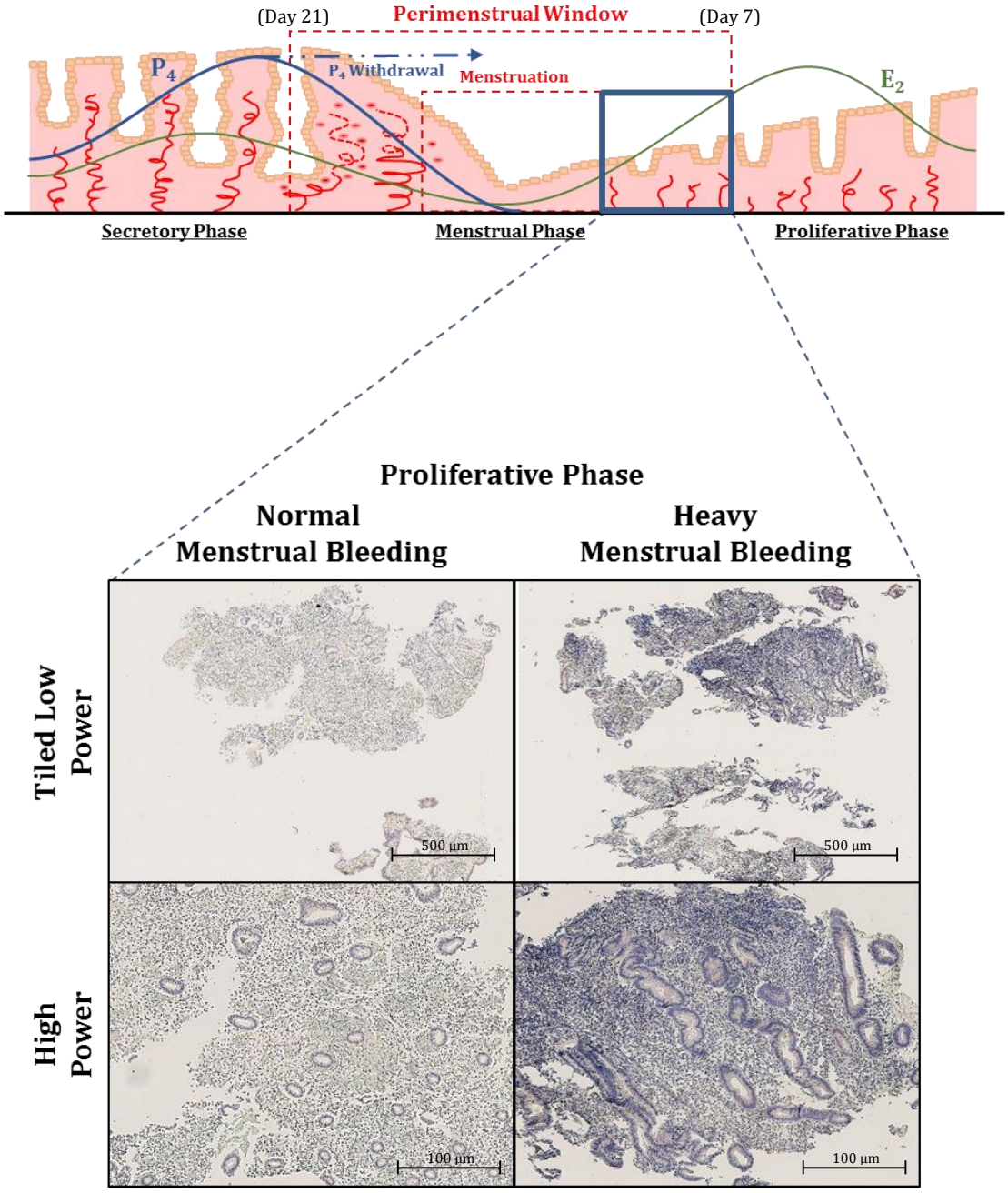

5.3.3 *CCL2*, *CXCL8, IL6* & *TNFA* Transcription across the Perimenstrual Window

Transcription of the chemokine *CXCL8* (*IL8*) was found to be significantly decreased in menstrual-phase endometrium of women with objectively-measured heavy menstrual bleeding compared to that of women with 'normal' menstrual bleeding ($p < 0.01$; **Figure 38B**), whereas no statistically significant transcriptional differences were apparent in comparisons made in the late secretory or early proliferative phases.

The leucocyte chemokine *CCL2* (*MCP1*) and the inflammatory cytokines *IL6* and *TNFA* all showed a trend of decreased transcription in menstrual-phase endometrium from women with heavy menstrual bleeding (**Figure 38A**, **C**, **D**), however none of these differences were found to be statistically significant. No differences in transcription of these chemokines and cytokines were found in comparisons made in the late secretory or early proliferative phases.

Figure 38. Transcription of the neutrophil chemokine *CXCL8* is decreased in the menstrual-phase endometrium of women with HMB. RT-qPCR quantification of chemokines *CCL2* and *CXCL8* (A and B), and of inflammatory cytokines *IL6* and *TNFA* (C and D) mRNA levels in the endometrium of women with objectively-measured heavy menstrual bleeding (MBL ≥ 80 mL) and normal menstrual bleeding (MBL < 80 mL), with data analysed by $\Delta\Delta C_q$ method and normalised to *ATP5B* mRNA levels. *** p < 0.01; error bars represent SEM; significance determined 2-way ANOVA with Sidak's multiple comparisons test (NMB vs. HMB). ATP5B = adenosine triphosphate synthase subunit beta, mitochondrial, CCL2 = C-C motif chemokine ligand 2, C_q = quantification cycle, CXCL8 = C-X-C chemokine ligand 8, E_2 = oestradiol, HMB = heavy menstrual bleeding, IL6 = interleukin-6, MBL = menstrual blood loss, mL = microlitre, NMB = normal menstrual bleeding, P_4 = progesterone, TNFA = tumour necrosis factor alpha.*

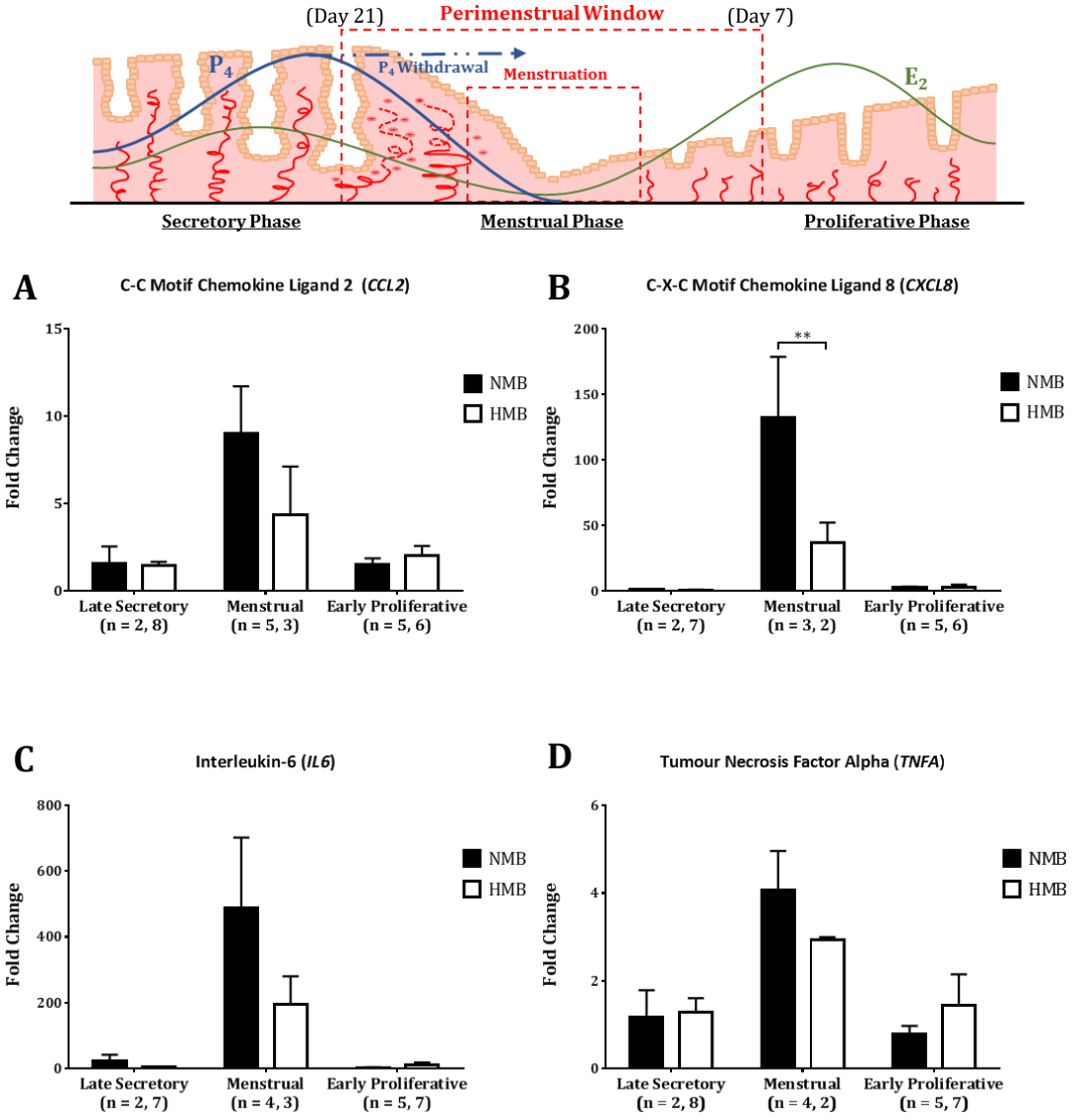

5.4 Discussion

5.4.1 Menstrual-Phase Apoptotic Gene Transcripts

Transcriptional decreases in the transcription factor *TBX2* (T-box 2), identified by whole genome array analysis of menstrual-phase endometrial biopsies from women with normal and heavy menstrual bleeding (NMB and HMB respectively; **Figure 31**, **Figure 32**), were validated in this chapter – differences in the transcription of this gene across the menstrual cycle were as yet undescribed in the literature.

T-box 2, named for its 200-amino-acid 'T-box' DNA-binding domain (Rowley *et al*., 2004), is a transcription factor more known for its contributions to embryonic development (Law *et al*., 1995) than any role in the endometrium or in menstruation. Though increased endometrial TBX2 expression (in the capacity of an oncogene) has been described in endometrial endometrioid adenocarcinoma samples relative to normal endometrium (Liu *et al*., 2010), these hysterectomy-derived samples were obtained from women with a mean age of 54 years (range: 36 – 70) – some of these women will very likely have been post-menopausal (though no such information was given), and no menstrual phase details were given for the women who were not. No inference can therefore be made from the authors' work (Liu *et al*., 2010) as to TBX2 expression with respect to menstrual phase, much less with respect to HMB.

Ismail and Bateman (2009) found that TBX2 expression in SW13 adrenocortical carcinoma cells greatly reduced caspase-3, -8 and -9 activation in response to apoptotic stimuli, and over-expression of TBX2 increased the expression of the apoptosis inhibitor cIAP2 (BIRC3). It is possible TBX2 plays a similar role in the menstrual endometrium, wherein the downregulation of TBX2 at menses may facilitate adequate caspase activation and thus apoptosis; the decreased levels of *TBX2* mRNA in the

endometrium of women with HMB are in theory supported by the modest (although non-significant) increases uncovered in glandular epithelial apoptosis – particularly as TBX2 expression is described as largely restricted to the cytoplasm of endometrial gland epithelial cells (Liu *et al*., 2010).

Transcription of cortactin (*CTTN*), heat shock 70 kDa protein 5 (*HSPA5*) and endothelial nitric oxide synthase (*NOS3*) was found decreased in the endometrium of women with HMB in work detailed in this chapter, though none of these decreases was statistically significant. Decreased transcription was found in all of these genes in the endometrium of women with HMB by our whole genome array (**Figure 31**, **Figure 32**).

The role of cortactin in menstruation and in heavy menstrual bleeding has not yet been described, though like TBX2, has been studied in connection with certain cancers, where it contributes to metastasis and tumour cell invasion (Su *et al*., 2014). Binding of cortactin to E-selectin and recruitment of cortactin to ligand-bound ICAM-1 and VCAM-1 are required to facilitate the deceleration of rolling leucocytes such as neutrophils as they extravasate from blood vessels (Vestweber *et al*., 2013). It is possible, therefore, that it is in this capacity that cortactin insufficiency may contribute to HMB, by inappropriately discouraging leucocyte infiltration from the spiral arterioles at menses – perhaps decreased leucocyte trafficking into the endometrium interferes with timely menstrual repair, as has been described in a mouse model of menses (Kaitu'u-Lino *et al*., 2006), and thereby prolongs menstrual bleeding.

Heat shock 70 kDa protein 5 (HSPA5; also known as glucose-regulated protein 78 kDa, GRP78) is the major chaperone protein of the endoplasmic reticulum, where it acts as a pro-survival factor in the maintenance of endoplasmic reticular homeostasis (Lin *et al*., 2015). HSPA5 also enacts a pro-survival/proliferative role in its binding of

phosphoinositide 3-kinase (PI3K) at the cell surface, regulating the PI3K/Akt signalling pathway and promoting proliferation and survival (Zhang *et al*., 2013). In a pseudo-decidualisation rat model, HSPA5 expression was increased in the endometrium at 5 days post-decidualisation stimulus, and was largely restricted to the glandular epithelium (Simmons and Kennedy, 2000). It is plausible that downregulation of *HSPA5* transcription in the menstrual endometrium of women with HMB delays the restoration of endometrial tissue integrity by re-epithelialisation during menses, thereby prolonging tissue 'injury' and bleeding.

Endothelial nitric oxide synthase (eNOS; also known as type III NOS, NOS3) catalyses the production of nitric oxide (NO), which functions as a vasodilator and platelet aggregation inhibitor (Palmer *et al*., 1987), as well as a neurotransmitter and cytotoxicity mediator (Lowenstein and Snyder, 1992) – it is in the former two capacities that NOS3 is likely to play a role in the endometrium at menstruation, contributing to the establishment of haemostasis in the wake of menstrual bleeding (Christiaens *et al*., 1980).

NOS3 has been described in the human endometrium (Telfer *et al*., 1995) in both mRNA transcript and protein form, and has further been shown to be expressed by endometrial glands throughout the menstrual cycle (Tseng *et al*., 1996). Chwalisz and Garfield (2000) demonstrated that in addition to being important in menstruation, NO species likely play roles in both endometrial receptivity and implantation.

Transcription of *NOS3* has been shown to be stimulated by progesterone in human primary endometrial cells, an effect which was abrogated in the presence of the progesterone receptor antagonist, mifepristone (RU486; Khorram and Han, 2009); 17β-oestradiol (E_2) was also found to stimulate *NOS3* transcription and protein

expression in human primary endometrial cells, with the introduction of progesterone at physiological concentrations augmenting this effect (Han *et al*., 2005).

Zervou *et al*. (1999) describe a cohort of patients with heavy menstrual bleeding in whom significantly higher levels of NO species were produced, an effect they ascribe to increased *NOS3* transcription as a consequence of oestradiol and progesterone. While the samples utilised in these studies were from pre-menopausal women with regular cycles undergoing hysterectomy for HMB, no objective measurements of menstrual blood loss were made in these patients. Since previous studies have found that up to 64% of women who subjectively report suffering HMB have sub-HMB objective measurements (<80 mL; NICE Clinical Guideline 44 on HMB, 2007; Wyatt *et al*., 2001), these findings must be interpreted in light of this caveat. Furthermore, it is difficult to support the assertion that increased *NOS3* transcription could occur in the endometrium of women with HMB as a consequence of oestradiol and progesterone, since no literature supports the premise that oestradiol and progesterone concentrations (or expression of their receptors) differ between the endometria of women with and without HMB (Critchley *et al*., 1994b).

Interestingly, the NOS-dependent endothelial production of NO was found to be enhanced by TNFα *in vitro* (Lamas *et al*., 1991), though the mechanism by which this occurs was not evaluated. This is not implausible in the context of this chapter's results, wherein both *NOS3* and *TNFA* transcription were found downregulated, though it must be noted that neither decrease was statistically significant – further work and increased numbers would be required before any such connection could be entertained.

Although non-significant decreases in transcription were found for thyroid receptor alpha (*THRA*) and direct IAP-binding protein, low pI (*DIABLO*) in the endometrium of

women with HMB in this chapter, these differences were in contradiction to those found by whole genome array (**Figure 31**, **Figure 32**), which showed transcriptional increases for these genes. Since both the whole genome array and the subsequent validation of the transcriptional changes it identified (undertaken in this chapter) made use of very carefully characterised tissues (see 2.1.2 Dating of Endometrial Biopsies and 2.1.1 Human Endometrial Tissue Collection), there are three possible explanations for the discrepancy:

1. Transcription of *THRA* and *DIABLO* is **increased** in the endometrium of women with HMB (supported by whole genome array; NMB, n = 4, HMB, n = 4), and RT-qPCR validation of these targets (NMB, n = 3, HMB, n = 3) failed to confirm this increase
2. There is **no differential transcription** of *THRA* and *DIABLO* in the human endometrium of women with HMB: the whole genome array misidentified the these genes as increased (i.e. false positives) and RT-qPCR validation of these targets failed (as would be expected) to find a difference
3. Transcription of *THRA* and *DIABLO* is **decreased** in the endometrium of women with HMB: the whole genome array misidentified these genes as increased, and RT-qPCR validation of these targets failed to confirm the decrease

Since the RT-qPCR validations described in this chapter are comparatively statistically underpowered, and moreover did not find any significant decreases, the first explanation is the likeliest – *THRA* and *DIABLO* are likely increased in the endometrium of women with HMB, despite the failure of these experiments to confirm this finding.

Thyroid hormone receptor alpha (THRA; also known as nuclear receptor subfamily 1, group A, member 1; NR1A1) is one of several receptors for the thyroid hormone

triiodothyronine (T_3), which participates in the regulation of metabolism, body temperature and growth (Harvey and Williams, 2002). Literature describing the role of THRA in the endometrium is limited, both with respect to menstruation specifically and indeed in general.

Transcription of *THRA* has been found by Catalano *et al*. (2007) to be significantly increased in the endometrium of the secretory phase relative to the proliferative phase, and to decline dramatically upon the arrival of menstruation (physiological progesterone withdrawal), as well as to be decreased in the mid-secretory-phase endometrium of women given the progesterone receptor antagonist mifepristone (pharmacological progesterone withdrawal).

Immunohistochemical and semi-quantitative investigation of THRA protein localisation in the human endometrium performed by Aghajanova *et al*. (2011) found that THRA was present in cells of the stroma and of the surface and glandular epithelia, and that immunoreactivity was highest in the mid-secretory phase (compared to the early secretory phase). The authors unfortunately did not examine THRA expression in the menstrual phase.

Studies undertaken by Zelenko *et al*. (2012) corroborate dynamic endometrial *THRA* transcription, describing levels several fold changes lower in the mid-secretory phase (when progesterone is highest) than in the early proliferative phase (when progesterone is lowest) in a cohort of control patients (i.e. not suffering endometriosis), but their work contains a number of serious methodological flaws. The most serious flaw is that 2 of the 4 patients from whom their proliferative-phase samples were taken were taking levothyroxine or Synthroid (levothyroxine sodium), synthetic forms of the thyroid hormone thyroxine (T_4). These medications could doubtless have an effect on *THRA* transcription, as could the medical necessity for these prescriptions (hypothyroidism) – hypothyroidism is also associated with an increased prevalence of

menstrual irregularities, such as HMB (Krassas *et al*., 1999). A further flaw unaddressed by Zelenko *et al.* is that the statistical significance for each of the 84 genes queried by targeted gene array (of which *THRA* was one) was assessed individually by unpaired t-tests, without appropriate correction for the number of statistical comparisons made.

DIABLO (alternatively known as second mitochondrial activator of caspases, SMAC) is a normally mitochondrially-restricted protein which is released into the cytosol upon induction of apoptosis (Chai *et al*., 2000). Once localised to the cytosol, DIABLO binds and neutralises inhibitors of apoptosis (IAPs), and promotes the proteolytic cleavage of procaspase-3 into cleaved caspase-3, a crucial 'executioner' mediator of apoptosis (Chai *et al*., 2000).

While little is known about the endometrial expression of DIABLO in the human endometrium, its expression in the uterus of the rat throughout the oestrous cycle has been well described (Leblanc *et al*., 2003; Veillette *et al*., 2013). The rodent oestrous cycle shares many similarities with the human menstrual cycle: the cycle begins with oestrogen-dominant phases in which the ovarian follicles develop (the proestrus and oestrus phases, analogous to the human proliferative phase), and is followed by progesterone-dominant phases in which corpus luteum is formed and active (the metoestrus and dioestrus phases, analogous to the human secretory phase). In the absence of pregnancy, as in humans, the corpus luteum regresses and progesterone concentrations decline; but unlike in humans, the rodent endometrium is reorganised in preparation for the following oestrous cycle rather than shed. Nevertheless, the rodent endometrium is also subject to apoptosis across the oestrous cycle (Dharma *et al*., 2001; Lai *et al*., 2000). Studies undertaken by Leblanc *et al*. (2003) showed that when apoptosis (as determined by cleaved caspase-3 expression) was highest in the

oestrous cycle, DIABLO was minimal, and vice versa. In the human, DIABLO immunoreactivity is suggested to have prognostic importance in endometrioid endometrial cancers (Dobrzycka *et al*., 2010).

While the transcriptional differences investigated in this chapter were felt to be especially rigorous, relying on the agreement of three independent criteria to evaluate menstrual phase (see 2.1.2 Dating of Endometrial Biopsies) and on objective measurements of menstrual blood loss to determine menstrual bleeding status (see 2.1.1 Human Endometrial Tissue Collection), this rigour presented something of a limitation in the undertaking of these experiments. Many of the significant changes found in this chapter would have been strengthened by increased numbers (which were only n = 3 – 4 (NMB) and n = 3 (HMB) for the transcriptional experiments) and many of the non-significant changes may have proved significant were tissue samples more numerous. Increased availability of appropriately-characterised samples would therefore be of great benefit for more successful validation of differential transcription of apoptotic gene targets.

5.4.2 Cleaved Caspase-3 & Apoptosis

Immunohistochemical and semi-quantitative histoscoring experiments performed in this chapter sought to compare the expression and localisation of cleaved caspase-3 in the endometrium of women with and without HMB. While no significant differences between the groups were revealed, these data are nevertheless a novel investigation into apoptosis in the endometrium of women suffering HMB, and represent a refinement on previous undertakings to study the same.

Glandular apoptosis had been previously investigated by TUNEL staining in proliferative-phase endometrial biopsies in women with and without symptomatic menstrual abnormalities (including, and mainly, HMB), and was found increased in the glands of women with such abnormalities (Stewart *et al*., 1999). The experiments described in this chapter used tissues of both the menstrual and proliferative phases, in women whose menstrual bleeding status had been more carefully characterised by objective measurements, and performed cleaved caspase-3 immunostaining, an apoptosis detection method superior to TUNEL staining.

Terminal deoxynucleotidyl transferase (TdT)-mediated dUTP-biotin nick end labelling (TUNEL) staining, while a standard and widely-used technique for the immunohistochemical detection of apoptosis (Gavrieli *et al*., 1992), relies on the late-stage apoptotic feature of chromatin fragmentation (Wyllie *et al*., 1984) to label apoptotic cells. As such, apoptotic cells at earlier, pre-DNA-degradation stages of apoptosis will be false negatives (Duan *et al*., 2003). TUNEL staining is also prone to the identification of false positives in the form of cells undergoing active gene transcription (Kockx *et al*., 1998), autolysis (Grasl-Kraupp *et al*., 1995) or which have been subjected to a number of DNA-strand-break-introducing tissue fixation, processing and pre-treatment protocols (Baron *et al*., 2000).

Other studies investigating apoptosis in the human endometrium have concerned ectopic endometrial apoptosis as a potential discriminator of ovarian endometriosis from adenomyosis (Suganuma *et al*., 1997), or have looked at the effects of levonorgestrel-releasing intrauterine systems (LNG-IUS) on endometrial apoptosis (Maia *et al*., 2005; Maruo *et al*., 2001). The latter two studies used patient cohorts who had been prescribed the use of LNG-IUSs to treat HMB associated with adenomyosis (Barrington and Bowen-Simpkins, 1997; Fedele *et al*., 1997), and were principally concerned with the effects that these systems had on the endometrium rather than

underlying differences in apoptosis that may exist in the endometrium of women with and without HMB.

Though cleaved caspase-3 immunoreactivity was very carefully characterised in endometrial tissues of the menstrual and proliferative phases (from women with and without HMB) in the experiments detailed in this chapter, it would be of great interest (if tissue availability would permit) to characterise differences in apoptosis between endometrial samples of the late secretory phase. Experiments described in Chapter 3 revealed that apoptosis first becomes extensive in the endometrial glands of the late secretory phase in women without HMB, though it is as yet unknown whether this is true of women with HMB: it is possible there exist differences in cleaved caspase-3, either in the extent of its expression, its localisation, or in the timing of its onset.

5.4.3 Inflammatory Gene Transcription

Transcriptional changes in the leucocyte chemokines *CCL2* (*MCP1*) and *CXCL8* (*IL8*) and in the inflammatory cytokines *IL6* and *TNFA* investigated in this chapter uncovered significantly lower levels of *CXCL8* mRNA transcript in the menstrual-phase endometrium of women with HMB, and lower (but not statistically significantly) levels of *CCL2*, *IL6* and *TNFA* transcript in the menstrual phase.

Though transcription and expression of *CXCL8* has been widely described in the human endometrium, no studies to date have shown differential transcription in the endometrium of women with HMB. Likewise, no studies exist investigating differences in the transcription of *CCL2*, *IL6* or *TNFA* in the endometrium of women with HMB.

CXCL8 (interleukin-8, IL-8), like its mouse counterpart CXCL1 (Oquendo *et al*., 1989; Scholten and Al-samman, 2012), is a C-X-C motif family chemokine selectively

chemoattractive for neutrophils, mediating not only their extravasation from peripheral blood into tissues, but also their mobilisation from bone marrow, adhesion to endothelial cells and activation and degranulation in tissues (Zhang *et al*., 2001). CXCL8 exerts its effects through the binding of its high-affinity cognate receptors, CXCR1 and 2 (IL8RA and B; Jones *et al*., 1997b), both of which are highly expressed on neutrophils (Huber *et al*., 1991) and also expressed on endothelial cells (Murdoch *et al*., 1999). The secretion of CXCL8 has been described in a multitude of cell types, including fibroblasts, endothelial and epithelial cells, monocytes and other leucocytes (Baggiolini *et al*., 1994; Saito *et al*., 1994), and is positively regulated by classically pro-inflammatory stimuli such as TNFα and interleukin-1β (IL-1β; Baggiolini *et al*., 1994). CXCL8 is reportedly a chemotactic factor for endothelial cells, and can function in an angiogenic capacity (Koch *et al*., 1992; Strieter *et al*., 1995a, 1995b).

CXCL8 expression has been described in the normal human endometrium across the menstrual cycle (Jones *et al*., 1997a; Maybin *et al*., 2011), in stromal cells (Arici *et al*., 1993, 1996) and in blood vessel perivascular cells (Critchley *et al*., 1994a; Milne *et al*., 1999). Maybin *et al*. (2011) reported significant increases in *CXCL8* transcription and protein expression in the menstrual phase, wherein it plays a putative role in menstrual repair.

These findings are corroborated by the *CXCL8* transcriptional data described in Chapter 3, and taken together, suggest that the decreased levels of *CXCL8* transcript observed in the endometrium of women with HMB may be pathologically insufficient, interfering with the timely and successful restoration of tissue and vasculature at menstruation.

CCL2 (also called monocyte chemoattractant protein 1; MCP1) is C-C motif family chemokine which exerts chemoattractive and activating effects on monocytes (as well as a handful of other leucocytes). Its expression and secretion has been described in

fibroblasts (Yoshimura and Leonard, 1990), endothelial cells (Sica et al., 1990a) and certain lymphocytes (Yoshimura *et al*., 1989a), as well as in monocytes themselves (Yoshimura *et al*., 1989b). Pro-inflammatory stimuli such as TNFα and IL-1β strongly potentiate CCL2 expression (Baggiolini *et al*., 1994). CCL2 acts primarily through its high-affinity C-C chemokine receptor, CCR2 (Charo *et al*., 1994; Graves *et al*., 1999). Binding of CCL2 to its receptors induces chemotaxis and activation in monocytes and macrophages (Charo *et al*., 1994), and in a variety of other leucocytes, including NK cells and basophil granulocytes (Allavena *et al*., 1994; Hartmann *et al*., 1995).

As in other tissues, where CCL2 is reported to induce vascular smooth muscle cell (VSMC) proliferation (Watanabe *et al*., 2001; Selzman *et al*., 2002), endometrial VSMC proliferation is influenced by CCL2 (Kayisli *et al*., 2015).

With respect to CCL2 and its role in early pregnancy, recent work by Gibson *et al*. (2015) demonstrated that uterine natural killer (uNK) cells are a major endometrial source of CCL2, and that CCL2 potently increased human endometrial endothelial cell (HEEC) network formation.

Across the menstrual cycle, CCL2 immunoreactivity has been reported by Jones *et al*. (1997a) to be highest in the premenstrual phase (with respect to the early secretory phase), though *CCL2* transcription was not investigated.

These menstrual cycle findings were not precisely recapitulated by the data presented in this chapter or in Chapter 3 – in which *CCL2* transcription was found to be significantly increased in the menstrual phase relative to late secretory and proliferative phases – though it is of course possible that the increases in *CCL2* mRNA transcript observed would not result in increases in CCL2 protein. Furthermore, Jones *et al.* (1997a) describe a significantly-increased CCL2 immunoreactivity in late secretory phase relative to early secretory phase, not to menstrual phase. Thus,

although not recapitulating the findings of Jones *et al.* (1997a), neither do the data presented in this chapter fundamentally dispute them.

IL-6 is an interleukin cytokine, long-considered to be exclusively pro-inflammatory due to its regulation of the production of acute phase inflammatory proteins (e.g. C-reactive protein, complement and serum amyloid A) in the liver during acute inflammation (Akira and Kishimoto, 1992). More recent studies have indicated, however, that IL-6 has a more nuanced role and is better regarded as both a pro- and anti-inflammatory cytokine: in mice, the introduction of IL-6-neutralising antibodies increased TNFα and interferon gamma (IFNγ) expression in response to staphylococcal enterotoxin B (SEB; Matthys *et al*., 1995) and in healthy humans, lipopolysaccharide- (LPS)-induced production of TNFα was inhibited by the introduction of recombinant IL-6 (Starkie *et al*., 2003). Still more recent work has implicated IL-6 in an inflammation-limiting role via the induction of alternative macrophage activation (Mauer *et al*., 2014)

In studies undertaken by (von Wolff *et al*., 2000), *IL6* is reported to be dynamically transcribed across the menstrual cycle, showing peak transcription in the late secretory phase. It is worth noting, however, that the authors assessed *IL6* mRNA transcript levels by RNase protection assay (in which a known RNA sequences is 'protected' by an antisense probe, then all other RNA is degraded by the introduction of a single-stranded RNA-specific ribonuclease) as an alternative to quantitative PCR, and that von Wolff *et al.* did not examine transcription in menstrual-phase samples. Subsequent work by several of the same authors confirmed this expression pattern (though again, excluding menstrual-phase samples), attributing the increased *IL6* transcription to endometrial leukocytes, epithelial and stromal cells (von Wolff *et al*., 2002), and also described increased IL-6 protein concentrations in the endometrial glands and its secretions in the late secretory phase.

In that no literature to date describes *IL6* transcription in the human endometrium in the menstrual phase, nor the differences therein in women with HMB, the data derived from these experiments may help elucidate the role IL-6 plays in the endometrium at menstruation.

Tumour necrosis factor alpha (TNFα) is an inflammatory cytokine first discovered in the serum of bacillus-Calmette-Guérin-(BCG)-infected mice following the administration of LPS (Carswell *et al*., 1975). It is produced primarily by activated macrophages and T-cells in a membrane-bound precursor form (pro-TNF), but is released by matrix-metalloproteinase- (MMP)-mediated cleavage as a soluble molecule (Black *et al*., 1997).

Despite what was thought to be its initial promise as a cancer treatment, TNFα quickly became recognised for its potent inflammatory activities: TNFα mediates neutrophil adherence to endothelial cells (Gamble *et al*., 1985), induces apoptosis in endothelial cells *in vitro* (Robaye *et al*., 1991), potentiates the expression of CXCL8 and CCL2 chemokines in endothelial cells (Sica *et al*., 1990a, 1990b) and is the central regulator of LPS-induced endotoxic shock (Beutler *et al*., 1985; Tracey *et al*., 1986).

TNFα expression and secretion has been described in the human endometrium (Hunt *et al*., 1992; Tabibzadeh, 1991; Tabibzadeh *et al*., 1995) and has been suggested to play an active role in menstrual tissue shedding (Tabibzadeh *et al*., 1995). Its transcription and expression are reported in endometrial epithelial and stromal cells (Tabibzadeh, 1991). Although *TNFA* transcription is reportedly increased in the late-secretory-phase endometrium (von Wolff *et al*., 2000), as with the authors' investigation of *IL6* transcription, no menstrual-phase samples were included in their sample cohort.

Interestingly, a study conducted by Malik *et al*. (2006) found significantly increased TNFα total protein in the menstrual effluent of women with objectively-verified HMB,

though its concentration was reportedly not significantly increased – this may merely reflect an increased volume of effluent, or at least a sufficiently increased volume to preclude the finding of a statistically significant difference.

Despite a relatively robust body of literature describing TNFα expression in the endometrium, no comparisons have been made of its endometrial expression between women with HMB and healthy controls. Data in these experiments may help further the understanding of how TNFα functions in the endometrium in normal physiology and in HMB.

The experiments performed in this chapter employed great rigour in the characterisation of endometrial tissue biopsies used, both in the criteria used to evaluate menstrual phase (see 2.1.2 Dating of Endometrial Biopsies) and in the criteria to evaluate menstrual bleeding status (see 2.1.1 Human Endometrial Tissue Collection). Unfortunately, while ultimately strengthening the work, this substantially limited the availability of endometrial tissues for experiments. Particularly for late-secretory- and menstrual-phase biopsies from women with objective menstrual blood loss measurements, sample numbers were prohibitively limiting.

The work detailed in this chapter would have benefitted greatly from augmented sample sizes, strengthening existing findings and perhaps uncovering further statistically significant differences. Increased tissue availability would also have facilitated the investigation of protein expression differences by Western blotting to corroborate changes uncovered in transcription.

5.4.4 Summary & Conclusions

RT-qPCR experiments undertaken in this chapter validated transcriptional decreases in the transcription factor T-box 2 (*TBX2*) found by whole genome array in the menstrual-phase endometrium of women with heavy menstrual bleeding, though failed to validate some of the other transcriptional changes identified in other apoptotic genes.

Immunohistochemical and semi-quantitative histoscoring data demonstrated the possibility of decreased cleaved caspase-3 expression in the endometrial glands at menses in women with heavy menstrual bleeding, though these differences were not statistically significant; cleaved caspase-3 expression and localisation were not significantly different in any tissue compartment in the proliferative phase of the menstrual cycle. These cleaved caspase-3 expression and localisation data are a novel investigation into apoptosis in the endometrium of women suffering HMB, and represent a methodological improvement on previous undertakings to study the same.

Transcription of the neutrophil chemokine *CXCL8* was found by RT-qPCR to be significantly decreased in the endometrium of women with heavy menstrual bleeding at menses, and though decreases were observed in the transcription of some other inflammatory chemokines and cytokines (*CCL2*, *IL6* and *TNFA*), these were not statistically significant.

These observations are summarised in (**Table 14**).

Table 14. Summary of differences observed in the human endometrium of women with heavy menstrual bleeding across the late secretory, menstrual and early proliferative phases of the menstrual cycle. Upward-facing arrows (↑) and shades of orange reflect increases in the observed quantity (relative to the endometrium of women with normal menstrual bleeding) described in this chapter; downward-facing arrows (↓) and shades of blue reflect decreases. White boxes without symbols reflect no differences in the quantity observed (cleaved caspase-3) or 'baseline' for transcriptional changes. 'N/A' and grey-shaded boxes represent time-points for which no data were available. Novel data to which the summary table refers can be found on the pages listed in the right-most column. *LS = late secretory phase, M = menstrual phase, EP = early proliferative phase. * denotes statistical significance ($p < 0.01$) for the observations described.*

Menstrual Phase	LS	M	EP	Pages
TBX2 transcription	*N/A*	↓↓/*	*N/A*	175
CTTN, HSPA5, *NOS3* transcription	*N/A*	↓	*N/A*	175
THRA, *DIABLO* transcription	*N/A*	↓	*N/A*	175
Apoptosis (cleaved caspase-3)	*N/A*	↑		177, 178, 179, 180
CXCL8 transcription		↓↓/*		182
CCL2, *IL6*, *TNFA* transcription		↓		182

6. Endometrial Repair and Proliferation in a Caspase-Inhibited Mouse Model of Induced Menstruation

6.1 Introduction

The oestrogen-primed human endometrium undergoes extensive differentiation under the influence of progesterone in the late secretory phase, termed 'decidualisation'. Decidualising endometrial stromal cells adopt a more spherical morphology and begin to express a number of factors, including prolactin and insulin-like growth factor-binding protein 1 (Brosens *et al*., 1999; Dunn *et al*., 2003). In most mammalian species decidualisation does not occur until embryonic/endometrial contact is established (i.e. implantation), however decidualisation occurs spontaneously in humans, even in the absence of implantation (Finn, 1998). In the event that implantation does not occur in the human endometrium, declining progesterone concentrations effected by the regression of the corpus luteum trigger endometrial breakdown and shedding, termed menstruation (Csapo and Resch, 1979).

Species whose endometria do not undergo spontaneous decidualisation, such as mice, do not menstruate in consequence of declining progesterone concentrations alone (Finn, 1998). Menstruation can be simulated in ovariectomised mice, however, by sequentially administering oestradiol and progesterone to prime the murine endometrium for decidualisation, and by administering oil to the lumen of the uterus to stimulate a decidualisation response (Finn and Pope, 1984). Declining progesterone concentrations following the final injections effect menstrual-like molecular and histological changes.

The studies described herein employ a refinement to the above model introduced by Brasted *et al*. (2003), in which progesterone injections are substituted by subcutaneously-implanted progesterone-releasing implants, the removal of which

mimics the regression of the corpus luteum in humans and triggers menstrual-like shedding of the endometrium.

As in the human menstrual endometrium (Finn, 1986; King *et al*., 1996; Evans and Salamonsen, 2012), the murine endometrium in this model shows inflammatory-like features subsequent to the withdrawal of progesterone, for instance leucocyte recruitment and chemokine expression (Cheng *et al*., 2007; Menning *et al*., 2012).

Apoptosis, a form of programmed cell death, is a biological process important to the maintenance of tissue homeostasis, disposal of infected and aged cells, remodelling tissue and resolution of acute inflammation (Kerr *et al*., 1972; Savill *et al*., 2002). Cysteine-aspartic acid proteases (caspases) are key effectors of apoptotic cell death, with the activation of caspase-3 occurring at the confluence of the intrinsic (initiated by caspase-9; Li *et al*., 1997) and extrinsic (initiated by caspase-8; Li *et al*., 1998) pathways of apoptotic induction (Slee *et al*., 2001; **Figure 3**).

In both the human endometrium (Chapter 3) and the mouse endometrium in a model of induced menses (Chapter 4), breakdown and shedding of the endometrium involves extensive apoptosis.

In the studies described herein, the effects of apoptosis inhibition on the events of menstruation were investigated by administering mice the pan-caspase inhibitor quinolyl-valyl-O-methylaspartyl-[2,6-difluorophenoxy]-methyl ketone (Q-VD-OPh), a potent and non-cytotoxic inhibitor of all major caspase-dependent apoptotic pathways (Caserta *et al*., 2003; **Figure 39**), at the time of progesterone withdrawal (**Figure 40**).

Figure 39. Inhibition of intrinsic and extrinsic apoptotic pathways by the pan-caspase inhibitor, Q-VD-OPh. Diagrammatic representation Q-VD-OPh inhibition of intrinsic and extrinsic apoptosis pathways (Caserta *et al.*, 2003). Caspase-3 cleavage is mediated by cleaved caspase-9 (intrinsic) or by cleaved caspase-8 (extrinsic). NB: simplified diagram omits many participants in the apoptosis pathway (see review by Danial and Korsmeyer, 2004). *Q-VD-OPh = quinolyl-valyl-O-methylaspartyl-[2,6-difluorophenoxy]-methyl ketone.*

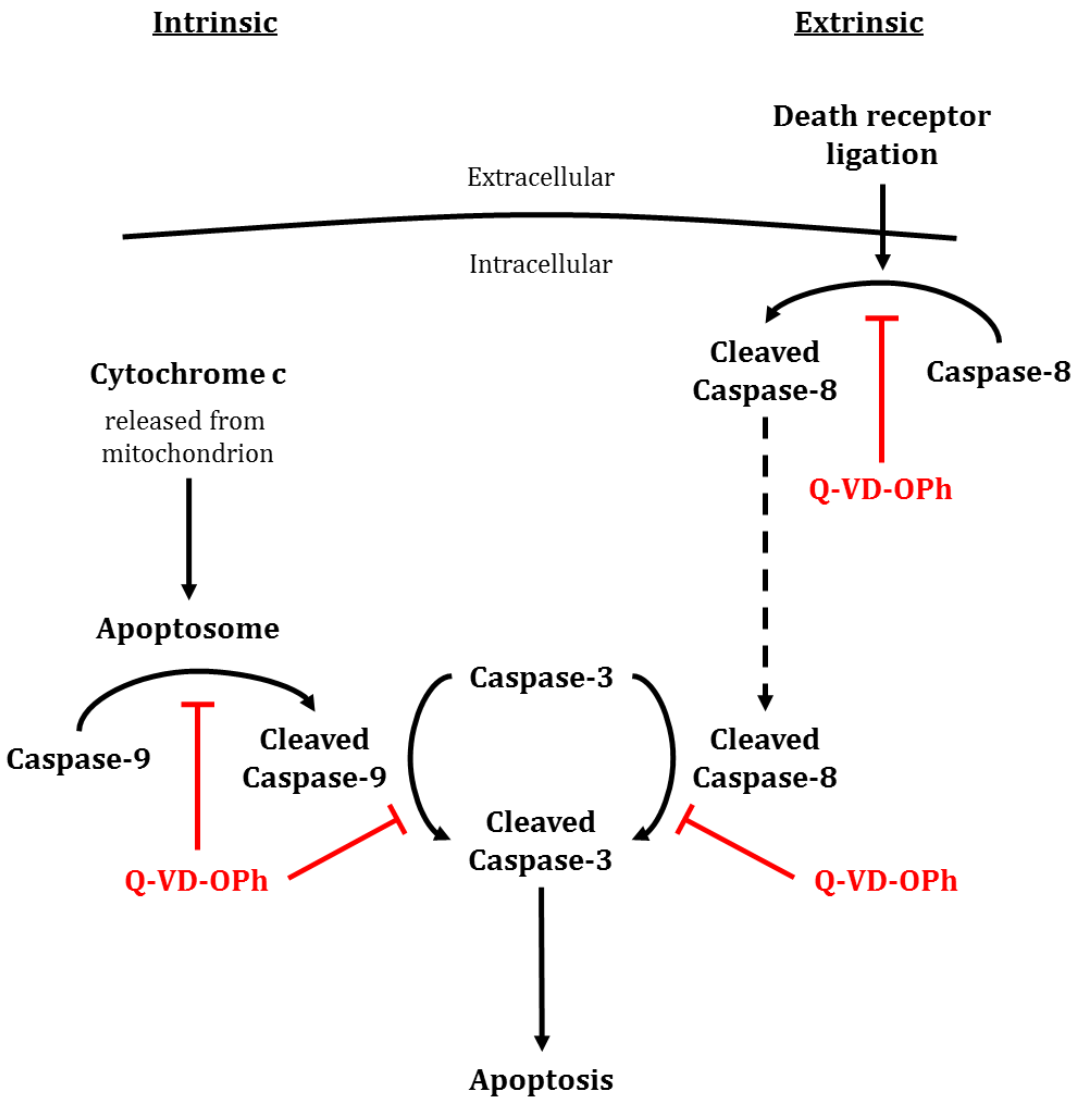

Figure 40. Mouse model of induced menstruation protocol with Q-VD-OPh caspase inhibition. Ovariectomised C57Bl/6 mice were administered oestradiol and progesterone to mimic human endocrine regulation of the endometrium through the menstrual cycle, with decidualisation induced via injection of oil into the lumen of the uterus; withdrawal of progesterone induced bleeding and menstrual-like endometrial changes (Finn and Pope, 1984; Brasted *et al*., 2003; Cheng *et al*., 2007; Cousins *et al*., 2014). The pan-caspase inhibitor Q-VD-OPh (or vehicle control) was administered intraperitoneally concomitant with progesterone withdrawal. *E_2 = oestradiol, i.p. = intraperitoneal, i.u. = intrauterine, kg = kilogram, mg = microgram, ng = nanogram, ovex = ovariectomy, P_4 = progesterone, Q-VD-OPh = quinolyl-valyl-O-methylaspartyl-[2,6-difluorophenoxy]-methyl ketone, s.c. = subcutaneous.*

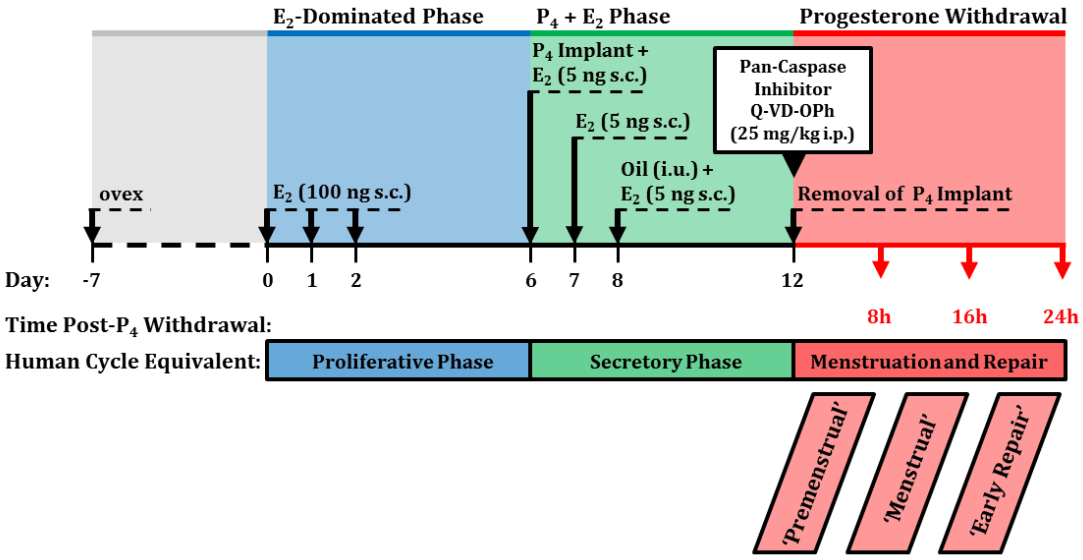

6.1.1 Hypothesis & Research Questions

Hypothesis: Experimental inhibition of apoptosis in a mouse model of induced menstruation will delay endometrial repair, delay the resolution of inflammation and lead to dysregulated proliferation

Following progesterone withdrawal in a mouse model of induced menstruation…

1. Does inhibition of apoptosis delay endometrial repair?
2. Does inhibition of apoptosis modulate the inflammatory environment of the mouse endometrium?
3. Does inhibition of apoptosis affect the intensity or distribution of proliferation and/or hypoxia in the mouse endometrium?

6.2 Materials & Methods

6.2.1 Caspase-Inhibited Mouse Model of Induced Menstruation

Although mice do not ordinarily menstruate, a mouse model of menses has been optimised in which endometrial decidualisation is stimulated, a number of menstrual-like features are effected and the tissue is subsequently repaired and restored (see 2.7 Mouse Model of Induced Menstruation).

The experiments described in this chapter sought to inhibit apoptosis at the time of progesterone withdrawal. Therefore while under isoflurane-induced anaesthesia for the removal of the progesterone pumps, mice in the treatment group were administered the pan-caspase inhibitor quinolyl-valyl-O-methylaspartyl-[2,6-difluorophenoxy]-methyl ketone (Q-VD-OPh; see **Figure 39**), a potent, non-cytotoxic inhibitor of the three major caspase-dependent apoptotic pathways (caspase-9/-3, caspase-8/-10 and caspase-12; Caserta *et al*., 2003).

Q-VD-OPh was administered at a dose of 25 mg/kg of body weight, dissolved in dimethyl sulphoxide (DMSO) and diluted 1:10 in sterile phosphate-buffered saline (PBS). Mice in the vehicle control group were administered 10% DMSO in PBS. Both the treatment and vehicle control were delivered as single-dose, 150-µL intraperitoneal injections.

A combined, 150-µL, single-dose intraperitoneal injection of 5'-bromo-2'-deoxyuridine (BrdU; 60 mg/kg) and pimonidazole hydrochloride (Hypoxyprobe; 60 mg/kg) was administered 1.5 hours before the mice were sacrificed and their tissues were harvested. BrdU immunoreactivity indicates active cell proliferation (Gratzner, 1982), whereas Hypoxyprobe immunoreactivity indicates partial oxygen pressures (pO_2) of

less than 10 mmHg (hypoxia; Varghese *et al*., 1976; Raleigh *et al*., 1985). Both compounds were dissolved in sterile PBS.

Mice were sacrificed at 8, 16 and 24 hours after removal of progesterone pumps and Q-VD-OPh/vehicle control injections (**Figure 40**). Uterine horns were removed and weighed, then split into two parts: one part was processed by 4% NBF fixation and embedded in paraffin for immunohistochemical studies, and the other was stored in RNA-stabilising reagent and stored at -80°C for RNA extraction.

Full details of these protocols can be found in 2.7 Mouse Model of Induced Menstruation.

6.2.2 Immunohistochemistry

Cleaved caspase-3, BrdU (a proliferation marker) and Hypoxyprobe (a marker of hypoxia) immunoreactivity and localisation was examined in endometrial tissues derived from vehicle-control- and Q-VD-OPh-treated mice following progesterone withdrawal (n = 32; see 2.7 Mouse Model of Induced Menstruation), according to the immunohistochemical protocols detailed in 2.2 Immunohistochemistry. Progesterone withdrawal time-points of 8 hours (n = 8), 16 hours (n = 12) and 24 hours (n = 12) were examined.

Tissues were additionally stained with haematoxylin and eosin (H&E) to facilitate the histological assessment of endometrial repair.

6.2.3 Semi-Quantitative Histoscoring

Localisation and expression intensity of cleaved caspase-3, BrdU and Hypoxyprobe were further investigated in Q-VD-OPh- and vehicle-control-treated mouse endometrial

tissues following progesterone withdrawal (n = 29; see 2.7 Mouse Model of Induced Menstruation) by means of a semi-quantitative histoscoring method (Aasmundstad *et al*., 1992; Wang *et al*., 1998; Critchley *et al*., 2006). Endometrial tissue sections were divided into cellular compartments (surface epithelium, glandular epithelium, decidual mass/stroma, basal stroma and perivascular cells/endothelium), to each of which a staining intensity grade of 0 – 3 was assigned: 0 represented no observed staining, 1 represented weak staining, 2 represented moderate staining and 3 represented strong staining. The staining intensity grade was multiplied by the estimated percentage of immunopositive tissue in that compartment (to the nearest 10%), yielding a histoscore of 0 – 300.

Each sample histoscore represents the average of histoscores from three 'complete' cross-sections through the tissue (in which the tissue was fully encircled by smooth muscle and all cellular compartments were present).

Full details of semi-quantitative histoscoring protocol can be found in 2.3 Semi-Quantitative Histoscoring.

6.2.4 Histological Assessment of Endometrial Repair

Progression of endometrial repair was assessed in haematoxylin- and eosin-stained tissue sections from Q-VD-OPh- and vehicle-control-treated mice following the withdrawal of progesterone (n = 33; see 2.7 Mouse Model of Induced Menstruation) according to a set of morphological features of endometrial breakdown and repair developed by Kaitu'u-Lino *et al*. (2006). A score of 1 – 5 was assigned to, where 1 corresponds to intact, decidualised endometrium, 3 corresponds to complete breakdown with no intact decidual tissue, and 5 corresponds to complete

re-epithelialisation and stromal restoration. Morphological breakdown and repair features are detailed in full in **Table 5**.

Each endometrial repair score represents the average of three different 'complete' cross-sections through the tissue (with all cellular compartments present and a fully smooth-muscle-encircled endometrium).

Further details of endometrial repair scoring can be found in 2.4 Histological Assessment of Endometrial Repair.

6.2.5 RNA Extraction & RT-qPCR

Total RNA was extracted from uterine tissues of mice treated with Q-VD-OPh or vehicle control following progesterone withdrawal (n = 25 – 31; see 2.7 Mouse Model of Induced Menstruation) and cDNA was synthesised according to the protocols described in 2.6 RNA Extraction & Reverse Transcription Quantitative Polymerase Chain Reaction (RT-qPCR). Progesterone withdrawal time-points of 8 hours (n = 9), 16 hours (8 – 10) and 24 hours (n = 9 – 12) were examined.

Cxcl1 and *Tnfa* mRNA transcript (see **Table 9**) levels were assayed by TaqMan-(hydrolysis probe) based RT-qPCR using triplicate technical replicates and normalising measurements to *Actb* mRNA transcript levels as a housekeeping control: cDNA extracted from mouse liver was included as a positive control and appropriate negative controls were also included. Data were analysed $\Delta\Delta C_q$ (quantification cycle) method as described by Applied Biosystems (Warrington, UK).

Full details of RT-qPCR and data analysis protocols can be found in 2.6 RNA Extraction & Reverse Transcription Quantitative Polymerase Chain Reaction (RT-qPCR).

6.3 Results

6.3.1 Q-VD-OPh Inhibition of Apoptosis at 8, 16 & 24 Hours Post-Progesterone Withdrawal

Administration of the pan-caspase inhibitor Q-VD-OPh completely abrogated cleaved caspase-3 expression (indicating apoptosis) in the mouse endometrium at 8 hours after progesterone withdrawal (simulated 'premenstrual' phase), whereas the endometrium of mice administered vehicle control showed cleaved caspase-3 expression (**Figure 41A**). Although the differences in apoptosis between the two treatment groups were most pronounced in the decidualised stroma, these were not statistically significant ($p = 0.1604$; **Figure 41B**); neither were differences in basal stromal apoptosis significant ($p = 0.3036$; **Figure 41C**). A panel of representative photomicrographs taken from cleaved-caspase-3-immunostained murine endometrial tissues at 8 hours after progesterone withdrawal is shown in **Figure 42**.

By 16 hours after Q-VD-OPh administration and progesterone withdrawal (simulated 'menstrual' phase), considerable cleaved caspase-3 expression was again seen in the endometrium, with mean histoscores showing no significant differences compared to vehicle-control-treated mice (**Figure 43A**). Levels of apoptosis were highest in the decidualised stroma of the endometrium of both Q-VD-OPh- and vehicle-control-treated mice (**Figure 43B**). Representative photomicrographs from endometrial tissues stained for cleaved caspase-3 at 16 hours after progesterone withdrawal are shown in a panel in **Figure 44**.

Levels of cleaved caspase-3 expression were comparable between the endometrium of mice treated with Q-VD-OPh and vehicle control at 24 hours after progesterone withdrawal (simulated 'early repair' phase; **Figure 45A**). Apoptosis was most extensive in the decidualised stroma of both treatment groups (**Figure 45B**). A panel of representative photomicrographs of cleaved-caspase-3-immunostained endometrial tissues taken at 24 hours after progesterone withdrawal is shown in **Figure 46**.

Figure 41. The pan-caspase inhibitor Q-VD-OPh abrogated cleaved caspase-3 expression in the decidualised and basal stroma at 8 hours post-progesterone withdrawal. Semi-quantitative immunoreactivity histoscoring (staining intensity multiplied by percentage of tissue staining positive) for cleaved caspase-3 (1:400, Cell Signalling Tech.) in endometrial tissues of mice administered Q-VD-OPh (n = 3) or vehicle control (n = 5), 8 hours following progesterone withdrawal. A) Individual data points plotted vs. histoscore, B) mean histoscores in the decidualised and basal stromae. *Each data point represents the average of three experiments; lines represent mean; error bars represent SEM.* E_2 *= oestradiol,* P_4 *= progesterone, Q-VD-OPh = quinolyl-valyl-O-methylaspartyl-[2,6-difluorophenoxy]-methyl ketone.*

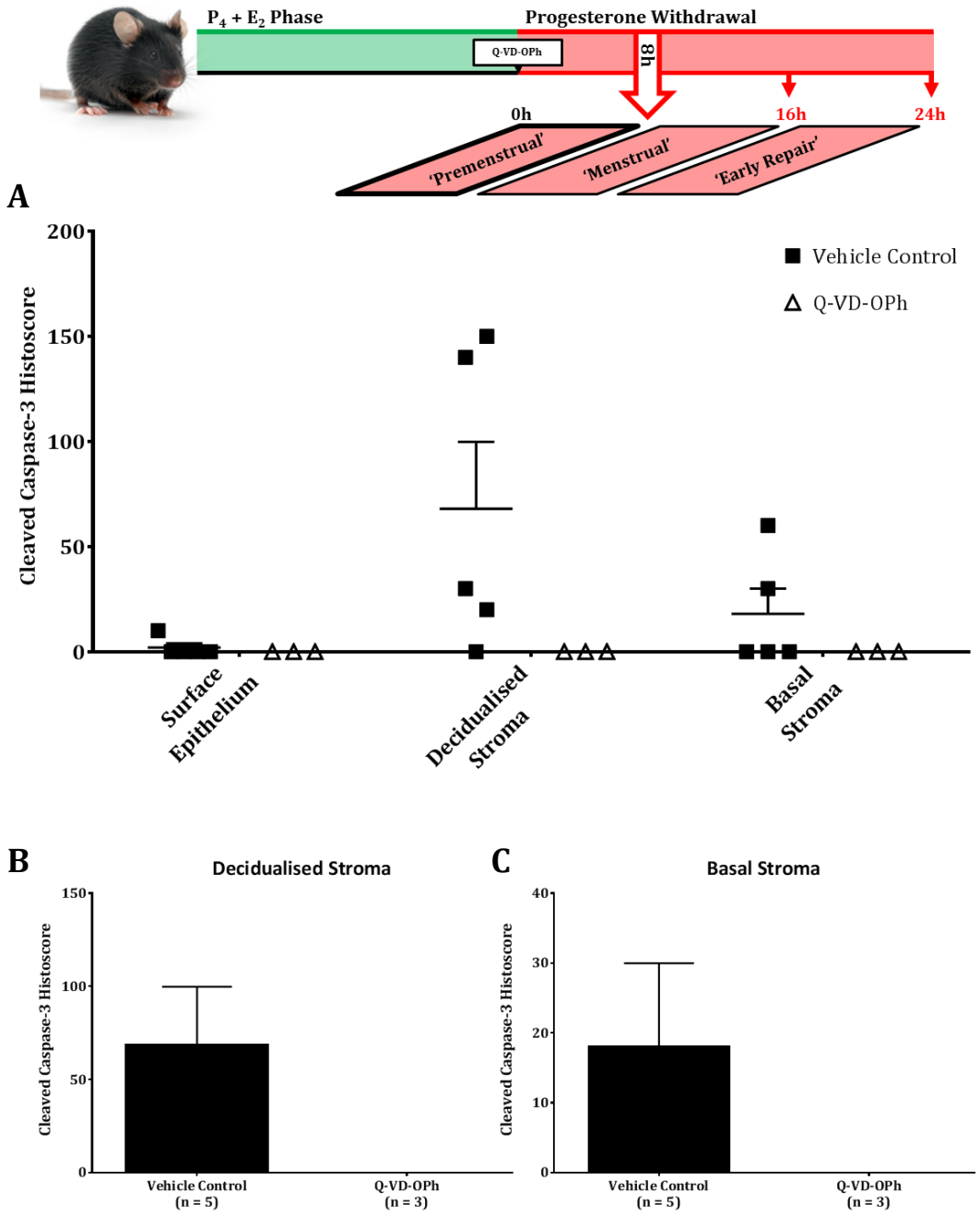

Figure 42. Cleaved caspase-3 expression undetectable in the endometrium of mice treated with Q-VD-OPh at 8 hours after progesterone withdrawal. Representative photomicrographs of cleaved caspase-3 (1:400, Cell Signalling Tech.) staining in serial sections of endometrium from mice administered Q-VD-OPh (n = 3) or vehicle control (n = 5), 8 hours following progesterone withdrawal. *Isotype control: non-immunised rabbit serum Ig fraction (Dako); nuclear counterstain: haematoxylin. Scale bars (500 µm, 50 µm) in image.* *E_2 = oestradiol, P_4 = progesterone, Q-VD-OPh = quinolyl-valyl-O-methylaspartyl-[2,6-difluorophenoxy]-methyl ketone.*

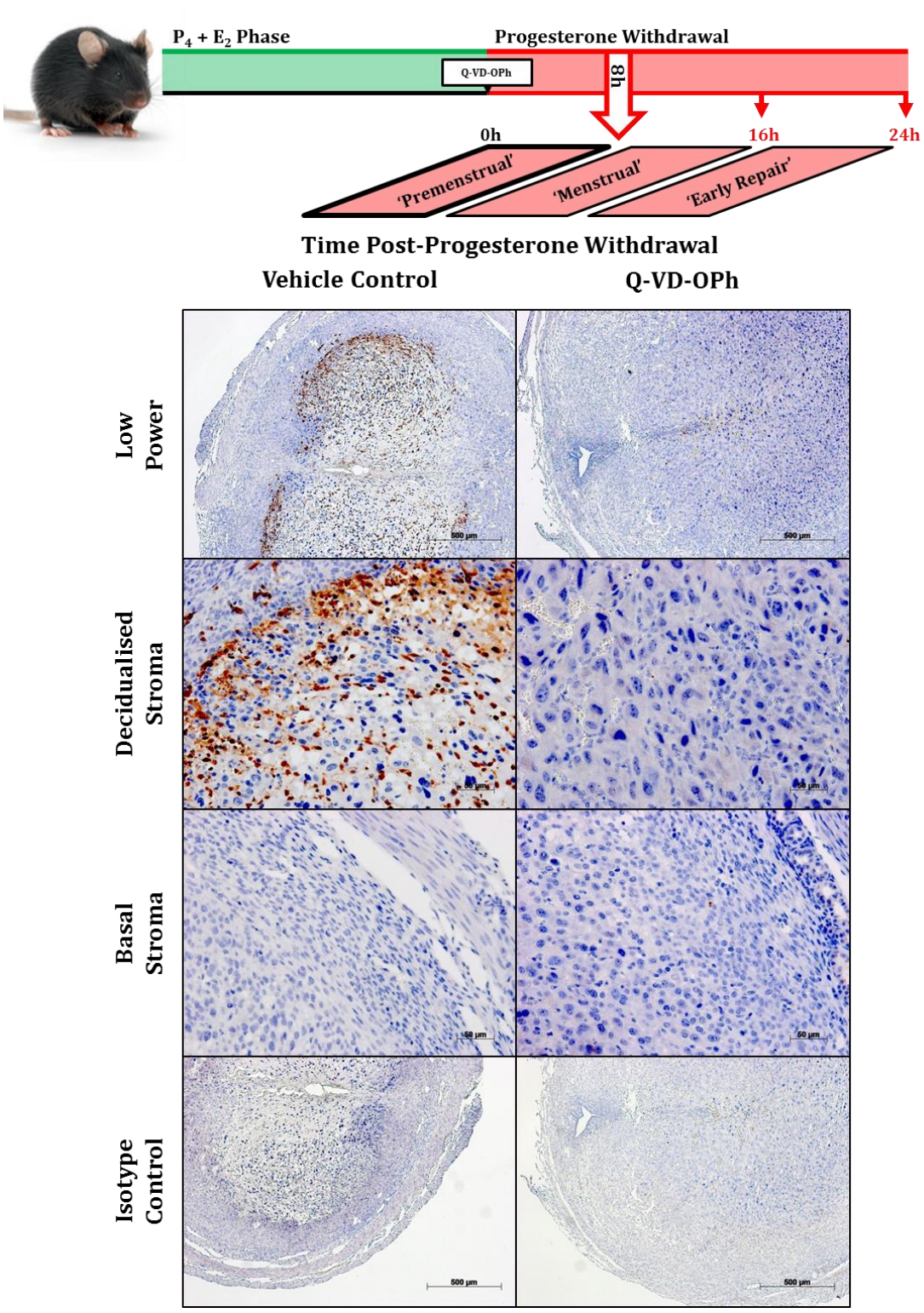

Figure 43. Cleaved caspase-3 expression returns to the Q-VD-OPh-treated mouse endometrium by 16 hours post-progesterone withdrawal. Semi-quantitative immunoreactivity histoscoring (staining intensity multiplied by percentage of tissue staining positive) for cleaved caspase-3 (1:400, Cell Signalling Tech.) in endometrial tissues of mice administered Q-VD-OPh (n = 8) or vehicle control (n = 4), 16 hours following progesterone withdrawal. A) Individual data points plotted vs. histoscore, B) mean histoscore in decidualised stroma. *Each data point represents the average of three experiments; lines represent mean; error bars represent SEM.* *E_2 = oestradiol, P_4 = progesterone, Q-VD-OPh = quinolyl-valyl-O-methylaspartyl-[2,6-difluorophenoxy]-methyl ketone.*

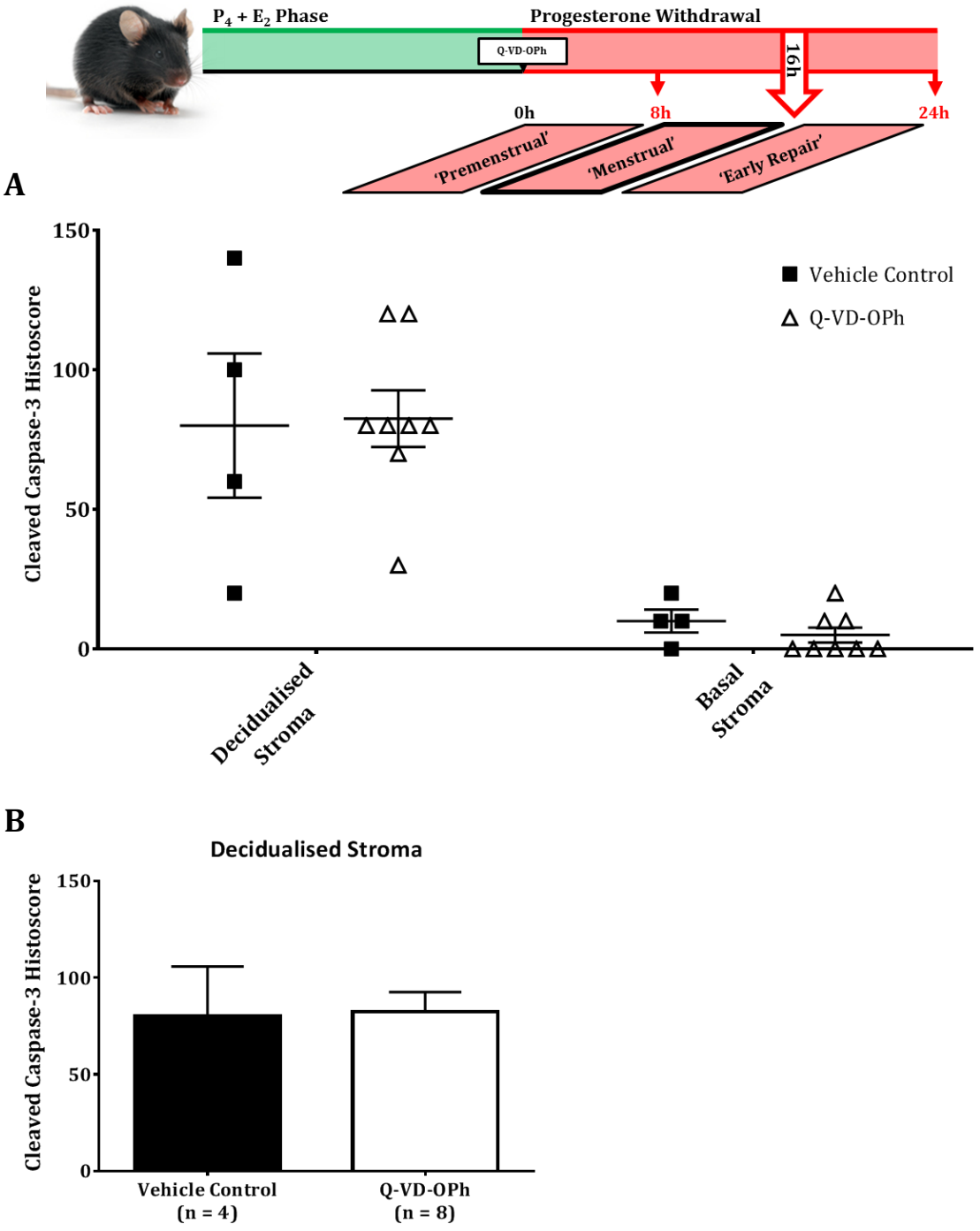

Figure 44. Cleaved caspase-3 expression detectable in the endometrium of both Q-VD-OPh- and vehicle-control-treated mice at 16 hours post-progesterone withdrawal. Representative photomicrographs of cleaved caspase-3 (1:400, Cell Signalling Tech.) staining in serial sections of endometrium from mice administered Q-VD-OPh (n = 8) or vehicle control (n = 4), 16 hours following progesterone withdrawal. *Isotype control: non-immunised rabbit serum Ig fraction (Dako); nuclear counterstain: haematoxylin. Scale bars (500 µm, 50 µm) in image.* E_2 *= oestradiol,* P_4 *= progesterone, Q-VD-OPh = quinolyl-valyl-O-methylaspartyl-[2,6-difluorophenoxy]-methyl ketone.*

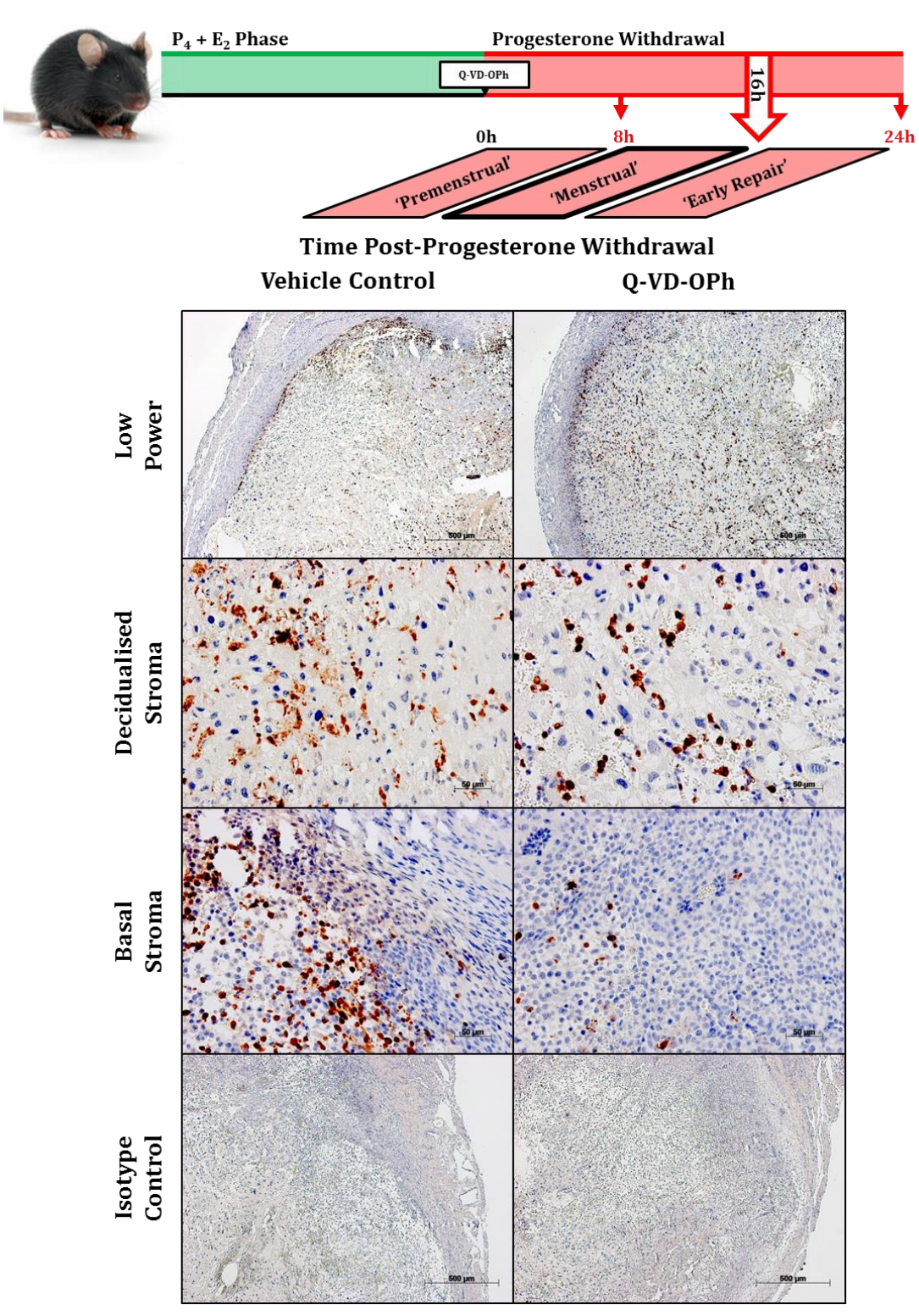

Figure 45. No differences in cleaved caspase-3 expression between the endometrium of Q-VD-OPh- and vehicle-control-treated mice at 24 hours after progesterone withdrawal. Semi-quantitative immunoreactivity histoscoring (staining intensity multiplied by percentage of tissue staining positive) for cleaved caspase-3 (1:400, Cell Signalling Tech.) in endometrial tissues of mice administered Q-VD-OPh (n = 5) or vehicle control (n = 7), 24 hours following progesterone withdrawal. A) Individual data points plotted vs. histoscore, B) mean histoscore in decidualised stroma. *Each data point represents the average of three experiments; lines represent mean; error bars represent SEM. E_2 = oestradiol, P_4 = progesterone, Q-VD-OPh = quinolyl-valyl-O-methylaspartyl-[2,6-difluorophenoxy]-methyl ketone.*

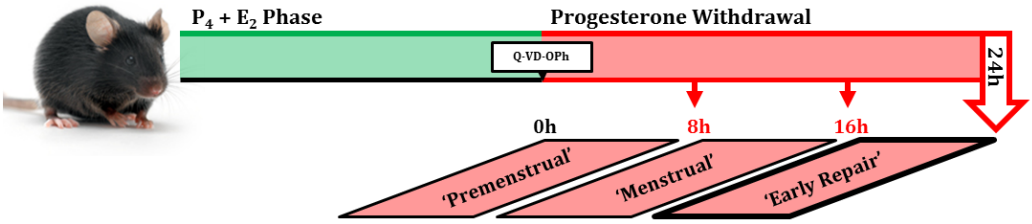

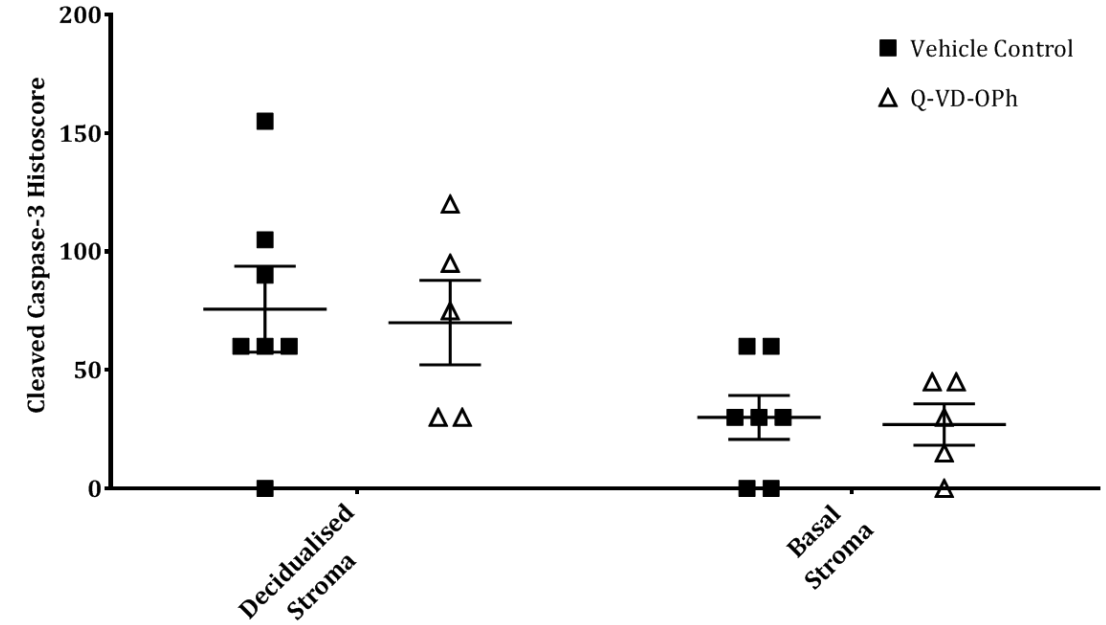

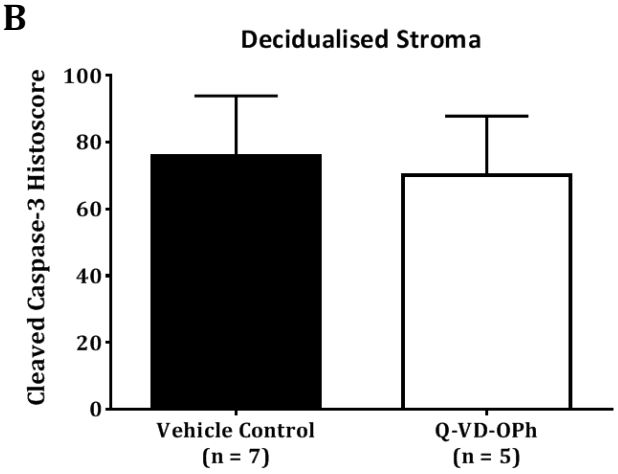

Figure 46. Cleaved caspase-3 expression is extensive in the endometrium of both Q-VD-OPh- and vehicle-control-treated mice at 24 hours after progesterone withdrawal. Representative photomicrographs of cleaved caspase-3 (1:400, Cell Signalling Tech.) staining in serial sections of endometrium from mice administered Q-VD-OPh (n = 5) or vehicle control (n = 7), 24 hours following progesterone withdrawal. *Isotype control: non-immunised rabbit serum Ig fraction (Dako); nuclear counterstain: haematoxylin. Scale bars (500 µm, 50 µm) in image.* E_2 *= oestradiol,* P_4 *= progesterone, Q-VD-OPh = quinolyl-valyl-O-methylaspartyl-[2,6-difluorophenoxy]-methyl ketone.*

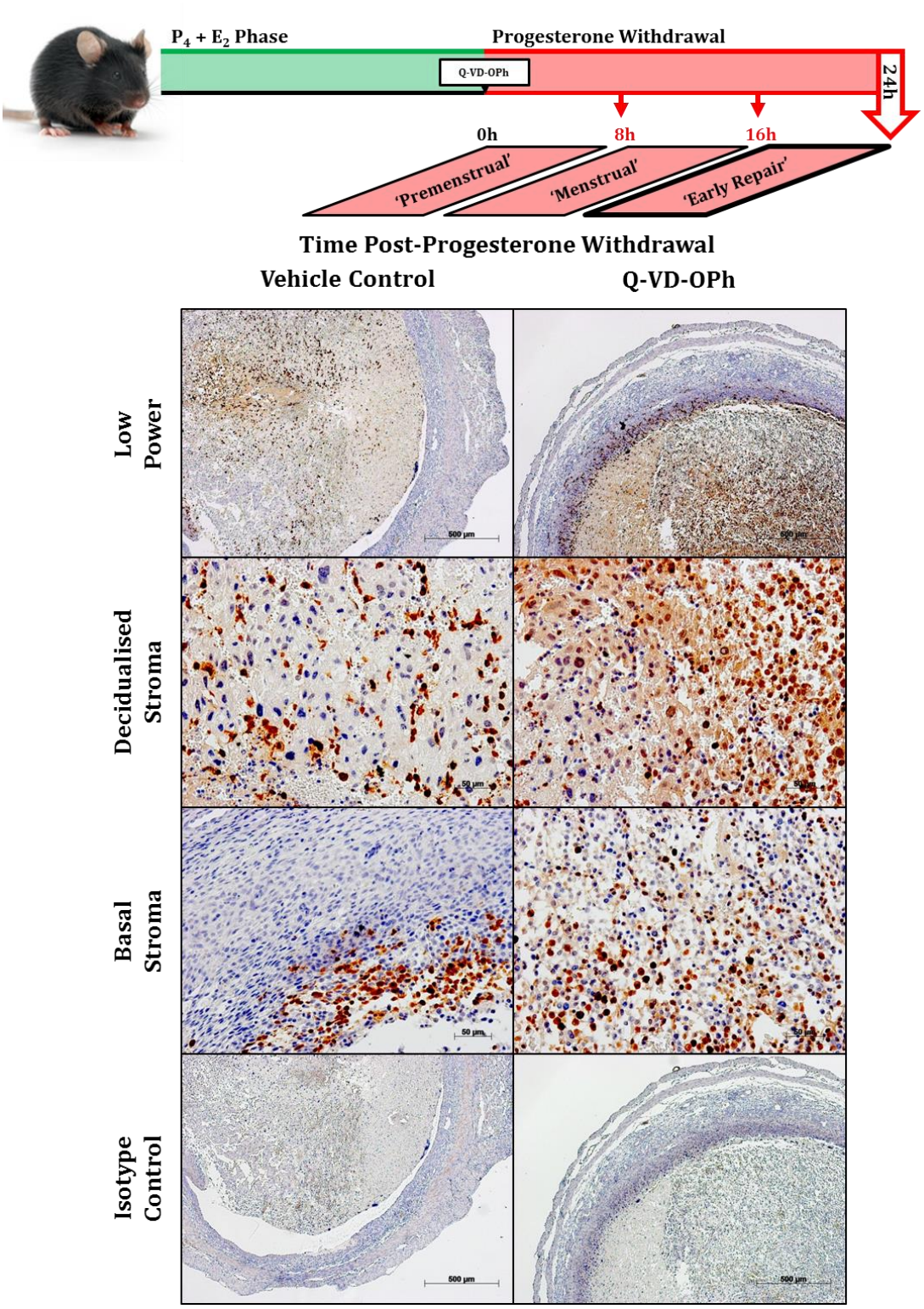

6.3.2 Endometrial Repair in Caspase-Inhibited Mice at 8, 16 & 24 Hours Post-Progesterone Withdrawal

At 8 hours following progesterone withdrawal (simulated 'premenstrual' phase), endometrial repair was found slightly retarded in Q-VD-OPh-treated mice relative to those administered vehicle control (see 2.4 Histological Assessment of Endometrial Repair for repair stage criteria as developed by Kaitu'u-Lino *et al*., 2006), though these data are not statistically significant ($p = 0.1705$; **Figure 47A**). Within the Q-VD-OPh treatment group, all mice ($n = 3$) showed a mostly intact decidua with some loss of structural integrity between decidual cells, consistent with repair stage 2 (**Figure 47B**). Fifty percent of the vehicle control treatment group showed signs consistent with a repair stage of 2 ($n = 3$), whereas 50% ($n = 3$) showed complete destruction of the decidual zone and sloughing of endometrium from the myometrium, features which were consistent with a repair stage of 3 (**Figure 47B**). These histological features are illustrated in a panel of representative photomicrographs from H&E-stained murine endometrial tissue sections at 8 hours post-progesterone withdrawal, shown in **Figure 48**.

By 16 hours after progesterone withdrawal (simulated 'menstrual' phase), differences in the progression of endometrial repair were less pronounced, with comparable mean repair stages between Q-VD-OPh- and vehicle-control-treated mice (**Figure 49A**). Twenty-five percent of Q-VD-OPh-treated mice ($n = 2$) showed a mostly intact decidua with some structurally disintegrated decidual cells, corresponding to a repair stage of 2; 50% showed complete decidual zone destruction with separation of the endometrium from the underlying myometrium (repair stage 3); and a final 25% showed further endometrial/myometrial separation and the beginnings of

re-epithelialisation (repair stage 4; **Figure 49B**). Amongst vehicle-control-treated mice, 50% (n = 2) scored a repair stage of 3 and 50% (n = 2) scored a repair stage of 4 (**Figure 49B**). A panel of representative photomicrographs illustrating endometrial repair stage features in tissue sections taken at 16 hours after progesterone withdrawal is given in **Figure 50**.

Twenty-four hours after the administration of Q-VD-OPh and the withdrawal of progesterone (simulated 'early repair' phase), differences in the progression of endometrial repair were less pronounced still between the treatment groups (**Figure 51A**). Of the Q-VD-OPh-treated mice, 80% (n = 4) were observed to have the histological features of complete decidual zone destruction alongside endometrial sloughing from the myometrium (repair stage 3) and 20% (n = 1) showed further endometrial sloughing and the beginnings of re-epithelialisation (repair stage 4; **Figure 51B**). Endometrial tissues derived from vehicle-control-treated mice showed a range of repair progression, with 14% (n = 1) showing only compromised decidual cell structural integrity, 57% (n = 4) showing features consistent with repair stage 3, and 29% (n = 2) achieving a repair stage of 4 (**Figure 51B**). These histological repair features are illustrated by a panel of photomicrographs of tissue sections taken at 24 hours post-progesterone withdrawal, given in **Figure 52**.

Figure 47. Q-VD-OPh treatment effected a slight but non-significant delay in endometrial repair at 8 hours post-progesterone withdrawal. Histological assessment of repair (1 – 5) in H&E-stained mouse endometrium based on established histological and morphological features (Kaitu'u-Lino *et al*., 2007) in mice administered Q-VD-OPh (n = 3) or vehicle control (n = 6), 8 hours following progesterone withdrawal. A) Mean repair score, B) parts of whole. *Each n-value represents the average of three experiments; error bars represent SEM. E_2 = oestradiol,P_4 = progesterone, Q-VD-OPh = quinolyl-valyl-O-methylaspartyl-[2,6-difluorophenoxy]-methyl ketone.*

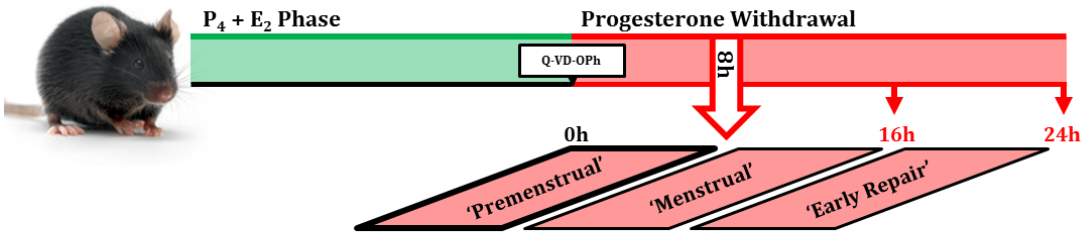

A

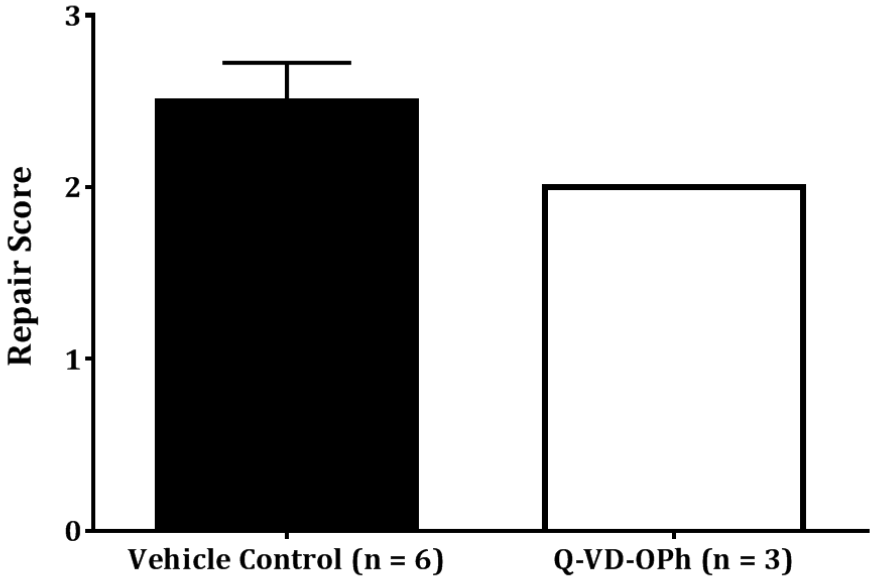

B

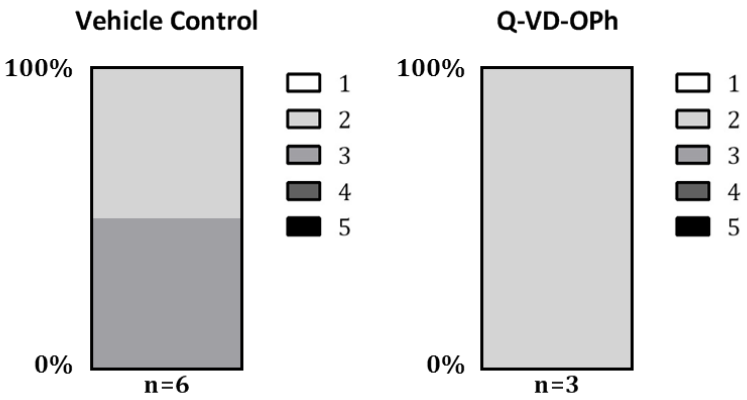

Figure 48. Some loss of endometrial decidual cell structural integrity at 8 hours post-progesterone withdrawal in both mice treated with Q-VD-OPh and with vehicle control. Representative photomicrographs of H&E-stained serial sections of endometrium used for histological assessment of repair in mice administered Q-VD-OPh (n = 3) or vehicle control (n = 5), 8 hours following progesterone withdrawal. **Black triangles** indicate loss of structural integrity between decidual cells; red-filled triangles indicate sloughing of endometrium from the myometrium. *Scale bars (500 µm, 50 µm) in image. E_2 = oestradiol, P_4 = progesterone, Q-VD-OPh = quinolyl-valyl-O-methylaspartyl-[2,6-difluorophenoxy]-methyl ketone.*

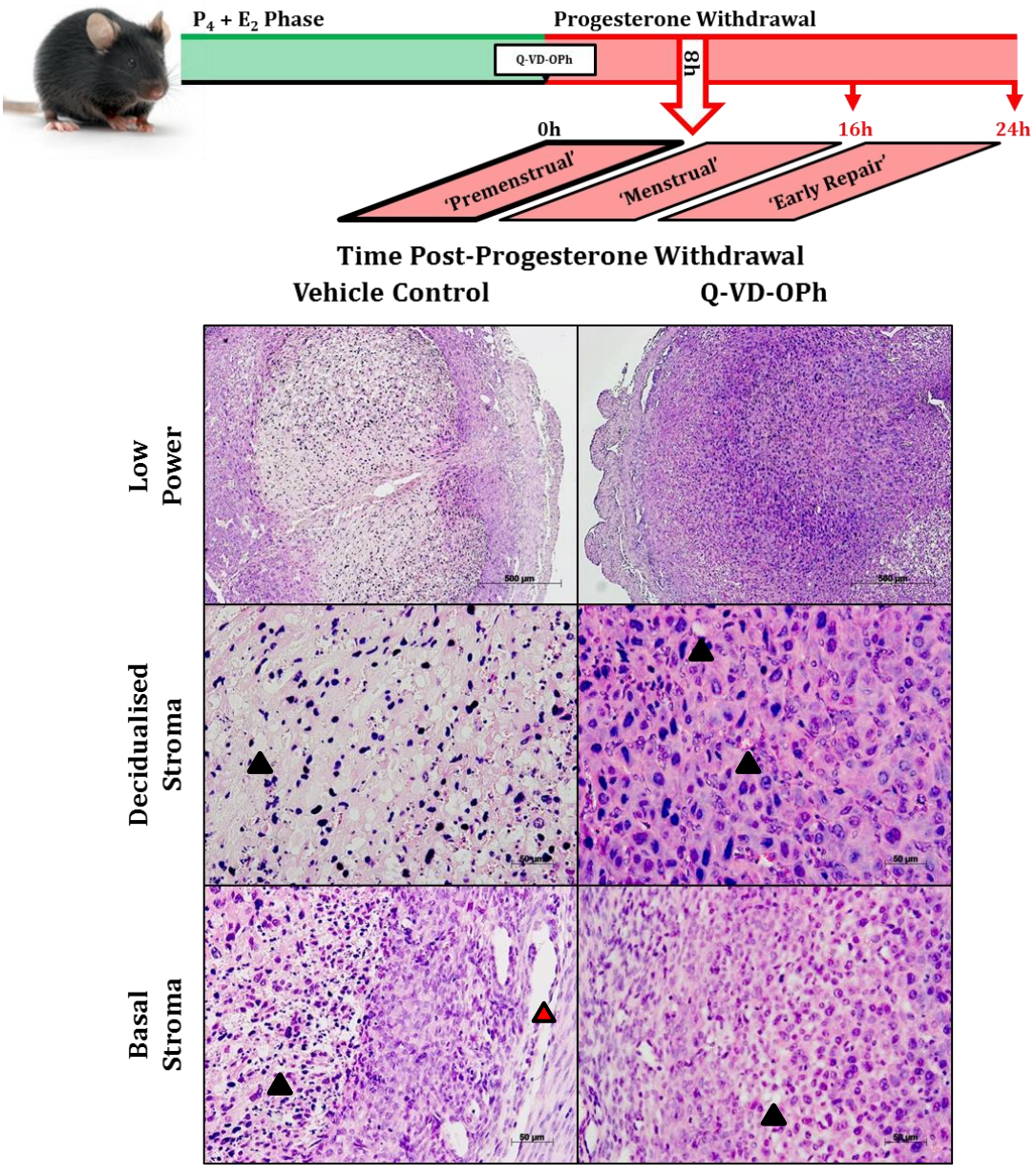

Figure 49. No differences in endometrial repair were apparent between Q-VD-OPh- and vehicle-control-treated mice at 16 hours post-progesterone withdrawal. Histological assessment of repair (1 – 5) in H&E-stained mouse endometrium based on established histological and morphological features (Kaitu'u-Lino *et al*., 2007) in mice administered Q-VD-OPh (n = 8) or vehicle control (n = 4), 16 hours following progesterone withdrawal. A) Mean repair score, B) parts of whole. *Each n-value represents the average of three experiments; error bars represent SEM.* *E_2 = oestradiol, P_4 = progesterone, Q-VD-OPh = quinolyl-valyl-O-methylaspartyl-[2,6-difluorophenoxy]-methyl ketone.*

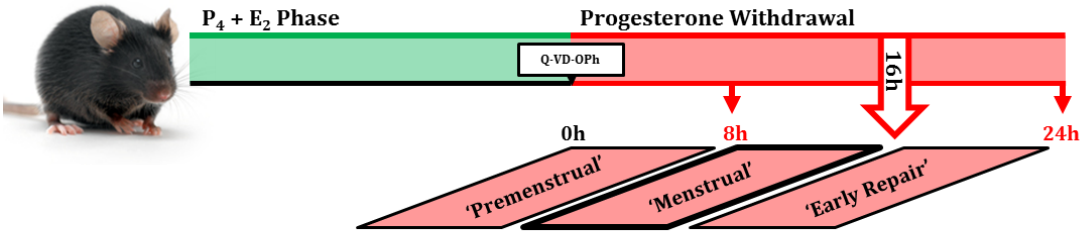

A

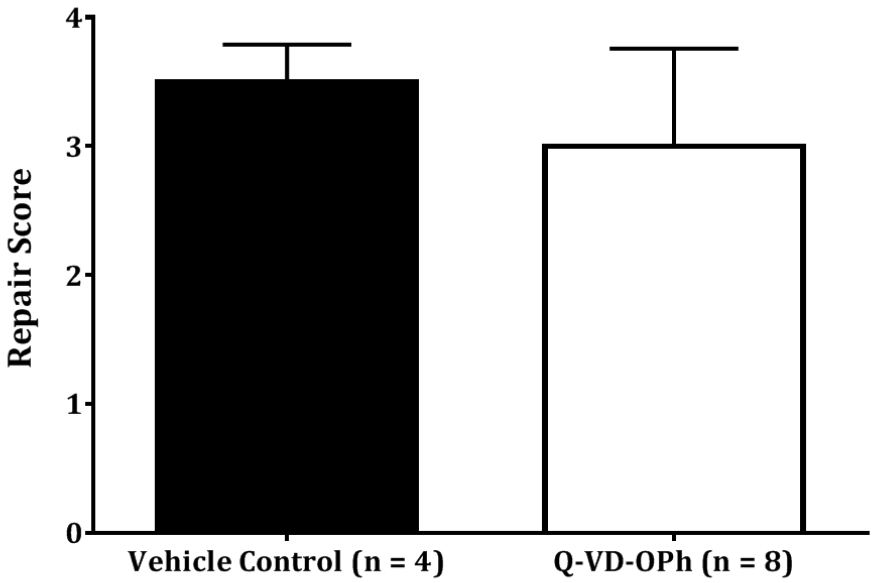

B

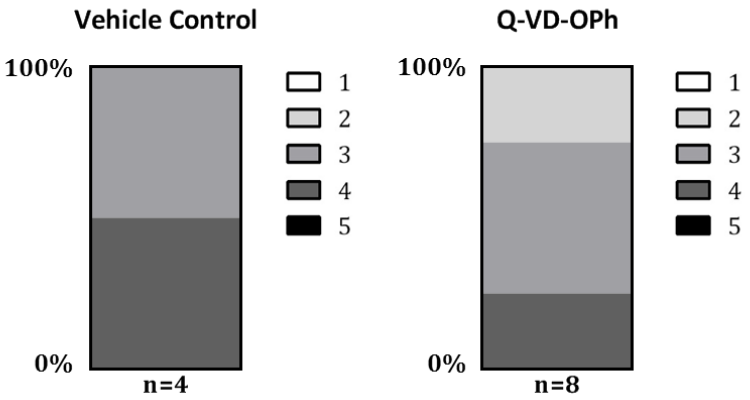

Figure 50. Endometrial separation from underlying myometrium and decidual zone destruction evident in the endometrium from both Q-VD-OPh- and vehicle-control-treated mice at 16 hours after progesterone withdrawal. Representative photomicrographs of H&E-stained serial sections of endometrium used for histological assessment of repair in mice administered Q-VD-OPh (n = 8) or vehicle control (n = 4), 16 hours following progesterone withdrawal. **Black triangles** indicate loss of structural integrity between decidual cells; red-filled triangles indicate sloughing of endometrium from the myometrium; blue-filled triangles indicate complete destruction of the decidual zone. *Scale bars (500 µm, 50 µm) in image.* *E_2 = oestradiol, P_4 = progesterone, Q-VD-OPh = quinolyl-valyl-O-methylaspartyl-[2,6-difluorophenoxy]-methyl ketone.*

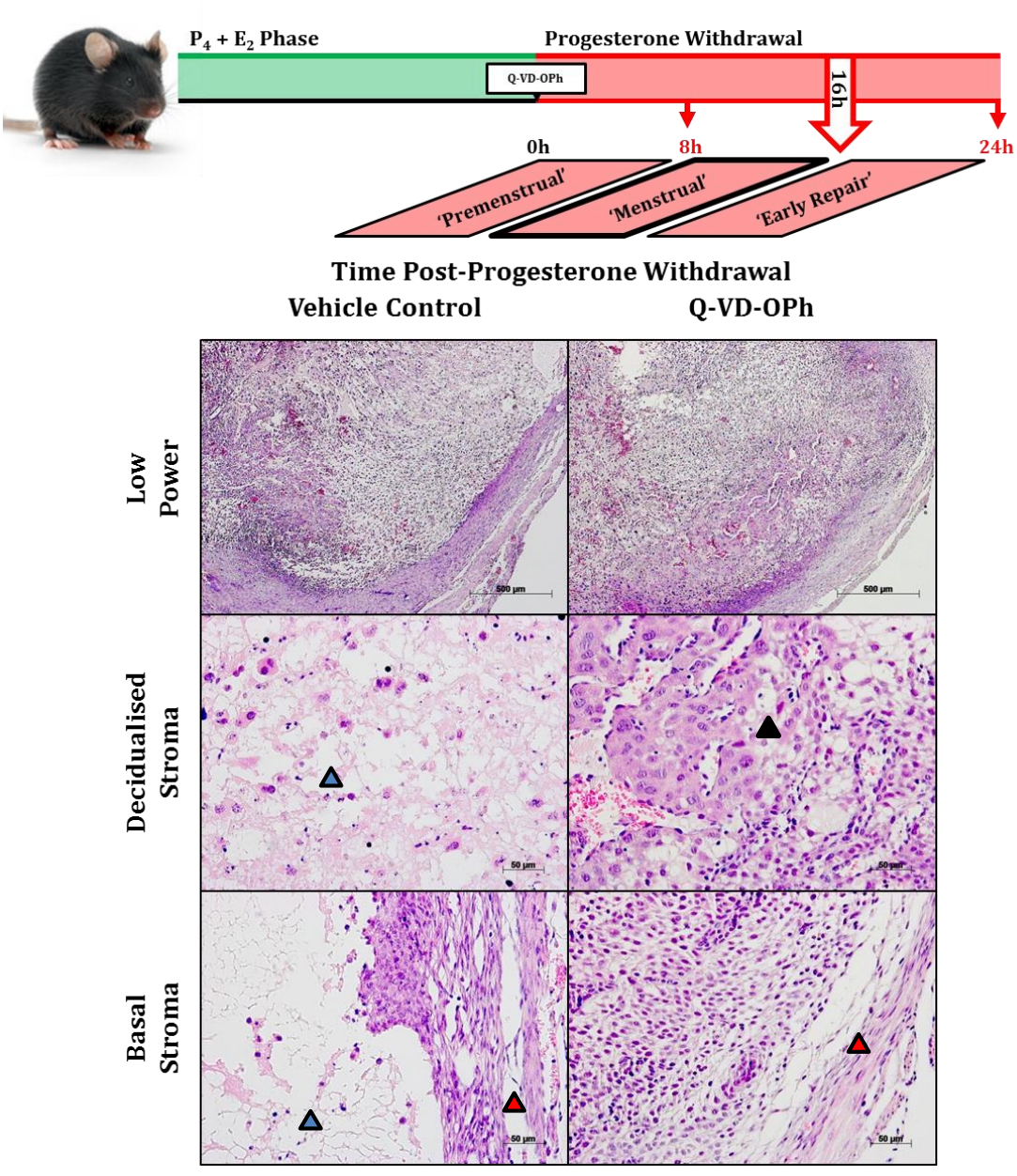

Figure 51. No differences in the progression of repair were observed between the endometrium of Q-VD-OPh- and vehicle-control-treated mice at 24 hours post-progesterone withdrawal. Histological assessment of repair (1 – 5) in H&E-stained mouse endometrium based on established histological and morphological features (Kaitu'u-Lino *et al*., 2007) in mice administered Q-VD-OPh (n = 5) or vehicle control (n = 7), 24 hours following progesterone withdrawal. A) Mean repair score, B) parts of whole. *Each n-value represents the average of three experiments; error bars represent SEM. E_2 = oestradiol, P_4 = progesterone, Q-VD-OPh = quinolyl-valyl-O-methylaspartyl-[2,6-difluorophenoxy]-methyl ketone.*

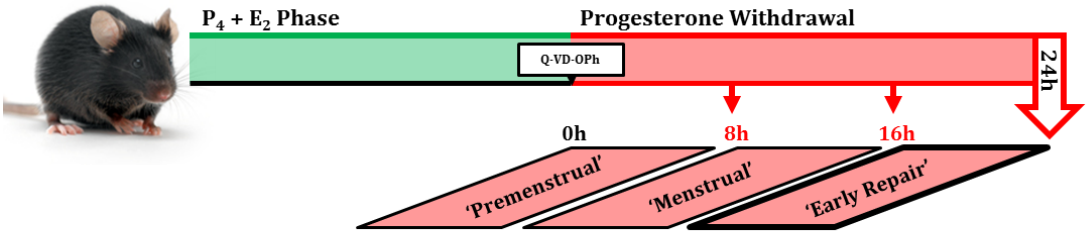

A

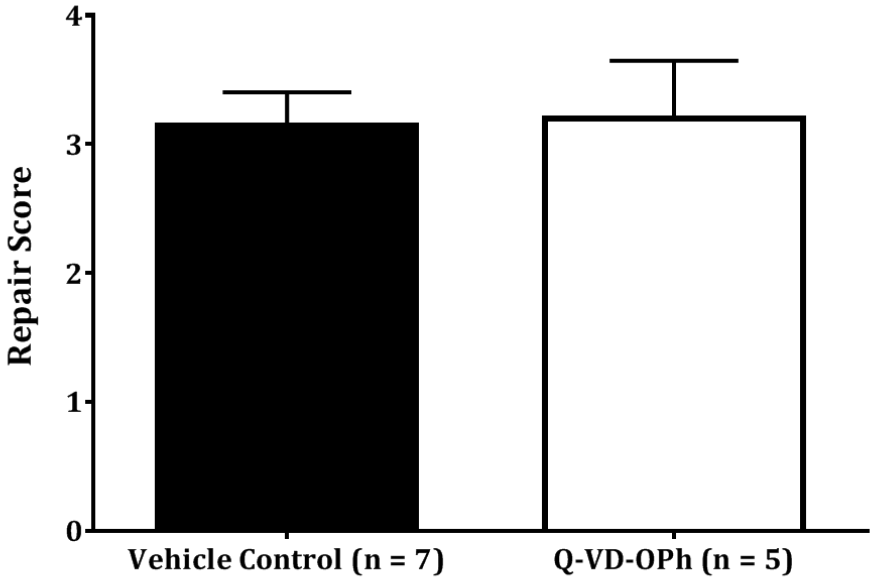

B

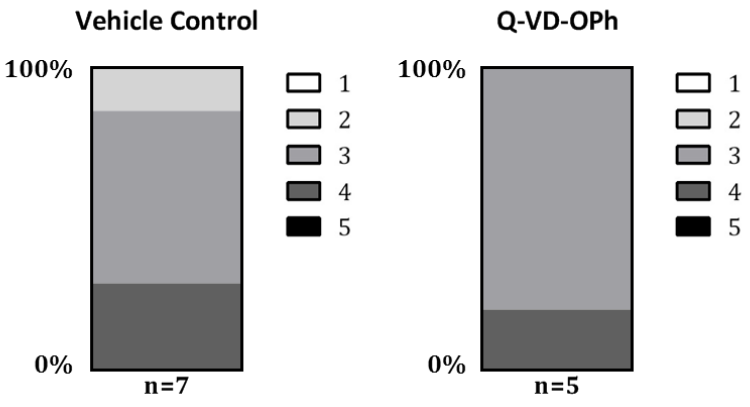

Figure 52. Beginning of re-epithelialisation and advanced sloughing of endometrium from underlying myometrium are apparent in mice treated with Q-VD-OPh and vehicle control at 24 hours after progesterone withdrawal. Representative photomicrographs of H&E-stained serial sections of endometrium used for histological assessment of repair in mice administered Q-VD-OPh (n = 5) or vehicle control (n = 7), 24 hours following progesterone withdrawal. **Black triangles** indicate loss of structural integrity between decidual cells; red-filled triangles indicate sloughing of endometrium from the myometrium; green-filled triangles indicate beginnings of re-epithelialisation. *Scale bars (500 µm, 50 µm) in image. E_2 = oestradiol, P_4 = progesterone, Q-VD-OPh = quinolyl-valyl-O-methylaspartyl-[2,6-difluorophenoxy]-methyl ketone.*

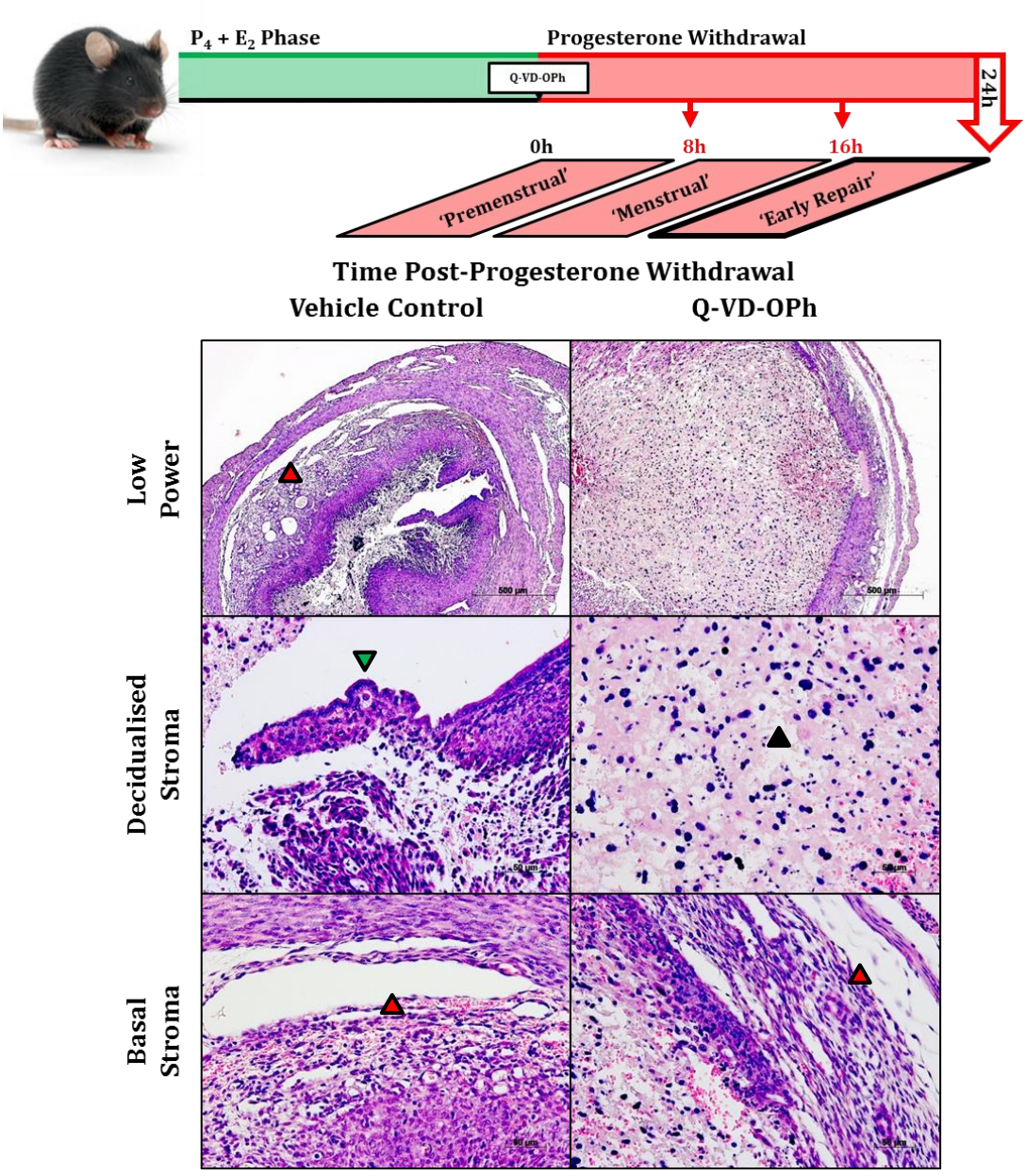

6.3.3 *Cxcl1* & *Tnfa* Transcription in the Endometrium of Caspase-Inhibited Mice at 8, 16 & 24 Hours Post-Progesterone Withdrawal

Transcription of the neutrophil chemokine *Cxcl1* (the homologue of human *CXCL8*/*IL8* in the mouse) was significantly decreased in the endometrium of Q-VD-OPh-treated mice at 16 hours after progesterone withdrawal (simulated 'menstrual' phase) relative to vehicle-control-treated mice at the same time-point ($p < 0.01$; **Figure 53A**). Endometrial *Cxcl1* transcription was significantly increased, however, in Q-VD-OPh-treated mice relative to mice treated with vehicle control at 24 hours after progesterone withdrawal (simulated 'early repair' phase; $p < 0.01$; **Figure 53A**).

Tumour necrosis factor alpha (*Tnfa*) showed significantly increased transcription in the endometrium of Q-VD-OPh-treated mice relative to vehicle-control-treated mice at 24 hours following the withdrawal of progesterone (simulated 'early repair' phase; $p < 0.01$; **Figure 53B**).

Figure 53. Endometrial transcription of the neutrophil chemokine *Cxcl1* is decreased in Q-VD-OPh-treated mice at 16 hours after progesterone withdrawal and increased at 24 hours; *Tnfa* transcription is increased at 24 hours after progesterone withdrawal. RT-qPCR quantification of *Cxcl1* (mouse homologue of human *CXCL8*/*IL8*; A) and *Tnfa* (B) mRNA levels in whole uterus RNA extracts, with data analysed by $\Delta\Delta C_q$ method and normalised to *Actb* (β-actin) mRNA levels. *** p < 0.01; error bars represent SEM; n = 3 – 9; significance determined by 2-way ANOVA and Sidak's multiple comparisons test (between treatment groups). Cxcl1 = C-X-C motif chemokine ligand 1, E_2 = oestradiol, P_4 = progesterone, Q-VD-OPh = quinolyl-valyl-O-methylaspartyl-[2,6-difluorophenoxy]-methyl ketone, Tnfa = tumour necrosis factor alpha.*

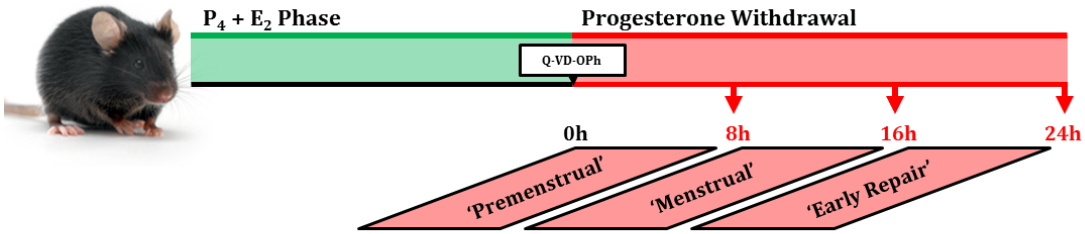

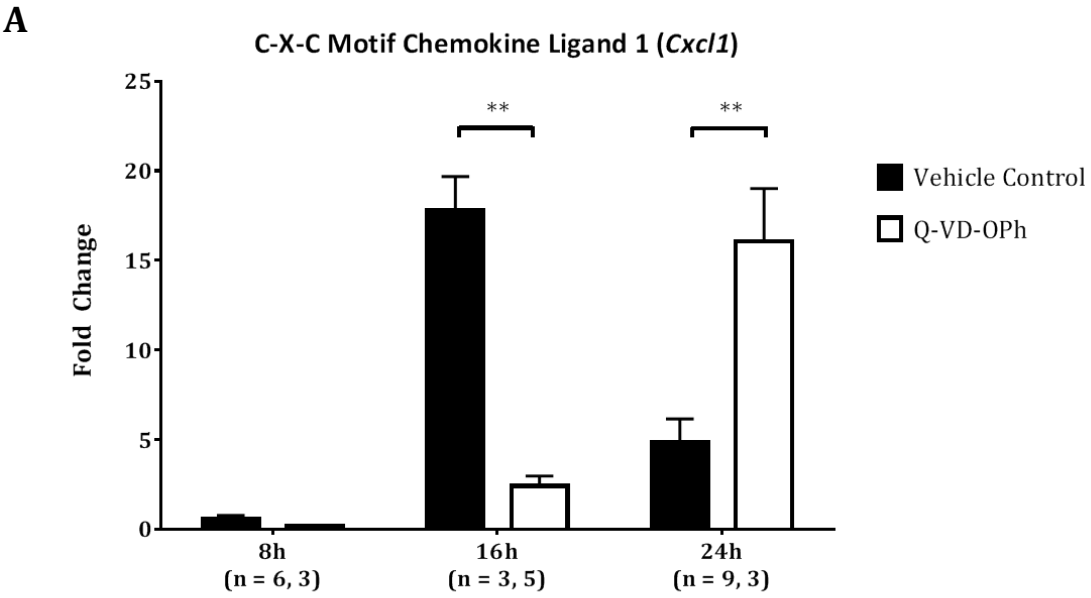

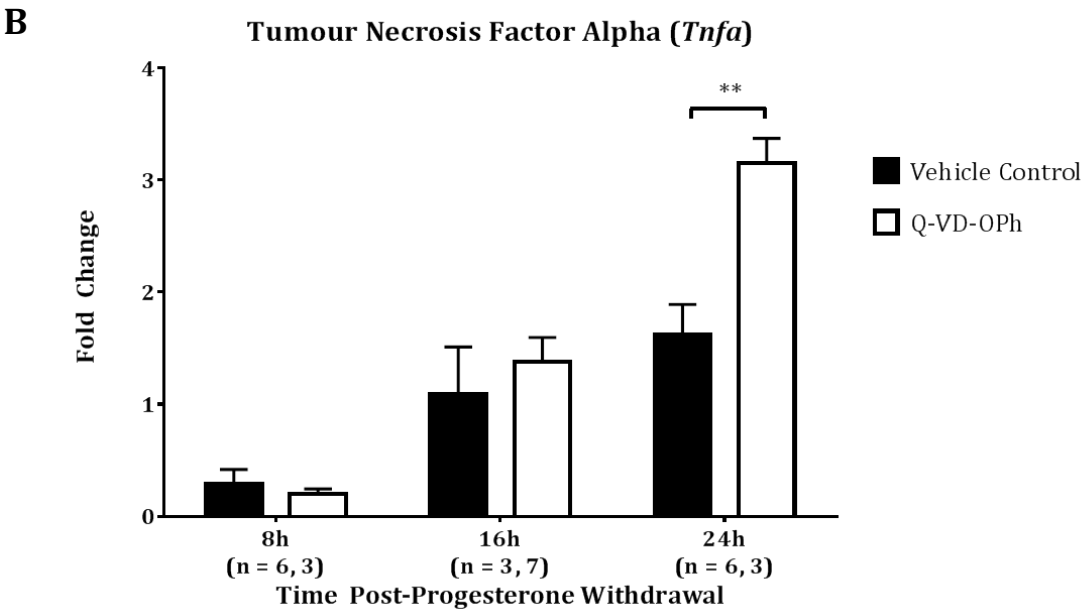

6.3.4 Proliferation in the Endometrium of a Caspase-Inhibited Mouse Model of Menstruation at 8, 16 & 24 Hours Post-Progesterone Withdrawal

BrdU-immunoreactive nuclei (indicating proliferating cells) were abundant in the basal stroma of the endometrium from both Q-VD-OPh- and vehicle-control-treated mice at 8 hours following progesterone withdrawal (simulated 'premenstrual' phase), though could also be found to a lesser extent in the decidualised stroma and surface and glandular epithelia (**Figure 54A**). Proliferation was significantly increased in the decidualised stroma of Q-VD-OPh-treated mice relative to that of vehicle-control-treated mice ($p < 0.05$; **Figure 54B**). A panel of representative photomicrographs taken from BrdU-immunostained endometrial tissue sections from mice at 8 hours after progesterone withdrawal is provided in **Figure 55**.

By 16 hours after progesterone withdrawal (simulated 'menstrual' phase), proliferation could no longer be found to any appreciable extent in the decidualised stroma of either treatment group (**Figure 56A**, **B**), and was instead found largely restricted to the surface epithelium (**Figure 56A**). No significant differences were found in BrdU immunoreactivity between treatment groups in any tissue compartment at this time. **Figure 57** provides a panel of representative photomicrographs of BrdU-immunostained endometrial tissue sections from mice at 16 hours after progesterone withdrawal.

Proliferation remained extensive in the surface epithelium of both treatment groups at 24 hours after progesterone withdrawal (simulated 'early repair' phase; **Figure 58A**), with no significant differences found in BrdU immunoreactivity in the decidualised endometrium (**Figure 58B**). No significant differences were found in any other tissue

compartment at this time. A panel of representative photomicrographs is shown in **Figure 59**, showing BrdU-immunostained endometrial tissues at 24 hours post-progesterone withdrawal.

Summaries of the endometrial BrdU immunoreactivity profiles across progesterone withdrawal time-points are given for vehicle-control-treated mice in **Figure 60A** and for Q-VD-OPh-treated mice in **Figure 60B**.

Plotted against time, the immunoreactivity data reveal significant increases in proliferation in the surface epithelium of vehicle-control-treated mice at 16 and 24 hours after progesterone withdrawal compared to 8 hours ($p < 0.001$, $p < 0.0001$ respectively; **Figure 60A**) and a significant decrease in basal stromal proliferation at 24 hours compared to 8 hours ($p < 0.01$; **Figure 60A**).

Relative to 8 hours after progesterone withdrawal, significant increases in surface epithelial proliferation were observed in Q-VD-OPh-treated mice at 16 and 24 hours ($p < 0.001$, $p < 0.05$ respectively; **Figure 60B**), while significant decreases were seen in decidualised stromal proliferation at 16 and 24 hours ($p < 0.05$; **Figure 60B**) and in basal stromal proliferation at 16 hours ($p < 0.05$; **Figure 60B**).

Figure 54. Proliferation increased in the decidualised endometrial stroma of Q-VD-OPh-treated mice at 8 hours after progesterone withdrawal. Semi-quantitative immunoreactivity histoscoring (staining intensity multiplied by percentage of tissue staining positive) for BrdU (1:600, Fitzgerald Ind.) in endometrial tissues of mice administered Q-VD-OPh (n = 3) or vehicle control (n = 6), 8 hours following progesterone withdrawal. A) Individual data points plotted vs. histoscore, B) mean histoscore in the decidualised stroma. *Each data point represents the average of three experiments; lines represent mean; error bars represent SEM; * p < 0.05; significance determined by unpaired t-test. BrdU = 5'-bromo-2'-deoxyuridine, E_2 = oestradiol, P_4 = progesterone, Q-VD-OPh = quinolyl-valyl-O-methylaspartyl-[2,6-difluorophenoxy]-methyl ketone.*

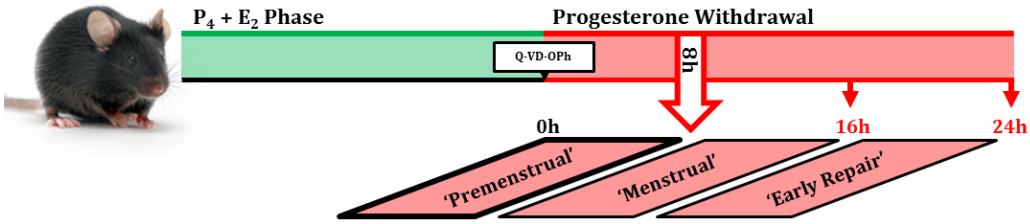

A

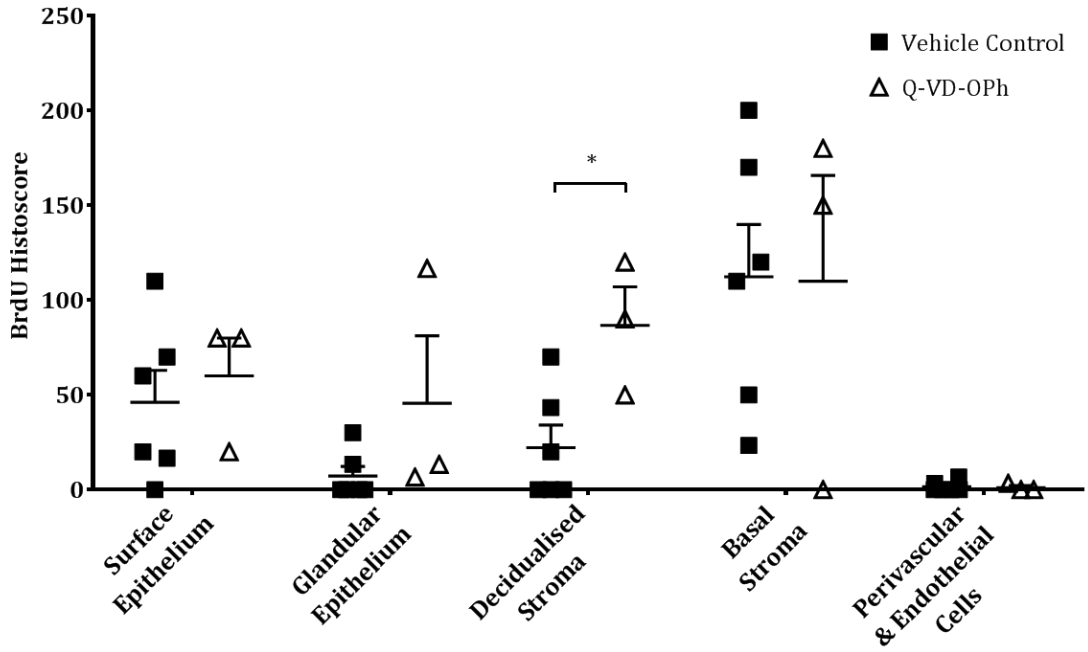

B

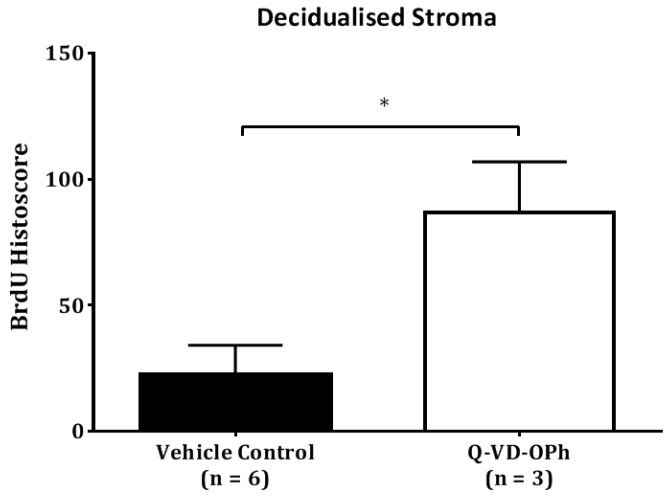

Figure 55. BrdU immunoreactivity detectable in the decidualised and basal endometrial stroma of Q-VD-OPh-treated mice at 8 hours post-progesterone withdrawal. Representative photomicrographs of BrdU (1:600, Fitzgerald Ind.) staining in serial sections of endometrium from mice administered Q-VD-OPh (n = 3) or vehicle control (n = 5), 8 hours following progesterone withdrawal. Brown-filled triangles indicate proliferating decidual cells. *Isotype control: sheep anti-digoxigenin (Roche); nuclear counterstain: haematoxylin. Scale bars (500 µm, 50 µm) in image. BrdU = 5'-bromo-2'-deoxyuridine, E_2 = oestradiol, P_4 = progesterone, Q-VD-OPh = quinolyl-valyl-O-methylaspartyl-[2,6-difluorophenoxy]-methyl ketone.*

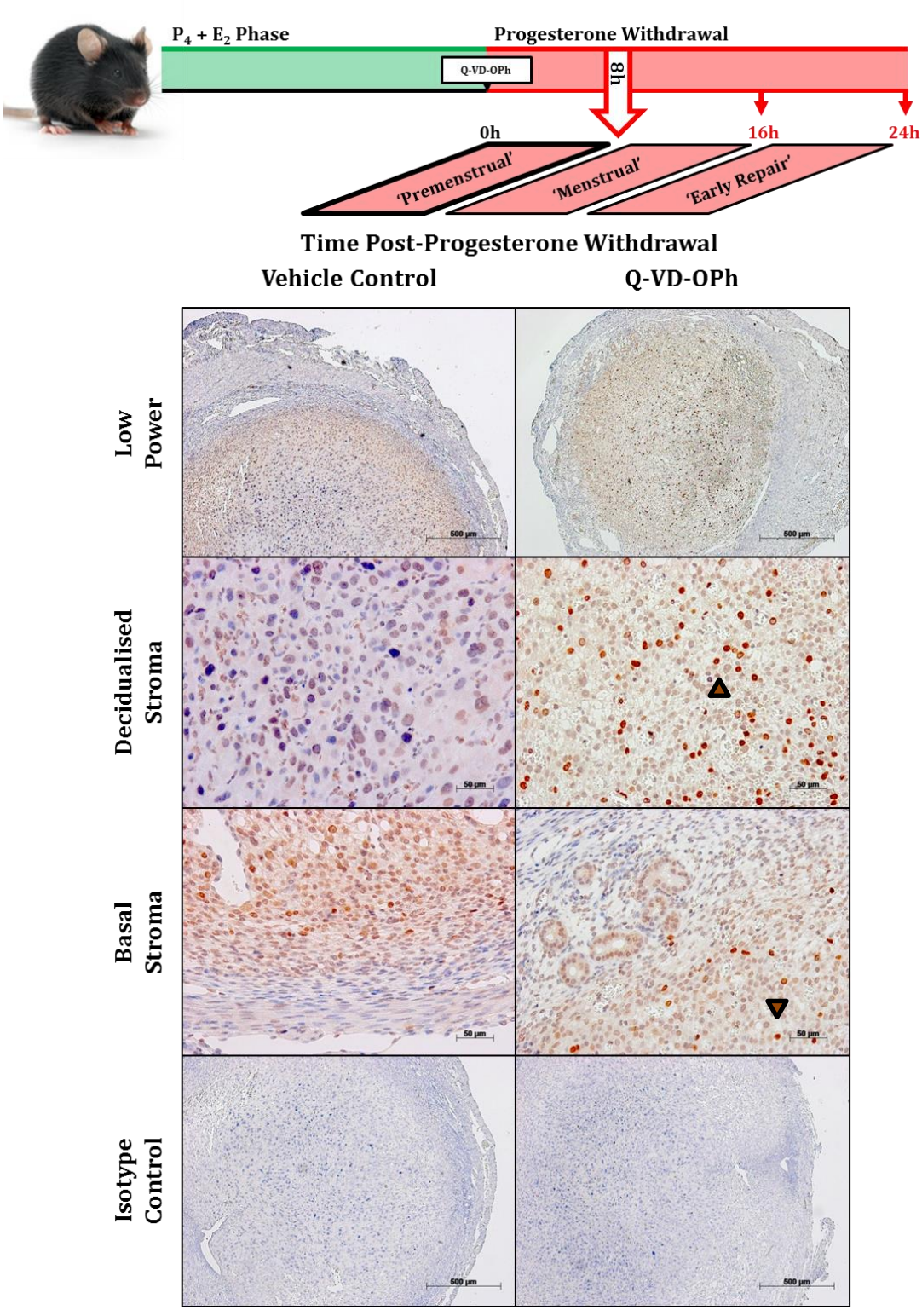

Figure 56. Proliferation no longer significantly increased in the decidualised endometrial stroma of Q-VD-OPh- and vehicle-control-treated mice at 16 hours post-progesterone withdrawal. Semi-quantitative immunoreactivity histoscoring (staining intensity multiplied by percentage of tissue staining positive) for BrdU (1:600, Fitzgerald Ind.) in endometrial tissues of mice administered Q-VD-OPh (n = 8) or vehicle control (n = 4), 16 hours following progesterone withdrawal. A) Individual data points plotted vs. histoscore, B) mean histoscore in the decidualised stroma. *Each data point represents the average of three experiments; lines represent mean; error bars represent SEM. BrdU = 5'-bromo-2'-deoxyuridine, E_2 = oestradiol, P_4 = progesterone, Q-VD-OPh = quinolyl-valyl-O-methylaspartyl-[2,6-difluorophenoxy]-methyl ketone.*

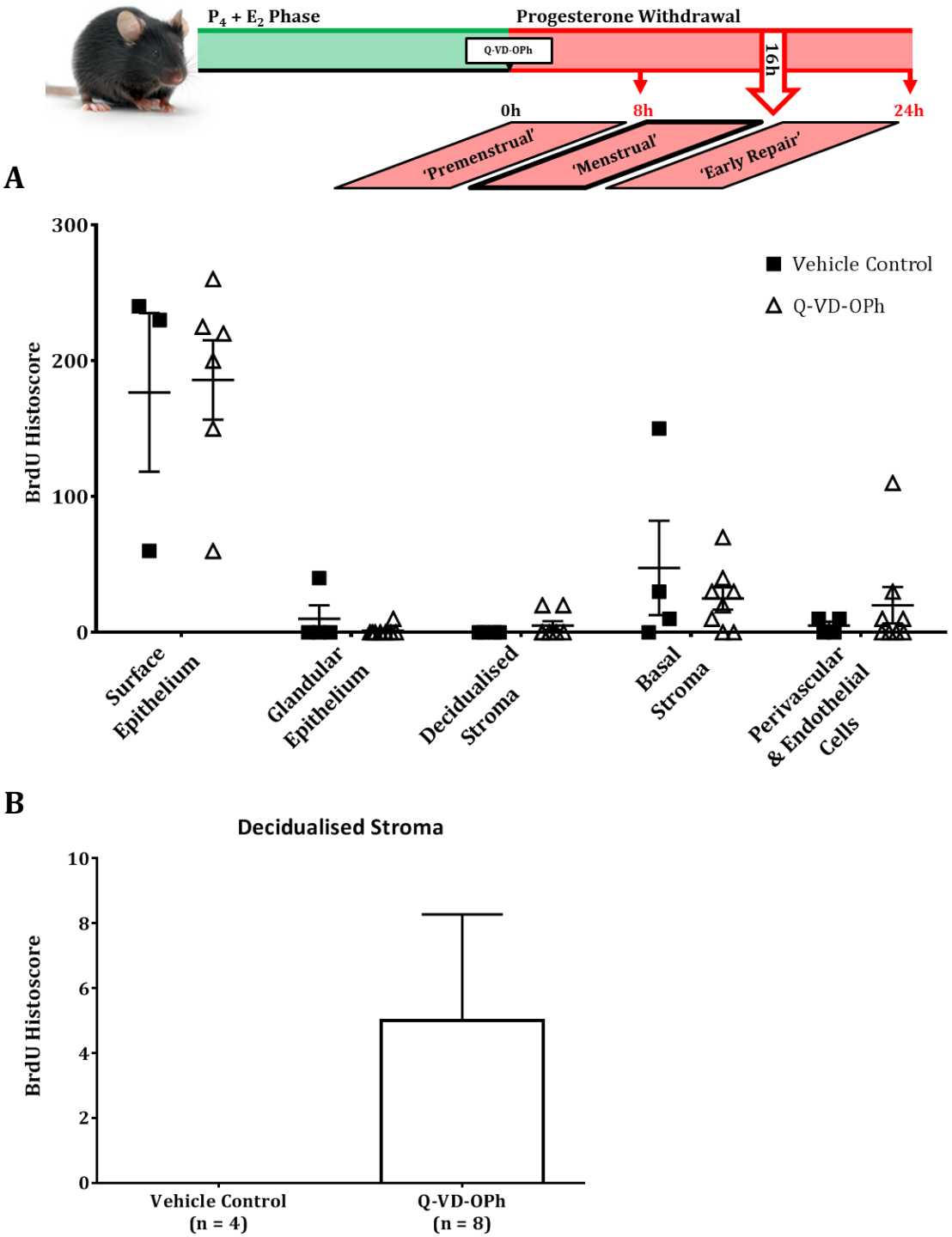

Figure 57. Comparable BrdU immunoreactivity in the decidualised and basal endometrial stroma of Q-VD-OPh- and vehicle-control-treated mice at 16 hours post-progesterone withdrawal. Representative photomicrographs of BrdU (1:600, Fitzgerald Ind.) staining in serial sections of endometrium from mice administered Q-VD-OPh (n = 8) or vehicle control (n = 4), 16 hours following progesterone withdrawal. *Isotype control: sheep anti-digoxigenin (Roche); nuclear counterstain: haematoxylin. Scale bars (500 µm, 50 µm) in image. BrdU = 5'-bromo-2'-deoxyuridine, E_2 = oestradiol, P_4 = progesterone, Q-VD-OPh = quinolyl-valyl-O-methylaspartyl-[2,6-difluorophenoxy]-methyl ketone.*

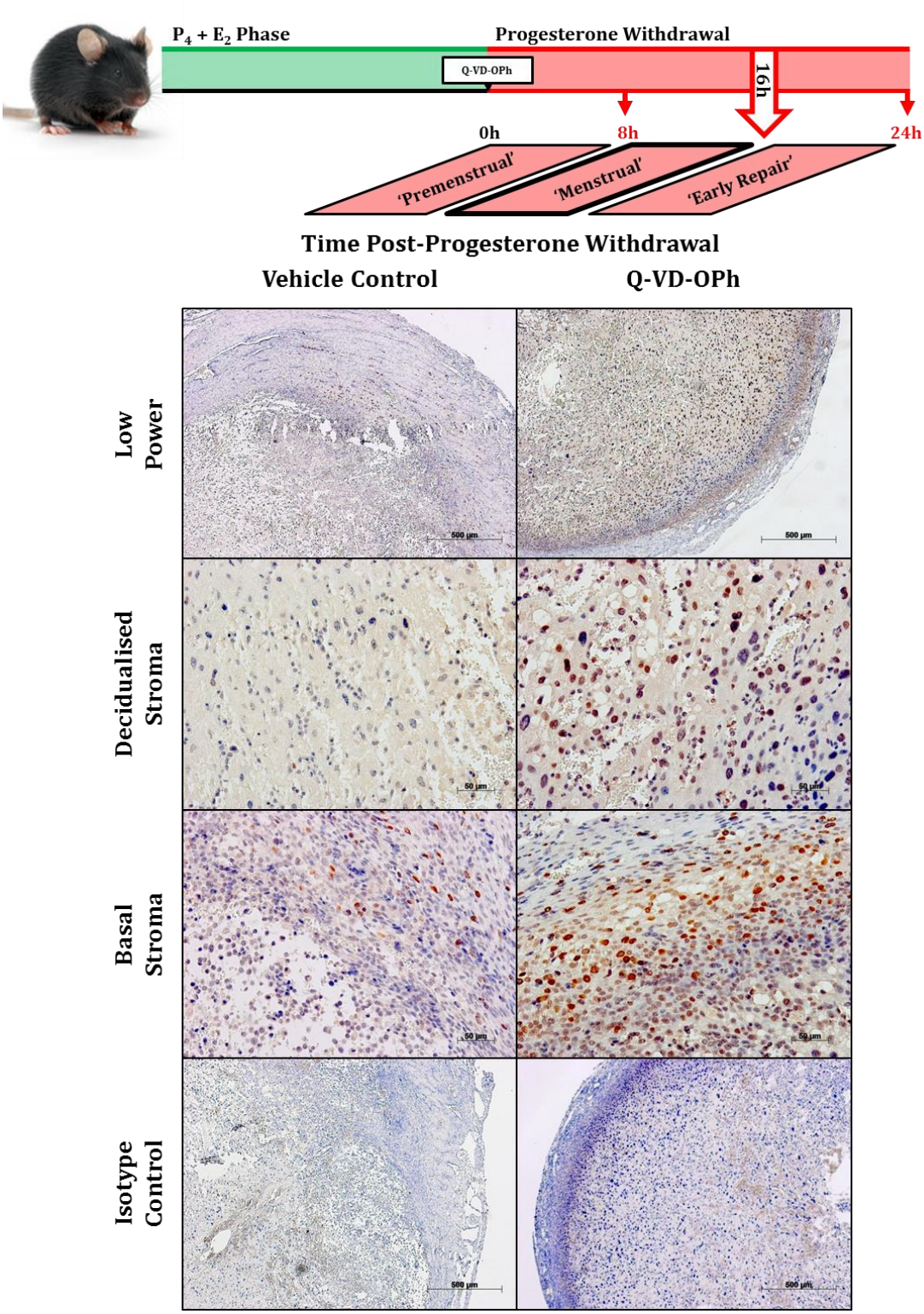

Figure 58. No differences in proliferation apparent between the endometrium of Q-VD-OPh- and vehicle-control-treated mice 24 hours after progesterone withdrawal. Semi-quantitative immunoreactivity histoscoring (staining intensity multiplied by percentage of tissue staining positive) for BrdU (1:600, Fitzgerald Ind.) in endometrial tissues of mice administered Q-VD-OPh (n = 5) or vehicle control (n = 7), 24 hours following progesterone withdrawal. A) Individual data points plotted vs. histoscore, B) mean histoscore in the decidualised stroma. *Each data point represents the average of three experiments; lines represent mean; error bars represent SEM. BrdU = 5'-bromo-2'-deoxyuridine, E_2 = oestradiol, P_4 = progesterone, Q-VD-OPh = quinolyl-valyl-O-methylaspartyl-[2,6-difluorophenoxy]-methyl ketone.*

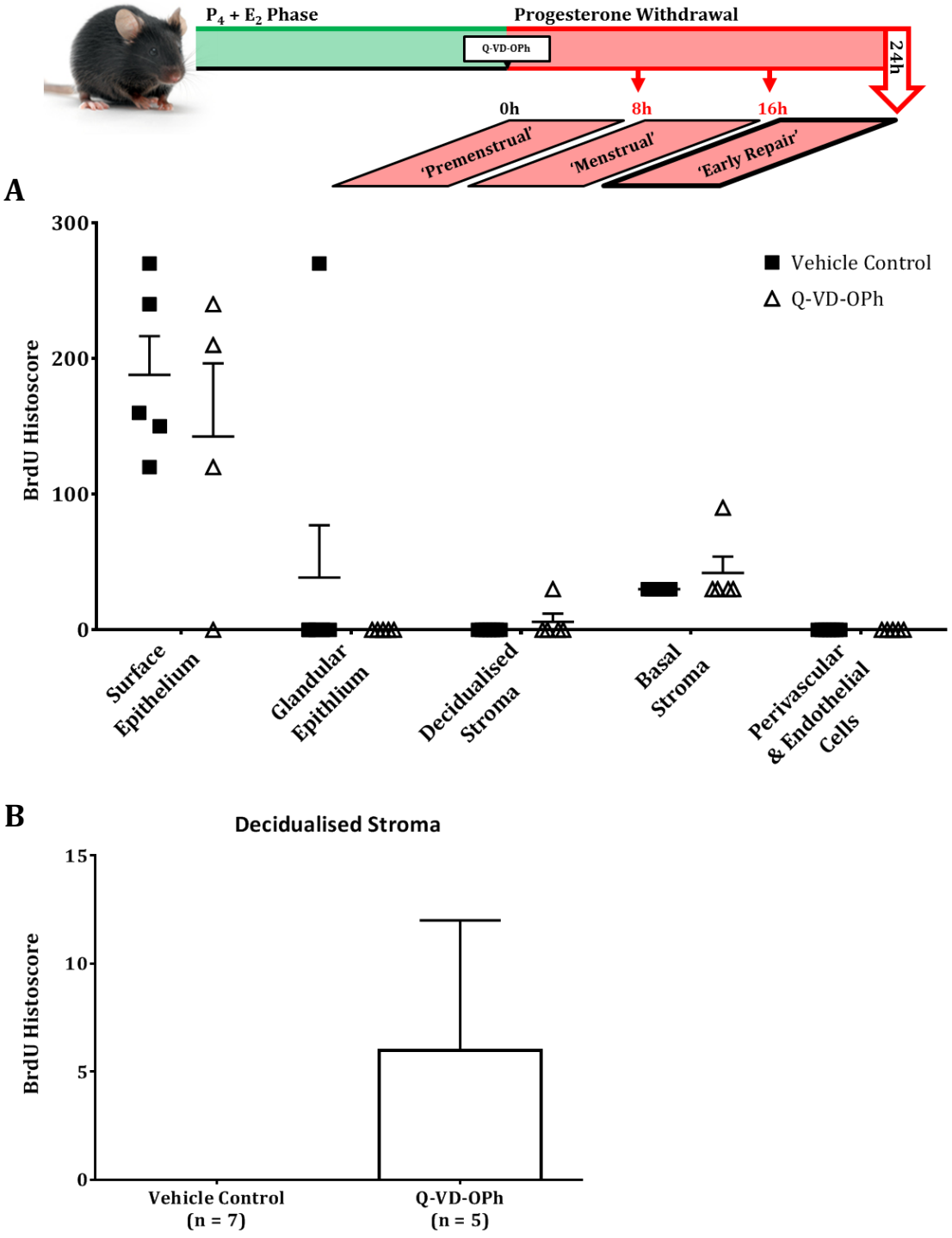

Figure 59. BrdU immunoreactivity is extensive in the basal endometrial stroma at 24 hours after progesterone withdrawal in mice administered Q-VD-OPh and vehicle control. Representative photomicrographs of BrdU (1:600, Fitzgerald Ind.) staining in serial sections of endometrium from mice administered Q-VD-OPh (n = 5) or vehicle control (n = 7), 24 hours following progesterone withdrawal. *Isotype control: sheep anti-digoxigenin (Roche); nuclear counterstain: haematoxylin. Scale bars (500 µm, 50 µm) in image. BrdU = 5'-bromo-2'-deoxyuridine, E_2 = oestradiol, P_4 = progesterone, Q-VD-OPh = quinolyl-valyl-O-methylaspartyl-[2,6-difluorophenoxy]-methyl ketone.*

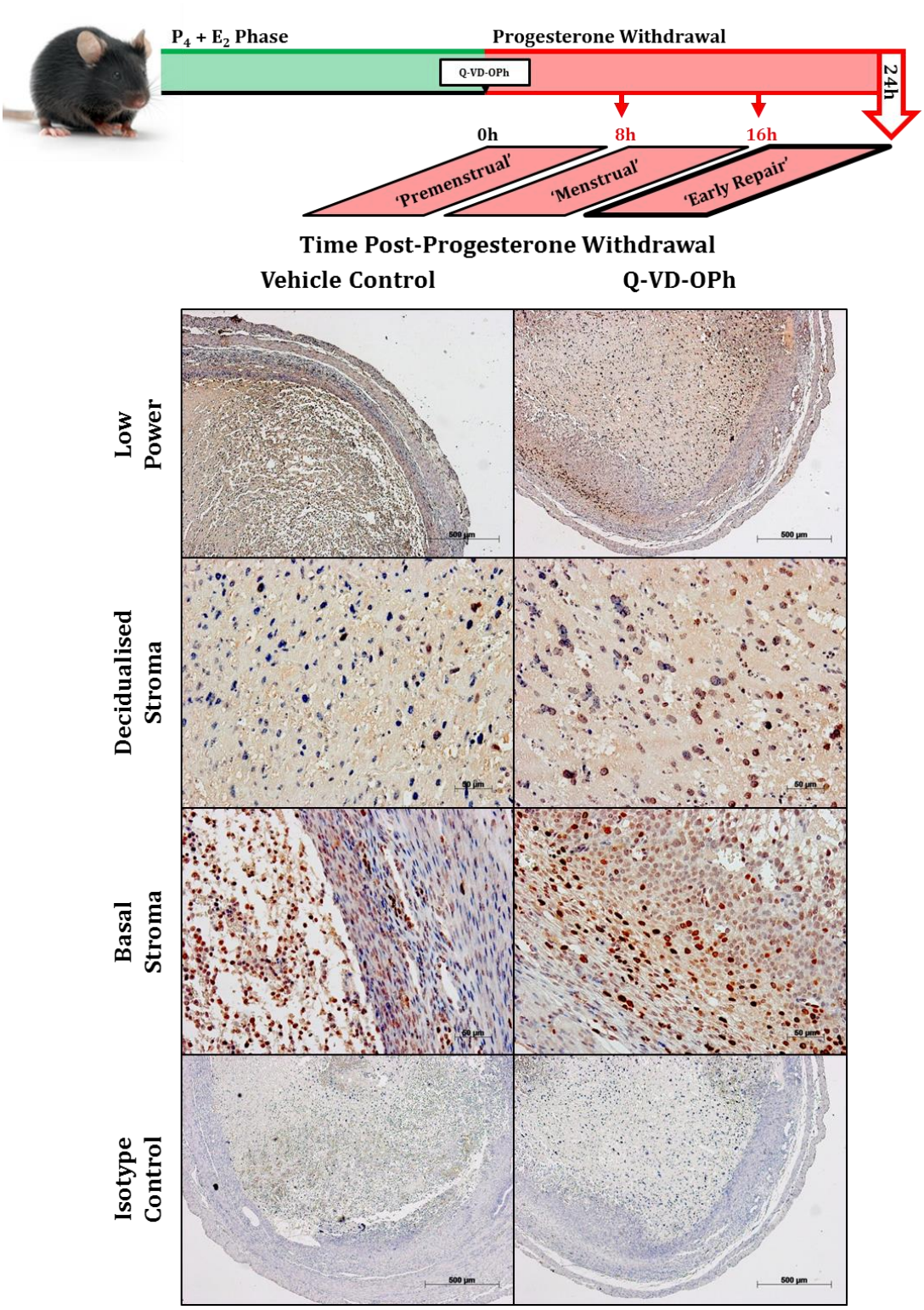

Figure 60. Summary changes in proliferation in the endometrium of mice administered Q-VD-OPh and vehicle control at 8, 16 and 24 hours after progesterone withdrawal. Semi-quantitative immunoreactivity histoscoring (staining intensity multiplied by percentage of tissue staining positive) for BrdU (1:600, Fitzgerald Ind.) in endometrial tissues of mice administered Q-VD-OPh (B; n = 16) or vehicle control (A; n = 17), 8, 16 and 24 hours following progesterone withdrawal. ** p < 0.05, ** p < 0.01, *** p < 0.001, **** p < 0.0001; error bars represent SEM; significance determined by 2-way ANOVA and Tukey's multiple comparisons test (all comparisons made to 8h). BrdU = 5'-bromo-2'-deoxyuridine, E_2 = oestradiol, P_4 = progesterone, Q-VD-OPh = quinolyl-valyl-O-methylaspartyl-[2,6-difluorophenoxy]-methyl ketone.*

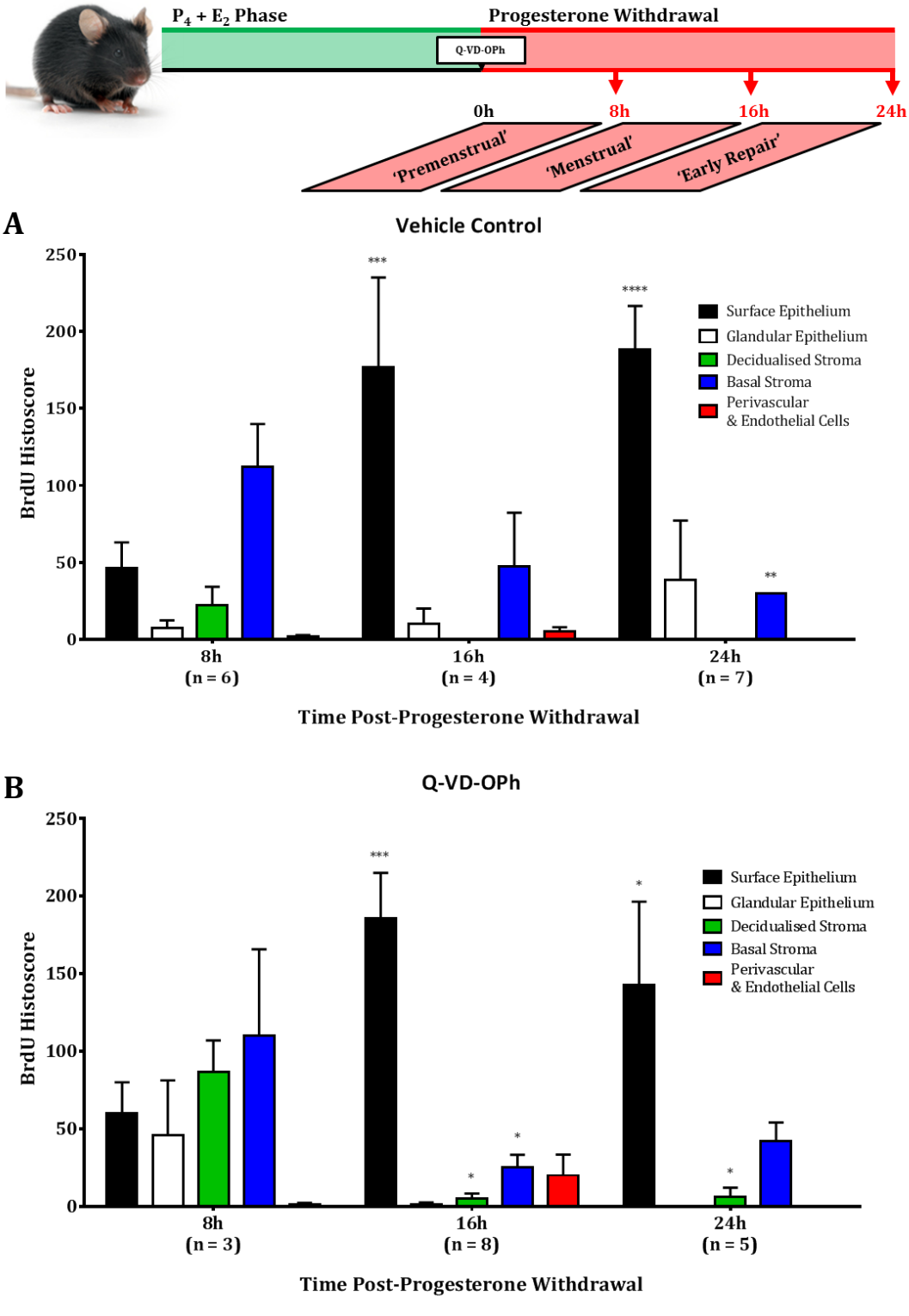

6.3.5 Hypoxia in the Endometrium of a Caspase-Inhibited Mouse Model of Menstruation at 8, 16 & 24 Hours Post-Progesterone Withdrawal

Hypoxia was extensive in the decidualised and basal endometrial stroma of both Q-VD-OPh- and vehicle-control-treated mice at 8 hours following progesterone withdrawal (simulated 'premenstrual' phase; **Figure 61A**), with hypoxic vessels observed in 1 of 3 Q-VD-OPh-treated mice (**Figure 61B**); nevertheless, no significant differences were found in Hypoxyprobe immunoreactivity between treatment groups in any tissue compartment. A panel of representative Hypoxyprobe-immunostained endometrial tissue photomicrographs from mice at 8 hours after progesterone withdrawal is given in **Figure 62.**

Perivascular and endothelial cell hypoxia was increased in both treatment groups at 16 hours after progesterone withdrawal (simulated 'menstrual' phase) and moderate hypoxia persisted in the decidualised stroma (**Figure 63**), though no significant Hypoxyprobe immunoreactivity differences were found in in any tissue compartment between treatment groups. **Figure 64** provides a panel of representative Hypoxyprobe-immunostained endometrial tissue photomicrographs from mice at 16 hours after progesterone withdrawal.

By 24 hours after progesterone withdrawal (simulated 'early repair' phase), mice of both treatment groups again showed little to no perivascular and endothelial cell hypoxia, but maintained moderate decidual zone hypoxia (**Figure 65**). No significant differences were found between treatment groups in any tissue compartment. A panel of representative photomicrographs is shown in **Figure 66**, showing Hypoxyprobe-immunostained endometrial tissues at 24 hours post-progesterone withdrawal.

Endometrial hypoxia profiles across progesterone withdrawal time-points are summarised for vehicle-control-treated mice in **Figure 67A** and for Q-VD-OPh-treated mice in **Figure 67B**.

Hypoxyprobe immunoreactivity data demonstrate a significant increase in perivascular and endothelial cell hypoxia in the endometrium of vehicle-control-treated mice at 16 hours after progesterone withdrawal, relative to both 8 and 24 hours ($p < 0.05$; **Figure 67A**).

In Q-VD-OPh-treated mice, no significant differences in endometrial hypoxia were observed in any tissue compartment between progesterone withdrawal time-points (**Figure 67B**).

Figure 61. Levels of endometrial hypoxia showed no significant differences at 8 hours post-progesterone withdrawal between mice administered Q-VD-OPh and vehicle control. Semi-quantitative immunoreactivity histoscoring (staining intensity multiplied by percentage of tissue staining positive) for pimonidazole (1:200, Hypoxyprobe Inc.) in endometrial tissues of mice administered Q-VD-OPh (n = 3) or vehicle control (n = 6), 8 hours following progesterone withdrawal. A) Individual data points plotted vs. histoscore, B) mean histoscore in the perivascular and endothelial cells. *Each data point represents the average of three experiments; lines represent mean; error bars represent SEM.* E_2 *= oestradiol,* P_4 *= progesterone, Q-VD-OPh = quinolyl-valyl-O-methylaspartyl-[2,6-difluorophenoxy]-methyl ketone.*

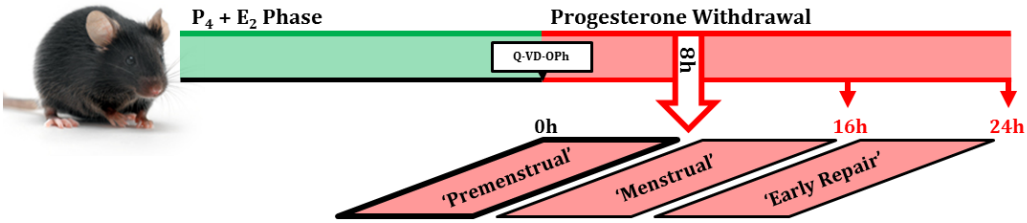

A

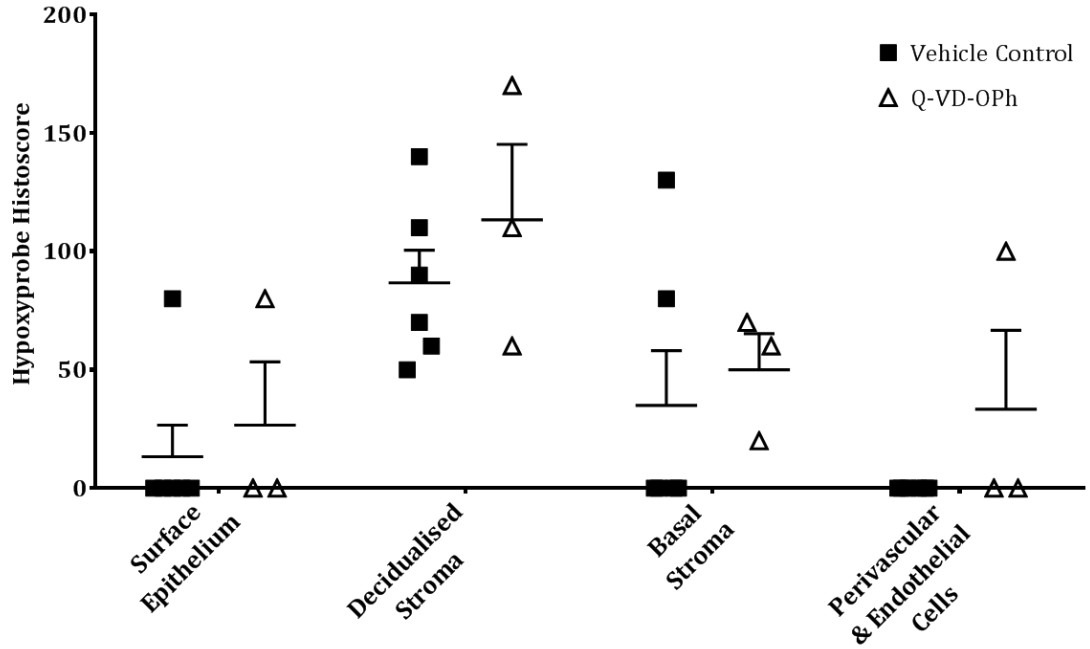

B

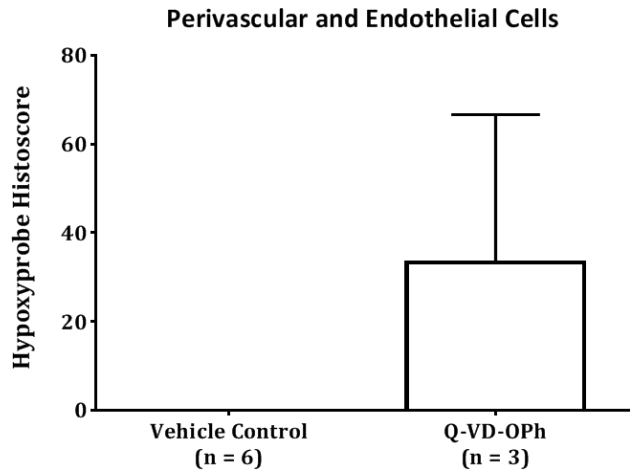

Figure 62. Hypoxia (Hypoxyprobe^{+}) is extensive in the decidualised endometrial stroma at 8 hours post-progesterone withdrawal in mice administered Q-VD-OPh and vehicle control; hypoxic vessels seen in Q-VD-OPh-treated mice. Representative photomicrographs of pimonidazole (1:200, Hypoxyprobe Inc.) staining in serial sections of endometrium from mice administered Q-VD-OPh (n = 3) or vehicle control (n = 6), 8 hours following progesterone withdrawal. **Black triangle** indicates hypoxic vessels. *Isotype control: mouse IgG1κ (Sigma-Aldrich); nuclear counterstain: haematoxylin. Scale bars (500 µm, 50 µm) in image. E_2 = oestradiol, P_4 = progesterone, Q-VD-OPh = quinolyl-valyl-O-methylaspartyl-[2,6-difluorophenoxy]-methyl ketone.*

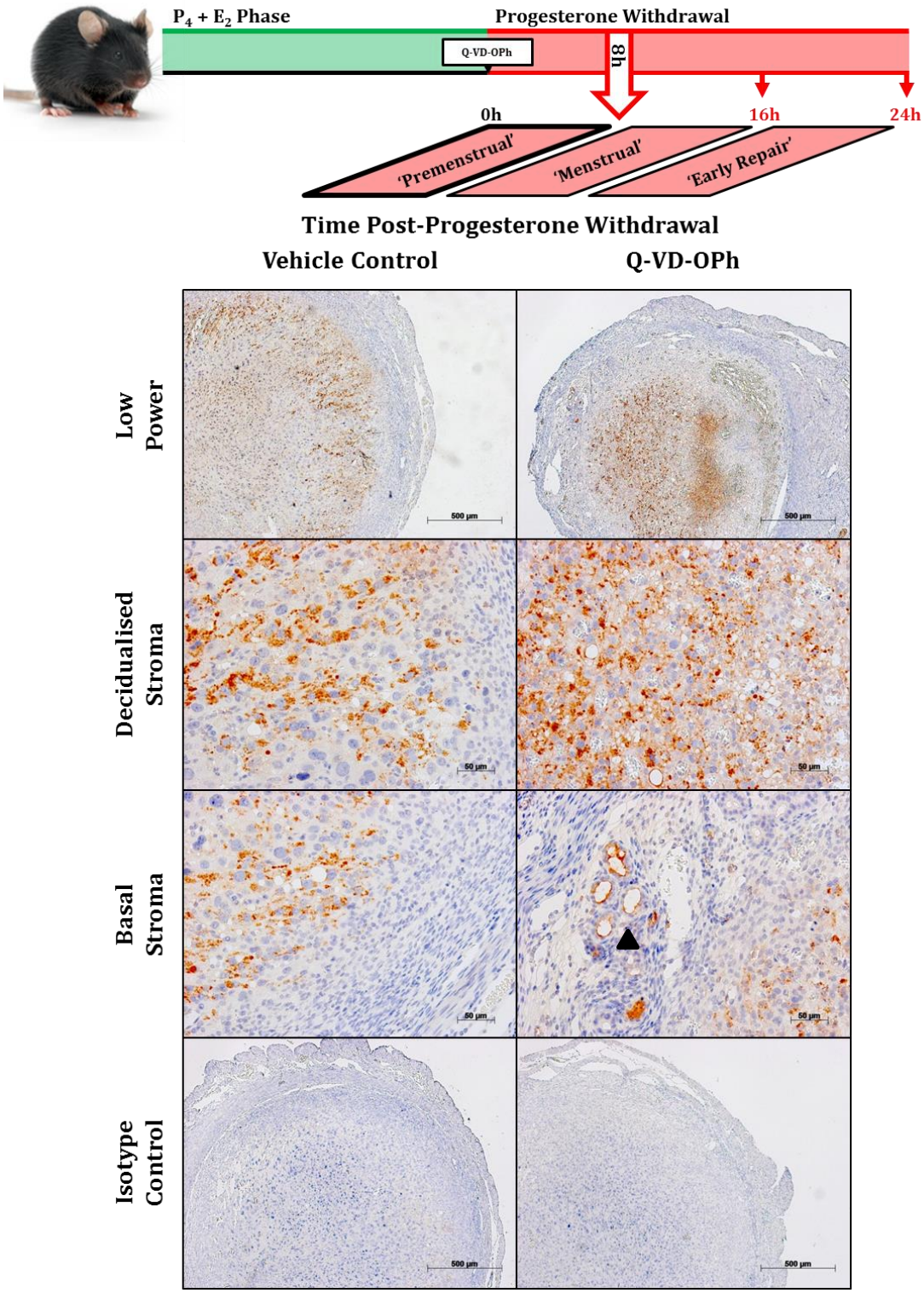

Figure 63. Q-VD-OPh effected no significant differences in endometrial hypoxia 16 hours after progesterone withdrawal. Semi-quantitative immunoreactivity histoscoring (staining intensity multiplied by percentage of tissue staining positive) for pimonidazole (1:200, Hypoxyprobe Inc.) in endometrial tissues of mice administered Q-VD-OPh (n = 8) or vehicle control (n = 4), 16 hours following progesterone withdrawal. *Each data point represents the average of three experiments; lines represent mean; error bars represent SEM. E_2 = oestradiol, P_4 = progesterone, Q-VD-OPh = quinolyl-valyl-O-methylaspartyl-[2,6-difluorophenoxy]-methyl ketone.*

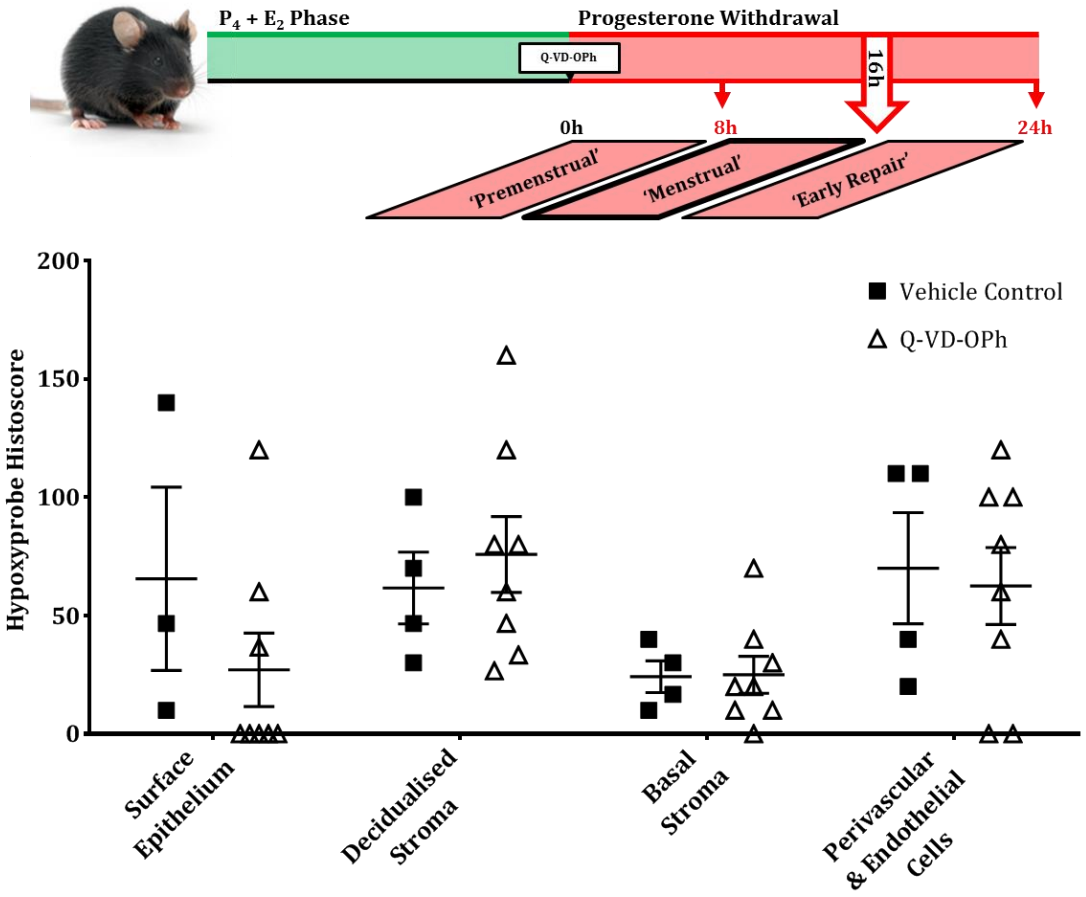

Figure 64. Endometrial hypoxia (Hypoxyprobe^{+}) is widespread in the mouse endometrium at 16 hours post-progesterone withdrawal in Q-VD-OPh- and vehicle-control-treated mice. Representative photomicrographs of pimonidazole (1:200, Hypoxyprobe Inc.) staining in serial sections of endometrium from mice administered Q-VD-OPh (n = 8) or vehicle control (n = 4), 16 hours following progesterone withdrawal. *Isotype control: mouse IgG1κ (Sigma-Aldrich); nuclear counterstain: haematoxylin. Scale bars (500 µm, 50 µm) in image. E_2 = oestradiol, P_4 = progesterone, Q-VD-OPh = quinolyl-valyl-O-methylaspartyl-[2,6-difluorophenoxy]-methyl ketone.*

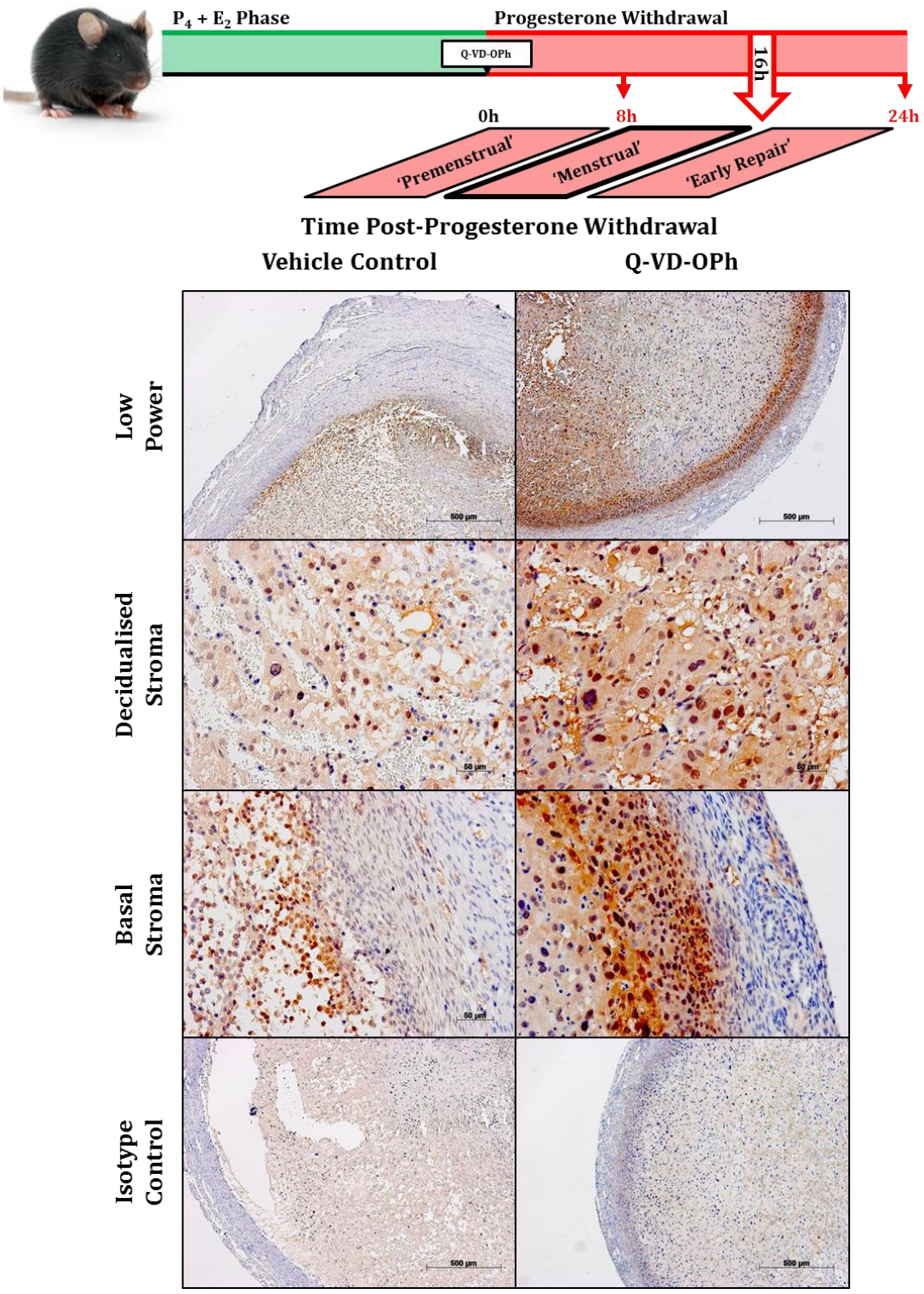

Figure 65. No significant differences in endometrial hypoxia were apparent in Q-VD-OPh-treated mice at 24 hours post-progesterone withdrawal. Semi-quantitative immunoreactivity histoscoring (staining intensity multiplied by percentage of tissue staining positive) for pimonidazole (1:200, Hypoxyprobe Inc.) in endometrial tissues of mice administered Q-VD-OPh (n = 5) or vehicle control (n = 7), 24 hours following progesterone withdrawal. *Each data point represents the average of three experiments; lines represent mean; error bars represent SEM. E_2 = oestradiol, P_4 = progesterone, Q-VD-OPh = quinolyl-valyl-O-methylaspartyl-[2,6-difluorophenoxy]-methyl ketone.*

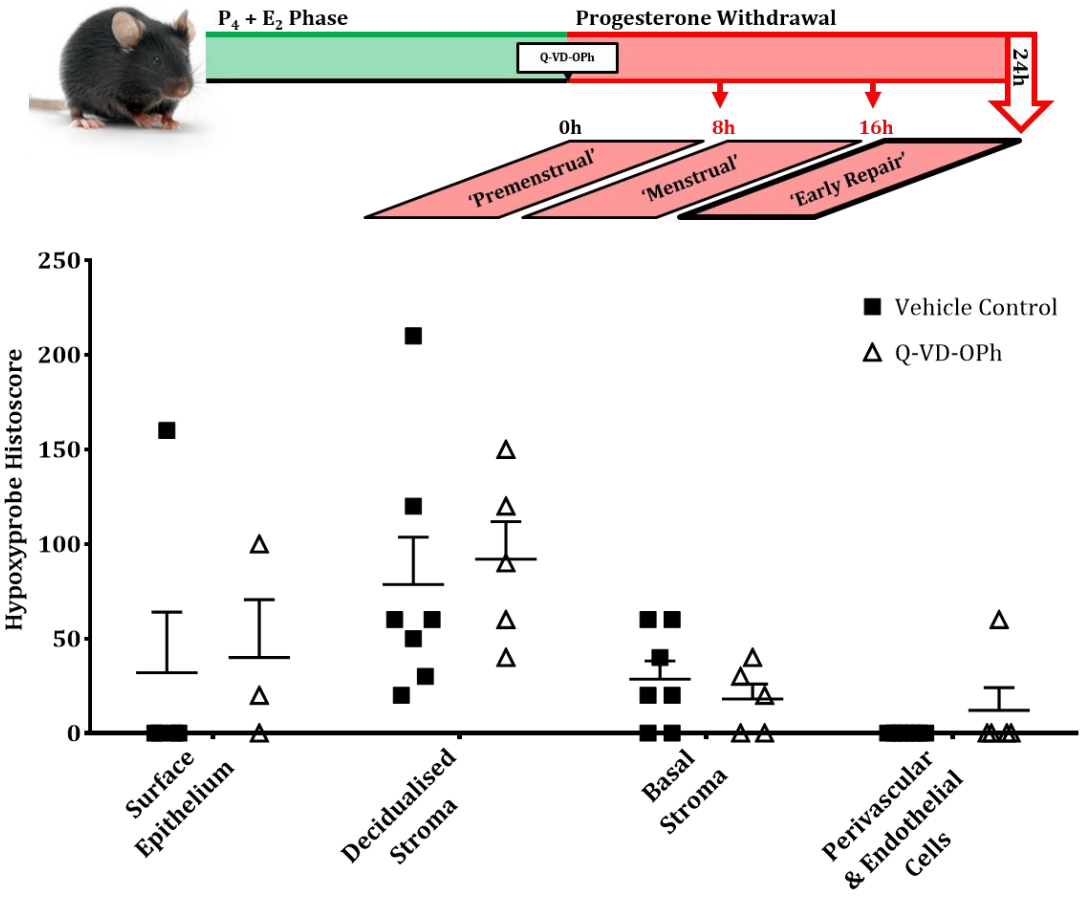

Figure 66. Hypoxia (Hypoxyprobe^{+}) remains extensive at 24 hours post-progesterone withdrawal in the endometrium of both mice treated with Q-VD-OPh and vehicle control. Representative photomicrographs of pimonidazole (1:200, Hypoxyprobe Inc.) staining in serial sections of endometrium from mice administered Q-VD-OPh (n = 5) or vehicle control (n = 7), 24 hours following progesterone withdrawal. *Isotype control: mouse IgG1κ (Sigma-Aldrich); nuclear counterstain: haematoxylin. Scale bars (500 µm, 50 µm) in image. E_2 = oestradiol, P_4 = progesterone, Q-VD-OPh = quinolyl-valyl-O-methylaspartyl-[2,6-difluorophenoxy]-methyl ketone.*

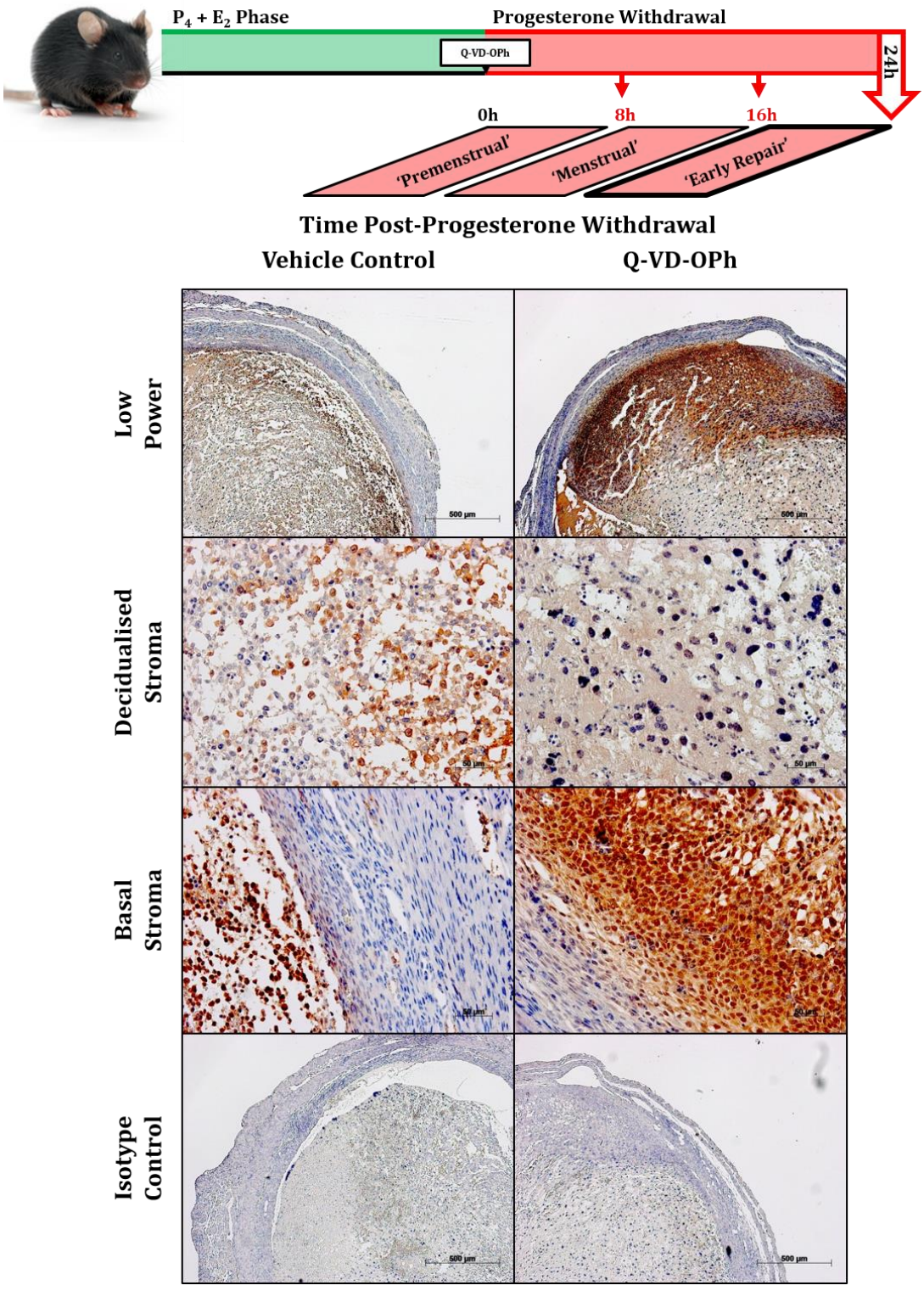

Figure 67. Summary changes in hypoxia in the endometrium of mice administered Q-VD-OPh and vehicle control at 8, 16 and 24 hours after progesterone withdrawal. Semi-quantitative immunoreactivity histoscoring (staining intensity multiplied by percentage of tissue staining positive) for Hypoxyprobe (1:200, Hypoxyprobe Inc.) in endometrial tissues of mice administered Q-VD-OPh (B; n = 16) or vehicle control (A; n = 17), 8, 16 and 24 hours following progesterone withdrawal. *# p < 0.05 (compared to 8h and 24h); error bars represent SEM; significance determined by 2-way ANOVA and Tukey's multiple comparisons test.* E_2 *= oestradiol,* P_4 *= progesterone, Q-VD-OPh = quinolyl-valyl-O-methylaspartyl-[2,6-difluorophenoxy]-methyl ketone.*

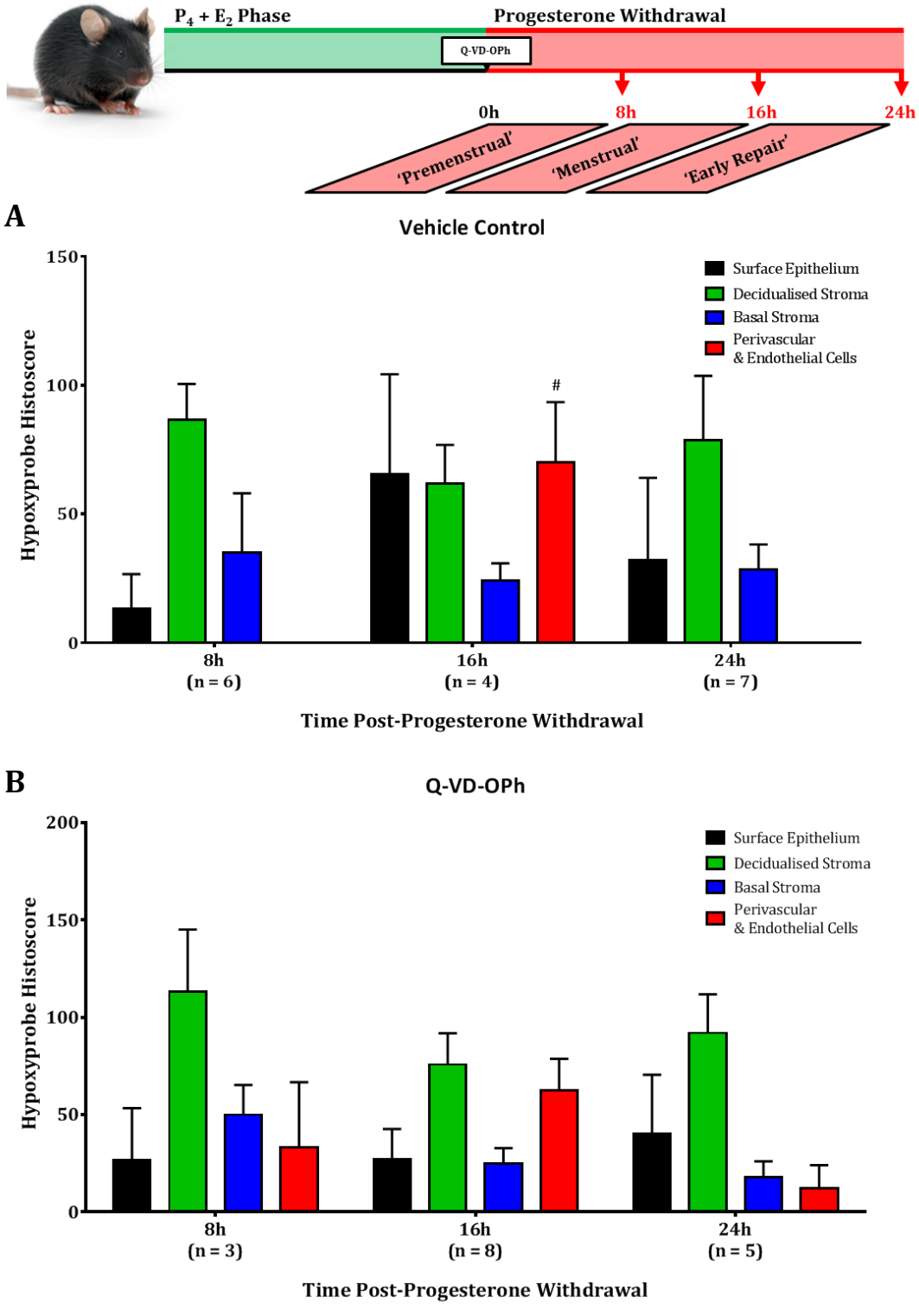

6.4 Discussion

6.4.1 Pan-Caspase Inhibitor Q-VD-OPh & Inhibition of Apoptosis

Immunohistochemical and semi-quantitative data described in this chapter demonstrate successful *in vivo* inhibition of apoptosis at 8 hours after progesterone withdrawal, with no cleaved caspase-3 expression seen in the endometrium of any of the mice administered the pan-caspase inhibitor Q-VD-OPh. In the endometrium of mice administered vehicle control (10% DMSO/PBS), cleaved caspase-3 expression was observed in the decidualised and basal endometrial stroma at 8 hours.

Whereas endometrial cleaved caspase-3 expression was completely abrogated in Q-VD-OPh-treated mice at 8 hours following progesterone withdrawal, by 16 hours and 24 hours, cleaved caspase-3 expression was again widespread in the endometrium and no differences were discernible between the treatment groups.

No studies to date have characterised the effects of *in vivo* inhibition of apoptosis on endometrial repair, inflammatory gene transcription, cellular proliferation or hypoxia – the data described herein are the first to do so.

Q-VD-OPh is a potent inhibitor of all three major, caspase-dependent apoptotic pathways: caspase-9/-3, caspase-8/-10 and caspase-12 (**Figure 39**; Caserta *et al*., 2003). It is reportedly functional in different species (including human and mouse) and various cell types, strongly inhibiting the activation of caspases, the cleavage of caspase substrates and the fragmentation of DNA that are characteristic of apoptosis (Kerr *et al*., 1972; Wyllie *et al*., 1984; Caserta *et al*., 2003). Its negligible cytotoxicity has been demonstrated *in vitro*, and *in vivo* at equivalent doses to those used in these experiments (Caserta *et al*., 2003; Liu *et al*., 2011).

The use of Q-VD-OPh as a caspase inhibitor represents a significant methodological improvement over studies employing the related fluoromethylketone- (fmk)-based caspase inhibitor compounds such as Boc-D-fmk or Z-VAD-fmk. Q-VD-OPh reportedly shows maximal caspase inhibition at one tenth the concentration of Boc-D-fmk in cell culture; and whereas Z-VAD-fmk and other fmk-based inhibitors show preferential inhibition of the caspase-9/-3 pathway, Q-VD-OPh is equally effective at inhibiting all three major apoptotic pathways (Caserta *et al*., 2003). Thus the use of Q-VD-OPh in the inhibition of apoptosis is more specific and effective, less cytotoxic and better tolerated by experimental animals.

The use of caspase-3 cleavage as a proxy for apoptosis is a well-established and powerful means of apoptosis detection, prone to fewer false negatives and positives than conventional detection methods such as TUNEL staining (Duan *et al*., 2003; Gavrieli *et al*., 1992). Cleaved caspase-3 is indicative of apoptosis at an earlier stage than morphological criteria such as cytoplasmic and nuclear condensation appear (Kerr *et al*., 1972; Duan *et al*., 2003) and represents an irreversible commitment to the apoptotic cascade – all three caspase activation pathways (caspase-9/-3, caspsase-8/-10, caspase-12), intrinsic and extrinsic, converge on the cleavage and activation of caspase-3 (Li *et al*., 1997, 1998; Slee *et al*., 2001).

Limiting numbers represented a weakness of the studies undertaken in this chapter, particularly for the demonstration of statistically significant inhibition of apoptosis in Q-VD-OPh-treated mice. While no cleaved caspase-3 expression was seen in the endometrium of any Q-VD-OPh-treated mouse at 8 hours' progesterone withdrawal, low sample size for this treatment group (n = 3) hampered the finding of a statistically significant difference compared to the vehicle control group. Increasing numbers of

Q-VD-OPh-treated mouse endometrial tissues at 8 hours after progesterone withdrawal would increase the likelihood of demonstrating significantly reduced cleaved caspase-3 expression, thereby strengthening the basic premise of the experiments – namely that the effects described in this chapter are due to early inhibition of apoptosis.

The data presented in this chapter nevertheless suggest that the administration of the pan-caspase inhibitor Q-VD-OPh inhibits caspase-3 cleavage and apoptosis until at least 8 hours after its injection and progesterone withdrawal. By 16 hours, apoptosis is re-established in the endometrium of mice administered Q-VD-OPh and persists until 24 hours.

6.4.2 Endometrial Repair

Haematoxylin- and eosin-staining of murine endometrial tissues and the subsequent characterisation of endometrial repair described in this chapter give the indication of a modestly retarded repair progression in the endometria of mice administered Q-VD-OPh compared to those administered vehicle control, though only early after progesterone withdrawal (8 hours) – these data were not statistically significant. By 16 hours after progesterone withdrawal, endometrial repair was equally progressed in mice of both treatment groups, suggesting that if there is an effect of caspase inhibition, it is only short-lived.

Though histological repair has been studied in the mouse endometrium following progesterone withdrawal, the effects of *in vivo* apoptosis inhibition on endometrial repair in a mouse model of menses are a novel line of experimental enquiry, as yet absent from the literature.

Since the mouse model of menstruation was first developed by Finn and Pope (1984), a number of excellent studies have emerged seeking to study endometrial breakdown and repair in this and in refined versions of this model.

Finn and Pope's seminal work on this model employed oestradiol and progesterone injections to prime the endometrium for decidualisation, and introduced intra-luminal uterine injections of arachis oil as a decidualisation stimulus. Sixty-four to sixty-six hours subsequent to the oil stimulus (70 hours after the final hormone injection), Finn and Pope discovered decidual responses in 83% of the mice undergoing the protocol; highly variable timings in the responses seen, however, discouraged the authors from further investigation.

Some 20 years later, Brasted *et al*. (2003) refined the original model, introducing in place of progesterone injections a subcutaneously-implanted, progesterone-releasing Silastic pump, as developed by Cohen and Milligan (1993). This refinement allowed the rapid withdrawal of progesterone from circulation (and by extension the uterus) via the pump's removal, facilitating more reliable timings of menstrual events in the model. The Brasted model saw progesterone support withdrawn from the mice 49 hours subsequent to the administration of the oil stimulus (Brasted *et al*., 2003).

Characterisation of uterine morphology undertaken in these studies showed that the endometrium was extensively remodelled in the decidualisation process, with endometrial glands pushed down toward the myometrium and closure of the lumen (Brasted *et al*., 2003). The authors describe the uterus as increasing in weight from 0 – 20 hours after progesterone withdrawal, but detail changes in the structural integrity of the decidual zone from 16 hours and the appearance of necrotic tissue from 20 hours. Maximal stromal destruction was described at 24 hours after progesterone

withdrawal, and (approximate) completion of the repair process by 48 hours (Brasted *et al*., 2003).

Further studies undertaken by Kaitu'u-Lino *et al*. (2006, 2007) using the Brasted model also found near-complete repair by 48 hours after progesterone withdrawal – the former study found this retarded in mice which had been administered a myeloid-cell-depleting neutralising antibody.

Studies undertaken in the same year by Xu *et al*. (2007) retained the use of the progesterone-releasing Silastic pump introduced by Brasted *et al.* but employed injection of the progesterone receptor antagonist mifepristone (RU486) in place of pump removal. Here they describe similar timings of breakdown and repair: they identified breakdown and shedding of epithelial cells by 8 hours after mifepristone injection, necrotic epithelium by 16 hours and sloughing of most of the decidualised stroma into the lumen by 24 hours. The authors corroborated observations of complete repair by 48 hours in the physiological progesterone withdrawal model (Brasted *et al*., 2003) with observations of the same in their pharmacological progesterone withdrawal model (Xu *et al*., 2007).

In studies undertaken more recently, in which the authors withdrew progesterone support 96 hours after the oil stimulus, Menning *et al*. (2012) describe many of the same features described above, including loss of structural integrity in the decidualised endometrium and its dissociation from the underlying myometrium. In contrast to previous studies, however, Menning *et al*. did not observe complete repair and re-epithelialisation until 72 hours after progesterone withdrawal.

Despite minor discrepancies, the timing of events involved in endometrial repair in a mouse model of menstruation is well-established and little disputed. Though endometrial repair has been studied extensively in a mouse model of menstruation however, both with (Kaitu'u-Lino *et al*., 2006) and without (Brasted *et al*., 2003) experimental manipulation of various parameters, no studies to date have investigated the effects of the inhibition of apoptosis on endometrial repair. The experiments described in this chapter are therefore a novel contribution to the existing literature.

As in other aspects of the studies described herein, limiting numbers represented a weakness in the characterisation of endometrial repair and the statistical analyses performed thereupon. Increasing sample sizes for mice of either treatment group at 16 and 24 hours after progesterone withdrawal are unlikely to uncover any significant differences in endometrial repair. Investigation into endometrial repair at 8 hours post-progesterone withdrawal, however, gave the indication of retarded repair progression in Q-VD-OPh-treated mice, warranting further investigation with increased numbers. If the Q-VD-OPh treatment group sample size were increased from n = 3, subsequent comparisons of repair progression may yield statistical significance.

Another question regarding this model which remains unanswered is whether the successful restoration of the endometrium is ultimately delayed in the Q-VD-OPh-treated mice: the latest progesterone withdrawal time-point examined in this chapter was 24 hours, but complete endometrial repair is thought not to occur until 48 to 72 hours (Brasted *et al*., 2003; Kaitu'u-Lino *et al*., 2006, 2007; Menning *et al*., 2012). Determination of the median endometrial repair time in Q-VD-OPh-treated mice could yield important data regarding the 'knock-on' effects of early inhibition of apoptosis.

The data comprising this chapter's characterisation of endometrial repair progression demonstrate that the effects of caspase inhibition are likely to be acute, limited to shortly after progesterone withdrawal (8 hours); any differences between Q-VD-OPh- and vehicle-control-treated mouse endometrium vanish (or are compensated for) by 16 and 24 hours after progesterone withdrawal.

6.4.3 Inflammatory Gene Transcription

The transcriptional data generated in the studies undertaken herein revealed significant differences in levels of endometrial *Cxc1* and *Tnfa* mRNA between treatment groups across the progesterone withdrawal time-points examined.

No such experiments investigating the effects of *in vivo* apoptosis inhibition on endometrial inflammatory cytokine transcription to my knowledge have yet been described in the literature, therefore these data are believed to represent entirely novel investigations.

Although transcription of *Cxcl1* (KC; a homologue of the human neutrophil chemokine *CXCL8*; Oquendo *et al*., 1989; Scholten and Al-samman, 2012) was significantly decreased in the caspase-inhibited endometrium at 16 hours' progesterone withdrawal, its transcription was significantly increased relative to vehicle control endometrium at 24 hours. Inhibition of *Cxcl1* transcription at one time-point and potentiation at another time-point may seem unusual, unless the *Cxcl1* transcriptional profile is regarded a 'curve' in which *Cxcl1* mRNA is maximally transcribed at 16 hours (simulated 'menstrual' phase) and decreases thereafter as the tissue is restored in vehicle-control-treated mice; in this view, Q-VD-OPh could be seen as retarding the 'menstrual' transcription of *Cxcl1*, such that its maximal expression is not observed

until 24 hours (simulated 'early repair' phase). Further investigation of the endometrial *Cxcl1* transcriptional profiles of Q-VD-OPh- and vehicle-control-treated mice at time-points subsequent to 24 hours' withdrawal could corroborate this hypothesis.

Q-VD-OPh-mediated caspase-inhibition resulted in a significant increase in endometrial *Tnfa* transcription at 24 hours' progesterone withdrawal as compared to vehicle-control-treated mice. Since apoptosis, evidenced by cleaved caspase-3 immunoreactivity, seems quickly restored in the Q-VD-OPh treatment group to vehicle-control-equivalent levels by 16 and 24 hours post-progesterone withdrawal, the potentiation of *Tnfa* transcription may be among the mechanisms by which apoptotic homeostasis is re-established in the endometrium of these mice.

Other studies undertaken have employed Q-VD-OPh and related caspase inhibitors, even in ovariectomised mice, but have done so to investigate the effects of caspase inhibition on other target tissues such as the heart (Liu *et al*., 2011) and have not investigated inflammatory mediator transcription in these contexts. Dynamic regulation of *Cxcl1* and *Tnfa* have been investigated and described, both in work presented in Chapter 4 and by other authors (Menning *et al*., 2012), though never before in the context of caspase inhibition.

The principal strength of the studies described herein therefore lies in their novelty – *in vivo* inhibition of apoptosis having never been studied in a mouse model of menstruation. These data are the first to show the effects of early caspase inhibition (i.e. at progesterone withdrawal) on the transcription of inflammatory cytokines later in the process of menstrual breakdown and repair.

The experiments described in this chapter would benefit from increased sample sizes, a limitation to the analyses without which must be acknowledged. In treatment groups of certain time-points, for instance, only as few as 3 mice successfully underwent endometrial decidualisation in the induced menses protocol – though we estimate the decidualisation success rate of this model in our hands at 60 – 75%, despite best efforts, fewer mice underwent endometrial decidualisation in some groups than had been hoped. Further work bolstering sample sizes at certain time-points would be of benefit, as would the investigation of further time-points following 24 hours' progesterone withdrawal.

Taken together, the data presented in this chapter suggest a nuanced role for apoptosis in the regulation of inflammatory cytokine and chemokine transcription in the endometrium of a mouse model of menses, influencing the magnitude of transcription and perhaps its timing. It is unknown for certain whether apoptosis plays a parallel role in the human endometrium in the regulation of inflammation at menses, a role perhaps disturbed in women with heavy menstrual bleeding. This hypothesis is not untenable, however, in light of evidence presented in Chapter 5, demonstrating disturbed apoptosis and inflammatory chemokine/cytokine transcriptional profiles in the endometrium of such women.

6.4.4 Endometrial Proliferation

The immunohistochemical and semi-quantitative BrdU histoscoring data generated in the experiments of this chapter demonstrated a number of statistically significant

changes in proliferation in the endometrium across progesterone withdrawal time-points.

Proliferation was significantly increased in the surface epithelium of both Q-VD-OPh- and vehicle-control-treated mice at 16 and 24 hours. In the basal stroma, proliferation was significantly increased in both treatment groups – at 24 hours for vehicle-control-treated mice and at 16 hours for Q-VD-OPh-treated mice.

Interestingly, however, proliferation in the decidualised stroma was only seen in mice treated with Q-VD-OPh: BrdU immunoreactivity was significantly higher at 8 hours than at 16 and 24 hours in Q-VD-OPh-treated mice, and significantly higher in Q-VD-OPh-treated mice at 8 hours than in vehicle-control-treated mice at the same time.

Although apoptosis has been inhibited in these mice, it does not necessarily follow that cells of the decidualised stroma, normally undergoing apoptosis at 8 hours' progesterone withdrawal, would actively proliferate in the absence of apoptosis – this was an unexpected and particularly interesting finding.

There have been no studies published as yet investigating changes in endometrial proliferation following progesterone withdrawal, in response to *in vivo* inhibition of apoptosis.

Despite the multitude of studies investigating endometrial repair in the mouse model of menstruation developed by Finn and Pope (1984) and refined by Brasted *et al*. (2003), as described earlier, somewhat fewer studies have investigated cellular proliferation specifically.

Kaitu'u-Lino *et al*. (2007) examined proliferation immunohistochemically by immunostaining for the proliferative marker Ki67, though only in mice sacrificed 24 and 48 hours after the withdrawal of progesterone. Here they found an abundance of

proliferation ($Ki67^+$) in the decidual zone, both of stromal cell and epithelial cell origin, noting that proliferation was more abundant in areas where breakdown was incomplete. The authors unfortunately did not attempt to quantify proliferation in the tissues, nor to analyse differences for statistical significance; no mention is made in their studies about which observations correspond to which progesterone withdrawal time-points.

The studies undertaken in this chapter investigated earlier time-points than did those undertaken by Kaitu'u-Lino *et al*. (2007), though both works examined proliferation in the mouse endometrium after 24 hours' progesterone withdrawal – here their Ki67 immunostaining photomicrographs match very closely to the BrdU immunostaining photomicrographs generated in this chapter.

In studies more recently undertaken by Cousins *et al*. (2014), proliferation was detailed by BrdU immunoreactivity, with mice sacrificed 4, 8, 12 and 24 hours after progesterone withdrawal. Cousins *et al.* found proliferating surface epithelial cells and basal stromal cells from 4 hours after progesterone withdrawal, consistent with the findings of this chapter, in which proliferation was found abundant in both of these tissue compartments at 8 hours. Cousins *et al.* further describe extensive surface epithelial proliferation at 12 hours, alongside the absence of proliferation in the decidualised mass – features, again, consistent with this chapter's findings at 8 and 16 hours. At 24 hours after progesterone withdrawal, Cousins *et al.* detail in their mice a still BrdU-immunopositive endometrial surface epithelium, with many BrdU-immunopositive basal stromal cells. These observations, too, are corroborated by investigations into BrdU immunoreactivity at 24 hours' progesterone withdrawal in the experiments of this chapter. The authors did not endeavour to quantify the changes

in proliferation observed in their experiments, though the broad observations they detail are nevertheless fully corroborated by the studies undertaken herein.

The experiments of this chapter sought to contribute to and refine the existing literature concerning endometrial proliferation after progesterone withdrawal in two main ways: firstly, by employing a semi-quantitative histoscoring method to better characterise the extent to which proliferation was occurring in various tissues of the endometrium; secondly, by determining what effects the inhibition of apoptosis had on proliferation in endometrial tissues. The former clarifies existing literature regarding cellular proliferation in the progesterone-withdrawn mouse endometrium, while the latter contributes a novel aspect to the current understanding of apoptosis and its importance to endometrial proliferation and restoration.

To address the principal shortcoming of these studies, namely limited sample sizes in treatment groups and time-points, some further work subjecting a small number of additional mice to the caspase-inhibited mouse model of menstruation protocol would help underscore and corroborate some of the proliferative changes detailed herein. Mice treated with Q-VD-OPh and culled at 8 hours after progesterone withdrawal in particular are lacking in these studies (n = 3), therefore these would be prioritised to help strengthen the finding of decidual cell proliferation in these mice.

The endometrial proliferation data presented in this chapter give a reasonable basis upon which to suppose that the widespread apoptosis observed in the mouse endometrium after progesterone withdrawal plays a role not only in the coordinated destruction of the decidualised endometrium, but plausibly in the inhibition of 'inappropriate' decidual cell proliferation.

One possibility is that in the absence of caspase inhibition, decidual cells that would otherwise be proliferating merely undergo apoptosis instead; thus the reason proliferation is not observed in vehicle-control-treated decidualised endometrium is that they die or are dying. Another possibility, however, is that cells undergoing apoptosis act to discourage neighbouring cells from proliferating, and that when this stimulus is removed by caspase-inhibition, cells are no longer prevented from undergoing proliferation. If the latter hypothesis is true, then apoptosis plays an important signalling role in the remodelling endometrium, in addition to being an effector of tissue destruction.

6.4.5 Endometrial Hypoxia

Hypoxyprobe immunostaining and semi-quantitative histoscoring data presented in this chapter delineate changes in the localisation and intensity of hypoxia in the endometrium across progesterone withdrawal time-points, revealing a number of interesting features therein.

Hypoxia was found most extensive in the decidualised endometrium of both Q-VD-OPh and vehicle control treatment groups, evident at 8 hours after progesterone withdrawal and persisting until at least 24 hours. Hypoxia was likewise consistently present, albeit to a lesser extent, in the surface epithelium and basal stroma of both treatment groups. No differences in hypoxia between progesterone withdrawal time-points were observed in these endometrial tissues.

Endometrial vasculature, in contrast, seems time-dependently hypoxic: Hypoxyprobe-immunonegative in the vehicle-control-treated mouse endometrium at 8 and 24 hours after progesterone withdrawal (indicating pO_2 > 10 mmHg; Varghese *et al*., 1976;

Raleigh *et al*., 1985), but briefly and significantly hypoxic at 16 hours after progesterone withdrawal (pO_2 < 10 mmHg).

No studies have been published to date investigating hypoxic changes in the mouse endometrium after progesterone withdrawal, nor have there been any studies published examining the differences in response to *in vivo* inhibition of apoptosis.

Hypoxyprobe (pimonidazole hydrochloride) forms adducts with thiol-containing amino acids at partial oxygen pressures of less than 10 mmHg (1.3% oxygen), and only in the presence of certain specific redox enzymes found in hypoxic cells (Varghese *et al*., 1976; Raleigh *et al*., 1985).

While physiological oxygen concentrations vary between different tissues and metabolic conditions, normal tissues are reported to have oxygen levels of 3 – 5% (pO_2 = 22 – 38 mmHg) and levels of 5 – 11% (pO_2 = 38 – 84 mmHg) are reported in circulation (Iyer *et al*., 1998; Caldwell *et al*., 2001).

Hypoxia is reportedly required for the synthesis of certain angiogenic factors, such as vascular endothelial growth factor (VEGF; Iyer *et al*., 1998; Fan *et al*., 2008), and thus may be important in the regulation of vascular proliferation.

In a pseudo-decidualisation mouse model (in which endometrial breakdown is stimulated not by direct withdrawal of progesterone, but by bilateral ovariectomy subsequent to oil decidualisation stimulus), work performed by Fan *et al*. (2008) demonstrated that VEGF was essential for the formation of new vessels, but not for the maintenance of mature vessels. Further, recent work in this model showed that *Vegf* transcription was regulated by the transcription factor, hypoxia inducible factor-1 alpha (HIF1α), facilitating maximal *Vegf* transcription at 12 hours after the (ovariectomy-mediated) withdrawal of progesterone (Chen *et al*., 2015).

The effects of hypoxia on leucocyte longevity and inhibition of apoptosis therein are well-documented (Hannah *et al*., 1995; Leuenroth *et al*., 2000; Walmsley *et al*., 2005; Cross *et al*., 2006).

While a considerable body of literature exists regarding the importance of hypoxia in regulating tissue and vascular repair, no experimental work has yet been undertaken to examine the effects of apoptosis and its inhibition on hypoxia in the mouse endometrium. The strength of these experiments therefore is born of the novelty of the experimental intervention in this model, investigating caspase inhibition on the extent and distribution of hypoxia in the progesterone-withdrawn mouse endometrium.

Although a brief spike in endometrial vascular hypoxia was described in these studies at 16 hours' progesterone withdrawal, further work investigating additional time-points around this time would be useful in better characterising endometrial hypoxia. The data in this chapter make clear that hypoxia is not established until sometime between 8 and 16 hours, and is not resolved until sometime between 16 and 24 hours, but any detail finer than this cannot be determined with the endometrial tissues available. 'When does vascular hypoxia begin', 'when is it resolved', and 'how long does it persist' or all questions of some interest in order to better understand hypoxia's contribution to menstruation and its resolution; thus it would be useful to further investigate 12 and 20 hour progesterone withdrawal time-points in the mouse endometrium.

The data presented in this chapter demonstrate that regions of hypoxia persist through progesterone withdrawal (at least from 8 to 24 hours) and may be a persistent feature of most tissues of the endometrium until its complete, successful restoration. Only the

vasculature of the endometrium appears subject to dynamic changes in hypoxia across progesterone withdrawal time-points, showing marked increases in hypoxia (i.e. decreases in oxygen concentrations) at 16 hours after progesterone withdrawal.

Hypoxia may play a role in the regulation of angiogenesis, immune cell recruitment and immune cell longevity. The effects of early apoptosis inhibition on endometrial (and in particular, perivascular and endothelial) hypoxia are unclear, but may interfere with coordinated hypoxic conditions in the vasculature.

6.4.6 Summary & Conclusions

Experimental manipulation of apoptosis in a mouse model of menstruation was achieved by the introduction of the pan-caspase inhibitor, Q-VD-OPh, and the inhibition of apoptosis in the endometrium was confirmed at 8 hours' progesterone withdrawal by immunohistochemistry and semi-quantitative histoscoring for cleaved caspase-3. Apoptosis was no longer inhibited by 16 hours.

Haematoxylin- and eosin-staining and histological assessment of endometrial repair uncovered a modest, but non-significant, retardation of endometrial repair in the caspase-inhibited mouse endometrium. No differences in repair were seen at 16 or 24 hours' progesterone withdrawal.

The inhibition of apoptosis in the progesterone-withdrawn mouse endometrium effected significant changes in the regulation of inflammatory cytokine and chemokine transcription at 16 and 24 hours after progesterone withdrawal, both in the magnitude of their transcription and conceivably in timing thereof.

Endometrial proliferation was found subject to significant changes across progesterone withdrawal time-points within treatment groups – where surface epithelial cell proliferation in particular was found significantly increased at 16 and 24 hours – but

also found significantly increased in the decidualised stroma in caspase-inhibited mice at 8 hours, a time-point at which decidual cell proliferation is ordinarily completely absent.

Caspase inhibition seemed to have little effect on hypoxia in the mouse endometrium following progesterone withdrawal, with levels hypoxia remaining fairly consistent across withdrawal time-points. Within mice of the vehicle control group, however, perivascular and endothelial cell hypoxia was found briefly and significantly increased at 16 hours.

These data, taken together, suggest a complex role for apoptosis in the endometrial remodelling process, influencing a wide range of molecular, cellular and histological features. The observations detailed herein are summarised in **Table 15**.

Table 15. Summary of observations in the caspase-inhibited mouse endometrium subsequent to the withdrawal of progesterone. Upward-facing arrows (↑) and shades of orange reflect increases in the observed quantity described in this chapter; downward-facing arrows (↓) and shades of blue reflect decreases. White boxes without symbols reflect the absence of observation (cleaved caspase-3, endometrial repair, BrdU, Hypoxyprobe) or 'baseline' for transcriptional changes. Novel data to which the summary table refers can be found on the pages listed in the right-most column. ** denotes statistical significance (p < 0.05 – 0.0001) for the observations described (compared to 8h for 'Vehicle Control' and 'Q-VD-OPh' data; compared to Vehicle Control for 'Q-VD vs. Ctrl' data). Ctrl = vehicle control.*

Hours Post-Progesterone Withdrawal		8	16	24	Pages
Apoptosis (cleaved caspase-3)	Vehicle Control	↑↑	↑↑↑	↑↑↑	213, 214, 215, 216, 217, 218
	Q-VD-OPh		↑↑↑	↑↑↑	
	Q-VD vs. Ctrl	↓↓			
Endometrial repair	Vehicle Control	↑	↑↑	↑↑	221, 222, 223, 224, 225, 226
	Q-VD-OPh		↑↑	↑↑	
	Q-VD vs. Ctrl	↓			
Cxcl1 transcription	Vehicle Control		↑↑↑	↑	228
	Q-VD-OPh			↑↑↑	
	Q-VD vs. Ctrl		↓↓/*	↑↑/*	
Tnfa transcription	Vehicle Control		↑	↑↑	228
	Q-VD-OPh		↑	↑↑↑	
	Q-VD vs. Ctrl			↑/*	

Table 15 continued.

Hours Post-Progesterone Withdrawal		8	16	24	Pages
Proliferation (BrdU) Surface epithelium	Vehicle Control	↑	↑↑↑/*	↑↑↑/*	231, 232, 233, 234 235, 236, 237
	Q-VD-OPh	↑	↑↑↑/*	↑↑↑/*	
	Q-VD vs. Ctrl				
Decidualised stroma	Vehicle Control				
	Q-VD-OPh	↑↑	*	*	
	Q-VD vs. Ctrl	↑↑/*			
Basal stroma	Vehicle Control	↑↑	↑	↑/*	
	Q-VD-OPh	↑↑	↑/*	↑	
	Q-VD vs. Ctrl				
Hypoxia (Hypoxyprobe) Surface epithelium	Vehicle Control	↑	↑↑	↑	240, 241, 242, 243, 244, 245, 246
	Q-VD-OPh	↑	↑	↑	
	Q-VD vs. Ctrl		↓		
Decidualised stroma	Vehicle Control	↑↑	↑↑	↑↑	
	Q-VD-OPh	↑↑	↑↑	↑↑	
	Q-VD vs. Ctrl				
Basal stroma	Vehicle Control	↑	↑	↑	
	Q-VD-OPh	↑	↑	↑	
	Q-VD vs. Ctrl				
Perivascular and endothelial	Vehicle Control		↑↑/*		
	Q-VD-OPh	↑	↑		
	Q-VD vs. Ctrl	↑	↓		

7. Summary, Future Directions

& Overall Conclusions

7.1 Synopsis of Results

The data presented in this thesis describe apoptosis and inflammation in the human endometrium across the perimenstrual window, meticulously characterised for menstrual phase and bleeding status, and in the mouse endometrium after withdrawal of progesterone in a murine model of induced menstruation.

Novel data regarding the spatial and temporal regulation of apoptosis in the normal human endometrium were presented, which were shown to be recapitulated in the endometrium of a mouse model of induced menstruation: endometrial apoptosis (cleaved caspase-3^{+}) was extensive prior to the onset of breakdown, shedding and bleeding.

Significant increases in menstrual-phase inflammatory cytokine transcription were demonstrated in the normal human endometrium, and these were further recapitulated in the endometrium of a mouse model: menstruation (in the human) and induced menstruation (in the mouse) effected significant increases in chemokine transcription (*CXCL8*, *CCL2, Cxcl1*) and in inflammatory cytokine transcription (*TNFA*, *IL6*, *Tnfa*).

Novel data concerning endometrial neutrophil population dynamics in the normal human endometrium were presented, demonstrating negligible abundance in the late secretory phase prior to a precipitous increase in numbers upon the advent of menstruation. Endometrial neutrophils (MPO^{+}, elastase^{+}) were revealed less numerous than previously supposed, though still constituted 5 – 10% of the endometrial stroma at menses. These data were recapitulated in the mouse endometrium, with substantial

increases observed in murine neutrophil numbers ($Ly6G^+$) by 24 hours post-progesterone withdrawal, constituting as much as 10% of the stroma.

Novel data regarding macrophage localisation ($CD68^+$) across the perimenstrual window in the normal human endometrium were presented, describing their trafficking to apoptotic glands at menses, phagocytosing apoptotic cells (cleaved caspase-3^+) and their subsequent movement into the stroma during the proliferative phase.

Investigating glucocorticoid receptor target gene transcription in a mouse model of menstruation produced novel data detailing significant changes in transcription across progesterone withdrawal time-points of 8, 16 and 24 hours, mirroring many of the transcriptional changes seen in the human endometrium across the perimenstrual window.

A novel series of experiments inhibiting apoptosis in a mouse model of menstruation detailed a multitude of acute cellular and histological effects, including dysregulated decidual cell proliferation ($BrdU^+$), altered inflammatory chemokine and cytokine transcriptional profiles (*Cxcl1*, *Tnfa*) and impaired repair.

Figure 68. Summary schematic of changes observed in the endometrium during simulated menstruation in an ovariectomised mouse model (top) and during menstruation in humans (bottom). Cellular and histological events which occur in the endometrium during simulated menstruation in the mouse model recapitulate those events which occur in the human endometrium at menstruation: significant apoptosis, preceding extensive neutrophil influx and inflammatory cytokine transcription. Coloured arrows depict approximate onset of change described. *P_4W/d = progesterone withdrawal, LMP = last menstrual period; 'PM' = 'pre-menstrual', 'M' = 'menstrual', 'ER' = 'early repair', LS = late secretory, M = menstrual, EP = early proliferative; NΦ = neutrophils, MΦ = macrophages.*

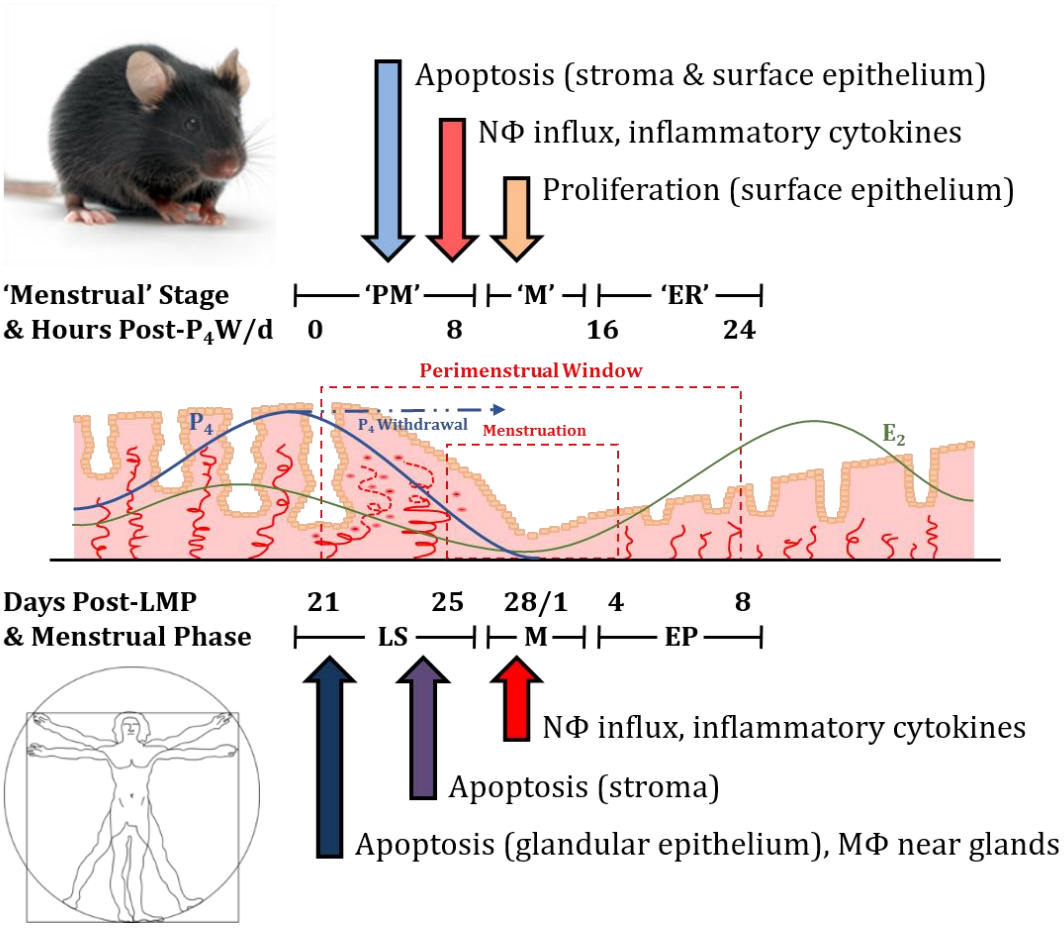

7.2 Areas for Future Study

This thesis provides robust descriptive data for the timing and extent of endometrial apoptosis and of neutrophil infiltration into the endometrium, obtained from precisely-characterised, 'full-thickness', hysterectomy-derived endometrial biopsies from women with normal menstrual bleeding (NMB). It would of considerable interest to characterise these phenomena in the endometrium of women with heavy menstrual bleeding (HMB) as carefully as was possible with the endometrium of women with NMB, though at this time impossible due to the scarcity of carefully-characterised, 'full thickness' endometrial biopsies from such women.

Even with the characterisation of inflammatory mediator transcription using endometrial biopsies obtained by the considerably less invasive means of endometrial suction curettage ('Pipelle' biopsies), the relatively poor availability of carefully-characterised samples greatly hindered optimal statistical analysis of differences between the endometrium of women with NMB and HMB.

As patient endometrial sample availability increases, particularly with accompanying objective menstrual blood loss measurements, many of the descriptive studies in the human endometrium detailed herein bear revisiting in order to strengthen the findings reported.

The studies described in this thesis concerning the mouse model of menstruation (both with and without caspase inhibition) exhaustively detailed apoptosis, proliferation, repair, hypoxia and inflammatory features across the progesterone withdrawal time-points investigated: 0, 4, 8, 16 and 24 hours post-progesterone withdrawal. As became increasingly clear, however, many of these features had yet to resolve by 24 hours post-progesterone withdrawal.

A number of not unreasonable research questions therefore suggest themselves:

1. When do levels of apoptosis return to 'baseline' in the mouse endometrium after progesterone withdrawal? Concomitant with or prior to successful, complete restoration of the endometrium?
2. No statistically significant differences in repair progression were uncovered in the caspase-inhibited mouse endometrium at ≤24 hours post-progesterone withdrawal, but neither treatment group exhibited a completely repaired endometrium by 24 hours. Is there a difference in the time taken to completely repair the endometrium after progesterone withdrawal between caspase-inhibited and vehicle-control-treated mice?
3. When do levels of inflammatory mediator transcription return to 'baseline' in the mouse endometrium after progesterone withdrawal? Is there a difference in the time taken to resolve these indicators of inflammation after progesterone withdrawal between caspase-inhibited and vehicle-control-treated mice?

Further studies might reasonably therefore investigate the above experimental endpoints at progesterone withdrawal time-points of 32, 40 and 48 hours.

Gene array studies were undertaken in this thesis, endeavouring to detail transcriptional changes in glucocorticoid receptor target genes in the mouse endometrium, which identified a number of gene transcripts dynamically regulated across the progesterone withdrawal time-points investigated (0, 8, 16 and 24 hours). Many of the putatively differentially-regulated transcripts require validation by RT-qPCR and corroboration with protein expression data to strengthen the legitimacy of these findings. These aspects would doubtless comprise the next stage of this line of inquiry.

7.3 Conclusions

This thesis presents data in support of a pivotal role for apoptosis in the events of menstruation in the human and mouse endometrium, preceding overt menstrual bleeding and endometrial shedding. The data presented herein further support regarding menstruation an inflammatory phenomenon, with significant increases observed in both the human and mouse endometrium in neutrophil abundance and inflammatory cytokine transcription. The legitimacy of a mouse model of menstruation is moreover strengthened by the exercises detailed in this thesis, demonstrating that many of the features characterising menstruation in the human endometrium are recapitulated in the mouse model employed herein.

With respect to menstrual pathologies, this thesis provides data describing dysregulation of apoptosis and inflammatory cytokine transcription in the endometrium of women with HMB. Interfering with normal physiological induction of apoptosis in a mouse model of menstruation effected a host of significant differences in proliferation and inflammation, underscoring the importance of apoptosis in the events of menstruation. Inhibition of apoptosis may therefore represent a powerful means by which to model disorders of menstruation in order to further understanding of the molecular and cellular events of menstruation.

Bibliography

Aasmundstad, T.A., Haugen, O.A., Johannesen, E., Høe, A.L., and Kvinnsland, S. (1992). Oestrogen receptor analysis: correlation between enzyme immunoassay and immunohistochemical methods. J. Clin. Pathol. *45*, 125–129.

Abadie, V., Badell, E., Douillard, P., Ensergueix, D., Leenen, P.J.M., Tanguy, M., Fiette, L., Saeland, S., Gicquel, B., and Winter, N. (2005). Neutrophils rapidly migrate via lymphatics after Mycobacterium bovis BCG intradermal vaccination and shuttle live bacilli to the draining lymph nodes. Blood *106*, 1843–1850.

Aghajanova, L., Stavreus-Evers, A., Lindeberg, M., Landgren, B.-M., Sparre, L.S., and Hovatta, O. (2011). Thyroid-stimulating hormone receptor and thyroid hormone receptors are involved in human endometrial physiology. Fertil. Steril. *95*, 230–237.e2.

Akira, S., and Kishimoto, T. (1992). IL-6 and NF-IL6 in acute-phase response and viral infection. Immunol. Rev. *127*, 25–50.

Allavena, P., Bianchi, G., Zhou, D., van Damme, J., Jílek, P., Sozzani, S., and Mantovani, A. (1994). Induction of natural killer cell migration by monocyte chemotactic protein-1, -2 and -3. Eur. J. Immunol. *24*, 3233–3236.

van Amerongen, M.J., Harmsen, M.C., van Rooijen, N., Petersen, A.H., and van Luyn, M.J.A. (2007). Macrophage Depletion Impairs Wound Healing and Increases Left Ventricular Remodeling after Myocardial Injury in Mice. Am. J. Pathol. *170*, 818–829.

Anggård, E. (1966). The biological activities of three metabolites of prostaglandin E 1. Acta Physiol. Scand. *66*, 509–510.

Anzick, S.L., Kononen, J., Walker, R.L., Azorsa, D.O., Tanner, M.M., Guan, X.Y., Sauter, G., Kallioniemi, O.P., Trent, J.M., and Meltzer, P.S. (1997). AIB1, a steroid receptor coactivator amplified in breast and ovarian cancer. Science *277*, 965–968.

Aplin, J.D. (1991). Implantation, trophoblast differentiation and h\a emochorial placentation: mechanistic evidence in vivo andin vitro. J Cell Sci *99*, 681–692.

Arcuri, F., Monder, C., Lockwood, C.J., and Schatz, F. (1996). Expression of 11 beta-hydroxysteroid dehydrogenase during decidualization of human endometrial stromal cells. Endocrinology *137*, 595–600.

Arici, A., Head, J.R., MacDonald, P.C., and Casey, M.L. (1993). Regulation of interleukin-8 gene expression in human endometrial cells in culture. Mol. Cell. Endocrinol. *94*, 195–204.

Arici, A., MacDonald, P.C., and Casey, M.L. (1996). Progestin regulation of interleukin-8 mRNA levels and protein synthesis in human endometrial stromal cells. J. Steroid Biochem. Mol. Biol. *58*, 71–76.

Ariel, A., Fredman, G., Sun, Y.-P., Kantarci, A., Van Dyke, T.E., Luster, A.D., and Serhan, C.N. (2006). Apoptotic neutrophils and T cells sequester chemokines during immune

response resolution through modulation of CCR5 expression. Nat. Immunol. *7*, 1209–1216.

Baggiolini, M., Dewald, B., and Moser, B. (1994). Interleukin-8 and related chemotactic cytokines--CXC and CC chemokines. Adv. Immunol. *55*, 97–179.

Ball, E., Bulmer, J., Ayis, S., Lyall, F., and Robson, S. (2006). Late sporadic miscarriage is associated with abnormalities in spiral artery transformation and trophoblast invasion. J. Pathol. *208*, 535–542.

Bamberger, A.-M., Milde-Langosch, K., Löning, T., and Bamberger, C.M. (2001). The Glucocorticoid Receptor Is Specifically Expressed in the Stromal Compartment of the Human Endometrium. J. Clin. Endocrinol. Metab.

Baron, D.A., La Perle, K.M., and Blomme, E.A. (2000). The use of computer-assisted image analysis in the evaluation of preclinical tumor efficacy models. Curr. Opin. Drug Discov. Devel. *3*, 79–93.

Barrington, J.W., and Bowen-Simpkins, P. (1997). The levonorgestrel intrauterine system in the management of menorrhagia. Br. J. Obstet. Gynaecol. *104*, 614–616.

Bazzoni, F., Cassatella, M.A., Rossi, F., Ceska, M., Dewald, B., and Baggiolini, M. (1991). Phagocytosing neutrophils produce and release high amounts of the neutrophil-activating peptide 1/interleukin 8. J. Exp. Med. *173*, 771–774.

Bennouna, S., Bliss, S.K., Curiel, T.J., and Denkers, E.Y. (2003). Cross-Talk in the Innate Immune System: Neutrophils Instruct Recruitment and Activation of Dendritic Cells during Microbial Infection. J. Immunol. *171*, 6052–6058.

Beutler, B., Milsark, I.W., and Cerami, A.C. (1985). Passive immunization against cachectin/tumor necrosis factor protects mice from lethal effect of endotoxin. Science *229*, 869–871.

Black, R.A., Rauch, C.T., Kozlosky, C.J., Peschon, J.J., Slack, J.L., Wolfson, M.F., Castner, B.J., Stocking, K.L., Reddy, P., Srinivasan, S., et al. (1997). A metalloproteinase disintegrin that releases tumour-necrosis factor-α from cells. Nature *385*, 729–733.

Blackwell, K., Zhang, L., Workman, L.M., Ting, A.T., Iwai, K., and Habelhah, H. (2013). Two Coordinated Mechanisms Underlie Tumor Necrosis Factor Alpha-Induced Immediate and Delayed IκB Kinase Activation. Mol. Cell. Biol. *33*, 1901–1915.

Bonatz, G., Hansmann, M.L., Buchholz, F., Mettler, L., Radzun, H.J., and Semm, K. (1992). Macrophage- and lymphocyte-subtypes in the endometrium during different phases of the ovarian cycle. Int. J. Gynaecol. Obstet. Off. Organ Int. Fed. Gynaecol. Obstet. *37*, 29–36.

Bonnar, J., and Sheppard, B.L. (1996). Treatment of menorrhagia during menstruation: randomised controlled trial of ethamsylate, mefenamic acid, and tranexamic acid. BMJ *313*, 579–582.

Brasted, M., White, C.A., Kennedy, T.G., and Salamonsen, L.A. (2003). Mimicking the Events of Menstruation in the Murine Uterus. Biol. Reprod. *69*, 1273–1280.

Braun, D.P., Ding, J., Shen, J., Rana, N., Fernandez, B.B., and Dmowski, W.P. (2002). Relationship between apoptosis and the number of macrophages in eutopic endometrium from women with and without endometriosis. Fertil. Steril. *78*, 830–835.

Brenner, R.M., Rudolph, L., Matrisian, L., and Slayden, O.D. (1996). Non-human primate models; artificial menstrual cycles, endometrial matrix metalloproteinases and s.c. endometrial grafts. Hum. Reprod. Oxf. Engl. *11 Suppl 2*, 150–164.

Brinkmann, V., Reichard, U., Goosmann, C., Fauler, B., Uhlemann, Y., Weiss, D.S., Weinrauch, Y., and Zychlinsky, A. (2004). Neutrophil Extracellular Traps Kill Bacteria. Science *303*, 1532–1535.

Brosens, J.J., Hayashi, N., and White, J.O. (1999). Progesterone receptor regulates decidual prolactin expression in differentiating human endometrial stromal cells. Endocrinology *140*, 4809–4820.

Buckley, C.D., Gilroy, D.W., Serhan, C.N., Stockinger, B., and Tak, P.P. (2013). The resolution of inflammation. Nat. Rev. Immunol. *13*, 59–66.

Buckley, C.D., Gilroy, D.W., and Serhan, C.N. (2014). Proresolving Lipid Mediators and Mechanisms in the Resolution of Acute Inflammation. Immunity *40*, 315–327.

Bulmer, J.N., Morrison, L., Longfellow, M., Ritson, A., and Pace, D. (1991). Granulated lymphocytes in human endometrium: histochemical and immunohistochemical studies. Hum. Reprod. Oxf. Engl. *6*, 791–798.

Burbelo, P.D., Drechsel, D., and Hall, A. (1995). A Conserved Binding Motif Defines Numerous Candidate Target Proteins for Both Cdc42 and Rac GTPases. J. Biol. Chem. *270*, 29071–29074.

Burrows, T.D., King, A., and Loke, Y.W. (1993). Expression of integrins by human trophoblast and differential adhesion to laminin or fibronectin. Hum. Reprod. *8*, 475–484.

Bustin, S.A. (2000). Absolute quantification of mRNA using real-time reverse transcription polymerase chain reaction assays. J. Mol. Endocrinol. *25*, 169–193.

Bustin, S.A., Benes, V., Garson, J.A., Hellemans, J., Huggett, J., Kubista, M., Mueller, R., Nolan, T., Pfaffl, M.W., Shipley, G.L., et al. (2009). The MIQE Guidelines: Minimum Information for Publication of Quantitative Real-Time PCR Experiments. Clin. Chem. *55*, 611–622.

Bygdeman, M. (2003). The possibility of using mifepristone for menstrual induction. Contraception *68*, 495–498.

Caldwell, C.C., Kojima, H., Lukashev, D., Armstrong, J., Farber, M., Apasov, S.G., and Sitkovsky, M.V. (2001). Differential Effects of Physiologically Relevant Hypoxic Conditions on T Lymphocyte Development and Effector Functions. J. Immunol. *167*, 6140–6149.

Cao, Y., Chen, C., Weatherbee, J.A., Tsang, M., and Folkman, J. (1995). gro-beta, a -C-X-C-chemokine, is an angiogenesis inhibitor that suppresses the growth of Lewis lung carcinoma in mice. J. Exp. Med. *182*, 2069–2077.

Carswell, E.A., Old, L.J., Kassel, R.L., Green, S., Fiore, N., and Williamson, B. (1975). An endotoxin-induced serum factor that causes necrosis of tumors. Proc. Natl. Acad. Sci. U. S. A. *72*, 3666–3670.

Caserta, T.M., Smith, A.N., Gultice, A.D., Reedy, M.A., and Brown, T.L. (2003). Q-VD-OPh, a broad spectrum caspase inhibitor with potent antiapoptotic properties. Apoptosis Int. J. Program. Cell Death *8*, 345–352.

Catalano, R.D., Critchley, H.O., Heikinheimo, O., Baird, D.T., Hapangama, D., Sherwin, J.R.A., Charnock-Jones, D.S., Smith, S.K., and Sharkey, A.M. (2007). Mifepristone induced progesterone withdrawal reveals novel regulatory pathways in human endometrium. Mol. Hum. Reprod. *13*, 641–654.

Chai, J., Du, C., Wu, J.-W., Kyin, S., Wang, X., and Shi, Y. (2000). Structural and biochemical basis of apoptotic activation by Smac/DIABLO. Nature *406*, 855–862.

Charo, I.F., Myers, S.J., Herman, A., Franci, C., Connolly, A.J., and Coughlin, S.R. (1994). Molecular cloning and functional expression of two monocyte chemoattractant protein 1 receptors reveals alternative splicing of the carboxyl-terminal tails. Proc. Natl. Acad. Sci. U. S. A. *91*, 2752–2756.

Chen, C.C., Sun, Y.T., Chen, J.J., and Chiu, K.T. (2000). TNF-alpha-induced cyclooxygenase-2 expression in human lung epithelial cells: involvement of the phospholipase C-gamma 2, protein kinase C-alpha, tyrosine kinase, NF-kappa B-inducing kinase, and I-kappa B kinase 1/2 pathway. J. Immunol. Baltim. Md 1950 *165*, 2719–2728.

Chen, X., Liu, J., He, B., Li, Y., Liu, S., Wu, B., Wang, S., Zhang, S., Xu, X., and Wang, J. (2015). Vascular endothelial growth factor (VEGF) regulation by hypoxia inducible factor-1 alpha (HIF1A) starts and peaks during endometrial breakdown, not repair, in a mouse menstrual-like model. Hum. Reprod. dev156.

Cheng, C. -w., Bielby, H., Licence, D., Smith, S.K., Print, C.G., and Charnock-Jones, D.S. (2007). Quantitative Cellular and Molecular Analysis of the Effect of Progesterone Withdrawal in a Murine Model of Decidualization. Biol. Reprod. *76*, 871–883.

Cheung-Flynn, J., Prapapanich, V., Cox, M.B., Riggs, D.L., Suarez-Quian, C., and Smith, D.F. (2005). Physiological Role for the Cochaperone FKBP52 in Androgen Receptor Signaling. Mol. Endocrinol. *19*, 1654–1666.

Christiaens, G.C., Sixma, J.J., and Haspels, A.A. (1980). Morphology of haemostasis in menstrual endometrium. Br. J. Obstet. Gynaecol. *87*, 425–439.

Chtanova, T., Schaeffer, M., Han, S.-J., van Dooren, G.G., Nollmann, M., Herzmark, P., Chan, S.W., Satija, H., Camfield, K., Aaron, H., et al. (2008). Dynamics of Neutrophil Migration in Lymph Nodes during Infection. Immunity *29*, 487–496.

Chukkapalli, S., Amessou, M., Dekhil, H., Dilly, A.K., Liu, Q., Bandyopadhyay, S., Thomas, R.D., Bejna, A., Batist, G., and Kandouz, M. (2014). Ehd3, a regulator of vesicular trafficking, is silenced in gliomas and functions as a tumor suppressor by controlling cell cycle arrest and apoptosis. Carcinogenesis *35*, 877–885.

Chwalisz, K., and Garfield, R.E. (2000). Role of nitric oxide in implantation and menstruation. Hum. Reprod. Oxf. Engl. *15 Suppl 3*, 96–111.

Cohen, P.E., and Milligan, S.R. (1993). Silastic implants for delivery of oestradiol to mice. J. Reprod. Fertil. *99*, 219–223.

Collart, M.A., Baeuerle, P., and Vassalli, P. (1990). Regulation of tumor necrosis factor alpha transcription in macrophages: involvement of four kappa B-like motifs and of constitutive and inducible forms of NF-kappa B. Mol. Cell. Biol. *10*, 1498–1506.

Colotta, F., Re, F., Polentarutti, N., Sozzani, S., and Mantovani, A. (1992). Modulation of granulocyte survival and programmed cell death by cytokines and bacterial products. Blood *80*, 2012–2020.

Cominelli, A., Chevronnay, H.P.G., Lemoine, P., Courtoy, P.J., Marbaix, E., and Henriet, P. (2014). Matrix metalloproteinase-27 is expressed in CD163+/CD206+ M2 macrophages in the cycling human endometrium and in superficial endometriotic lesions. Mol. Hum. Reprod. *20*, 767–775.

Corner, G.W., and Allen, W.M. (1929). Physiology of the corpus luteum II: production of a special uterine reaction (progestational proliferation) by extracts of the corpus luteum. Am. J. Physiol. *88*, 326–346.

Coulter, A., Peto, V., and Doll, H. (1994). Patients' Preferences and General Practitioners' Decisions in the Treatment of Menstrual Disorders. Fam. Pract. *11*, 67–74.

Cousins, F.L., Murray, A., Esnal, A., Gibson, D.A., Critchley, H.O.D., and Saunders, P.T.K. (2014). Evidence from a Mouse Model That Epithelial Cell Migration and Mesenchymal-Epithelial Transition Contribute to Rapid Restoration of Uterine Tissue Integrity during Menstruation. PLoS ONE *9*, e86378.

Cox, G., Crossley, J., and Xing, Z. (1995). Macrophage engulfment of apoptotic neutrophils contributes to the resolution of acute pulmonary inflammation in vivo. Am. J. Respir. Cell Mol. Biol. *12*, 232–237.

Critchley, H., and Maybin, J. (2011). Molecular and Cellular Causes of Abnormal Uterine Bleeding of Endometrial Origin. Semin. Reprod. Med. *29*, 400–409.

Critchley, H.O., Kelly, R.W., and Kooy, J. (1994a). Perivascular location of a chemokine interleukin-8 in human endometrium: a preliminary report. Hum. Reprod. Oxf. Engl. *9*, 1406–1409.

Critchley, H.O., Abberton, K.M., Taylor, N.H., Healy, D.L., and Rogers, P.A. (1994b). Endometrial sex steroid receptor expression in women with menorrhagia. Br. J. Obstet. Gynaecol. *101*, 428–434.

Critchley, H.O.D., Jones, R.L., Lea, R.G., Drudy, T.A., Kelly, R.W., Williams, A.R.W., and Baird, D.T. (1999). Role of Inflammatory Mediators in Human Endometrium during Progesterone Withdrawal and Early Pregnancy. J. Clin. Endocrinol. Metab. *84*, 240–248.

Critchley, H.O.D., Kelly, R.W., Brenner, R.M., and Baird, D.T. (2002). The endocrinology of menstruation–a role for the immune system. Clin. Endocrinol. (Oxf.) *55*, 701–710.

Critchley, H.O.D., Osei, J., Henderson, T.A., Boswell, L., Sales, K.J., Jabbour, H.N., and Hirani, N. (2006). Hypoxia-Inducible Factor-1α Expression in Human Endometrium and Its Regulation by Prostaglandin E-Series Prostanoid Receptor 2 (EP2). Endocrinology *147*, 744–753.

Cromwell, D., Mahmood, T., Templeton, A., and van der Meulen, J. (2009). Surgery for menorrhagia within English regions: variation in rates of endometrial ablation and hysterectomy. BJOG Int. J. Obstet. Gynaecol. *116*, 1373–1379.

Cross, A., Barnes, T., Bucknall, R.C., Edwards, S.W., and Moots, R.J. (2006). Neutrophil apoptosis in rheumatoid arthritis is regulated by local oxygen tensions within joints. J. Leukoc. Biol. *80*, 521–528.

Csapo, A.I., and Pulkkinen, M. (1978). Indispensability of the human corpus luteum in the maintenance of early pregnancy. Luteectomy evidence. Obstet. Gynecol. Surv. *33*, 69–81.

Csapo, A.I., and Resch, B. (1979). Prevention of implantation by antiprogesterone. J. Steroid Biochem. *11*, 963–969.

Daems, W.T., and De Bakker, J.M. (1982). Do Resident Macrophages Proliferate? Immunobiology *161*, 204–211.

Daley, J.M., Thomay, A.A., Connolly, M.D., Reichner, J.S., and Albina, J.E. (2007). Use of Ly6G-specific monoclonal antibody to deplete neutrophils in mice. J. Leukoc. Biol. *83*, 64–70.

Damsky, C.H., Librach, C., Lim, K.H., Fitzgerald, M.L., McMaster, M.T., Janatpour, M., Zhou, Y., Logan, S.K., and Fisher, S.J. (1994). Integrin switching regulates normal trophoblast invasion. Development *120*, 3657–3666.

Dancey, J.T., Deubelbeiss, K.A., Harker, L.A., and Finch, C.A. (1976). Neutrophil kinetics in man. J. Clin. Invest. *58*, 705–715.

Danial, N.N., and Korsmeyer, S.J. (2004). Cell Death: Critical Control Points. Cell *116*, 205–219.

Denkers, E.Y., Del Rio, L., and Bennouna, S. (2003). Neutrophil production of IL-12 and other cytokines during microbial infection. Chem. Immunol. Allergy *83*, 95–114.

Dharma, S.J., Kholkute, S.D., and Nandedkar, T.D. (2001). Apoptosis in endometrium of mouse during estrous cycle. Indian J. Exp. Biol. *39*, 218–222.

Dobrzycka, B., Terlikowski, S.J., Bernaczyk, P.S., Garbowicz, M., Niklinski, J., Chyczewski, L., and Kulikowski, M. (2010). Prognostic significance of smac/DIABLO in endometrioid endometrial cancer. Folia Histochem. Cytobiol. *48*, 678–681.

Doulatov, S., Notta, F., Eppert, K., Nguyen, L.T., Ohashi, P.S., and Dick, J.E. (2010). Revised map of the human progenitor hierarchy shows the origin of macrophages and dendritic cells in early lymphoid development. Nat. Immunol. *11*, 585–593.

Dransfield, I., Stocks, S.C., and Haslett, C. (1995). Regulation of cell adhesion molecule expression and function associated with neutrophil apoptosis. Blood *85*, 3264–3273.

Duan, W.R., Garner, D.S., Williams, S.D., Funckes-Shippy, C.L., Spath, I.S., and Blomme, E.A.G. (2003). Comparison of immunohistochemistry for activated caspase-3 and cleaved cytokeratin 18 with the TUNEL method for quantification of apoptosis in histological sections of PC-3 subcutaneous xenografts. J. Pathol. *199*, 221–228.

Duckitt, K., and Collins, S. (2008). Menorrhagia. BMJ Clin. Evid. *2008*.

Dunican, A.L., Leuenroth, S.J., Ayala, A., and Simms, H.H. (2000). CXC chemokine suppression of polymorphonuclear leukocytes apoptosis and preservation of function is oxidative stress independent. Shock Augusta Ga *13*, 244–250.

Dunn, C.L., Critchley, H.O.D., and Kelly, R.W. (2002). IL-15 Regulation in Human Endometrial Stromal Cells. J. Clin. Endocrinol. Metab. *87*, 1898–1898.

Dunn, C.L., Kelly, R.W., and Critchley, H.O.D. (2003). Decidualization of the human endometrial stromal cell: an enigmatic transformation. Reprod. Biomed. Online *7*, 151–161.

Endrikat, J., Vilos, G., Muysers, C., Fortier, M., Solomayer, E., and Lukkari-Lax, E. (2011). The levonorgestrel-releasing intrauterine system provides a reliable, long-term treatment option for women with idiopathic menorrhagia. Arch. Gynecol. Obstet. *285*, 117–121.

Ensor, C.M., and Tai, H.-H. (1995). 15-Hydroxyprostaglandin dehydrogenase. J. Lipid Mediat. Cell Signal. *12*, 313–319.

Ertel, W., Keel, M., Infanger, M., Ungethüm, U., Steckholzer, U., and Trentz, O. (1998). Circulating mediators in serum of injured patients with septic complications inhibit neutrophil apoptosis through up-regulation of protein-tyrosine phosphorylation. J. Trauma *44*, 767–775; discussion 775–776.

Evans, J., and Salamonsen, L.A. (2012). Inflammation, leukocytes and menstruation. Rev. Endocr. Metab. Disord. *13*, 277–288.

Evans, J., and Salamonsen, L.A. (2014). Decidualized Human Endometrial Stromal Cells Are Sensors of Hormone Withdrawal in the Menstrual Inflammatory Cascade. Biol. Reprod. *90*, 14.

Fadok, V.A., Bratton, D.L., Frasch, S.C., Warner, M.L., and Henson, P.M. (1998). The role of phosphatidylserine in recognition of apoptotic cells by phagocytes. Cell Death Differ. *5*, 551–562.

Fadok, V.A., Bratton, D.L., and Henson, P.M. (2001). Phagocyte receptors for apoptotic cells: recognition, uptake, and consequences. J. Clin. Invest. *108*, 957–962.

Fan, X., Krieg, S., Kuo, C.J., Wiegand, S.J., Rabinovitch, M., Druzin, M.L., Brenner, R.M., Giudice, L.C., and Nayak, N.R. (2008). VEGF blockade inhibits angiogenesis and reepithelialization of endometrium. FASEB J. *22*, 3571–3580.

Fedele, L., Bianchi, S., Raffaelli, R., Portuese, A., and Dorta, M. (1997). Treatment of adenomyosis-associated menorrhagia with a levonorgestrel-releasing intrauterine device. Fertil. Steril. *68*, 426–429.

Feroze-Zaidi, F., Fusi, L., Takano, M., Higham, J., Salker, M.S., Goto, T., Edassery, S., Klingel, K., Boini, K.M., Palmada, M., et al. (2007). Role and Regulation of the Serum- and Glucocorticoid-Regulated Kinase 1 in Fertile and Infertile Human Endometrium. Endocrinology *148*, 5020–5029.

Finn, C.A. (1986). Implantation, menstruation and inflammation. Biol. Rev. Camb. Philos. Soc. *61*, 313–328.

Finn, C.A. (1996). Why do women menstruate? Historical and evolutionary review. Eur. J. Obstet. Gynecol. Reprod. Biol. *70*, 3–8.

Finn, C.A. (1998). Menstruation: a nonadaptive consequence of uterine evolution. Q. Rev. Biol. *73*, 163–173.

Finn, C.A., and Keen, P.M. (1963). The Induction of Deciduomata in the Rat. J. Embryol. Exp. Morphol. *11*, 673–682.

Finn, C.A., and Pope, M. (1984). Vascular and cellular changes in the decidualized endometrium of the ovariectomized mouse following cessation of hormone treatment: a possible model for menstruation. J. Endocrinol. *100*, 295–300.

Fleming, T.J., Fleming, M.L., and Malek, T.R. (1993). Selective expression of Ly-6G on myeloid lineage cells in mouse bone marrow. RB6-8C5 mAb to granulocyte-differentiation antigen (Gr-1) detects members of the Ly-6 family. J. Immunol. *151*, 2399–2408.

Fraser, I., Critchley, H., Broder, M., and Munro, M. (2011). The FIGO Recommendations on Terminologies and Definitions for Normal and Abnormal Uterine Bleeding. Semin. Reprod. Med. *29*, 383–390.

Fraser, I.S., McCarron, G., and Markham, R. (1984). A preliminary study of factors influencing perception of menstrual blood loss volume. Am. J. Obstet. Gynecol. *149*, 788–793.

Fraser, I.S., Langham, S., and Uhl-Hochgraeber, K. (2009). Health-related quality of life and economic burden of abnormal uterine bleeding. Expert Rev. Obstet. Gynecol. *4*, 179–189.

Frazier, K., Williams, S., Kothapalli, D., Klapper, H., and Grotendorst, G.R. (1996). Stimulation of fibroblast cell growth, matrix production, and granulation tissue formation by connective tissue growth factor. J. Invest. Dermatol. *107*, 404–411.

Gaide Chevronnay, H.P., Galant, C., Lemoine, P., Courtoy, P.J., Marbaix, E., and Henriet, P. (2009). Spatiotemporal Coupling of Focal Extracellular Matrix Degradation and Reconstruction in the Menstrual Human Endometrium. Endocrinology *150*, 5094–5105.

Gaide Chevronnay, H.P., Selvais, C., Emonard, H., Galant, C., Marbaix, E., and Henriet, P. (2012). Regulation of matrix metalloproteinases activity studied in human endometrium as a paradigm of cyclic tissue breakdown and regeneration. Biochim. Biophys. Acta BBA - Proteins Proteomics *1824*, 146–156.

Galant, C., Berlière, M., Dubois, D., Verougstraete, J.-C., Charles, A., Lemoine, P., Kokorine, I., Eeckhout, Y., Courtoy, P.J., and Marbaix, E. (2004). Focal Expression and Final Activity of Matrix Metalloproteinases May Explain Irregular Dysfunctional Endometrial Bleeding. Am. J. Pathol. *165*, 83–94.

Galperin, E., Benjamin, S., Rapaport, D., Rotem-Yehudar, R., Tolchinsky, S., and Horowitz, M. (2002). EHD3: A Protein That Resides in Recycling Tubular and Vesicular Membrane Structures and Interacts with EHD1. Traffic *3*, 575–589.

Gamble, J.R., Harlan, J.M., Klebanoff, S.J., and Vadas, M.A. (1985). Stimulation of the adherence of neutrophils to umbilical vein endothelium by human recombinant tumor necrosis factor. Proc. Natl. Acad. Sci. U. S. A. *82*, 8667–8671.

Gannon, M.J., Day, P., Hammadieh, N., and Johnson, N. (1996). A new method for measuring menstrual blood loss and its use in screening women before endometrial ablation. Br. J. Obstet. Gynaecol. *103*, 1029–1033.

Garry, R., Hart, R., Karthigasu, K., and Burke, C. (2010). Structural changes in endometrial basal glands during menstruation. BJOG Int. J. Obstet. Gynaecol. *117*, 1175–1185.

Gavrieli, Y., Sherman, Y., and Ben-Sasson, S.A. (1992). Identification of programmed cell death in situ via specific labeling of nuclear DNA fragmentation. J. Cell Biol. *119*, 493–501.

Gibson, D.A., Greaves, E., Critchley, H.O.D., and Saunders, P.T.K. (2015). Estrogen-dependent regulation of human uterine natural killer cells promotes vascular remodelling via secretion of CCL2. Hum. Reprod. *30*, 1290–1301.

Gilroy, D., and De Maeyer, R. (2015). New insights into the resolution of inflammation. Semin. Immunol.

Goeman, J.J., Geer, S.A. van de, Kort, F. de, and Houwelingen, H.C. van (2004). A global test for groups of genes: testing association with a clinical outcome. Bioinformatics *20*, 93–99.

Grasl-Kraupp, B., Ruttkay-Nedecky, B., Koudelka, H., Bukowska, K., Bursch, W., and Schulte-Hermann, R. (1995). In situ detection of fragmented DNA (TUNEL assay) fails to discriminate among apoptosis, necrosis, and autolytic cell death: a cautionary note. Hepatol. Baltim. Md *21*, 1465–1468.

Gratzner, H.G. (1982). Monoclonal antibody to 5-bromo- and 5-iododeoxyuridine: A new reagent for detection of DNA replication. Science *218*, 474–475.

Graves, D.T., Jiang, Y., and Valente, A.J. (1999). The expression of monocyte chemoattractant protein-1 and other chemokines by osteoblasts. Front. Biosci. J. Virtual Libr. *4*, D571–D580.

Grigg, J.M., Silverman, M., Savill, J.S., Sarraf, C., and Haslett, C. (1991). Neutrophil apoptosis and clearance from neonatal lungs. The Lancet *338*, 720–722.

Gubbay, O., Critchley, H.O.D., Bowen, J.M., King, A., and Jabbour, H.N. (2002). Prolactin Induces ERK Phosphorylation in Epithelial and CD56+ Natural Killer Cells of the Human Endometrium. J. Clin. Endocrinol. Metab. *87*, 2329–2335.

Hallberg, L., and Nilsson, L. (1964). Constancy of Individual Menstrual Blood Loss. Acta Obstet. Gynecol. Scand. *43*, 352–359.

Hallberg, L., Högdahl, A.M., Nilsson, L., and Rybo, G. (1966a). Menstrual blood loss and iron deficiency. Acta Med. Scand. *180*, 639–650.

Hallberg, L., Högdahl, A.M., Nilsson, L., and Rybo, G. (1966b). Menstrual blood loss--a population study. Variation at different ages and attempts to define normality. Acta Obstet. Gynecol. Scand. *45*, 320–351.

Hamlett, G.W.D. (1934). Uterine bleeding in a bat, Glossophaga soricina. Anat. Rec. *60*, 9–17.

Han, G., Magee, T., and Khorram, O. (2005). Regulation of nitric oxide synthase isoforms by estrogen in the human endometrium. Fertil. Steril. *84, Supplement 2*, 1220–1227.

Hannah, S., Mecklenburgh, K., Rahman, I., Bellingan, G.J., Greening, A., Haslett, C., and Chilvers, E.R. (1995). Hypoxia prolongs neutrophil survival in vitro. FEBS Lett. *372*, 233–237.

Hapangama, D.K., Critchley, H.O.D., Henderson, T.A., and Baird, D.T. (2002). Mifepristone-Induced Vaginal Bleeding Is Associated with Increased Immunostaining for Cyclooxygenase-2 and Decrease in Prostaglandin Dehydrogenase in Luteal Phase Endometrium. J. Clin. Endocrinol. Metab. *87*, 5229–5234.

Harlow, S.D., and Campbell, O.M.R. (2004). Epidemiology of menstrual disorders in developing countries: a systematic review. BJOG Int. J. Obstet. Gynaecol. *111*, 6–16.

Harrison, J.E., and Schultz, J. (1976). Studies on the chlorinating activity of myeloperoxidase. J. Biol. Chem. *251*, 1371–1374.

Hartmann, K., Beiglböck, F., Czarnetzki, B.M., and Zuberbier, T. (1995). Effect of CC chemokines on mediator release from human skin mast cells and basophils. Int. Arch. Allergy Immunol. *108*, 224–230.

Harvey, C.B., and Williams, G.R. (2002). Mechanism of Thyroid Hormone Action. Thyroid *12*, 441–446.

Haskill, S., Beg, A.A., Tompkins, S.M., Morris, J.S., Yurochko, A.D., Sampson-Johannes, A., Mondal, K., Ralph, P., and Baldwin Jr., A.S. (1991). Characterization of an immediate-early gene induced in adherent monocytes that encodes IκB-like activity. Cell *65*, 1281–1289.

Henderson, T.A., Saunders, P.T.K., Moffett-King, A., Groome, N.P., and Critchley, H.O.D. (2003). Steroid Receptor Expression in Uterine Natural Killer Cells. J. Clin. Endocrinol. Metab. *88*, 440–449.

Henson, P.M., Bratton, D.L., and Fadok, V.A. (2001). The phosphatidylserine receptor: a crucial molecular switch? Nat. Rev. Mol. Cell Biol. *2*, 627–633.

Heximer, S.P., Watson, N., Linder, M.E., Blumer, K.J., and Hepler, J.R. (1997). RGS2/G0S8 is a selective inhibitor of Gqα function. Proc. Natl. Acad. Sci. *94*, 14389–14393.

Hiby, S.E., King, A., Sharkey, A.M., and Loke, Y.W. (1997). Human uterine NK cells have a similar repertoire of killer inhibitory and activatory receptors to those found in blood, as demonstrated by RT-PCR and sequencing. Mol. Immunol. *34*, 419–430.

Hishikawa, K., Nakaki, T., and Fujii, T. (2000). Connective tissue growth factor induces apoptosis via caspase 3 in cultured human aortic smooth muscle cells. Eur. J. Pharmacol. *392*, 19–22.

van der Horst, C.J., and Gillman, J. (1941). The menstrual cycle in Elephantulus myuras jamesoni p amily Macroscelididae. South Afr. J. Med. Sci. *6*, 27–47.

Huang, Z.P., Ni, H., Yang, Z.M., Wang, J., Tso, J.K., and Shen, Q.X. (2003). Expression of regulator of G-protein signalling protein 2 (RGS2) in the mouse uterus at implantation sites. Reproduction *126*, 309–316.

Huber, A.R., Kunkel, S.L., Todd, R.F., 3rd, and Weiss, S.J. (1991). Regulation of transendothelial neutrophil migration by endogenous interleukin-8. Science *254*, 99–102.

Hunt, J.S., Chen, H.L., Hu, X.L., and Tabibzadeh, S. (1992). Tumor necrosis factor-alpha messenger ribonucleic acid and protein in human endometrium. Biol. Reprod. *47*, 141–147.

Hurst, S.M., Wilkinson, T.S., McLoughlin, R.M., Jones, S., Horiuchi, S., Yamamoto, N., Rose-John, S., Fuller, G.M., Topley, N., and Jones, S.A. (2001). IL-6 and Its Soluble Receptor Orchestrate a Temporal Switch in the Pattern of Leukocyte Recruitment Seen during Acute Inflammation. Immunity *14*, 705–714.

Huynh, M.-L.N., Fadok, V.A., and Henson, P.M. (2002). Phosphatidylserine-dependent ingestion of apoptotic cells promotes TGF-β1 secretion and the resolution of inflammation. J. Clin. Invest. *109*, 41–50.

Igarashi, A., Okochi, H., Bradham, D.M., and Grotendorst, G.R. (1993). Regulation of connective tissue growth factor gene expression in human skin fibroblasts and during wound repair. Mol. Biol. Cell *4*, 637–645.

Iida, S., Kohro, T., Kodama, T., Nagata, S., and Fukunaga, R. (2005). Identification of CCR2, flotillin, and gp49B genes as new G-CSF targets during neutrophilic differentiation. J. Leukoc. Biol. *78*, 481–490.

Irvine, G.A., Campbell-Brown, M.B., Lumsden, M.A., Heikkilä, A., Walker, J.J., and Cameron, I.T. (1998). Randomised comparative trial of the levonorgestrel intrauterine

system and norethisterone for treatment of idiopathic menorrhagia. Br. J. Obstet. Gynaecol. *105*, 592–598.

Ismail, A., and Bateman, A. (2009). Expression of TBX2 promotes anchorage-independent growth and survival in the p53-negative SW13 adrenocortical carcinoma. Cancer Lett. *278*, 230–240.

Isomaa, V.V., Ghersevich, S.A., Mäentausta, O.K., Peltoketo, E.H., Poutanen, M.H., and Vihko, R.K. (1993). Steroid biosynthetic enzymes: 17 beta-hydroxysteroid dehydrogenase. Ann. Med. *25*, 91–97.

Ivkovic, S., Yoon, B.S., Popoff, S.N., Safadi, F.F., Libuda, D.E., Stephenson, R.C., Daluiski, A., and Lyons, K.M. (2003). Connective tissue growth factor coordinates chondrogenesis and angiogenesis during skeletal. Development *130*, 2779–2791.

Iyer, N.V., Kotch, L.E., Agani, F., Leung, S.W., Laughner, E., Wenger, R.H., Gassmann, M., Gearhart, J.D., Lawler, A.M., Yu, A.Y., et al. (1998). Cellular and developmental control of O2 homeostasis by hypoxia-inducible factor 1α. Genes Dev. *12*, 149–162.

Jabbour, H.N., Sales, K.J., Smith, O.P.M., Battersby, S., and Boddy, S.C. (2006). Prostaglandin receptors are mediators of vascular function in endometrial pathologies. Mol. Cell. Endocrinol. *252*, 191–200.

Jenkins, S.J., Ruckerl, D., Cook, P.C., Jones, L.H., Finkelman, F.D., Rooijen, N. van, MacDonald, A.S., and Allen, J.E. (2011). Local Macrophage Proliferation, Rather than Recruitment from the Blood, Is a Signature of TH2 Inflammation. Science *332*, 1284–1288.

Jeong, J.-W., Lee, H.S., Lee, K.Y., White, L.D., Broaddus, R.R., Zhang, Y.-W., Woude, G.F.V., Giudice, L.C., Young, S.L., Lessey, B.A., et al. (2009). Mig-6 modulates uterine steroid hormone responsiveness and exhibits altered expression in endometrial disease. Proc. Natl. Acad. Sci. *106*, 8677–8682.

Johnston, M.G., Hay, J.B., and Movat, H.Z. (1976). The modulation of enhanced vascular permeability by prostaglandins through alterations in blood flow (hyperemia). Agents Actions *6*, 705–711.

Jones, R.L., Kelly, R.W., and Critchley, H.O. (1997a). Chemokine and cyclooxygenase-2 expression in human endometrium coincides with leukocyte accumulation. Hum. Reprod. *12*, 1300–1306.

Jones, S.A., Dewald, B., Clark-Lewis, I., and Baggiolini, M. (1997b). Chemokine Antagonists That Discriminate between Interleukin-8 Receptors SELECTIVE BLOCKERS OF CXCR2. J. Biol. Chem. *272*, 16166–16169.

Jutila, D.B., Kurk, S., and Jutila, M.A. (1994). Differences in the expression of Ly-6C on neutrophils and monocytes following PI-PLC hydrolysis and cellular activation. Immunol. Lett. *41*, 49–57.

Jutila, M.A., Kroese, G.M., Jutila, K.L., Stall, A.M., Fiering, S., Herzenberg, L.A., And, E.L.B., and Butcher, E.C. (1988). Ly-6C is a monocyte/macrophage and endothelial cell differentiation antigen regulated by interferon-gamma. Eur. J. Immunol. *18*, 1819–1826.

Kägi, J.H., and Kojima, Y. (1987). Chemistry and biochemistry of metallothionein. Experientia. Suppl. *52*, 25–61.

Kaitu'u, T.J., Shen, J., Zhang, J., Morison, N.B., and Salamonsen, L.A. (2005). Matrix Metalloproteinases in Endometrial Breakdown and Repair: Functional Significance in a Mouse Model. Biol. Reprod. *73*, 672–680.

Kaitu'u-Lino, T.J., Morison, N.B., and Salamonsen, L.A. (2006). Neutrophil depletion retards endometrial repair in a mouse model. Cell Tissue Res. *328*, 197–206.

Kaitu'u-Lino, T.J., Morison, N.B., and Salamonsen, L.A. (2007). Estrogen Is Not Essential for Full Endometrial Restoration after Breakdown: Lessons from a Mouse Model. Endocrinology *148*, 5105–5111.

Kamat, B.R., and Isaacson, P.G. (1987). The immunocytochemical distribution of leukocytic subpopulations in human endometrium. Am. J. Pathol. *127*, 66–73.

Kamei, Y., Hattori, M., Hatazawa, Y., Kasahara, T., Kanou, M., Kanai, S., Yuan, X., Suganami, T., Lamers, W.H., Kitamura, T., et al. (2014). FOXO1 activates glutamine synthetase gene in mouse skeletal muscles through a region downstream of 3′-UTR: possible contribution to ammonia detoxification. Am. J. Physiol. - Endocrinol. Metab. *307*, E485–E493.

Kats, R., Al-Akoum, M., Guay, S., Metz, C., and Akoum, A. (2005). Cycle-dependent expression of macrophage migration inhibitory factor in the human endometrium. Hum. Reprod. *20*, 3518–3525.

Kaunitz, D.A.M., and Inki, P. (2012). The Levonorgestrel-Releasing Intrauterine System in Heavy Menstrual Bleeding. Drugs *72*, 193–215.

Kaunitz, A.M., Meredith, S., Inki, P., Kubba, A., and Sanchez-Ramos, L. (2009). Levonorgestrel-releasing intrauterine system and endometrial ablation in heavy menstrual bleeding: a systematic review and meta-analysis. Obstet. Gynecol. *113*, 1104–1116.

Kawai, K., Liu, S.-X., Tyurin, V.A., Tyurina, Y.Y., Borisenko, G.G., Jiang, J.F., St. Croix, C.M., Fabisiak, J.P., Pitt, B.R., and Kagan, V.E. (2000). Antioxidant and Antiapoptotic Function of Metallothioneins in HL-60 Cells Challenged with Copper Nitrilotriacetate. Chem. Res. Toxicol. *13*, 1275–1286.

Kayisli, U.A., Guzeloglu-Kayisli, O., and Arici, A. (2004). Endocrine-Immune Interactions in Human Endometrium. Ann. N. Y. Acad. Sci. *1034*, 50–63.

Kayisli, U.A., Basar, M., Guzeloglu-Kayisli, O., Semerci, N., Atkinson, H.C., Shapiro, J., Summerfield, T., Huang, S.J., Prelle, K., Schatz, F., et al. (2015). Long-acting progestin-only contraceptives impair endometrial vasculature by inhibiting uterine vascular smooth muscle cell survival. Proc. Natl. Acad. Sci. 201424814.

Keightley, M.C., Brown, P., Jabbour, H.N., and Sales, K.J. (2010). F-Prostaglandin receptor regulates endothelial cell function via fibroblast growth factor-2. BMC Cell Biol. *11*, 8.

Kelly, E.J., Sandgren, E.P., Brinster, R.L., and Palmiter, R.D. (1997). A pair of adjacent glucocorticoid response elements regulate expression of two mouse metallothionein genes. Proc. Natl. Acad. Sci. *94*, 10045–10050.

Kerr, J.F.R., Wyllie, A.H., and Currie, A.R. (1972). Apoptosis: a basic biological phenomenon with wide-ranging implications in tissue kinetics. Br. J. Cancer *26*, 239.

Khatri, R., and Gupta, A.N. (1978). Effect of childbirth on menstrual pattern. Indian J. Med. Res. *67*, 66–72.

Khorram, O., and Han, G. (2009). Influence of progesterone on endometrial nitric oxide synthase expression. Fertil. Steril. *91*, 2157–2162.

King, A., Jokhi, P.P., Burrows, T.D., Gardner, L., Sharkey, A.M., and Loke, Y.W. (1996). Functions of human decidual NK cells. Am. J. Reprod. Immunol. N. Y. N 1989 *35*, 258–260.

Koch, A.E., Polverini, P.J., Kunkel, S.L., Harlow, L.A., DiPietro, L.A., Elner, V.M., Elner, S.G., and Strieter, R.M. (1992). Interleukin-8 as a macrophage-derived mediator of angiogenesis. Science *258*, 1798–1801.

Kockx, M.M., Muhring, J., Knaapen, M.W., and de Meyer, G.R. (1998). RNA synthesis and splicing interferes with DNA in situ end labeling techniques used to detect apoptosis. Am. J. Pathol. *152*, 885–888.

Kondo, Y., Rusnak, J.M., Hoyt, D.G., Settineri, C.E., Pitt, B.R., and Lazo, J.S. (1997). Enhanced Apoptosis in Metallothionein Null Cells. Mol. Pharmacol. *52*, 195–201.

Krassas, G.E., Pontikides, N., Kaltsas, T., Papadopoulou, P., Paunkovic, J., Paunkovic, N., and H. Duntas, L. (1999). Disturbances of menstruation in hypothyroidism. Clin. Endocrinol. (Oxf.) *50*, 655–659.

Kunsch, C., and Rosen, C.A. (1993). NF-kappa B subunit-specific regulation of the interleukin-8 promoter. Mol. Cell. Biol. *13*, 6137–6146.

Lai, M.D., Lee, L.R., Cheng, K.S., and Wing, L.Y. (2000). Expression of proliferating cell nuclear antigen in luminal epithelium during the growth and regression of rat uterus. J. Endocrinol. *166*, 87–93.

Lamas, S., Michel, T., Brenner, B.M., and Marsden, P.A. (1991). Nitric oxide synthesis in endothelial cells: evidence for a pathway inducible by TNF-alpha. Am. J. Physiol.-Cell Physiol. *261*, C634–C641.

Law, D.J., Gebuhr, T., Garvey, N., Agulnik, S.I., and Silver, L.M. (1995). Identification, characterization, and localization to chromosome 17q21-22 of the human TBX2 homolog, member of a conserved developmental gene family. Mamm. Genome Off. J. Int. Mamm. Genome Soc. *6*, 793–797.

Lazarus, H.M., Cruikshank, W.W., Narasimhan, N., Kagan, H.M., and Center, D.M. (1995). Induction of human monocyte motility by lysyl oxidase. Matrix Biol. J. Int. Soc. Matrix Biol. *14*, 727–731.

Lea, R.G., and Clark, D.A. (1991). Macrophages and migratory cells in endometrium relevant to implantation. Baillières Clin. Obstet. Gynaecol. *5*, 25–59.

Leblanc, V., Dery, M.-C., Shooner, C., and Asselin, E. (2003). Opposite regulation of XIAP and Smac/DIABLO in the rat endometrium in response to 17β-estradiol at estrus. Reprod. Biol. Endocrinol. *1*, 59.

Lee, D.K., Carrasco, J., Hidalgo, J., and Andrews, G.K. (1999). Identification of a signal transducer and activator of transcription (STAT) binding site in the mouse metallothionein-I promoter involved in interleukin-6-induced gene expression. Biochem. J. *337*, 59–65.

Lessey, B.A., Killam, A.P., Metzger, D.A., Haney, A.F., Greene, G.L., and McCARTY, K.S. (1988). Immunohistochemical Analysis of Human Uterine Estrogen and Progesterone Receptors Throughout the Menstrual Cycle*. J. Clin. Endocrinol. Metab. *67*, 334–340.

Lessin, D.L., Hunt, J.S., King, C.R., and Wood, G.W. (1988). Antigen expression by cells near the maternal-fetal interface. Am. J. Reprod. Immunol. Microbiol. AJRIM *16*, 1–7.

Leuenroth, S.J., Grutkoski, P.S., Ayala, A., and Simms, H.H. (2000). Suppression of PMN apoptosis by hypoxia is dependent on Mcl-1 and MAPK activity. Surgery *128*, 171–177.

Li, H., Zhu, H., Xu, C., and Yuan, J. (1998). Cleavage of BID by Caspase 8 Mediates the Mitochondrial Damage in the Fas Pathway of Apoptosis. Cell *94*, 491–501.

Li, P., Nijhawan, D., Budihardjo, I., Srinivasula, S.M., Ahmad, M., Alnemri, E.S., and Wang, X. (1997). Cytochrome c and dATP-dependent formation of Apaf-1/caspase-9 complex initiates an apoptotic protease cascade. Cell *91*, 479–489.

Li, W., Liu, G., Chou, I.-N., and Kagan, H.M. (2000). Hydrogen peroxide-mediated, lysyl oxidase-dependent chemotaxis of vascular smooth muscle cells. J. Cell. Biochem. *78*, 550–557.

Li, X.F., Charnock-Jones, D.S., Zhang, E., Hiby, S., Malik, S., Day, K., Licence, D., Bowen, J.M., Gardner, L., King, A., et al. (2001). Angiogenic Growth Factor Messenger Ribonucleic Acids in Uterine Natural Killer Cells. J. Clin. Endocrinol. Metab. *86*, 1823–1834.

Liang, L., Fu, K., Lee, D.K., Sobieski, R.J., Dalton, T., and Andrews, G.K. (1996). Activation of the complete mouse metallothionein gene locus in the maternal deciduum. Mol. Reprod. Dev. *43*, 25–37.

Liaw, S.-H., Kuo, I., and Eisenberg, D. (1995). Discovery of the ammonium substrate site on glutamine synthetase, A third cation binding site. Protein Sci. *4*, 2358–2365.

Lin, Y.G., Shen, J., Yoo, E., Liu, R., Yen, H.-Y., Mehta, A., Rajaei, A., Yang, W., Mhawech-Fauceglia, P., DeMayo, F.J., et al. (2015). Targeting the glucose-regulated protein-78 abrogates Pten-null driven AKT activation and endometrioid tumorigenesis. Oncogene.

Liu, F., Lang, J., Li, J., Benashski, S.E., Siegel, M., Xu, Y., and McCullough, L.D. (2011). Sex Differences in the Response to Poly(ADP-ribose) Polymerase-1 Deletion and Caspase Inhibition After Stroke. Stroke *42*, 1090–1096.

Liu, W.-K., Jiang, X.-Y., and Zhang, Z.-X. (2010). Expression of PSCA, PIWIL1, and TBX2 in Endometrial Adenocarcinoma. Onkologie *33*, 241–245.

Liu, Y., Cousin, J.M., Hughes, J., Damme, J.V., Seckl, J.R., Haslett, C., Dransfield, I., Savill, J., and Rossi, A.G. (1999). Glucocorticoids Promote Nonphlogistic Phagocytosis of Apoptotic Leukocytes. J. Immunol. *162*, 3639–3646.

Lowenstein, C.J., and Snyder, S.H. (1992). Nitric oxide, a novel biologic messenger. Cell *70*, 705–707.

Lucero, H.A., and Kagan, H.M. (2006). Lysyl oxidase: an oxidative enzyme and effector of cell function. Cell. Mol. Life Sci. CMLS *63*, 2304–2316.

Lumsden, M.A., Kelly, R.W., and Baird, D.T. (1983). Primary dysmenorrhoea: the importance of both prostaglandins E2 and F2 alpha. Br. J. Obstet. Gynaecol. *90*, 1135–1140.

Lydon, J.P., DeMayo, F.J., Funk, C.R., Mani, S.K., Hughes, A.R., Montgomery, C.A., Shyamala, G., Conneely, O.M., and O'Malley, B.W. (1995). Mice lacking progesterone receptor exhibit pleiotropic reproductive abnormalities. Genes Dev. *9*, 2266–2278.

Maia, J. Hugo, Maltez, A., Studart, E., Athayde, C., and Coutinho, E.M. (2005). Effect of menstrual cycle and hormonal treatment on ki-67 and bcl-2 expression and adenomyosis. Gynecol. Endocrinol. *20*, 127–131.

Maletto, B.A., Ropolo, A.S., Alignani, D.O., Liscovsky, M.V., Ranocchia, R.P., Moron, V.G., and Pistoresi-Palencia, M.C. (2006). Presence of neutrophil-bearing antigen in lymphoid organs of immune mice. Blood *108*, 3094–3102.

Malik, S., Day, K., Perrault, I., Charnock-Jones, D.S., and Smith, S.K. (2006). Reduced levels of VEGF-A and MMP-2 and MMP-9 activity and increased TNF-α in menstrual endometrium and effluent in women with menorrhagia. Hum. Reprod. *21*, 2158–2166.

Maling, H.M., Webster, M.E., Williams, M.A., Saul, W., and Anderson, W. (1974). Inflammation Induced by Histamine, Serotonin, Bradykinin and Compound 48/80 in the Rat: Antagonists and Mechanisms of Action. J. Pharmacol. Exp. Ther. *191*, 300–310.

Marbaix, E., Kokorine, I., Moulin, P., Donnez, J., Eeckhout, Y., and Courtoy, P.J. (1996). Menstrual breakdown of human endometrium can be mimicked in vitro and is selectively and reversibly blocked by inhibitors of matrix metalloproteinases. Proc. Natl. Acad. Sci. U. S. A. *93*, 9120–9125.

Maruo, T., Laoag-Fernandez, J.B., Pakarinen, P., Murakoshi, H., Spitz, I.M., and Johansson, E. (2001). Effects of the levonorgestrel-releasing intrauterine system on proliferation and apoptosis in the endometrium. Hum. Reprod. *16*, 2103–2108.

Marwick, J.A., Dorward, D.A., Lucas, C.D., Jones, K.O., Sheldrake, T.A., Fox, S., Ward, C., Murray, J., Brittan, M., Hirani, N., et al. (2013). Oxygen levels determine the ability of glucocorticoids to influence neutrophil survival in inflammatory environments. J. Leukoc. Biol. jlb.0912462.

Matthys, P., Mitera, T., Heremans, H., Damme, J.V., and Billiau, A. (1995). Anti-gamma interferon and anti-interleukin-6 antibodies affect staphylococcal enterotoxin B-induced weight loss, hypoglycemia, and cytokine release in D-galactosamine-sensitized and unsensitized mice. Infect. Immun. *63*, 1158–1164.

Mauer, J., Chaurasia, B., Goldau, J., Vogt, M.C., Ruud, J., Nguyen, K.D., Theurich, S., Hausen, A.C., Schmitz, J., Brönneke, H.S., et al. (2014). Signaling by IL-6 promotes alternative activation of macrophages to limit endotoxemia and obesity-associated resistance to insulin. Nat. Immunol. *15*, 423–430.

Maybin, J.A., Hirani, N., Jabbour, H.N., and Critchley, H.O.D. (2011). Novel Roles for Hypoxia and Prostaglandin E2 in the Regulation of IL-8 During Endometrial Repair. Am. J. Pathol. *178*, 1245–1256.

Maybin, J.A., Barcroft, J., Thiruchelvam, U., Hirani, N., Jabbour, H.N., and Critchley, H.O.D. (2012). The presence and regulation of connective tissue growth factor in the human endometrium. Hum. Reprod. *27*, 1112–1121.

McDonald, S.E., Henderson, T.A., Gomez-Sanchez, C.E., Critchley, H.O.D., and Mason, J.I. (2006). 11Beta-hydroxysteroid dehydrogenases in human endometrium. Mol. Cell. Endocrinol. *248*, 72–78.

McLoughlin, R.M., Witowski, J., Robson, R.L., Wilkinson, T.S., Hurst, S.M., Williams, A.S., Williams, J.D., Rose-John, S., Jones, S.A., and Topley, N. (2003). Interplay between IFN-γ and IL-6 signaling governs neutrophil trafficking and apoptosis during acute inflammation. J. Clin. Invest. *112*, 598–607.

Menning, A., Walter, A., Rudolph, M., Gashaw, I., Fritzemeier, K.-H., and Roese, L. (2012). Granulocytes and Vascularization Regulate Uterine Bleeding and Tissue Remodeling in a Mouse Menstruation Model. PLoS ONE *7*, e41800.

Merad, M., Manz, M.G., Karsunky, H., Wagers, A., Peters, W., Charo, I., Weissman, I.L., Cyster, J.G., and Engleman, E.G. (2002). Langerhans cells renew in the skin throughout life under steady-state conditions. Nat. Immunol. *3*, 1135–1141.

Milne, S.A., and Jabbour, H.N. (2003). Prostaglandin (PG) $F_{2\alpha}$ Receptor Expression and Signaling in Human Endometrium: Role of $PGF_{2\alpha}$ in Epithelial Cell Proliferation. J. Clin. Endocrinol. Metab. *88*, 1825–1832.

Milne, S.A., Critchley, H.O.D., Drudy, T.A., Kelly, R.W., and Baird, D.T. (1999). Perivascular Interleukin-8 Messenger Ribonucleic Acid Expression in Human Endometrium Varies across the Menstrual Cycle and in Early Pregnancy Decidua [1]. J. Clin. Endocrinol. Metab. *84*, 2563–2567.

Milne, S.A., Perchick, G.B., Boddy, S.C., and Jabbour, H.N. (2001). Expression, Localization, and Signaling of PGE2 and EP2/EP4 Receptors in Human Nonpregnant Endometrium across the Menstrual Cycle. J. Clin. Endocrinol. Metab.

Moffett, A., and Colucci, F. (2014). Uterine NK cells: active regulators at the maternal-fetal interface. J. Clin. Invest. *124*, 1872–1879.

Moffett, A., and Loke, C. (2006). Immunology of placentation in eutherian mammals. Nat. Rev. Immunol. *6*, 584–594.

Moffett-King, A. (2002). Natural killer cells and pregnancy. Nat. Rev. Immunol. *2*, 656–663.

Moreno-Bueno, G., Salvador, F., Martín, A., Floristán, A., Cuevas, E.P., Santos, V., Montes, A., Morales, S., Castilla, M.A., Rojo-Sebastián, A., et al. (2011). Lysyl oxidase-like 2 (LOXL2), a new regulator of cell polarity required for metastatic dissemination of basal-like breast carcinomas: LOXL2 in metastatic basal-like breast carcinomas. EMBO Mol. Med. *3*, 528–544.

Munro, M.G., Critchley, H.O.D., and Fraser, I.S. (2011a). The FIGO classification of causes of abnormal uterine bleeding in the reproductive years. Fertil. Steril. *95*, 2204–2208.e3.

Munro, M.G., Critchley, H.O.D., Broder, M.S., and Fraser, I.S. (2011b). FIGO classification system (PALM-COEIN) for causes of abnormal uterine bleeding in nongravid women of reproductive age. Int. J. Gynecol. Obstet. *113*, 3–13.

Munro, M.G., Critchley, H.O.D., and Fraser, I.S. (2012). The FIGO systems for nomenclature and classification of causes of abnormal uterine bleeding in the reproductive years: who needs them? Am. J. Obstet. Gynecol. *207*, 259–265.

Murdoch, C., Monk, P.N., and Finn, A. (1999). CXC Chemokine Receptor Expression on Human Endothelial Cells. Cytokine *11*, 704–712.

Murray, J., Barbara, J.A.J., Dunkley, S.A., Lopez, A.F., Ostade, X.V., Condliffe, A.M., Dransfield, I., Haslett, C., and Chilvers, E.R. (1997). Regulation of Neutrophil Apoptosis by Tumor Necrosis Factor-α: Requirement for TNFR55 and TNFR75 for Induction of Apoptosis In Vitro. Blood *90*, 2772–2783.

Nakamura, M., Takakura, M., Fujii, R., Maida, Y., Bono, Y., Mizumoto, Y., Zhang, X., Kiyono, T., and Kyo, S. (2013). The PRB-dependent FOXO1/IGFBP-1 axis is essential for progestin to inhibit endometrial epithelial growth. Cancer Lett. *336*, 68–75.

Nakao, S., Ogtata, Y., Shimizu, E., Yamazaki, M., Furuyama, S., and Sugiya, H. (2002). Tumor necrosis factor alpha (TNF-alpha)-induced prostaglandin E2 release is mediated by the activation of cyclooxygenase-2 (COX-2) transcription via NFkappaB in human gingival fibroblasts. Mol. Cell. Biochem. *238*, 11–18.

Naslavsky, N., McKenzie, J., Altan-Bonnet, N., Sheff, D., and Caplan, S. (2009). EHD3 regulates early-endosome-to-Golgi transport and preserves Golgi morphology. J. Cell Sci. *122*, 389–400.

Nathan, C.F. (1987). Neutrophil activation on biological surfaces. Massive secretion of hydrogen peroxide in response to products of macrophages and lymphocytes. J. Clin. Invest. *80*, 1550–1560.

Nathan, C., Srimal, S., Farber, C., Sanchez, E., Kabbash, L., Asch, A., Gailit, J., and Wright, S.D. (1989). Cytokine-induced respiratory burst of human neutrophils: dependence on extracellular matrix proteins and CD11/CD18 integrins. J. Cell Biol. *109*, 1341–1349.

National Collaborating Centre for Women's and Children's Health, and National Institute for Health and Care Excellence (NICE) (2007). Heavy Menstrual Bleeding Clinical Guideline No. 44.

National Institute for Health and Care Excellence (NICE) (2004). Hysterectomy - Draft Scope for Consultation.

Nayak, N.R., Critchley, H.O.D., Slayden, O.D., Menrad, A., Chwalisz, K., Baird, D.T., and Brenner, R.M. (2000). Progesterone Withdrawal Up-Regulates Vascular Endothelial Growth Factor Receptor Type 2 in the Superficial Zone Stroma of the Human and Macaque Endometrium: Potential Relevance to Menstruation [1]. J. Clin. Endocrinol. Metab. *85*, 3442–3452.

Noyes, R.W., Hertig, A.T., and Rock, J. (1950). Dating the Endometrial Biopsy. Fertil. Steril. *1*, 3–25.

Nunn, C., Zou, M.-X., Sobiesiak, A.J., Roy, A.A., Kirshenbaum, L.A., and Chidiac, P. (2010). RGS2 inhibits β-adrenergic receptor-induced cardiomyocyte hypertrophy. Cell. Signal. *22*, 1231–1239.

Office for National Statistics UK (2013). Full report - Women in the labour market, September 2013.

Ohmori, Y., Fukumoto, S., and Hamilton, T.A. (1995). Two structurally distinct kappa B sequence motifs cooperatively control LPS-induced KC gene transcription in mouse macrophages. J. Immunol. *155*, 3593–3600.

Oñate, S.A., Tsai, S.Y., Tsai, M.J., and O'Malley, B.W. (1995). Sequence and characterization of a coactivator for the steroid hormone receptor superfamily. Science *270*, 1354–1357.

Oquendo, P., Alberta, J., Wen, D.Z., Graycar, J.L., Derynck, R., and Stiles, C.D. (1989). The platelet-derived growth factor-inducible KC gene encodes a secretory protein related to platelet alpha-granule proteins. J. Biol. Chem. *264*, 4133–4137.

Ottonello, L., Frumento, G., Arduino, N., Bertolotto, M., Dapino, P., Mancini, M., and Dallegri, F. (2002). Differential regulation of spontaneous and immune complex-induced neutrophil apoptosis by proinflammatory cytokines. Role of oxidants, Bax and caspase-3. J. Leukoc. Biol. *72*, 125–132.

Palmer, R.M.J., Ferrige, A.G., and Moncada, S. (1987). Nitric oxide release accounts for the biological activity of endothelium-derived relaxing factor. Nature *327*, 524–526.

Papayannopoulos, V., Metzler, K.D., Hakkim, A., and Zychlinsky, A. (2010). Neutrophil elastase and myeloperoxidase regulate the formation of neutrophil extracellular traps. J. Cell Biol. *191*, 677–691.

Park, D., Tosello-Trampont, A.-C., Elliott, M.R., Lu, M., Haney, L.B., Ma, Z., Klibanov, A.L., Mandell, J.W., and Ravichandran, K.S. (2007). BAI1 is an engulfment receptor for apoptotic cells upstream of the ELMO/Dock180/Rac module. Nature *450*, 430–434.

Peinado, H., del Carmen Iglesias-de la Cruz, M., Olmeda, D., Csiszar, K., Fong, K.S.K., Vega, S., Nieto, M.A., Cano, A., and Portillo, F. (2005). A molecular role for lysyl oxidase-like 2 enzyme in Snail regulation and tumor progression. EMBO J. *24*, 3446–3458.

Pertoft, H., Laurent, T.C., Låås, T., and Kågedal, L. (1978). Density gradients prepared from colloidal silica particles coated by polyvinylpyrrolidone (Percoll). Anal. Biochem. *88*, 271–282.

Peters, A.M., Saverymuttu, S.H., Keshavarzian, A., Bell, R.N., and Lavender, J.P. (1985). Splenic pooling of granulocytes. Clin. Sci. Lond. Engl. 1979 *68*, 283–289.

Pijnenborg, R., Bland, J.M., Robertson, W.B., and Brosens, I. (1983). Uteroplacental arterial changes related to interstitial trophoblast migration in early human pregnancy. Placenta *4*, 397–413.

Pijnenborg, R., Anthony, J., Davey, D.A., Rees, A., Tiltman, A., Vercruysse, L., and van Assche, A. (1991). Placental bed spiral arteries in the hypertensive disorders of pregnancy. Br. J. Obstet. Gynaecol. *98*, 648–655.

Pillay, J., Braber, I. den, Vrisekoop, N., Kwast, L.M., Boer, R.J. de, Borghans, J.A.M., Tesselaar, K., and Koenderman, L. (2010). In vivo labeling with 2H2O reveals a human neutrophil lifespan of 5.4 days. Blood *116*, 625–627.

Pirone, D.M., Carter, D.E., and Burbelo, P.D. (2001). Evolutionary expansion of CRIB-containing Cdc42 effector proteins. Trends Genet. TIG *17*, 370–373.

Polow, K., Lübbert, H., Boquoi, E., Kreutzer, G., Jeske, R., and Pollow, B. (1975). Studies on 17beta-hydroxysteroid dehydrogenase in human endometrium and endometrial carcinoma I. Subcellular distribution and variations of specific enzyme activity. Acta Endocrinol. (Copenh.) *79*, 134–145.

Popovici, R.M., Irwin, J.C., Giaccia, A.J., and Giudice, L.C. (1999). Hypoxia and cAMP Stimulate Vascular Endothelial Growth Factor (VEGF) in Human Endometrial Stromal Cells: Potential Relevance to Menstruation and Endometrial Regeneration. J. Clin. Endocrinol. Metab. *84*, 2245–2245.

Poropatich, C., Rojas, M., and Silverberg, S.G. (1987). Polymorphonuclear leukocytes in the endometrium during the normal menstrual cycle. Int. J. Gynecol. Pathol. Off. J. Int. Soc. Gynecol. Pathol. *6*, 230–234.

Prentice, A. (1999). Health care implications of dysfunctional uterine bleeding. Baillières Best Pract. Res. Clin. Obstet. Gynaecol. *13*, 181–188.

Raleigh, J.A., Franko, A.J., Koch, C.J., and Born, J.L. (1985). Binding of misonidazole to hypoxic cells in monolayer and spheroid culture: evidence that a side-chain label is bound as efficiently as a ring label. Br. J. Cancer *51*, 229–235.

Ramsey, E.M., Houston, M.L., and Harris, J.W. (1976). Interactions of the trophoblast and maternal tissues in three closely related primate species. Am. J. Obstet. Gynecol. *124*, 647–652.

Reichel, C.A., Rehberg, M., Lerchenberger, M., Berberich, N., Bihari, P., Khandoga, A.G., Zahler, S., and Krombach, F. (2009). Ccl2 and Ccl3 Mediate Neutrophil Recruitment via Induction of Protein Synthesis and Generation of Lipid Mediators. Arterioscler. Thromb. Vasc. Biol. *29*, 1787–1793.

Ren, Y., Silverstein, R.L., Allen, J., and Savill, J. (1995). CD36 gene transfer confers capacity for phagocytosis of cells undergoing apoptosis. J. Exp. Med. *181*, 1857–1862.

Ribechini, E., Leenen, P.J.M., and Lutz, M.B. (2009). Gr-1 antibody induces STAT signaling, macrophage marker expression and abrogation of myeloid-derived suppressor cell activity in BM cells. Eur. J. Immunol. *39*, 3538–3551.

Robaye, B., Mosselmans, R., Fiers, W., Dumont, J.E., and Galand, P. (1991). Tumor necrosis factor induces apoptosis (programmed cell death) in normal endothelial cells in vitro. Am. J. Pathol. *138*, 447–453.

Roberts, D.K., Parmley, T.H., Walker, N.J., and Horbelt, D.V. (1992). Ultrastructure of the microvasculature in the human endometrium throughout the normal menstrual cycle. Am. J. Obstet. Gynecol. *166*, 1393–1406.

Roberts, T.E., Tsourapas, A., Middleton, L.J., Champaneria, R., Daniels, J.P., Cooper, K.G., Bhattacharya, S., and Barton, P.M. (2011). Hysterectomy, endometrial ablation, and levonorgestrel releasing intrauterine system (Mirena) for treatment of heavy menstrual bleeding: cost effectiveness analysis. BMJ *342*, d2202.

Rosas, M., Thomas, B., Stacey, M., Gordon, S., and Taylor, P.R. (2010). The myeloid 7/4-antigen defines recently generated inflammatory macrophages and is synonymous with Ly-6B. J. Leukoc. Biol. *88*, 169–180.

Rossi, A.G., McCutcheon, J.C., Roy, N., Chilvers, E.R., Haslett, C., and Dransfield, I. (1998). Regulation of Macrophage Phagocytosis of Apoptotic Cells by cAMP. J. Immunol. *160*, 3562–3568.

Rowley, M., Grothey, E., and Couch, F.J. (2004). The role of Tbx2 and Tbx3 in mammary development and tumorigenesis. J. Mammary Gland Biol. Neoplasia *9*, 109–118.

Royal College of Obstetricians and Gynaecologists (RCOG), London School of Hygiene and Tropical Medicine, and Ipsos MORI (2012). RCOG National Heavy Menstrual Bleeding Audit - Second Annual Report.

Rudolph, M., Docke, W.-D., Muller, A., Menning, A., Rose, L., Zollner, T.M., and Gashaw, I. (2012). Induction of Overt Menstruation in Intact Mice. PLoS ONE *7*.

Rudolph-Owen, L.A., Slayden, O.D., Matrisian, L.M., and Brenner, R.M. (1998). Matrix Metalloproteinase Expression in Macaca mulatta Endometrium: Evidence for Zone-Specific Regulatory Tissue Gradients. Biol. Reprod. *59*, 1349–1359.

Saito, S., Kasahara, T., Sakakura, S., Enomoto, M., Umekage, H., Harada, N., Morii, T., Nishikawa, K., Narita, N., and Ichijo, M. (1994). Interleukin-8 Production by CD16−CD56bright Natural Killer Cells in the Human Early Pregnancy Decidua. Biochem. Biophys. Res. Commun. *200*, 378–383.

Salamonsen, L.A., and Lathbury, L.J. (2000). Endometrial leukocytes and menstruation. Hum. Reprod. Update *6*, 16–27.

Salamonsen, L.A., and Woolley, D.E. (1999). Menstruation: induction by matrix metalloproteinases and inflammatory cells. J. Reprod. Immunol. *44*, 1–27.

Salamonsen, L.A., Zhang, J., Hampton, A., and Lathbury, L. (2000). Regulation of matrix metalloproteinases in human endometrium. Hum. Reprod. *15*, 112–119.

Sales, K.J., List, T., Boddy, S.C., Williams, A.R.W., Anderson, R.A., Naor, Z., and Jabbour, H.N. (2005). A Novel Angiogenic Role for Prostaglandin F2α-FP Receptor Interaction in Human Endometrial Adenocarcinomas. Cancer Res. *65*, 7707–7716.

Sales, K.J., Maldonado-Pérez, D., Grant, V., Catalano, R.D., Wilson, M.R., Brown, P., Williams, A.R.W., Anderson, R.A., Thompson, E.A., and Jabbour, H.N. (2009). Prostaglandin F2α-F-prostanoid receptor regulates CXCL8 expression in endometrial adenocarcinoma cells via the calcium–calcineurin–NFAT pathway. Biochim. Biophys. Acta *1793*, 1917–1928.

Salker, M.S., Christian, M., Steel, J.H., Nautiyal, J., Lavery, S., Trew, G., Webster, Z., Al-Sabbagh, M., Puchchakayala, G., Föller, M., et al. (2011). Deregulation of the serum- and glucocorticoid-inducible kinase SGK1 in the endometrium causes reproductive failure. Nat. Med. *17*, 1509–1513.

Santos, I.S., Minten, G.C., Valle, N.C., Tuerlinckx, G.C., Silva, A.B., Pereira, G.A., and Carriconde, J.F. (2011). Menstrual bleeding patterns: A community-based cross-sectional study among women aged 18-45 years in Southern Brazil. BMC Womens Health *11*, 26.

Sanui, H., Yoshida, S., Nomoto, K., Ohhara, R., and Adachi, Y. (1982). Peritoneal macrophages which phagocytose autologous polymorphonuclear leucocytes in guinea-pigs. I: induction by irritants and microorgansisms and inhibition by colchicine. Br. J. Exp. Pathol. *63*, 278–284.

Savill, J., and Haslett, C. (1995). Granulocyte clearance by apoptosis in the resolution ofinflammation. Semin. Cell Biol. *6*, 385–393.

Savill, J., Smith, J., Sarraf, C., Ren, Y., Abbott, F., and Rees, A. (1992). Glomerular mesangial cells and inflammatory macrophages ingest neutrophils undergoing apoptosis. Kidney Int. *42*, 924–936.

Savill, J., Dransfield, I., Gregory, C., and Haslett, C. (2002). A blast from the past: clearance of apoptotic cells regulates immune responses. Nat. Rev. Immunol. *2*, 965–975.

Savill, J.S., Wyllie, A.H., Henson, J.E., Walport, M.J., Henson, P.M., and Haslett, C. (1989a). Macrophage phagocytosis of aging neutrophils in inflammation. Programmed cell death in the neutrophil leads to its recognition by macrophages. J. Clin. Invest. *83*, 865–875.

Savill, J.S., Henson, P.M., and Haslett, C. (1989b). Phagocytosis of aged human neutrophils by macrophages is mediated by a novel “charge-sensitive” recognition mechanism. J. Clin. Invest. *84*, 1518–1527.

Scapini, P., Lapinet-Vera, J.A., Gasperini, S., Calzetti, F., Bazzoni, F., and Cassatella, M.A. (2000). The neutrophil as a cellular source of chemokines. Immunol. Rev. *177*, 195–203.

Schneider, C.A., Rasband, W.S., and Eliceiri, K.W. (2012). NIH Image to ImageJ: 25 years of image analysis. Nat. Methods *9*, 671–675.

Scholten, D., and Al-samman, M. (2012). CXCR3 Ligands induce Expression of CXCL1 (KC/murine IL8 homolog) in Mouse Hepatic Stellate Cells. J. Cell Sci. Ther. *01*.

Schröder, A.K., Von Der Ohe, M., Kolling, U., Altstaedt, J., Uciechowski, P., Fleischer, D., Dalhoff, K., Ju, X., Zenke, M., Heussen, N., et al. (2006). Polymorphonuclear leucocytes selectively produce anti-inflammatory interleukin-1 receptor antagonist and chemokines, but fail to produce pro-inflammatory mediators. Immunology *119*, 317–327.

Schulz, C., Perdiguero, E.G., Chorro, L., Szabo-Rogers, H., Cagnard, N., Kierdorf, K., Prinz, M., Wu, B., Jacobsen, S.E.W., Pollard, J.W., et al. (2012). A Lineage of Myeloid Cells Independent of Myb and Hematopoietic Stem Cells. Science *336*, 86–90.

Selzman, C.H., Miller, S.A., Zimmerman, M.A., Gamboni-Robertson, F., Harken, A.H., and Banerjee, A. (2002). Monocyte chemotactic protein-1 directly induces human vascular smooth muscle proliferation. Am. J. Physiol. - Heart Circ. Physiol. *283*, H1455–H1461.

Serhan, C.N., Brain, S.D., Buckley, C.D., Gilroy, D.W., Haslett, C., O'Neill, L.A.J., Perretti, M., Rossi, A.G., and Wallace, J.L. (2007). Resolution of inflammation: state of the art, definitions and terms. FASEB J. *21*, 325–332.

Shakhov, A.N., Collart, M.A., Vassalli, P., Nedospasov, S.A., and Jongeneel, C.V. (1990). Kappa B-type enhancers are involved in lipopolysaccharide-mediated transcriptional activation of the tumor necrosis factor alpha gene in primary macrophages. J. Exp. Med. *171*, 35–47.

Shankar, M., Chi, C., and Kadir, R.A. (2008). Review of quality of life: menorrhagia in women with or without inherited bleeding disorders. Haemophilia *14*, 15–20.

Shapley, M., Jordan, K., and Croft, P.R. (2002). Why women consult with increased vaginal bleeding: a case-control study. Br J Gen Pr. *52*, 108–113.

Shapley, M., Jordan, K., and Croft, P.R. (2004). An epidemiological survey of symptoms of menstrual loss in the community. Br. J. Gen. Pract. *54*, 359–363.

Sica, A., Wang, J.M., Colotta, F., Dejana, E., Mantovani, A., Oppenheim, J.J., Larsen, C.G., Zachariae, C.O., and Matsushima, K. (1990a). Monocyte chemotactic and activating factor gene expression induced in endothelial cells by IL-1 and tumor necrosis factor. J. Immunol. *144*, 3034–3038.

Sica, A., Matsushima, K., Van Damme, J., Wang, J.M., Polentarutti, N., Dejana, E., Colotta, F., and Mantovani, A. (1990b). IL-1 transcriptionally activates the neutrophil chemotactic factor/IL-8 gene in endothelial cells. Immunology *69*, 548–553.

Siderovski, D. p., Heximer, S. p., and Forsdyke, D. r. (1994). A Human Gene Encoding a Putative Basic Helix–Loop–Helix Phosphoprotein Whose mRNA Increases Rapidly in Cycloheximide-Treated Blood Mononuclear Cells. DNA Cell Biol. *13*, 125–147.

da Silva, A.J., and Pieniazek, N.J. (2003). Latest Advances and Trends in PCR-Based Diagnostic Methods. In Textbook-Atlas of Intestinal Infections in AIDS, D.D. M.D, ed. (Springer Milan), pp. 397–412.

Simmons, D.G., and Kennedy, T.G. (2000). Induction of Glucose-Regulated Protein 78 in Rat Uterine Glandular Epithelium During Uterine Sensitization for the Decidual Cell Reaction. Biol. Reprod. *62*, 1168–1176.

Slayden, O.D., and Brenner, R.M. (2006). A critical period of progesterone withdrawal precedes menstruation in macaques. Reprod. Biol. Endocrinol. *4*, S6.

Slee, E.A., Adrain, C., and Martin, S.J. (2001). Executioner Caspase-3, -6, and -7 Perform Distinct, Non-redundant Roles during the Demolition Phase of Apoptosis. J. Biol. Chem. *276*, 7320–7326.

Smith, O.P.M., Jabbour, H.N., and Critchley, H.O.D. (2007). Cyclooxygenase enzyme expression and E series prostaglandin receptor signalling are enhanced in heavy menstruation. Hum. Reprod. *22*, 1450–1456.

Smith, R.E., Salamonsen, L.A., Komesaroff, P.A., Li, K.X.Z., Myles, K.M., Lawrence, M., and Krozowski, Z. (1997). 11β-Hydroxysteroid Dehydrogenase Type II in the Human Endometrium: Localization and Activity during the Menstrual Cycle [1]. J. Clin. Endocrinol. Metab. *82*, 4252–4257.

Smith, S.K., Abel, M.H., Kelly, R.W., and Baird, D.T. (1981a). Prostaglandin synthesis in the endometrium of women with ovular dysfunctional uterine bleeding. Br. J. Obstet. Gynaecol. *88*, 434–442.

Smith, S.K., Abel, M.H., Kelly, R.W., and Baird, D.T. (1981b). A role for prostacyclin (PGi2) in excessive menstrual bleeding. Lancet Lond. Engl. *1*, 522–524.

Smyth, G.K. (2005). limma: Linear Models for Microarray Data. In Bioinformatics and Computational Biology Solutions Using R and Bioconductor, R. Gentleman, V.J. Carey, W. Huber, R.A. Irizarry, and S. Dudoit, eds. (Springer New York), pp. 397–420.

Smyth, Gordon K., Yang, Yee-Hwa, (second), and Speed, Terry P., (third) (2003). Statistical Issues in cDNA Microarray Data Analysis - Springer. M.J. Brownstein, and A.B. Khodursky, eds. (Humana Press),.

Spornitz, U.M. (1992). The functional morphology of the human endometrium and decidua. Adv. Anat. Embryol. Cell Biol. *124*, 1–99.

Starkie, R., Ostrowski, S.R., Jauffred, S., Febbraio, M., and Pedersen, B.K. (2003). Exercise and IL-6 infusion inhibit endotoxin-induced TNF-alpha production in humans. FASEB J. Off. Publ. Fed. Am. Soc. Exp. Biol. *17*, 884–886.

Stern, M., Savill, J., and Haslett, C. (1996). Human monocyte-derived macrophage phagocytosis of senescent eosinophils undergoing apoptosis. Mediation by alpha v beta

3/CD36/thrombospondin recognition mechanism and lack of phlogistic response. Am. J. Pathol. *149*, 911–921.

Stewart, Campbell-Brown, Critchley, and Farquharson (1999). Endometrial apoptosis in patients with dysfunctional uterine bleeding. Histopathology *34*, 99–105.

Strieter, R.M., Kasahara, K., Allen, R., Showell, H.J., Standiford, T.J., and Kunkel, S.L. (1990). Human neutrophils exhibit disparate chemotactic factor gene expression. Biochem. Biophys. Res. Commun. *173*, 725–730.

Strieter, R.M., Polverini, P.J., Kunkel, S.L., Arenberg, D.A., Burdick, M.D., Kasper, J., Dzuiba, J., Van Damme, J., Walz, A., and Marriott, D. (1995a). The functional role of the ELR motif in CXC chemokine-mediated angiogenesis. J. Biol. Chem. *270*, 27348–27357.

Strieter, R.M., Polverini, P.J., Arenberg, D.A., Walz, A., Opdenakker, G., Van Damme, J., and Kunkel, S.L. (1995b). Role of C-X-C chemokines as regulators of angiogenesis in lung cancer. J. Leukoc. Biol. *57*, 752–762.

Su, C.-M., Su, Y.-H., Chiu, C.-F., Chang, Y.-W., Hong, C.-C., Yu, Y.-H., Ho, Y.-S., Wu, C.-H., Yen, C.-S., and Su, J.-L. (2014). Vascular Endothelial Growth Factor-C Upregulates Cortactin and Promotes Metastasis of Esophageal Squamous Cell Carcinoma. Ann. Surg. Oncol. *21*, 767–775.

Suganuma, N., Harada, M., Furuhashi, M., Nawa, A., and Kikkawa, F. (1997). Apoptosis in human endometrial and endometriotic tissues. Horm. Res. *48 Suppl 3*, 42–47.

Sugino, N., Karube-Harada, A., Taketani, T., Sakata, A., and Nakamura, Y. (2004). Withdrawal of Ovarian Steroids Stimulates Prostaglandin F2α Production Through Nuclear Factor-κB Activation via Oxygen Radicals in Human Endometrial Stromal Cells: Potential Relevance to Menstruation. J. Reprod. Dev. *50*, 215–225.

Sun, S.C., Ganchi, P.A., Ballard, D.W., and Greene, W.C. (1993). NF-kappa B controls expression of inhibitor I kappa B alpha: evidence for an inducible autoregulatory pathway. Science *259*, 1912–1915.

Tabibzadeh, S. (1991). Ubiquitous expression of TNF-alpha/cachectin immunoreactivity in human endometrium. Am. J. Reprod. Immunol. N. Y. N 1989 *26*, 1–4.

Tabibzadeh, S., Zupi, E., Babaknia, A., Liu, R., Marconi, D., and Romanini, C. (1995). Site and menstrual cycle-dependent expression of proteins of the tumour necrosis factor (TNF) receptor family, and BCL-2 oncoprotein and phase-specific production of TNF alpha in human endometrium. Hum. Reprod. Oxf. Engl. *10*, 277–286.

Talbi, S., Hamilton, A.E., Vo, K.C., Tulac, S., Overgaard, M.T., Dosiou, C., Le Shay, N., Nezhat, C.N., Kempson, R., Lessey, B.A., et al. (2006). Molecular Phenotyping of Human Endometrium Distinguishes Menstrual Cycle Phases and Underlying Biological Processes in Normo-Ovulatory Women. Endocrinology *147*, 1097–1121.

Telfer, J.F., Lyall, F., Norman, J.E., and Cameron, I.T. (1995). Identification of nitric oxide synthase in human uterus. Hum. Reprod. Oxf. Engl. *10*, 19–23.

Tepper, R.I., Coffman, R.L., and Leder, P. (1992). An eosinophil-dependent mechanism for the antitumor effect of interleukin-4. Science *257*, 548–551.

Thiruchelvam, U., Dransfield, I., Saunders, P.T.K., and Critchley, H.O.D. (2012). The importance of the macrophage within the human endometrium. J. Leukoc. Biol.

Thompson, A., Han, V.K.M., and Yang, K. (2002). Spatial and Temporal Patterns of Expression of 11β-Hydroxysteroid Dehydrogenase Types 1 and 2 Messenger RNA and Glucocorticoid Receptor Protein in the Murine Placenta and Uterus During Late Pregnancy. Biol. Reprod. *67*, 1708–1718.

Tracey, K.J., Beutler, B., Lowry, S.F., Merryweather, J., Wolpe, S., Milsark, I.W., Hariri, R.J., Fahey, T.J., 3rd, Zentella, A., and Albert, J.D. (1986). Shock and tissue injury induced by recombinant human cachectin. Science *234*, 470–474.

Tranguch, S., Cheung-Flynn, J., Daikoku, T., Prapapanich, V., Cox, M.B., Xie, H., Wang, H., Das, S.K., Smith, D.F., and Dey, S.K. (2005). Cochaperone immunophilin FKBP52 is critical to uterine receptivity for embryo implantation. Proc. Natl. Acad. Sci. U. S. A. *102*, 14326–14331.

Trump, B.F., Goldblatt, P.J., and Stowell, R.E. (1965). Studies of necrosis in vitro of mouse hepatic parenchymal cells. Ultrastructural alterations in endoplasmic reticulum, Golgi apparatus, plasma membrane, and lipid droplets. Lab. Investig. J. Tech. Methods Pathol. *14*, 2000–2028.

Tseng, L., and Gurpide, E. (1974). Estradiol and 20α-Dihydroprogesterone Dehydrogenase Activities in Human Endometrium During the Menstrual Cycle. Endocrinology *94*, 419–423.

Tseng, L., and Gurpide, E. (1975a). Induction of human endometrial estradiol dehydrogenase by progestins. Endocrinology *97*, 825–833.

Tseng, L., and Gurpide, E. (1975b). Effects of progestins on estradiol receptor levels in human endometrium. J. Clin. Endocrinol. Metab. *41*, 402–404.

Tseng, L., Zhang, J., Peresleni TYu, and Goligorsky, M.S. (1996). Cyclic expression of endothelial nitric oxide synthase mRNA in the epithelial glands of human endometrium. J. Soc. Gynecol. Investig. *3*, 33–38.

Urban, C.F., Ermert, D., Schmid, M., Abu-Abed, U., Goosmann, C., Nacken, W., Brinkmann, V., Jungblut, P.R., and Zychlinsky, A. (2009). Neutrophil Extracellular Traps Contain Calprotectin, a Cytosolic Protein Complex Involved in Host Defense against Candida albicans. PLoS Pathog *5*, e1000639.

Ussov, W.Y., Aktolun, C., Myers, M.J., Jamar, F., and Peters, A.M. (1995). Granulocyte margination in bone marrow: comparison with margination in the spleen and liver. Scand. J. Clin. Lab. Invest. *55*, 87–96.

Uzumcu, M., Homsi, M.F.A., Ball, D.K., Coskun, S., Jaroudi, K., Hollanders, J.M.G., and Brigstock, D.R. (2000). Localization of connective tissue growth factor in human uterine tissues. Mol. Hum. Reprod. *6*, 1093–1098.

Varghese, A.J., Gulyas, S., and Mohindra, J.K. (1976). Hypoxia-dependent Reduction of 1-(2-Nitro-1-imidazolyl)-3-methoxy-2-propanol by Chinese Hamster Ovary Cells and KHT Tumor Cells in Vitro and in Vivo. Cancer Res. *36*, 3761–3765.

Vassilev, V., Pretto, C.M., Cornet, P.B., Delvaux, D., Eeckhout, Y., Courtoy, P.J., Marbaix, E., and Henriet, P. (2005). Response of Matrix Metalloproteinases and Tissue Inhibitors of Metalloproteinases Messenger Ribonucleic Acids to Ovarian Steroids in Human Endometrial Explants Mimics Their Gene- and Phase-Specific Differential Control *in Vivo*. J. Clin. Endocrinol. Metab. *90*, 5848–5857.

Veillette, A., Grenier, K., Brasseur, K., Fréchette-Frigon, G., Leblanc, V., Parent, S., and Asselin, E. (2013). Regulation of the PI3-K/Akt Survival Pathway in the Rat Endometrium. Biol. Reprod. *88*, 79.

Verma, S., Hiby, S.E., Loke, Y.W., and King, A. (2000). Human Decidual Natural Killer Cells Express the Receptor for and Respond to the Cytokine Interleukin 15. Biol. Reprod. *62*, 959–968.

Vestweber, D., Zeuschner, D., Rottner, K., and Schnoor, M. (2013). Cortactin regulates the activity of small GTPases and ICAM-1 clustering in endothelium. Tissue Barriers *1*, e23862.

Walmsley, S.R., Print, C., Farahi, N., Peyssonnaux, C., Johnson, R.S., Cramer, T., Sobolewski, A., Condliffe, A.M., Cowburn, A.S., Johnson, N., et al. (2005). Hypoxia-induced neutrophil survival is mediated by HIF-1α–dependent NF-κB activity. J. Exp. Med. *201*, 105–115.

Wang, H., Critchley, H.O., Kelly, R.W., Shen, D., and Baird, D.T. (1998). Progesterone receptor subtype B is differentially regulated in human endometrial stroma. Mol. Hum. Reprod. *4*, 407–412.

Ward, C., Chilvers, E.R., Lawson, M.F., Pryde, J.G., Fujihara, S., Farrow, S.N., Haslett, C., and Rossi, A.G. (1999). NF-kappaB activation is a critical regulator of human granulocyte apoptosis in vitro. J. Biol. Chem. *274*, 4309–4318.

Warner, P.E., Critchley, H.O.D., Lumsden, M.A., Campbell-Brown, M., Douglas, A., and Murray, G.D. (2004). Menorrhagia II: is the 80-mL blood loss criterion useful in management of complaint of menorrhagia? Am. J. Obstet. Gynecol. *190*, 1224–1229.

Watanabe, T., Pakala, R., Katagiri, T., and Benedict, C.R. (2001). Monocyte chemotactic protein 1 amplifies serotonin-induced vascular smooth muscle cell proliferation. J. Vasc. Res. *38*, 341–349.

Whyte, M.K., Meagher, L.C., MacDermot, J., and Haslett, C. (1993). Impairment of function in aging neutrophils is associated with apoptosis. J. Immunol. *150*, 5124–5134.

Wick, M., Bürger, C., Funk, M., and Müller, R. (1995). Identification of a Novel Mitogen-Inducible Gene (mig-6): Regulation during G1 Progression and Differentiation. Exp. Cell Res. *219*, 527–535.

Wilkens, J., Male, V., Ghazal, P., Forster, T., Gibson, D.A., Williams, A.R.W., Brito-Mutunayagam, S.L., Craigon, M., Lourenco, P., Cameron, I.T., et al. (2013). Uterine NK

Cells Regulate Endometrial Bleeding in Women and Are Suppressed by the Progesterone Receptor Modulator Asoprisnil. J. Immunol. *191*, 2226–2235.

Witko-Sarsat, V., Pederzoli-Ribeil, M., Hirsh, E., Sozzani, S., and Cassatella, M.A. (2011). Regulating neutrophil apoptosis: new players enter the game. Trends Immunol. *32*, 117–124.

von Wolff, M., Thaler, C.J., Strowitzki, T., Broome, J., Stolz, W., and Tabibzadeh, S. (2000). Regulated expression of cytokines in human endometrium throughout the menstrual cycle: dysregulation in habitual abortion. Mol. Hum. Reprod. *6*, 627–634.

von Wolff, M., Thaler, C.J., Zepf, C., Becker, V., Beier, H.M., and Strowitzki, T. (2002). Endometrial expression and secretion of interleukin-6 throughout the menstrual cycle. Gynecol. Endocrinol. Off. J. Int. Soc. Gynecol. Endocrinol. *16*, 121–129.

Wong, C.-W., Komm, B., and Cheskis, B.J. (2001). Structure−Function Evaluation of ER α and β Interplay with SRC Family Coactivators. ER Selective Ligands. Biochemistry (Mosc.) *40*, 6756–6765.

Wyatt, K.M., Dimmock, P.W., Walker, T.J., and O'Brien, P.M.S. (2001). Determination of total menstrual blood loss. Fertil. Steril. *76*, 125–131.

Wyllie, A.H. (1980). Glucocorticoid-induced thymocyte apoptosis is associated with endogenous endonuclease activation. Nature *284*, 555–556.

Wyllie, A.H., Kerr, J.F., and Currie, A.R. (1972). Cellular events in the adrenal cortex following ACTH deprivation. J. Pathol. *106*, Pix.

Wyllie, A.H., Morris, R.G., Smith, A.L., and Dunlop, D. (1984). Chromatin cleavage in apoptosis: association with condensed chromatin morphology and dependence on macromolecular synthesis. J. Pathol. *142*, 67–77.

Xiao, B., von Hertzen, H., Zhao, H., and Piaggio, G. (2003). Menstrual induction with mifepristone and misoprostol☆. Contraception *68*, 489–494.

Xu, X.B., He, B., and Wang, J.D. (2007). Menstrual-like changes in mice are provoked through the pharmacologic withdrawal of progesterone using mifepristone following induction of decidualization. Hum. Reprod. *22*, 3184–3191.

Yamamoto, K., Arakawa, T., Ueda, N., and Yamamoto, S. (1995). Transcriptional Roles of Nuclear Factor B and Nuclear Factor-Interleukin-6 in the Tumor Necrosis Factor - Dependent Induction of Cyclooxygenase-2 in MC3T3-E1 Cells. J. Biol. Chem. *270*, 31315–31320.

Yang, H., Zhou, Y., Edelshain, B., Schatz, F., Lockwood, C.J., and Taylor, H.S. (2012). FKBP4 is regulated by HOXA10 during decidualization and in endometriosis. Reproduction *143*, 531–538.

Yang, Z., Wolf, I.M., Chen, H., Periyasamy, S., Chen, Z., Yong, W., Shi, S., Zhao, W., Xu, J., Srivastava, A., et al. (2006). FK506-Binding Protein 52 Is Essential to Uterine Reproductive Physiology Controlled by the Progesterone Receptor A Isoform. Mol. Endocrinol. *20*, 2682–2694.

Yellon, S.M., Dobyns, A.E., Beck, H.L., Kurtzman, J.T., Garfield, R.E., and Kirby, M.A. (2013). Loss of Progesterone Receptor-Mediated Actions Induce Preterm Cellular and Structural Remodeling of the Cervix and Premature Birth. PLoS ONE *8*.

Yoshimura, T., and Leonard, E.J. (1990). Secretion by human fibroblasts of monocyte chemoattractant protein-1, the product of gene JE. J. Immunol. Baltim. Md 1950 *144*, 2377–2383.

Yoshimura, T., Yuhki, N., Moore, S.K., Appella, E., Lerman, M.I., and Leonard, E.J. (1989a). Human monocyte chemoattractant protein-1 (MCP-1) Full-length cDNA cloning, expression in mitogen-stimulated blood mononuclear leukocytes, and sequence similarity to mouse competence gene JE. FEBS Lett. *244*, 487–493.

Yoshimura, T., Robinson, E.A., Tanaka, S., Appella, E., Kuratsu, J., and Leonard, E.J. (1989b). Purification and amino acid analysis of two human glioma-derived monocyte chemoattractants. J. Exp. Med. *169*, 1449–1459.

You, H., Jang, Y., You-Ten, A.I., Okada, H., Liepa, J., Wakeham, A., Zaugg, K., and Mak, T.W. (2004). p53-dependent inhibition of FKHRL1 in response to DNA damage through protein kinase SGK1. Proc. Natl. Acad. Sci. U. S. A. *101*, 14057–14062.

Yue, T.L., Wang, X., Sung, C.P., Olson, B., McKenna, P.J., Gu, J.L., and Feuerstein, G.Z. (1994). Interleukin-8. A mitogen and chemoattractant for vascular smooth muscle cells. Circ. Res. *75*, 1–7.

Zelenko, Z., Aghajanova, L., Irwin, J.C., and Giudice, L.C. (2012). Nuclear Receptor, Coregulator Signaling, and Chromatin Remodeling Pathways Suggest Involvement of the Epigenome in the Steroid Hormone Response of Endometrium and Abnormalities in Endometriosis. Reprod. Sci. *19*, 152–162.

Zervou, S., Klentzeris, L.D., and Old, R.W. (1999). Nitric oxide synthase expression and steroid regulation in the uterus of women with menorrhagia. Mol. Hum. Reprod. *5*, 1048–1054.

Zhang, X.W., Liu, Q., Wang, Y., and Thorlacius, H. (2001). CXC chemokines, MIP-2 and KC, induce P-selectin-dependent neutrophil rolling and extravascular migration in vivo. Br. J. Pharmacol. *133*, 413–421.

Zhang, Y., Tseng, C.-C., Tsai, Y.-L., Fu, X., Schiff, R., and Lee, A.S. (2013). Cancer Cells Resistant to Therapy Promote Cell Surface Relocalization of GRP78 Which Complexes with PI3K and Enhances PI(3,4,5)P3 Production. PLoS ONE *8*, e80071.

Appendix

Oral Presentations

- "Inhibition of Apoptosis in a Mouse Model of Menstruation"
  GM Armstrong, AA Murray, PTK Saunders, AG Rossi, HOD Critchley

  1st Congress of Society for Endometriosis and Uterine Disorder (2015)
  Paris, France

- "Womb for Improvement"
  GM Armstrong

  MRC Centenary/Bright Club Edinburgh "eMpiRiC" Comedy Night (2013)
  Edinburgh, UK

Poster Presentations

- "Apoptosis and Resolution of Inflammation in a Mouse Model of Induced Menstruation"
  GM Armstrong, AA Murray, JA Maybin, PTK Saunders, AG Rossi, HOD Critchley

  62nd Annual Meeting for Society of Reproductive Investigation (2015)
  San Francisco, USA

- "Apoptosis and Neutrophil Infiltration in the Human Endometrium at Menstruation Recapitulated in Mouse Model of Induced Menses"
  GM Armstrong, AA Murray, JA Maybin, AG Rossi, HOD Critchley

  World Congress of Reproductive Biology (2014)
  Edinburgh, UK

- "A Whole Genome Array of Menstrual Endometrium from Women with Normal and Heavy Menstrual Bleeding Identifies Apoptosis as an Important Differentially-Regulated Function"
  JA Maybin, GM Armstrong, E Marshall, PTK Saunders, HOD Critchley

  2nd Biomarker Meeting on Personalized Reproductive Medicine (2014)
  Valencia, Spain

Original Research Papers

- "Cortisol Regulates the Paracrine Action of Macrophages by Inducing Vasoactive Gene Expression in Endometrial Cells"
  U Thiruchelvam, JA Maybin, GM Armstrong, E Greaves, PTK Saunders, HOD Critchley
  Accepted for publication in J Leuk Biol (December 2015)

Prizes & Awards

- "Glucocorticoid Signalling in Endometrial Repair in a Mouse Model of Menstruation"
  Society for Endocrinology (SfE) Summer Studentship (for student assistance)

  Awarded to assist undergraduate students in gaining research experience (2015)

- "Resolution of Inflammation in the Uterine Endometrium"
  Moray Endowment Fund research endowment

  Awarded to support promising research in any scientific discipline (2015)

- "Inhibition of Apoptosis in a Mouse Model of Menstruation and Repair"
  Barbour Watson Trust research endowment

  Awarded to support research in gynaecology (2014)